

Cooperative multiple hydrogen bonding in supramolecular chemistry

Citation for published version (APA):

Beijer, F. H. (1998). *Cooperative multiple hydrogen bonding in supramolecular chemistry*. [Phd Thesis 1 (Research TU/e / Graduation TU/e), Chemical Engineering and Chemistry]. Technische Universiteit Eindhoven. <https://doi.org/10.6100/IR508563>

DOI:

[10.6100/IR508563](https://doi.org/10.6100/IR508563)

Document status and date:

Published: 01/01/1998

Document Version:

Publisher's PDF, also known as Version of Record (includes final page, issue and volume numbers)

Please check the document version of this publication:

- A submitted manuscript is the version of the article upon submission and before peer-review. There can be important differences between the submitted version and the official published version of record. People interested in the research are advised to contact the author for the final version of the publication, or visit the DOI to the publisher's website.
- The final author version and the galley proof are versions of the publication after peer review.
- The final published version features the final layout of the paper including the volume, issue and page numbers.

[Link to publication](#)

General rights

Copyright and moral rights for the publications made accessible in the public portal are retained by the authors and/or other copyright owners and it is a condition of accessing publications that users recognise and abide by the legal requirements associated with these rights.

- Users may download and print one copy of any publication from the public portal for the purpose of private study or research.
- You may not further distribute the material or use it for any profit-making activity or commercial gain
- You may freely distribute the URL identifying the publication in the public portal.

If the publication is distributed under the terms of Article 25fa of the Dutch Copyright Act, indicated by the "Taverne" license above, please follow below link for the End User Agreement:

www.tue.nl/taverne

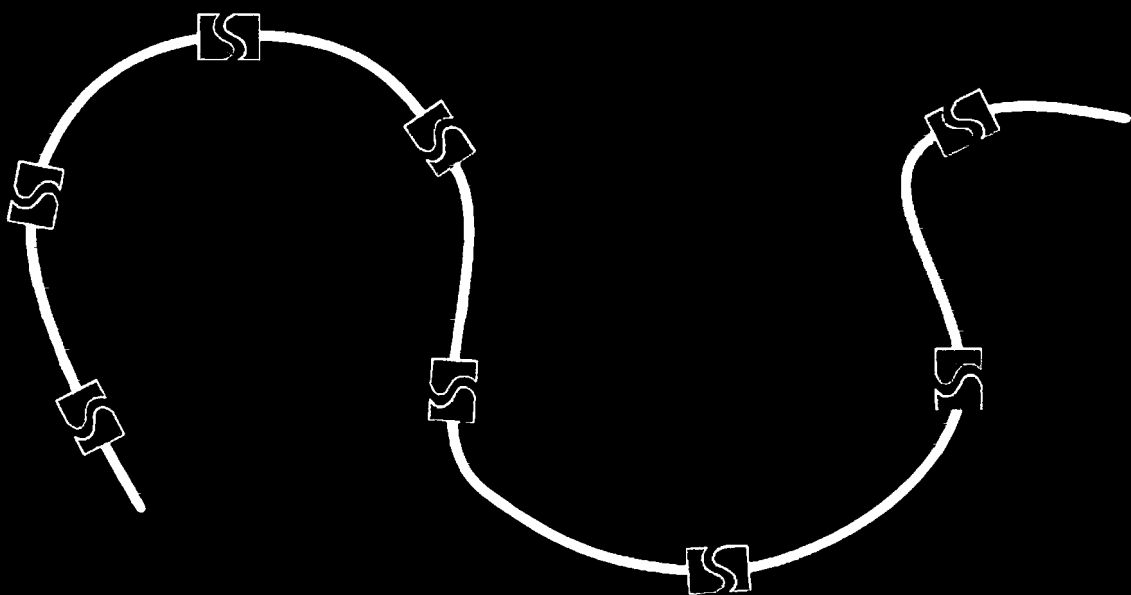
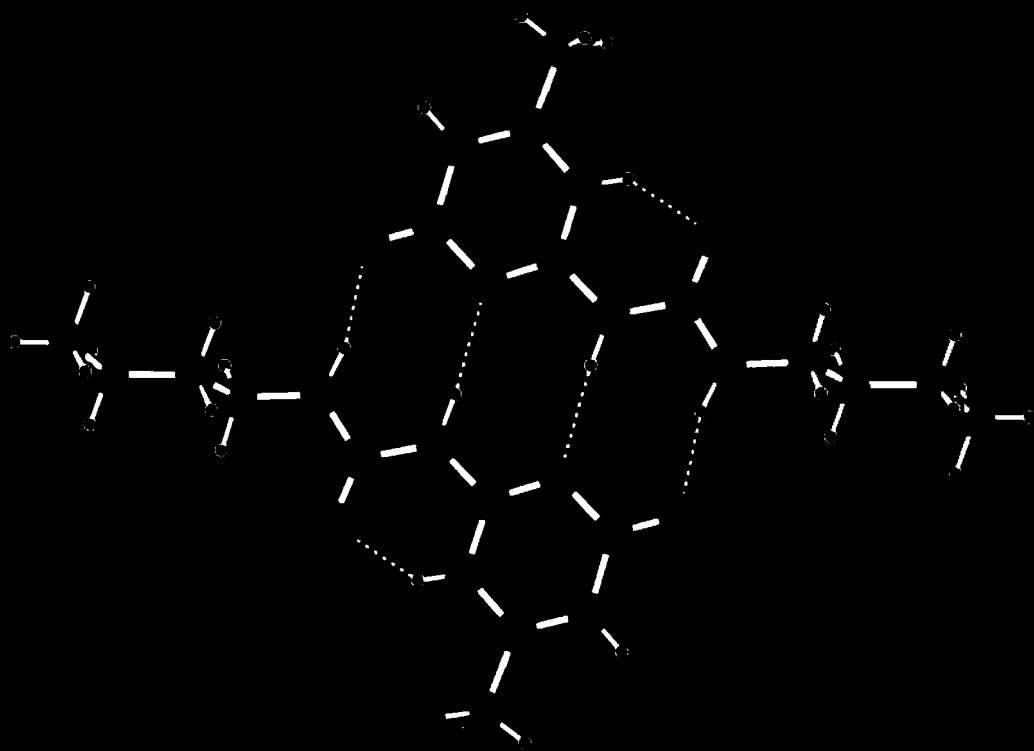
Take down policy

If you believe that this document breaches copyright please contact us at:

openaccess@tue.nl

providing details and we will investigate your claim.

Cooperative Multiple Hydrogen Bonding in Supramolecular Chemistry



Felix H. Beijer

Cooperative Multiple Hydrogen Bonding in Supramolecular Chemistry

Cooperative Multiple Hydrogen Bonding in Supramolecular Chemistry

PROEFSCHRIFT

ter verkrijging van de graad van doctor aan de
Technische Universiteit Eindhoven, op gezag van
de Rector Magnificus, prof.dr. M. Rem, voor een
commissie aangewezen door het College voor
Promoties in het openbaar te verdedigen op
maandag 18 mei 1998 om 16.00 uur.

door

Felix Hugo Beijer

geboren te Tiel

Dit proefschrift is goedgekeurd door de promotoren:

prof.dr. E.W. Meijer

en

prof.dr.ir. D.N. Reinhoudt

copromotor: dr. R.P. Sijbesma

The research described in this thesis was financially supported in part by DSM Research, Geleen, The Netherlands.

Kaftontwerp: Erik R. Beijer

Druk: Universiteitsdrukkerij TUE

CIP-DATA LIBRARY TECHNISCHE UNIVERSITEIT EINDHOVEN

Beijer, Felix H.

Cooperative Multiple Hydrogen Bonding in Supramolecular Chemistry / by Felix H. Beijer. - Eindhoven : Technische Universiteit Eindhoven, 1998

Proefschrift

ISBN 90-386-0698-2

NUGI 813

Trefwoorden: supramoleculaire chemie / waterstofbruggen / complexatie / dimerisatie / kristalontwerp.

Subject headings: supramolecular chemistry / hydrogen bonds / complexation / dimerization / crystal engineering.

Aan mijn ouders.

Voorwoord

Ondanks het toenemende aantal promoties is het voltooien van een proefschrift ook tegenwoordig geen sinecure. Bovendien is er een sterk contrast tussen enerzijds de tijd en moeite die je je als AIO getroost om tot een inhoudelijk mooi en goed leesbaar proefschrift te komen, en anderzijds de tijd die je publiek erin leest. Na gezorgd te hebben voor mooie resultaten vergde het opschrijven ervan tot een goed leesbaar en begrijpelijk verhaal met een duidelijke lijn veel moeite. Hierbij werd zowel mijn geduld als dat van mijn begeleider danig op de proef gesteld, maar na stug doorzetten is het dan zover: het boekje is nu eindelijk af.

Voor het schrijven van het dankwoord daarentegen, ongetwijfeld het meest gelezen deel van een proefschrift en door de meesten die daarin vernoemd worden vaak ook wel het meest gewaardeerde, heb je ironisch genoeg veel minder tijd nodig, hoewel dit schrijven soms ook behoorlijk lastig kan zijn. Gedurende mijn promotietijd zijn er vele mensen geweest die, elk op hun eigen wijze, een bijdrage hebben geleverd cq. invloed hebben gehad die geleid heeft tot het resultaat zoals dat nu voor je ligt. Van deze gelegenheid maak ik dan ook graag gebruik om desbetreffende personen voor hun bijdrage te bedanken.

Als eerste wil ik mijn (eerste) promotor, Bert Meijer, bedanken voor de geboden gelegenheid om een promotieonderzoek in zijn lab uit te voeren, voor het zeer motiverende en enerverende onderwerp waaraan ik heb mogen werken, voor de vrijheid die hij mij in het uitvoeren van het onderzoek heeft gegeven, en voor zijn aanhoudende stimulering cq. prikkeling om te komen tot 'de gemiddelde AIO ontstijgende' resultaten. Bert, meer nog wil ik je bedanken voor het inzicht dat je me hebt gegeven dat het verkrijgen van mooie resultaten één ding is, maar dat de vaardigheden om deze te kunnen 'verkoop' soms/vaak zo mogelijk nog belangrijker gevonden worden en dus kunnen zijn. Hoewel de lijn en targets van het onderzoek, de strategie om te komen tot de resultaten, en een (mogelijke) strategie tot presentatie, mij altijd duidelijk zijn geweest, heeft jouw visie op de grote lijnen, en op de optimale 'verkoop' strategie, me veel inzicht gegeven in de mogelijke succesfactoren in de moderne wetenschappelijke wereld. Daarom heeft dit me op diverse punten veel geholpen, oa bij het schrijven van het proefschrift. Bij deze wil ik eveneens mijn tweede promotor, David Reinhoudt, bedanken om mijn tweede promotor te willen zijn.

Als begeleider en tevens copromotor was jij, Rint Sijbesma, altijd nauw bij mijn onderzoek betrokken, vooral toen na het vinden van de sterke en unidirectionele dimerisatie via viervoudige waterstofbruggen één van je doelstellingen gerealiseerd leek te kunnen worden. Deze nauwe betrokkenheid heeft als positief effect het behalen van de mooie resultaten danig bespoedigd. Het bleek helaas echter nogal lastig om dit inhoudelijke succes, en het dientengevolge kunnen realiseren van Lehn's mooie concepten, om te zetten in persoonlijk succes (een Science artikel), maar jij hebt me laten zien dat een aanhouder

uiteindelijk kan winnen. Verder wil ik je volhardendheid in het verbeteren van mijn manuscripten, en de snelheid van doorkijken daarbij, niet onvermeld laten.

Jef Vekemans, jou wil ik bedanken voor je steun in raad en daad door, mijns insziens, je diepgaand inzicht in persoonlijke gezichtspunten, waarden en normen. Je had altijd wel een minuutje (of meer) tijd. Beste Jef, van je vermogen om alles in een bredere context te plaatsen, en dat zelfs vanuit verschillende perspectieven, heb ik veel waardevolle dingen geleerd. Behalve op menselijk gebied heb je zeker ook op wetenschappelijk gebied een belangrijke bijdrage geleverd, voor mij met name bij het schrijven van het proefschrift.

Tijdens mijn promotie hebben diverse studenten een waardevolle inbreng geleverd aan mijn onderzoek. Toch is deze inbreng, om verschillende redenen, niet altijd even expliciet in de inhoud van mijn proefschrift terug te vinden. Justin Hommes, als mijn eerste research-stage student heb je je bezig gehouden met iets wat uiteindelijk helaas een dood spoor bleek. Toch heb ik jouw voorliefde voor, en succes in ruige chemie zeer gewaardeerd. Jacco de Kraker, ook jouw onderzoek bleek later helaas een doodlopend spoor, hoewel je jouw specifieke research-stage opdracht met succes hebt volbracht. Jij hebt inzicht gegeven in de moeilijke ketoester chemie. Hoang Hirschberg, omdat jij gelukkig op een tijdstip kwam dat mijn onderzoek meer vorm had gekregen, zijn jouw waardevolle syntheseresultaten terug te vinden in hoofdstuk 3. Luc Brunsveld, jij kwam werkelijk op het meest ideaal denkbare tijdstip in mijn onderzoek terecht, maar het is toch zéker ook zo dat jij zelfstandig een zeer waardevolle bijdrage hebt geleverd. Het inhoudelijke succes met de supramoleculaire polymeren is voor een substantieel deel mede te danken aan jouw buitengewone inzet, en de daaruit volgende resultaten. Ky Hirschberg, als afstudeerstudent heb jij laten zien dat jouw aanvankelijke opdracht intrinsiek gedoemd was niet mooi te gelukken, waarna je je echter meester gemaakt hebt van een eigen stuk expertise: de 'siliconen'chemie. Ky, door je gave om gemakkelijk contacten te leggen heb je hierbij de kennis en ervaring van Huub van Aert in de (siliconen)polymeerchemie gemobiliseerd. Dat heeft geleid tot resultaten die een substantiële en nieuwe bijdrage geleverd hebben aan het succes van de supramoleculaire polymeren, nl. het rheologisch gedrag in bulk. Tenslotte wil ik ook Michel Pepers bedanken voor het inzicht dat hij heeft gegeven in de heterodimeeruitwisseling. Michel, ten gevolge van je voetbalongelukje kon je niet veel anders dan het 2D-NMR werk voor de heterodimeeruitwisseling doen. Daaraan heb je met zeer veel inbreng en enthousiasme gewerkt, en je hebt de moeilijke wiskunde van de kinetiek begrepen en kunnen toepassen.

Veel dank ben ik verschuldigd aan Huub Kooijman en Anton Spek (Universiteit Utrecht, vakgroep Kristal- en Structuurchemie) voor hun zeer grote inzet en enthousiasme bij het meten van kristalstructuren. Huub, de kristalstructuren zijn van enorme waarde geweest voor (het verloop van) het onderzoek, mede dankzij jouw hulp in de interpretatie hiervan. Ook wil ik prof.dr. J. Van der Maas en Bert Lutz (Universiteit Utrecht, vakgroep Analytische Molekuulspectrometrie) hartelijk bedanken voor de geboden

gelegenheid om bij hen Infrarood te meten op geavanceerde apparatuur, en het assisteren daarbij. Hendrik-Jan Luinge wil ik bedanken voor zijn specialistische inbreng in de kwantitatieve evaluatie van de meetgegevens. Bert en Hendrik-Jan, jullie inzet heeft geleid tot een betrouwbare bepaling van de dimerisatieconstanten van verbindingen 10 en 11 in hoofdstuk 3, wat van zeer grote waarde is geweest. Hartmut Fischer, jou wil ik hartelijk bedanken voor je waardevolle hulp die je mij als totale leek in het gebied van de vloeibare kristallen hebt gegeven, alsmede voor het meten van X-ray verstrooiing van diverse verbindingen in hoofdstuk 5, en jouw interpretatie en uitleg hiervan. Tenslotte wil ik ook Jos van Wolput hartelijk bedanken voor het meten van IR spectra bij hoge temperaturen.

De vaste staf wil ik bedanken voor het kritisch volgen van mijn onderzoek (o.a. tijdens de lunches en als commentaar op het kwartaalverslag). Joost van Dongen wil ik bedanken voor het meten van ESI-MS spectra, hoewel ik zijn actie samen met Brigitte om het spectrum in figuur 6.4 op mijn zuurkast te plakken, en dan vooral de bijgeschreven tekst, lange tijd niet zo heb kunnen waarderen. Henk Eding wil ik bedanken voor het uitvoeren van de elementanalyses (Henk, en dan vooral voor het geduld dat jij met mij moest hebben toen je nog op het oude apparaat mat) alsmede voor het verzorgen van voor een prettige werksfeer zorgende activiteiten zoals borrels. Hans Damen dank ik voor de snelle zorg voor chemicaliën en glaswerk. Marcel van Genderen dank ik voor zijn inbreng van NMR expertise, en ook voor zijn correcties en suggesties op diverse proefschrift hoofdstukken.

Alle (oud)-collega's en studenten wil ik bedanken voor de gezelligheid en open sfeer op het lab. Een speciaal woord van dank richt ik tot Huub van Aert voor zijn spontaan geboden hulp in de polymeerchemie bij de begeleiding van Ky. Koen Pieterse en Michiel Bouman dank ik voor hun hulp met het vaak onbegrijpelijke ding dat (im)personal computer heet; Anja Palmans bedank ik voor suggesties en gegeven kennis over vloeibare kristallen voor hoofdstuk 5 van het proefschrift; Henk Janssen en Toine Biemans bedank ik eveneens voor suggesties bij andere hoofdstukken; Brigitte Folmer bedank ik voor VPO-metingen. Een speciaal woord van dank wil ik in deze rij tot Ronald Lange richten. Beste Ronald, hoewel ik mijn onderzoek altijd zoveel mogelijk een eigen identiteit heb willen meegeven, en we mede daarom in verschillende richtingen hebben gewerkt, is het begin van mijn onderzoek voor een belangrijk deel aan jouw werk te danken geweest. Hiervoor wil ik je hartelijk danken, mede omdat het me tijdens mijn promotietijd namelijk aan de hand van ervaringen van sommige collega's steeds duidelijker geworden is hoe afhankelijk je als AIO bent van het geluk om een onderwerp te (mogen) bewerken dat ook potentie tot succes heeft.

Tenslotte wil ik mijn ouders en broers bedanken voor hun stimulerende steun tijdens mijn promotie-periode, en hun interesse in mijn onderzoek.

Felix

Contents

Chapter 1: Introduction	1
1.1 Supramolecular Chemistry	1
1.2 Fundamentals of Hydrogen Bonding	2
1.3 Arrays of Multiple Hydrogen Bonds, and the Jorgensen Model	3
1.4 Hydrogen Bonding in Supramolecular Chemistry	5
1.5 Aim and scope of this Research	12
1.6 Outline of this Thesis	13
 Chapter 2: Triply Hydrogen Bonded Complexes of Diaminopyridines and Diaminotriazines with Uracils: Opposite Effect of Acylation on Complex Stabilities	 17
2.1 Introduction	18
2.2 Results	18
2.2.1 Synthesis	18
2.2.2 Association studies in solution	21
2.2.3 Complexation in the solid state; X-ray single crystal structures	24
2.3 Discussion	28
2.3.1 Dimerization of uracil derivatives	28
2.3.2 Comparison of diaminotriazines and (acylated) diaminopyridines Dimerization and complexation with <i>N</i> -propylthymine and uracil derivatives	29
2.3.3 Persistence of the triazine-uracil triple hydrogen bonding motif in the solid state	30
2.3.4 Opposite effect of acylation on the stability of complexes of diaminopyridine and diaminotriazine. Dimerization and complexation with <i>N</i> -propylthymine	31
2.4 Conclusion	34
2.5 Experimental Section	34
 Chapter 3: The DADA Motif in Quadruply Hydrogen Bonded Dimers of Triazines and Pyrimidines	 45
3.1 Introduction	46
3.2 Quadruple Hydrogen Bonding in Acylated Diaminotriazine Derivatives	49
3.2.1 Synthesis	49
3.2.2 Hydrogen bonding pattern in the solid state	51

3.2.3	Association studies in chloroform solution	53
3.3	Quadruple Hydrogen Bonding in Acylated Diaminopyrimidine Derivatives	59
3.3.1	Introduction	59
3.3.2	Synthesis	59
3.3.3	Hydrogen bonding pattern in the solid state	60
3.3.4	Association in chloroform solution; Dimerization constants	62
3.4	Evaluation of Relative Strength of Dimerization	66
3.5	Conclusion	68
3.6	Experimental Section	68

Chapter 4: The DDAA Quadruple Hydrogen Bonding Motif in 2-Ureido-4-pyrimidinones **79**

4.1	Introduction	80
4.2	Results and Discussion	81
4.2.1	The DDAA motif in dimers of 2-butylureido-6-methyl-4[1H]-pyrimidinone	81
4.2.2	Tautomeric equilibrium between dimeric 2-ureido-4[1H]-pyrimidinone and 2-ureido-pyrimidin-4-ol tautomers	84
4.2.3	Dilution studies to obtain dimerization constants	92
4.2.4	Exchange of dimers: heterodimers	98
4.3	Evaluation	100
4.3.1	Monomer-Dimer, and tautomeric equilibria in solution	100
4.3.2	Relative strength of dimerization	103
4.4	Conclusion	104
4.5	Experimental Section	104

Chapter 5: Discotic Liquid Crystals from Quadruply Hydrogen Bonded Dimers **115**

5.1	Introduction	116
5.2	Results	120
5.2.1	Synthesis	120
5.2.2	Studies of liquid crystalline properties	121
5.3	Discussion and Conclusion	127
5.3.1	Discotic entity	127
5.3.2	Mesophase temperature stability	128
5.4	Conclusion	129
5.5	Experimental Section	129

**Chapter 6: Reversible Linear Supramolecular Polymers,
by Self-Complementary Quadruple Hydrogen
Bonding of Bifunctional Compounds** **133**

6.1	Introduction	134
6.2	Results and Discussion	137
	6.2.1 Synthesis and characterization of supramolecular polymer	137
	6.2.2 Polymer properties in solution	140
	6.2.3 Polymer properties in bulk	143
6.3	Conclusion	145
6.4	Experimental Section	146

Chapter 7: Crystal Engineering of Melamine–Uracil Complexes **151**

7.1	Introduction	152
7.2	Results	153
	7.2.1 Cocrystallization	153
	7.2.2 Crystal structures	154
7.3	Discussion of Complex Stoichiometries	162
7.4	Conclusion	164
7.5	Experimental Section	164

Samenvatting	167
--------------	-----

Summary	170
---------	-----

Curriculum Vitae	173
------------------	-----

List of Publications	175
----------------------	-----

Chapter 1

Introduction

1.1 Supramolecular Chemistry

Inspired by Nature and motivated by the desire to understand and design complex multi-molecular structures, supramolecular chemistry has become one of the most fascinating and largest fields in modern organic chemistry.¹ Supramolecular chemistry is generally described as the chemistry beyond the covalent bond, and deals with the organization of molecules into larger structures via spontaneous assembly that is governed by non-covalent interactions between—or within—molecules.² Compared to the relatively inert covalent or ionic bonds (with typical enthalpies of 100–400 kJ.mol⁻¹ and ~250 kJ.mol⁻¹, respectively), non-covalent interactions are relatively weak, and often reversible. Non-covalent interactions comprise of hydrogen bonds (with typical bond enthalpies of 10–65 kJ.mol⁻¹ for normal hydrogen bonds), dipole–dipole and VanderWaals interactions (with typical bond enthalpies of 2–10 kJ.mol⁻¹), and hydrophobic interactions. Despite the weakness of non-covalent interactions, thermodynamically stable complexes can be obtained by the cooperative action of many weak interactions.

In natural systems, a delicate balance between covalent and the different kinds of non-covalent interactions results in the formation of large and complex, yet very well-defined structures. Spontaneous organization, governed by non-covalent interactions, and its reversibility, allows for controlled building of complex structures, with the possibility of spontaneous repair of mismatches. As a consequence, in almost all life processes, such as signalling, recognition, transport, replication, and construction, the association or complexation of two or more molecules is involved, ranging from the molecular to the cellular scale.

An example of the effect of assembly on the molecular scale in biological systems is the folding of polypeptides into their tertiary structure, governed by a delicate balance between the different non-covalent interactions in their aqueous environment. The specific activity of enzymes, e.g. which catalyze nearly all metabolic processes, arises from this tertiary structure, as well as the complexation of the substrate to the active site. The high tensile strength of cellulose, the major construction material in plants, as well as that of chitin, contained in the exoskeleton of insects and crustacea as construction material, arises for a large part from stabilization of the long and straight polymer chains of cellulose and

chitin by intramolecular hydrogen bonds, and hydrogen bonds between the chains.³ Collagen, the main fibrous element of skin, bone, tendon, cartilage, blood vessels and teeth of mammals, consists of three polypeptide chains in a helical conformation, wound around each other and kept together by non-covalent interactions to form a stiff cable with remarkable strength.

Within the area of applying the principles of supramolecular chemistry to polymer chemistry—with the intention to obtain novel, self-assembled, functional materials—the specific aim of this thesis is to investigate the possibilities of the application of multiple hydrogen bonding in polymer chemistry. By virtue of its unique combination of strength, directionality and specificity, multiple hydrogen bonding is the favorite intermolecular force in self-associating systems. Multiple hydrogen bonding is therefore one of the most attractive candidates for application as the organizing interaction to obtain well-defined structures in supramolecular polymer chemistry.

1.2 Fundamentals of Hydrogen Bonding

Hydrogen bonds are attractive interactions between a positively charged hydrogen atom bonded to an electronegative element (the donor: $D^{\delta-}-H^{\delta+}$), and a negatively charged atom with a lone pair of electrons (the acceptor: $A^{\delta-}$).⁴ Hydrogen bonding is most often associated with the functional groups summarized in table 1.1.⁵

Table 1.1: Functional groups that can form hydrogen bonds, arranged by element.

element	Donors	Donor strength	Acceptors	Acceptor strength
fluorine	F-H	very strong	F ⁻ , F-H	very strong strong
oxygen	O-H (in an acid)	strong	⁻ O-P, ⁻ O-S ⁻ , ⁻ O-C,	strong strong
oxygen	O-H (in water, or alcohols)	medium	O=P, O=S, O=C, H ₂ O, H-O-C, C-O-C	medium-strong medium
nitrogen	N ⁺ -H	strong	C=N-C	medium
nitrogen	N-H	medium	N(R) ₃ ,	medium
sulfur	S-H	weak	S=C	medium-weak
carbon	C-H	weak	π -electrons	weak

In a certain medium, the strength of a single hydrogen bond depends mainly on the Donor (D) strength and the Acceptor (A) strength of the functional groups involved. Several

scales for hydrogen bonding acidity and basicity have been developed, and a qualitative idea of the donor and acceptor strength of the possible functional groups is given in table 1.1.⁶ These hydrogen bonding donor and acceptor strengths do generally not correlate with the proton acidity and atom basicity (pK_a and pK_b) of the groups involved, but a proportional relation has been established within hydrogen bonding functionalities of one type of functional groups.

The strongest hydrogen bonds are formed between a strong donor, i.e. a hydrogen atom bonded to a very electronegative element (like F–H, and O–H in acids), and a strong acceptor, i.e. a strongly electronegative element (F). Positively charged donors (N^+H), or negatively charged acceptors (F^- , O^-P , O^-S , O^-C), also give rise to strong hydrogen bonds. However, by far the most hydrogen bonds occurring in natural systems, such as $N-H\cdots N$, $N-H\cdots O=C$, and $O-H\cdots O$, have neutral atoms and are of medium strength. The existence and importance of weak hydrogen bonding, with C–H and S–H donors, has become generally accepted only recently. This kind of hydrogen bonding has been suggested to be in fact very important, particularly in crystal engineering.⁷

The strength of hydrogen bonds is divided into three categories. Weak hydrogen bonds have energies less than $5\text{ kJ}\cdot\text{mol}^{-1}$, hydrogen bonds of medium strength have energies between 5 and $40\text{ kJ}\cdot\text{mol}^{-1}$, and strong hydrogen bonds have energies between 40 and $100\text{ kJ}\cdot\text{mol}^{-1}$. Very strong hydrogen bonds with energies exceeding $100\text{ kJ}\cdot\text{mol}^{-1}$ are exceptional, and only occur with the element fluorine. Whereas hydrogen bonds of weak and medium type can be considered as electrostatic interactions between a positive and a negative charge (or dipole), strong hydrogen bonds are more of a covalent bond type. As a result of their nature, hydrogen bonds are one of the most reliable and predictable non-covalent interactions: (i) they are among the strongest of non-covalent interactions, (ii) they are specific and directional because donor (D) and acceptor (A) functionalities are involved.

1.3 Arrays of Multiple Hydrogen Bonds, and the Jorgensen model

Arrays of multiple parallel or near parallel hydrogen bonds are frequently encountered in molecular recognition, both in natural as well as in man-made systems. The cooperative action of the hydrogen bonds in such arrays increases strength, and especially specificity and directionality of the interaction. The binding strength of multiple hydrogen bonded complexes is of course dependent on the strength of the individual hydrogen bonds in the array, and the number of hydrogen bonds. However, the particular arrangement of donor (D) and acceptor (A) groups in the array was found also to be very important. Although the large difference in bonding strength between the triply hydrogen bonded DNA base pairs

Adenine•Thymine/Uracil (a DAD•ADA couple) and Guanine•Cytosine (a DAA•ADD couple) has been observed long ago (for models, see figure 1.1a–b),⁸ Jorgensen was the first to realize that this anomaly could be explained by the order of hydrogen bonding functional groups (*vide infra*).⁹ Zimmerman has taken a lot of synthetic effort to prepare the DDD•AAA couple (figure 1.1c),¹⁰ of which the bonding strength ($K_a > 10^5 \text{ M}^{-1}$) was fully in line with the trend observed for the DAD•ADA and the DAA•ADD couple.

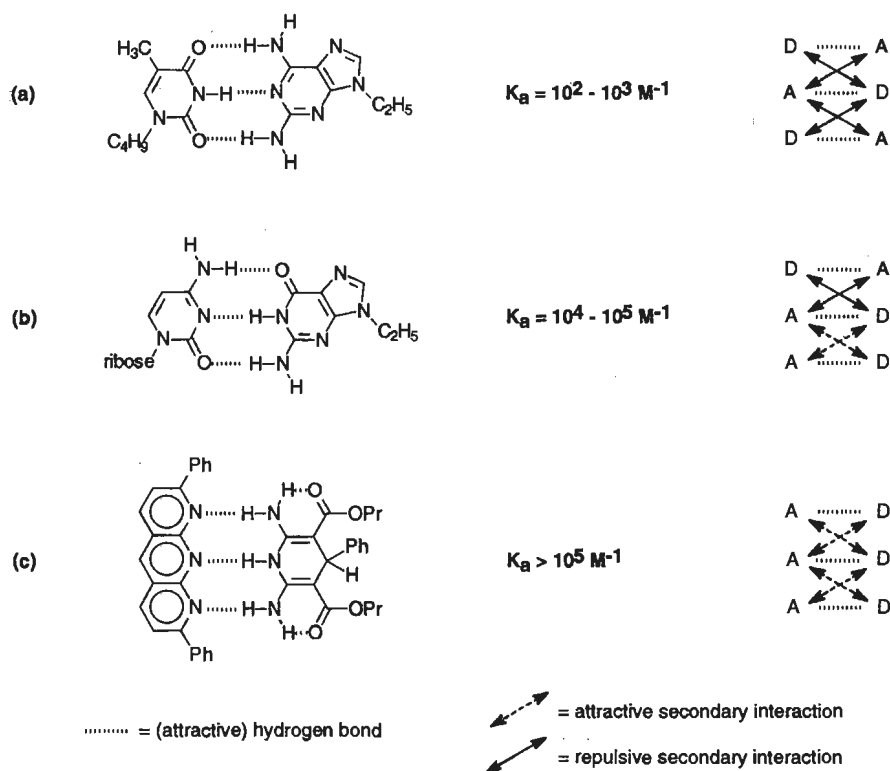


Figure 1.1: Bonding strength of, and secondary interactions in, triply hydrogen bonded complexes.^{8–10}

Because of the functional groups involved, the hydrogen bonds in multiple hydrogen bonding arrays are of intermediate strength, and can as a consequence be considered as electrostatic interactions between charges. In an array of hydrogen bonding functionalities, the distances between a functionality and the neighbour of the opposing functionality are still relatively short. With the typical bond lengths of the primary hydrogen bonds of approximately 1.9–2.0 Å between donor and acceptor in the triply hydrogen bonded DNA base pairs, these distances are between 2.3 and 3.7 Å. Hence, these cross-interactions invoke a substantial secondary electrostatic interaction (depicted in figure 1.1 by double headed arrows). Obviously, similar charges cause a repulsive electrostatic interaction, and opposite charges cause an attractive interaction.

In several excellent papers,⁸ Jorgensen modelled this effect by quantum mechanical calculations, resulting in a calculated ΔG -value of $-31.4 \text{ kJ.mol}^{-1}$ for every primary interaction (the attractive hydrogen bond), and $+10.5 \text{ kJ.mol}^{-1}$ and $-10.5 \text{ kJ.mol}^{-1}$ for every repulsive or attractive secondary interaction, respectively. Although his theory give trends in the right direction, the calculated energy of the effects upon association are probably too large (vide infra). Also using quantummechanical calculations, Burrows has discerned between secondary interactions resulting from an atom in the array that is also involved in (primary) hydrogen bonding (effect $\pm 7 \text{ kJ.mol}^{-1}$), and additional secondary interactions, resulting from a spectator atom that is not involved in primary hydrogen bonding ($\pm 11 \text{ kJ.mol}^{-1}$). Recently, Schneider has proposed an empirical free energy relationship for the stability of multiple hydrogen bonded complexes in chloroform.¹¹ Derived from a large number of experimental association data of heterocyclic compounds with spatially fixed arrays, he showed that the complex stability in chloroform may be estimated reasonably well by a simple sum of increments: ΔG is a sum of -7.9 kJ.mol^{-1} for each hydrogen bond, and $+ \text{ or } - 2.9 \text{ kJ.mol}^{-1}$ for each attractive or repulsive secondary electrostatic interaction, respectively.

1.4 Hydrogen Bonding in Supramolecular Chemistry

Artificial receptors. Many biologically active molecules contain multiple hydrogen bonding sites. Consequently, it has been a challenge for supramolecular chemists to develop and synthesize artificial receptor molecules that form complexes with these substrates with high binding strength and selectivity. For example, barbiturates, a class of compounds widely used for their physiological action on animals as sedatives and anticonvulsants, have a well-defined functional-group structure consisting of 2 donor and 6 acceptor functionalities capable of hydrogen bonding (figure 1.2).

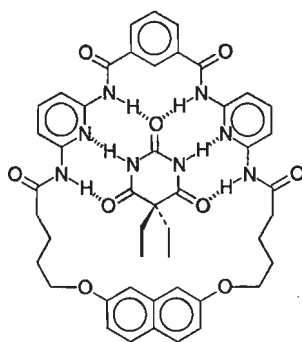


Figure 1.2: Complex of diethyl-barbiturate and an artificial receptor designed by Hamilton. The barbiturate molecule in the centre is complexed by the receptor by six hydrogen bonds.¹²

Hamilton¹² has designed a complementary unit that complexes the barbiturate strongly by six hydrogen bonds (figure 1.2). The synthesis of the receptor molecule involved a high-dilution coupling of a di(acid chloride) with a diamine, which gave a yield of the desired product of only 12–14 %. The structure of the complex was confirmed by NMR in solution and X-ray diffraction studies of crystals.

Such receptors have been covalently attached onto solid supports, such as silica and polymers. The first example was reported by Feibush et al,¹³ who functionalized silica with a chiral di(acylamino)pyridine unit (figure 1.3); a long and tedious 9-step synthesis was required. With these silica materials as stationary phase, mixtures of barbiturates and uracil derivatives could be separated chromatographically. The separation is based on difference in association constants of the complexes with the di(acylamino)pyridine unit on the silica. Because the receptor carried one enantiomer in the acylamino group, separation into enantiomers was also feasible. The same concept has been applied by Tanabe¹⁴ and Zimmerman,¹⁵ with other functional groups and/or solid supports.

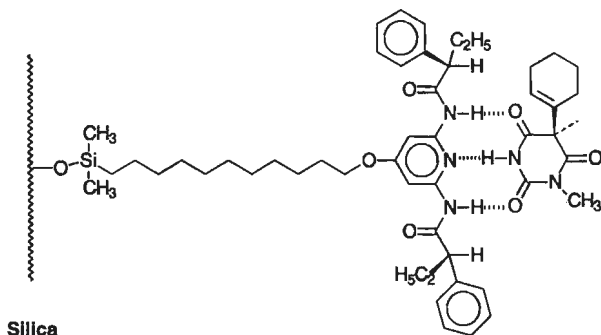


Figure 1.3: Complex of a receptor on silica with a barbiturate molecule via three directional hydrogen bonds reported by Feibush.¹³

Programmed self-assembly. Several structures have been designed and synthesized that assemble spontaneously into a well-defined structure, similar to the spontaneous folding of proteins into a well-defined architecture by a delicate balance of the different non-covalent interactions. Mendoza and Rebek¹⁶ have designed a large class of self-complementary molecules, capable of the formation of a molecular container by folding like the two halves of a tennis-ball (a simple example is given in figure 1.4). The formation of the container is driven by hydrogen bond formation. It is also shown that it is possible to include neutral guest molecules of the appropriate size within the containers (or capsules), and this inclusion is in many cases very size-specific.

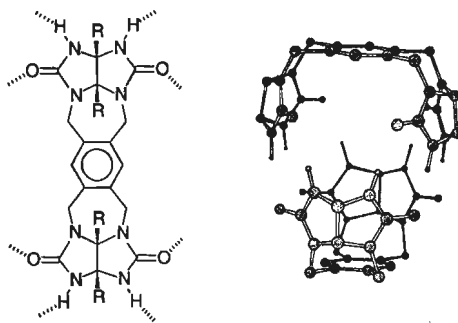


Figure 1.4: Self-complementary molecule that self-assembles into a molecular container reported by Rebek.¹⁶

Supramolecular structures based on the six-membered, hydrogen bonded cyclic motif of three substituted melamine/2,4,6-triaminopyrimidine and three substituted barbituric acid/cyanuric acid molecules have been reported by the groups of Lehn,¹⁷ Whitesides,¹⁸ and Reinhoudt.¹⁹ The latter demonstrated the self-assembly of a complex molecular box with 36 hydrogen bonds, consisting of two stacked cyclic rosettes (figure 1.5). The cyclic rosettes are formed by 3 melamine moieties (attached onto bifunctional calixarene molecules) and 3 diethylbarbiturate molecules. The two stacked rosettes are linked by calixarene molecules.

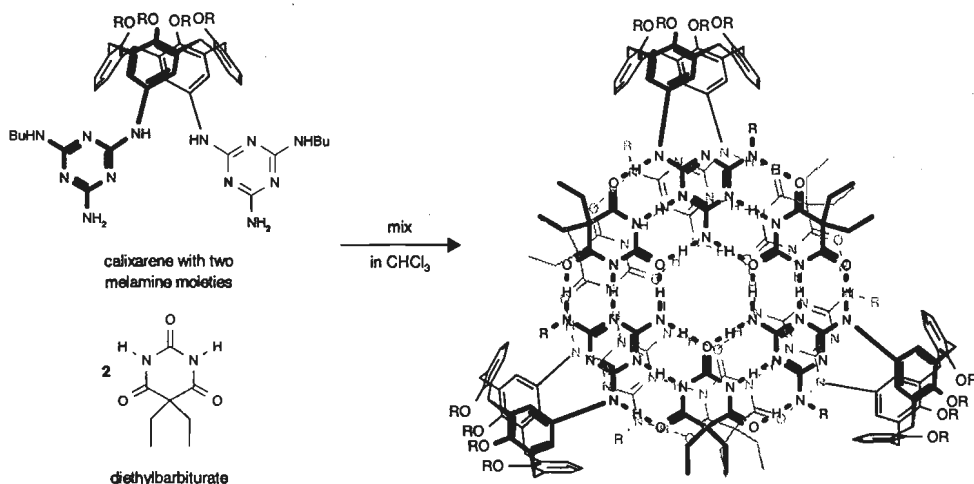


Figure 1.5: Self-assembled stacked rosette structure of Reinhoudt in solution.¹⁹

Crystal engineering. Crystallographers have tried for long to correlate molecular structure and solid-state structure. In general, their attempts were not very successful, since a large variety of crystal packing factors determines the crystal structure. However, their attempts were relatively successful in cases where hydrogen bonding interactions are used.²⁰

Recently, Desiraju introduced the term crystal engineering, the design of solid structures using supramolecular entities.²¹ Crystal engineering has become one of the central topics in supramolecular design. As a good example of crystal engineering, Whitesides has shown that subtle structural modifications may lead to different solid state structures in cocrystals of barbiturate and melamine molecules (see figure 1.6).²²

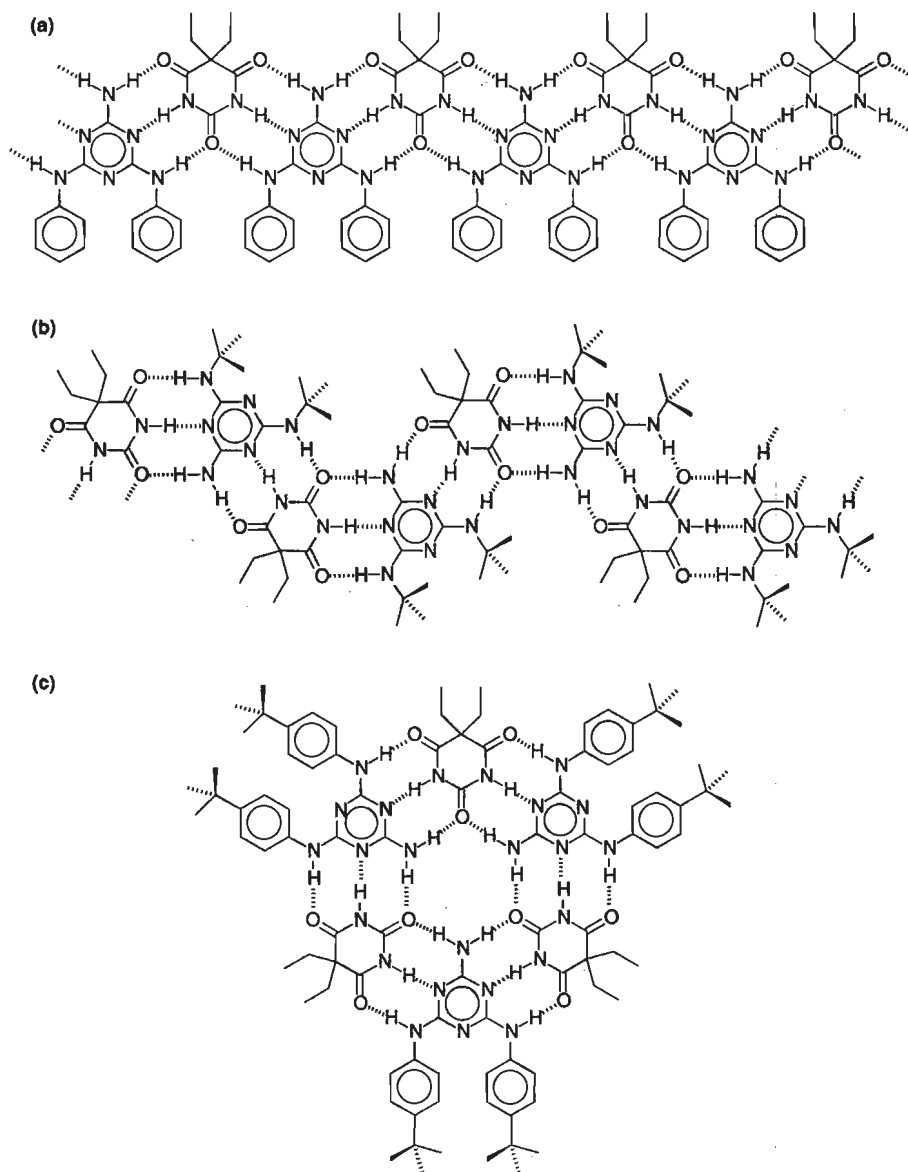


Figure 1.6: Crystal structures of melamine and cyanuric acid derivatives reported by Whitesides,²² (a) linear extended tape, (b) crinkled tape, (c) rosette (= cyclic hexamer).

A similar example includes the formation of infinite tapes of type (a) from self-complementary units, and from complementary units in a 1:1 ratio, as reported by Lehn.²³ Müllen also showed that solid state structure in cocrystals of 5-alkoxyisophthalic acid derivatives with various nitrogen heterocycles was governed by delicate structural variations,²⁴ while Mascal demonstrated the 'programmed' formation of a macrocycle from self-complementary molecules, by using the directionality and specificity of multiple hydrogen bonding arrays.²⁵

Self-assembly of bilayers, membranes, or fibers. In natural systems, the spontaneous assembly of membranes and fibers from small molecules is governed by non-covalent interactions. This has also been mimicked successfully in artificial systems.²⁶ Kunitake²⁷ and Ringsdorf²⁸ have reported the spontaneous formation of monolayers on the air-water interface, or even bilayers by hydrogen bonding (figure 1.7). Furthermore, the spontaneous formation of tube-like nanostructures in water by association of complementary hydrogen bonding units has been reported.²⁹

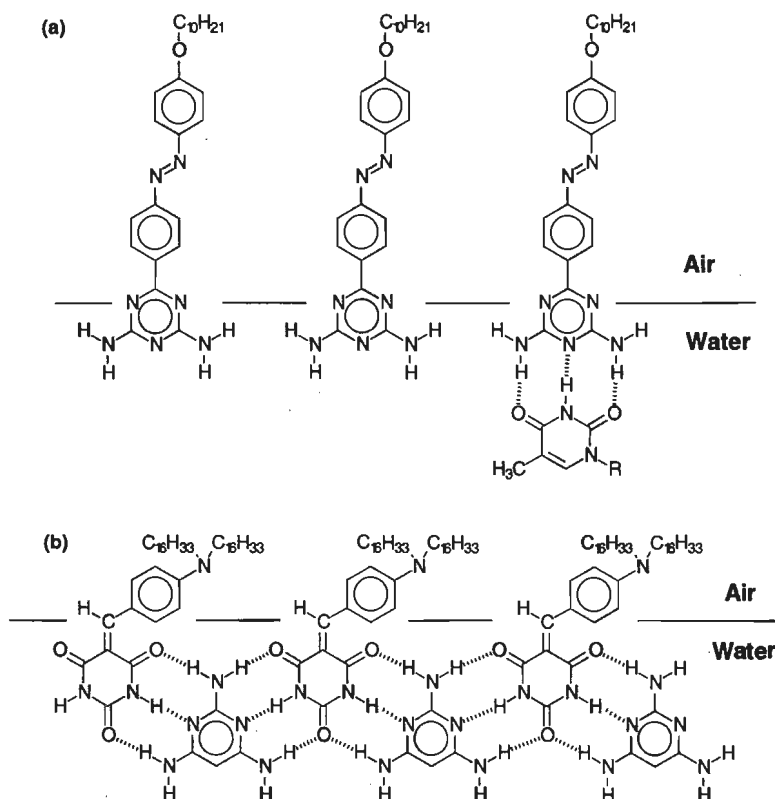


Figure 1.7: (a) monolayer on the air water interface of Kunitake,²⁷
(b) monolayer structure of Ringsdorf.²⁸

Non-covalent assembly of polymers. The concept of obtaining linear polymers by association of monomeric units via non-covalent interactions was already described by Lehn in 1988 as an interesting challenge in supramolecular chemistry.² Lehn realised the formation of supramolecular polymers by using bifunctional molecules with complementary hydrogen bonding functionalities (figure 1.8).³⁰ Mixing of solutions of both molecules resulted in the precipitation of a liquid crystalline material consisting of polymeric chains. As was shown by electron microscopy and X-ray diffraction, these chains are wound around each other in a helical fashion.

Other examples of self-assembled polymers are reported by Griffin,³¹ who uses bifunctional molecules of the pyridine–acid couple, by Fréchet,³² using the combination of pyridine and acid with trifunctional molecules, and by others.³³

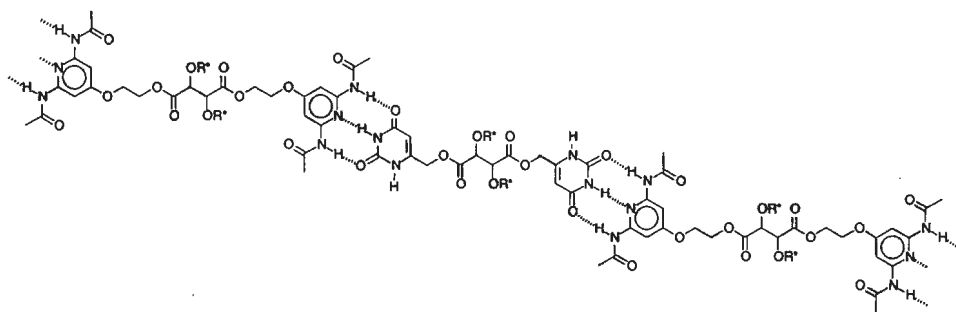


Figure 1.8: Supramolecular linear polymer reported by Lehn.³⁰

Modification of polymer properties. Several research groups have tried to obtain special polymer properties by using non-covalent interactions. Stadler³⁴ grafted functional groups capable of hydrogen bonding onto a polyisobutylene polymer (figure 1.9a). Rheological studies showed that clustering of these functional groups enhanced the mechanical properties. A number of interesting publications³⁵ deals with side-chain functionalized polymers, with the side-groups complexing another molecule by hydrogen bonds—using the pyridine–acid combination—inducing liquid crystalline behavior (figure 1.9b). Lange³⁶ has shown that the alternating styrene–maleimide copolymer can molecularly dissolve melamine in a 3:1 ratio between imide groups and melamine (figure 1.9c). A cross-linked material with new properties is obtained.

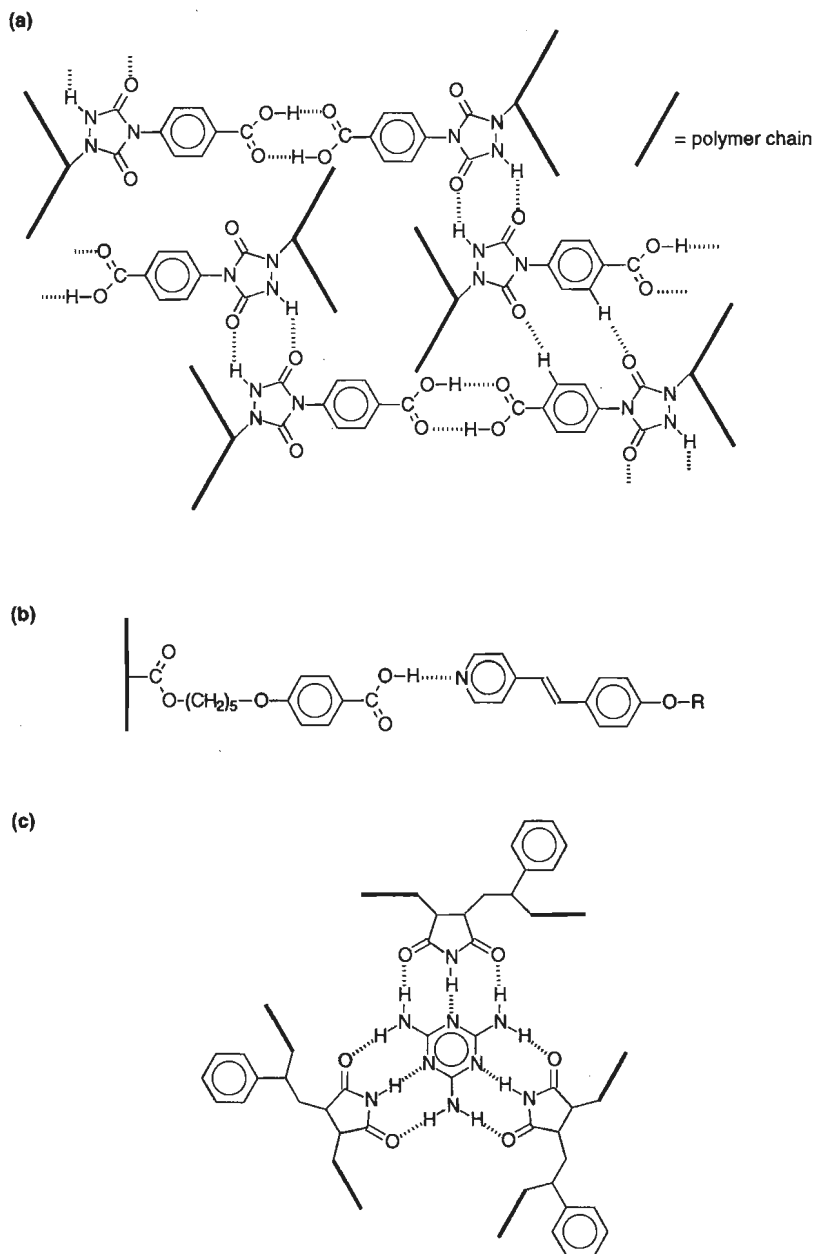


Figure 1.9: Engineering of polymer properties using hydrogen bonding:

(a) cross-linking of polymers by hydrogen bonding,³⁴

(b) side-chain functionalization of polymers by hydrogen bonding,³⁵

(c) molecular dissolution of melamine in the alternating styrene-maleimide copolymer.³⁶

1.5 Aim and Scope of this Research

New supramolecular concepts and structures are currently reported in an ever increasing rate, acknowledging the interest and impact of this field. The molecular structures have evolved from quite simple ones in the beginning to more complex ones now. Inspired by the wealth of biomacromolecules, it is a challenge in the field of materials science to obtain novel functional materials by combining the strengths of organic chemistry (having well-defined structures), supramolecular chemistry (using non-covalent interactions) and polymer chemistry (having large structures).

Ease of synthesis is a prerequisite in materials science, since substantial quantities of material are often needed. For the predictability and reliability of aggregate formation, building blocks that combine a large binding strength with specificity and directionality are desirable. In our studies to obtain such units, we decided to use multiple hydrogen bonding as the non-covalent interactions, because of their nature. Multiple hydrogen bonding has already been used extensively in supramolecular chemistry, but the combination of strong binding and ease of synthesis is rare, if not unknown (illustrated in figure 1.10). Components of complexes that bind strongly ($K_a > 10^5 \text{ M}^{-1}$), such as the DDD•AAA couple,¹⁰ multipoint receptors for barbiturates,¹² urea,³⁷ flavin,³⁸ guanines,³⁹ and melamine⁴⁰, nanotubes formed from cyclic peptides,⁴¹ and also in other examples,⁴² require multistep syntheses, obstructing their use in materials science.

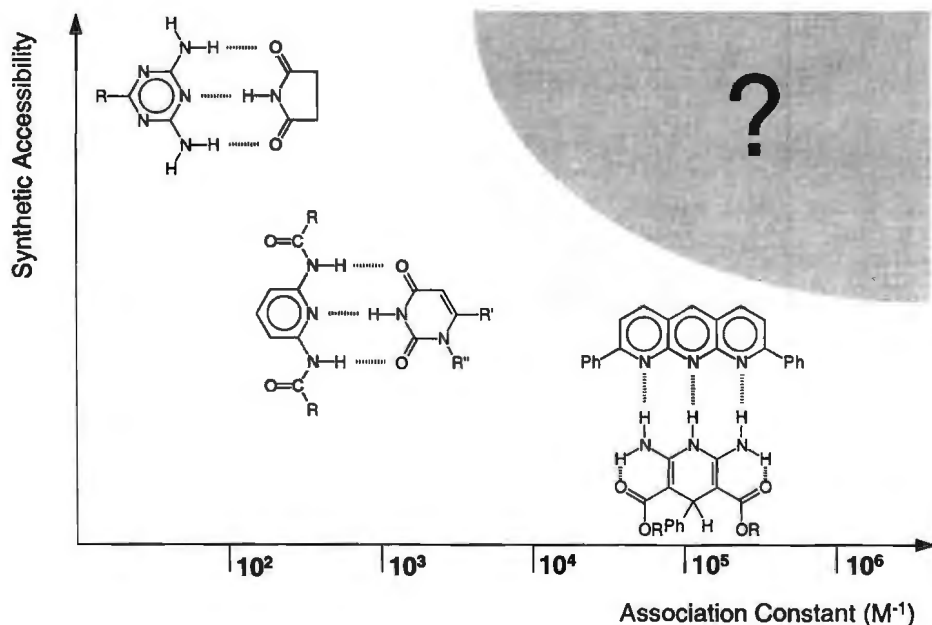


Figure 1.10: The synthetic accessibility of multiple hydrogen bonding units versus binding strength.

In order to obtain synthetically easily accessible units that bind very strongly, insight into the factors that determine the strength of multiple hydrogen bonding is of great value, since this gives the possibility for rational design. Hence, obtaining a good understanding of these factors is one of the aims in this research. It has been only recently that the importance of secondary interactions as described by Jorgensen was recognized.

We started our search for strongly associating and synthetically well accessible units with the known, but only scarcely used,⁴³ combination of diaminotriazine and uracil. It was anticipated that by acylating the amino groups of the diaminotriazine units, more stable complexes would be obtained, in analogy to 2,6-diaminopyridine. In binding experiments, however, we actually found the opposite effect. The unexpectedly low association constants prompted us to look in detail into the conformation of acylaminotriazines. Using insights from that study, and from the work of Jorgensen that brought the importance of secondary interactions to our attention, we designed new, self-complementary, quadruple hydrogen bonding units. These units were required to be simple to synthesize, yet they should form very strong dimers. The present thesis is a report on the preparation and characterization of such heterocyclic recognition units, and their use in supramolecular systems.

1.6 Outline of this Thesis

Chapter 1 gives a general introduction into the field of supramolecular chemistry, focussing on hydrogen bonding. To give insight into the strength of multiple hydrogen bonded complexes, Jorgensen's model for arrays of multiple hydrogen bonds is elaborated. A survey of applications of hydrogen bonding in supramolecular chemistry is then given to show the potential of hydrogen bonding in supramolecular chemistry. Finally, it is described that exciting new prospects arise from combining of the fields of polymer chemistry, organic chemistry, and supramolecular chemistry.

Detailed studies to obtain insight into the effect of acylation of diaminopyridines and diaminotriazines on complexation with uracils, and on dimerization, are described in *chapter 2*. The complexation behavior in solution is studied by a combination of ¹H-NMR and FT-IR, while the hydrogen bonding patterns in the solid state in cocrystals are studied by X-ray diffraction.⁴⁴ In *chapter 3*, the possibilities of obtaining strong dimerization of DADA arrays in acylated derivatives of diaminotriazine and diaminopyrimidine are investigated. Stronger dimerization is achieved by applying Jorgensen's model, as well as by pre-organization of the array by an intramolecular hydrogen bond.⁴⁵ Studies of quadruple hydrogen bonding in 2-ureido-4-pyrimidinones are given in *chapter 4*, disclosing the possibilities of DDAA arrays.⁴⁶

With several interesting new hydrogen bonding units available, our attention focused on applications in supramolecular systems. In *chapter 5*, a new type of discotic liquid

crystalline materials, in which the core is formed by a quadruply hydrogen bonded dimer, is presented.⁴⁷ **Chapter 6** describes an initial move towards supramolecular polymers, in which the polymeric chain is built non-covalently by association of bifunctional monomeric units via strong and directional hydrogen bonding of the ureidopyrimidinone units.⁴⁸ Finally, **chapter 7** describes crystal engineering in melamine–uracil complexes, disclosing the programmable formation of 1:2 herring-bone structures and 1:3 rosette-like structures.⁴⁹

References

- 1) S.P. Newton, J.F. Stoddart, W. Hayes, *Supramol. Sci.*, **1996**, 3, 221.
- 2) (a) J.-M. Lehn, *Angew. Chem. Int. Ed. Engl.*, **1988**, 27, 89, (b) J.-M. Lehn, *Angew. Chem. Int. Ed. Engl.*, **1990**, 29, 1304, (c) C. Fouquey, J.-M. Lehn, A.-M. Levelut, *Adv. Mater.*, **1990**, 2, 254, (d) J.-M. Lehn, *Makromol. Chem. Makromol. Symp.*, **1993**, 69, 1.
- 3) L. Stryer, *Biochemistry*, 3rd Edn., W.H. Freeman and Company, New York, **1988**.
- 4) G.A. Jeffrey, *An Introduction to Hydrogen Bonding*, Oxford University Press, Oxford, **1997**.
- 5) G.A. Jeffrey, W. Saenger, *Hydrogen Bonding in Biological Structures*, Springer, Berlin, **1994**.
- 6) (a) M.H. Abraham, *J. Phys. Org. Chem.*, **1993**, 6, 660, (b) M.H. Abraham, *Chem. Soc. Rev.*, **1993**, 22, 73.
- 7) (a) T. Suzuki, H. Fujii, T. Miyashi, Y. Yamashita, *J. Org. Chem.*, **1992**, 57, 6477, (b) D.S. Reddy, B.S. Goud, K. Panneerselvam, G.R. Desiraju, *J. Chem. Soc., Chem. Comm.*, **1993**, 663, (c) K. Biradha, C.V. Krishnamahan Sharma, K. Panneerselvam, L. Shimoni, H.L. Karrell, D.E. Zacherias, G.R. Desiraju, *J. Chem. Soc., Chem. Comm.*, **1993**, 1473, (d) M.A. Viswamitra, R. Radhakrishnan, J. Bandekar, G.R. Desiraju, *J. Am. Chem. Soc.*, **1993**, 115, 4868, (e) G.R. Desiraju, *Acc. Chem. Res.*, **1996**, 29, 441, (f) G.R. Desiraju, *Angew. Chem. Int. Ed. Engl.*, **1995**, 34, 2311.
- 8) R.R. Shoup, H.T. Miles, E.D. Becker, *Biochim. Biophys. Res. Comm.*, **1966**, 23, 194.
- 9) (a) W.L. Jorgensen, J. Pranata, *J. Am. Chem. Soc.*, **1990**, 112, 2008, (b) J. Pranata, S.G. Wierschke, W.L. Jorgensen, *J. Am. Chem. Soc.*, **1991**, 113, 2810.
- 10) (a) T.J. Murray, S.C. Zimmerman, *J. Am. Chem. Soc.*, **1992**, 114, 4010, (b) S.C. Zimmerman, T.J. Murray, *Phil. Trans. R. Soc. London, series A*, **1993**, 345, 49, (c) E.E. Fenton, T.J. Murray, M.H. Baloga, S.C. Zimmerman, *J. Org. Chem.*, **1993**, 58, 6625, (d) S.C. Zimmerman, T.J. Murray, *Tetrahedron Lett.*, **1994**, 35, 4077, (e) T.J. Murray, S.C. Zimmermann, S.V. Kolotuchin, *Tetrahedron*, **1995**, 51, 635.
- 11) J. Sartorius, H.-J. Schneider, *Chemistry, Eur. J.* **1996**, 2, 1446.
- 12) (a) A. D. Hamilton, D. van Engen, *J. Am. Chem. Soc.*, **1987**, 109, 5035, (b) A.D. Hamilton, N. Pant, A.V. Muehldorf, *Pure & Appl. Chem.*, **1988**, 60, 533, (c) A.D. Hamilton, A. Muehldorf, S.-K. Chang, N. Pant, S. Goswami, D. Van Engen, *J. Incl. Phenom. Molec. Rec. Chem.*, **1989**, 7, 27, (d) S.K. Chang, D. Van Engen, E. Fan, A.D. Hamilton, *J. Am. Chem. Soc.*, **1991**, 113, 7640.
- 13) B. Feibush, A. Figueroa, R. Charles, K.D. Onari, P. Feibush, B.L. Karger, *J. Am. Chem. Soc.*, **1986**, 108, 3310.
- 14) K. Tanabe, T. Takeuchi, J. Matsui, K. Ikebukuro, K. Yano, I. Karube, *J. Chem. Soc., Chem. Comm.*, **1995**, 2303.
- 15) S.C. Zimmermann, W.-S. Kwan, *Angew. Chem. Int. Ed. Engl.*, **1995**, 34, 2404.

- 16) (a) R. Wyler, J. de Mendoza, J. Rebek Jr., *Angew. Chem.*, **1993**, *105*, 1820, (b) C. Valdés, U.P. Spitz, L.M. Toledo, S.W. Kubik, J. Rebek, Jr., *J. Am. Chem. Soc.*, **1995**, *117*, 12733, (c) M. Grotzfeld, N. Branda, J. Rebek Jr., *Science*, **1996**, *271*, 487, (c), J. Rebek Jr., *Chemical Society Reviews*, **1996**, 255.
- 17) C.M. Drain, K.C. Russell, J.-M. Lehn, *Chem. Comm.*, **1996**, 337.
- 18) J.P. Mathias, C.T. Seto, E.E. Simanek, G.M. Whitesides, *J. Am. Chem. Soc.*, **1994**, *116*, 1725, (b) J.P. Mathias, E.E. Simanek, J.A. Zerkowski, C.T. Seto, G.M. Whitesides, *J. Am. Chem. Soc.*, **1994**, *116*, 4316, (c) J.P. Mathias, E.E. Simanek, G.M. Whitesides, *J. Am. Chem. Soc.*, **1994**, *116*, 4326.
- 19) R.H. Vreekamp, J.P.M. van Duynhoven, M. Hubert, W. Verboom, D.N. Reinhoudt, *Angew. Chem.*, **1996**, *108*, 1306.
- 20) (a) L. Leiserowitz, M. Tuval, *Acta Cryst*, **1978**, *B34*, 1230, (b) L. Leiserowitz, A.T. Hagler, *Proc. R. Soc. London, series A*, **1983**, *388*, 133, (c) M.C. Etter, *Acc. Chem. Res.*, **1990**, *23*, 120, (d) C.B. Aakeröy, K.R. Seddon, *Chem. Soc. Rev.*, **1993**, 397.
- 21) G.R. Desiraju, *Angew. Chem. Int. Ed. Engl.*, **1995**, *34*, 2311.
- 22) (a) J.P. Mathias, J.C. MacDonald, C.T. Seto, D.A. Wierda, G.M. Whitesides, *J. Am. Chem. Soc.*, **1994**, *116*, 2382, (b) J.A. Zerkowski, G.M. Whitesides, *J. Am. Chem. Soc.*, **1994**, *116*, 4298, (c) J.A. Zerkowski, J.P. Mathias, G.M. Whitesides, *J. Am. Chem. Soc.*, **1994**, *116*, 4305.
- 23) (a) J.-M. Lehn, M. Mascal, A. deCian, J. Fischer, *J. Chem. Soc, Chem. Comm.*, **1990**, 479, (b) J.-M. Lehn, M. Mascal, A. deCian, J. Fischer, *J. Chem. Soc, Perkin Trans. 1*, **1992**, 461.
- 24) S. Vallyaveettil, V. Enkelmann, K. Müllen, *J. Chem. Soc., Chem. Comm.*, **1994**, 2097.
- 25) M. Mascal, N.M. Hecht, R. Warmuth, M.H. Moore, J.P. Turkenburg, *Angew. Chem.*, **1996**, *108*, 2348.
- 26) Reviewed by: C.M. Paleos, D. Tsiourvas, *Adv. Mater.*, **1997**, *9*, 695.
- 27) (a) K. Kurihara, K. Ohto, Y. Honda, T. Kunitake, *J. Am. Chem. Soc.*, **1991**, *113*, 5077, (b) Y. Honda, K. Kurihara, T. Kunitake, *Chem. Lett.*, **1991**, 681, (c) D.Y. Sasaki, K. Kurihara, T. Kunitake, *J. Am. Chem. Soc.*, **1992**, *114*, 10994, (d) T. Kawahara, K. Kurihara, T. Kunitake, *Chem. Lett.*, **1992**, 1839, (e) N. Kimizuka, T. Kawasaki, T. Kunitake, *J. Am. Chem. Soc.*, **1993**, *115*, 4387, (f) H. Koyano, P. Bissel, K. Yoshihara, K. Ariga, T. Kunitake, *Chem. Eur. J.*, **1997**, *3*, 1077, (g) K. Ariga, A. Kamino, H. Koyano, T. Kunitake, *J. Mater. Chem.*, **1997**, *7*, 1155.
- 28) (a) A. Laschewsky, E. Wischerhoff, S. Denzinger, H. Ringsdorf, A. Delcorte, P. Bertrand, *Chem. Eur. J.*, **1997**, *3*, 34, (b) T.M. Bohanon, S. Denzinger, R. Fink, W. Paulus, H. Ringsdorf, M. Weck, *Angew. Chem. Int. Ed. Engl.*, **1995**, *34*, 58, (c) R. Ahuja, P.-L. Caruso, D. Möbius, W. Paulus, H. Ringsdorf, G. Wildburg, *Angew. Chem.*, **1993**, *105*, 1082, (d) Z. Whang, L. wang, X. Zhang, J. Shen, S. Denzinger, H. Ringsdorf, *Macromol. Chem. Phys.*, **1997**, *198*, 573.
- 29) N. Kimizuka, T. Kawasaki, K. Hirata, T. Kunitake, *J. Am. Chem. Soc.*, **1995**, *117*, 6360, (b) N. Kimizuka, S. Fujikawa, H. Kuwahara, T. Kunitake, A. Marsh, J.-M. Lehn, *J. Chem. Soc., Chem. Comm.*, **1995**, 2103.
- 30) (a) C. Fouquey, J.-M. Lehn, A.-M. Levelut, *Adv. Mater.* **1990**, *2*, 254, (b) M. Kotera, J.-M. Lehn, J.-P. Vigneron, *J. Chem. Soc. Chem. Commun.*, **1994**, 197.
- 31) (a) P. Bladon, A.C. Griffin, *Macromolecules*, **1993**, *26*, 6604, (b) C. Alexander, C.P. Jariwala, C.-M. Lee, A.C. Griffin, *Macromol. Symp.*, **1994**, *77*, 283, (c) C.B. St. Pourcain, A.C. Griffin, *Macromolecules*, **1995**, *28*, 4116,
- 32) H. Kihara, K. Kato, T. Uryu, J.M.J. Fréchet, *Chem. Mater.*, **1996**, *8*, 961.

- 33) (a) C.D. Eisenbach, A. Gödel, M. Terskan-Reinold, U.S. Schubert, *Makromol. Chem. Phys.*, **1995**, *196*, 1077, (b) C.P. Lillya, R.J. Baker, S. Huetten, H.H. Winter, Y.-G. Lin, J. Shi, L.C. Dickinson, J. C.W. Chien, *Macromolecules*, **1992**, *25*, 2076, (c) Y. Ducharme, J.D. Wuest, *J. Org. Chem.* **1988**, *53*, 5787, (d) U. Seidel, J. Hellman, D. Schollmeyer, C. Hilger, R. Stadler, *Supramol. Science*, **1995**, *2*, 45.
- 34) M. Müller, A. Dardin, U. Seidel, V. Balsamo, B. Iván, H.W. Spiess, R. Stadler, *Macromolecules*, **1996**, *29*, 2577.
- 35) (a) Reviewed by C.T. Imrie in *Trends in Polymer Chemistry*, **1995**, *3*, 22, (b) U. Kumar, T. Kato, J.M.J. Fréchet, *J. Am. Chem. Soc.*, **1992**, *114*, 6630, (c) T. Kato, H. Kihara, T. Uryu, A. Fujishima, J.M.J. Fréchet, *Macromolecules*, **1992**, *25*, 6836, (d) S. Malik, P.K. Dhal, R.A. Mashelkar, *Macromolecules* **1995**, *28*, 2159, (e) T. Kato, N. Hirota, A. Fujishima, J.M.J. Fréchet, *J. Polym. Sci., part A: Polym. Chem.*, **1996**, *34*, 57.
- 36) (a) R.F.M. Lange, E.W. Meijer, *Macromolecules*, **1995**, *28*, 782, (b). R.F.M. Lange, Ph.D. Thesis, Eindhoven, **1997**.
- 37) (a) T.W. Bell, J. Liu, *J. Am. Chem. Soc.*, **1988**, *110*, 3673, (b) S. Goswami, R. Mukherjee, *Tetrahedron Lett.*, **1997**, *38*, 1619, (c) T.W. Bell, Z. Hou, *Angew. Chem. Int. Ed. Engl.*, **1997**, *36*, 1536.
- 38) (a) N. Tamura, T. Kajiki, T. Nabeshima, Y. Yano, *J. Chem. Soc., Chem. Comm.*, **1994**, 2583, (b) N. Tamura, K. Mitsui, T. Nabeshima, Y. Yano, *J. Chem. Soc., Perkin Trans. 2*, **1994**, 2229.
- 39) T.W. Bell, Z. Hou, S.C. Zimmerman, P.A. Thiesen, *Angew. Chem.*, **1995**, *107*, 2321.
- 40) J.S. Lindsey, P.C. Kearney, R.J. Duff, P.J. Tjivikua, J. Rebek Jr., *J. Am. Chem. Soc.*, **1988**, *110*, 6575.
- 41) M.R. Ghadiri, J.R. Granja, R.A. Milligan, D.E. McRee, N. Khazanovich, *Nature*, **1993**, *366*, 324.
- 42) Other examples of arrays of more than three hydrogen bonds (a) T.R. Kelly, C. Zhao, G.J. Bridger, *J. Am. Chem. Soc.*, **1989**, *111*, 3744, (b) A.D. Hamilton, D. Little, *J. Chem. Soc., Chem. Comm.*, **1990**, 297, (c) S.C. Hirst, A.D. Hamilton, *Tetrahedron Lett.*, **1990**, *31*, 2401, (d) M.S. Goodman, S.D. Rose, *J. Am. Chem. Soc.*, **1991**, *113*, 9380, (e) S.J. Geib, S.C. Hirst, C. Vicent, A.D. Hamilton, *J. Chem. Soc., Chem. Commun.*, **1991**, 1283.
- 43) (a) Y. Honda, K. Kurihara, T. Kunitake, *Chem. Lett.*, **1991**, 681, (b) T.K. Park, J. Schroeder, J. Rebek Jr., *J. Am. Chem. Soc.*, **1991**, *113*, 5125, (c) T. K. Park, Q. Feng, J. Rebek Jr., *J. Am. Chem. Soc.*, **1992**, *114*, 4529.
- 44) F.H. Beijer, R.P. Sijbesma, J.A.J.M. Vekemans, E.W. Meijer, H. Kooijman, A.L. Spek, *J. Org. Chem.*, **1996**, *61*, 6371.
- 45) F.H. Beijer, H. Kooijman, R.P. Sijbesma, A.L. Spek, E.W. Meijer, *Angew. Chem.*, **1998**, *110*, 79; *Angew. Chem. Int. Ed. Engl.*, **1998**, *37*, 75.
- 46) F.H. Beijer, R.P. Sijbesma, H. Kooijman, A.L. Spek, E.W. Meijer, *J. Am. Chem. Soc.*, submitted.
- 47) F.H. Beijer, H. Fischer, R.P. Sijbesma, E.W. Meijer, *Chem. Eur. J.*, in preparation.
- 48) R.P. Sijbesma, F.H. Beijer, L. Brunsveld, B.J.B. Folmer, K. Hirschberg, R.F.M. Lange, J.K.L. Lowe, E.W. Meijer, *Science*, **1997**, *278*, 1601.
- 49) R.F.M. Lange, F.H. Beijer, R.P. Sijbesma, R.W.W. Hooft, H. Kooijman, A.L. Spek, J. Kroon, E.W. Meijer, *Angew. Chem. Int. Ed. Engl.*, **1997**, *36*, 969.

Chapter 2

Triply Hydrogen Bonded Complexes of Diaminopyridines and Diaminotriazines with Uracils:

Opposite Effect of Acylation on Complex Stabilities

Abstract:

The complexation behavior of several 2,4-diamino-s-triazines and 2,6-diaminopyridine with uracil derivatives was studied, with special emphasis on the effect of acylation of the aminogroups on binding. ^1H -NMR and IR-spectroscopy were used for characterization of the complexation in solution, while X-ray diffraction was used to ascertain the hydrogen bonding patterns in the solid state in (co)crystals.

Acylation of the amino groups of 2,6-diaminopyridine leads to a stepwise increase of the association constant of the complexes with N-propylthymine in CDCl_3 from 84 to 460 – 920 M^{-1} , presumably due to an increased donor strength of the N–H groups of diaminopyridine involved in the triple hydrogen bonding. However, acylation of the amino groups of 2,4-diamino-s-triazines leads to a dramatic decrease of the association constant of the complexes with N-propylthymine, from 890 to approximately 6 M^{-1} .

This phenomenon is related to different conformational preferences of the amides in these compounds. The amide groups in di(acylamino)pyridines prefer a trans-conformation, with the carbonyl group anti with respect to the ring nitrogen, and coplanar with the aromatic ring. However, the amides of di(acylamino)triazines reside predominantly in a cis-conformation. Repulsive secondary electrostatic interactions between the cis-amide and uracil carbonyl groups are thought to be responsible for the low association constant of complexes of di(acylamino)triazines with uracils.

The higher dimerization constants of di(acylamino)triazines compared to di(acylamino)pyridines have been rationalized by dimerization via quadruple hydrogen bonding of the ADADA array of di(acylamino)triazines, formed by extension from the DAD-array of a diaminotriazine with two cis-amide acceptor sites.

2.1 Introduction

The use of multiple hydrogen bonding for the assembly of supramolecular structures is now a well-established principle.¹ Multiple hydrogen bonding is a particularly good way to achieve recognition, because of its strength, directionality and specificity. In a program aimed at the use of multiple hydrogen bonding for the assembly of supramolecular polymer complexes,² we are aiming at (self)-complementary hydrogen bonding units that offer an optimal balance between synthetic accessibility, strength, and specificity.

A complementary pair frequently encountered in supramolecular chemistry consists of a di(acylamino)pyridine as the Donor–Acceptor–Donor (DAD) unit and an imide as the Acceptor–Donor–Acceptor (ADA) unit. Examples include complexes of 2,6-di(acylamino)pyridines with uracils, succinimides or glutarimides,³ with association constants in CDCl₃ in the range of 50–500 M⁻¹. Recently, the use of melamines,⁴ 2,4,6-triaminopyrimidines,⁵ aminoalkyl-*s*-triazines,⁶ and 2,4-diamino-*s*-triazines⁷ as DAD groups was also reported.

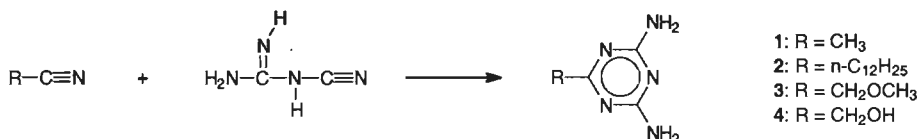
We decided to compare the hydrogen bonding properties of synthetically well-accessible 6-alkyl-2,4-diamino-*s*-triazine derivatives with the well-studied 2,6-diaminopyridine, with special emphasis on the effect of acylation on binding strength with uracils/thymines, and dimerization. ¹H-NMR titrations and IR spectroscopy in chloroform solution are used to study the complexation via hydrogen bonding of parent and of acylated diaminotriazines and diaminopyridine with uracil derivatives, as well as the amide conformations of acylated compounds in solution. Additional information is gathered from (co)crystallization experiments giving access to crystal structures and hence to detailed information about the geometry of the hydrogen bonded complexes. Taking into account the decisive role of amide conformations, the results of the complexation experiments are discussed in the framework of the model of Jorgensen.⁸ This model uses secondary electrostatic interactions to explain differences in strength between arrays of hydrogen bonding groups.

2.2 Results

2.2.1 Synthesis

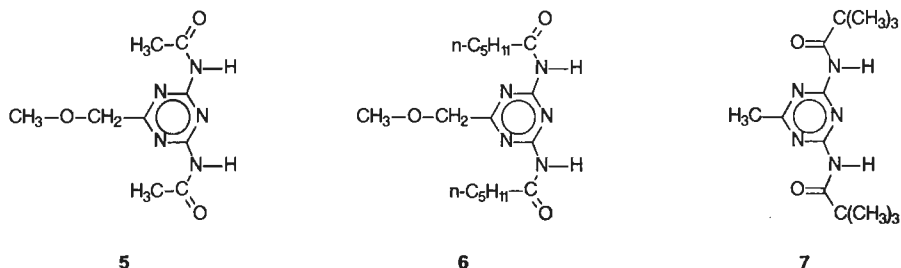
Synthesis of diamino-*s*-triazine derivatives. 2,4-Diamino-*s*-triazines can be prepared conveniently by condensation of the appropriate nitrile with dicyanodiamide in alcohol at reflux temperature (scheme 2.1).⁹ This well-known route was applied to synthesize compounds 1–3 from commercially available nitriles. To study the effect of substitution with

groups capable of additional hydrogen bonding interactions, the water soluble 6-hydroxymethyl substituted 2,4-diamino-*s*-triazine **4** was prepared. The synthesis of **4** was performed according to the method of Sims¹⁰ via a three-step synthesis. Glycolonitrile¹¹ was protected as its butyl vinyl ether (yield 53%), which product was subsequently converted to the corresponding 2,4-diamino-*s*-triazine (59%). Finally, triazine **4** was obtained by deprotection with acid (63%).



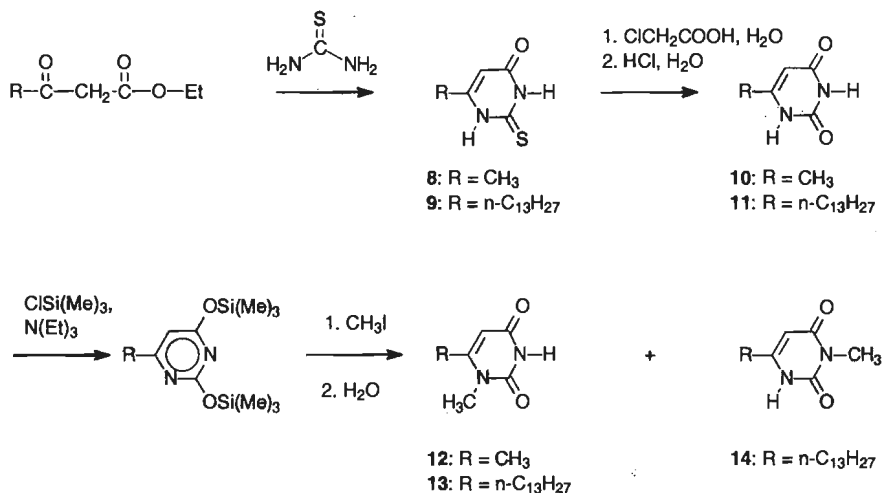
Scheme 2.1: General route for the synthesis of 2,4-diamino-*s*-triazines.

The solubility of 2,4-diamino-*s*-triazines **1**, **3**, and **4** in chloroform was unfortunately too low to use these compounds in association studies. The solubility of diamino-triazines was enhanced considerably by attaching a long alkyl chain to the 6-position, as in compound **2**. Acylated 2,4-diamino-*s*-triazines were prepared with the expectation that the amide N–H protons would display stronger hydrogen bonding than the parent NH₂ protons. Di(acetylamino)triazine **5** was prepared by boiling diaminotriazine **3** in acetic anhydride;¹² di(hexanoylamino)triazine **6** and di(pivaloylamino)triazine **7** were prepared using two equivalents of the appropriate acid chloride in refluxing pyridine. The acylated triazines **5** and **6** readily undergo hydrolysis in water at room temperature.^{12c}



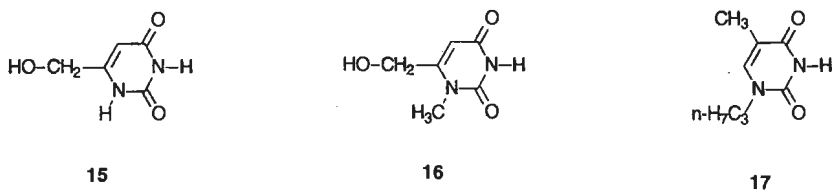
Synthesis of uracil derivatives. Uracil derivatives **10** and **11** were synthesized according to the well-known sequence of condensation of β -keto esters with thiourea, followed by conversion of the thiouracils **8** and **9** to the corresponding uracils by hydrolysis of the thiogroup with chloroacetic acid¹³ (see scheme 2.2). The limited solubility of 6-methyluracil **10** and even of 6-tridecyluracil **11** in chloroform prevented their use in NMR-complexation experiments. The proton on *N*-1, which does not participate in formation of a triply hydrogen bonded complex and is capable of additional hydrogen bonding, was removed by *N*-1-methylation, with the hope of increased solubility. Selective *N*-1-methylation of uracils **10** and **11** was accomplished by silylation of these uracils with trimethylsilylchloride

and triethylamine in THF, followed by reaction of the intermediate silyl derivatives with methyl iodide, and then deprotection with water. This sequence afforded uracil derivatives **12** and **13**, respectively.¹⁴ The solubility of uracil **12** in chloroform was low, but, fortunately, uracil **13** was readily soluble in CHCl_3 . 3-*N*-Methyl-6-tridecyluracil (**14**) was isolated as a minor byproduct (7%) in the synthesis of **13**.



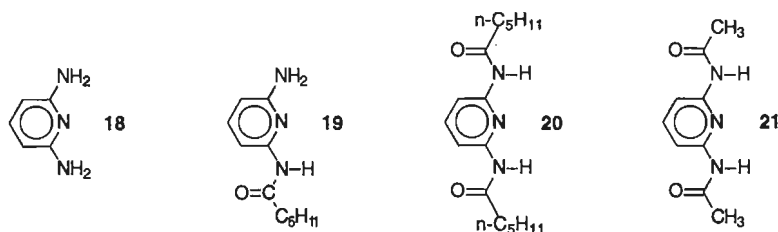
Scheme 2.2: General route for the synthesis of uracil derivatives.

To study the effect of substitution with additional groups capable of hydrogen bonding interactions besides the ADA array, 6-hydroxymethyl substituted uracil **15** was prepared by reduction of the butyl ester of 6-carboxyuracil.¹⁵ The sequence of silylation and *N*-1-methylation via the silyl-Hilbert-Johnson reaction could also be applied to this uracil, affording derivative **16**. Deprotection of the silylated hydroxymethyl substituent was achieved by prolonged acid treatment in water. *N*-1-propylthymine (**17**) was prepared by direct alkylation of thymine according to a literature procedure.¹⁶



Synthesis of 2,6-diaminopyridine derivatives. Acylation of 2,6-diaminopyridine (**18**) with one equivalent of hexanoyl chloride in THF at 0°C gave a mixture of the starting material, and of mono- and di(acylated) compound. From this mixture, mono(hexanoyl)diaminopyridine **19** was obtained in 57% yield after purification by column

chromatography. Attempts to synthesize mono(acylated) derivatives of 2,6-diaminopyridine with acetic anhydride, acetyl chloride, hexanoyl chloride or palmitoyl chloride were unsuccessful when performed in pyridine at 0°C; only formation of bis-acylated compound was observed. Bis(acylamino)pyridines **20** and **21** were prepared by acylation of diaminopyridine under standard conditions¹⁷ with hexanoyl chloride and acetic anhydride, respectively.



2.2.2 Association Studies in Solution

Association constants of hydrogen bonded complexes may be determined from evaluation of ¹H-NMR titration data by computer fitting with non-linear least squares methods. Provided the proper binding model is used, this method guarantees a more reliable treatment of data than the use of graphical methods. In the present investigation, we were specifically interested in dimerization, and we certainly did not want to neglect its effect on the calculated hetero-association constants. Therefore, dimerization constants were determined separately, and the titration data of hetero-complexation were analysed using a model that explicitly takes dimerization into account. The reader is referred to the experimental section for detailed information.

Dimerization. Dimerization constants in CDCl₃ at 298 K were determined by monitoring the N-H proton shift in ¹H-NMR as a function of concentration. The concentration dependence of the dilution data could be fitted well to the dimerization model.¹⁸ The fitting procedure afforded dimerization constants, as well as the monomer and dimer shifts (Table 2.1). In some cases, for example derivatives **5** and **7**, several of the C-H signals of the aromatic ring or the CH₂ signals adjacent to the N-H group in **20** also showed a concentration dependent shift large enough to allow reliable monitoring. Fitting of these data afforded the same dimerization constants within experimental error (± 15%). The dimerization constants of 2,6-diaminopyridine (**18**) and of 2,6-di(acetylamino)pyridine (**21**) could not be determined due to the limited solubility of these compounds. K_{dim} values are generally very low, except those of di(acylamino)triazines **5** and **6**, and of 3-*N*-methyluracil **14**.

Table 2.1: Dimerization constants (K_{dim}) and complexation induced shift (CIS) values of N–H protons in dimers of diaminotriazine-, diaminopyridine- and uracil derivatives.

Entry	Compound	K_{dim} (M^{-1}) ^a	CIS (ppm)
1	2-amino-6-hexanoylamino-pyridine (19)	<1	3.0
2	2,6-Di(hexanoylamino)pyridine (20)	<1	2.9
3	2,4-Diamino-6-dodecyl- <i>s</i> -triazine (2)	2.2	2.37
4	2,4-Di(acetylamino)-6-methoxymethyl- <i>s</i> -triazine (5)	37	2.35
5	2,4-Di(hexanoylamino)-6-methoxymethyl- <i>s</i> -triazine (6)	24	2.33
6	2,4-Di(pivaloylamino)-6-methyl- <i>s</i> -triazine (7)	1.7	0.76
7	1- <i>N</i> -propylthymine (17)	4.3	3.40
8	1- <i>N</i> -methyl-6-tridecyluracil (13)	7.0	3.52
9	3- <i>N</i> -methyl-6-tridecyluracil (14)	94	3.93

^a estimated relative error in K_{dim} is 15%.

Hetero-complexation. Job-plots of the DAD–ADA hydrogen bonded complexes of (acylated) derivatives of diaminopyridine and -triazine with uracils show a maximum at mol fraction = 0.5, indicating a 1:1 stoichiometry in the complex formation. Job plots of diaminotriazine **2** and di(acetylamino)triazine **5** with *N*-propylthymine **17** are shown in figure 2.1.¹⁹ The results of the titration experiments, affording association constants corrected for dimerization of the titrant,²⁰ are summarized in table 2.2.

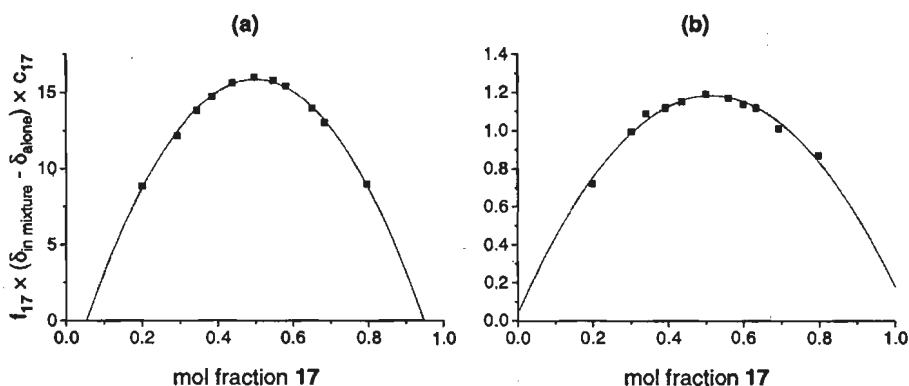


Figure 2.1: Job plots, measured at total concentrations of 8–10 mM, for:
 (a) diaminotriazine **2** with *N*-propylthymine **17**,
 (b) di(acetylamino)triazine **5** with **17**.

Table 2.2: Association constants (K_a), and complexation induced shift (CIS) values of complexes of diaminopyridine- and diaminotriazine derivatives with (thio)uracil derivatives.

Entry	diaminopyridine-, diaminotriazine- derivative	<i>N</i> -propylthymine/ uracil derivative	K_a (M^{-1}) ^a	CIS (ppm) of NH proton; (probe)
1	diaminopyridine 18	<i>N</i> -propylthymine 17	84	1.36; (18)
2	(hexanoyl)diaminopyridine 19	<i>N</i> -propylthymine 17	230	2.82; (19)
3	di(hexanoylamino)pyridine 20	<i>N</i> -propylthymine 17	460	2.81; (20)
4	di(acetylamino)pyridine 21	<i>N</i> -propylthymine 17	920	2.86; (21)
5	di(hexanoylamino)pyridine 20	<i>N</i> -1-methyluracil 13	530	2.80; (20)
6	diaminotriazine 2	<i>N</i> -propylthymine 17	890	5.65; (17)
7	diaminotriazine 2	<i>N</i> -1-methyluracil 13	750	5.61; (13)
8	di(acetylamino)triazine 5	<i>N</i> -propylthymine 17	5.7	1.39; (5)
9	di(hexanoylamino)triazine 6	<i>N</i> -propylthymine 17	6.4	1.68; (6)
10	di(pivaloylamino)triazine 7	<i>N</i> -propylthymine 17	4.7	1.28; (7)
11	diaminotriazine 2	thiouracil 9	107	3.76; (9)
12	diaminotriazine 2	<i>N</i> -3-methyluracil 14	< 2	-

^a estimated relative error in K_a is 15%.

Substituents on the uracil/thymine, or on di(acylamino)pyridine strongly effect the association constants of the complexes, but barely influence the chemically induced shift of the protons in the complexes (compare entries 2, 3, 4, and 5, and entry 6 with 7 in table 2.2). High association constants are observed for the complexes of 2,6-di(acylamino)pyridines **20** and **21** with uracils **13** and **17**, respectively, and also for the complexes of diaminotriazine **2** with uracils **13** and **17**. These association constants are comparable with literature values of complexation of triazines with uracils^{7b,7c} and with flavine derivatives.³ⁿ Complexes of 2,6-diaminopyridine (**18**) and 2-amino-6-hexanoylamino-pyridine (**19**) with *N*-propylthymine **17** have lower association constants, whereas very low association constants are observed for the complexes of di(acylamino)triazines **5**, **6**, and **7** with *N*-propylthymine (**17**).

IR Spectroscopy of (acylamino)pyridines and di(acylamino)triazines. IR-spectra of compounds **2**, **5**, **6**, **7**, and **18–21** were recorded in dry chloroform solutions, generally at 50 mM. For di(acylamino)triazines **5** and **6**, compounds with substantial dimerization, concentrations in the range 1–5 mM were applied to obtain the monomer spectrum. Wavenumbers of the monomer N–H stretch vibrations are reported in Table 2.3. Di(acylamino)pyridines **20** and **21**, monohexanoylamino-pyridine **19**, and di(pivaloylamino)-

triazine **7** show their amide N–H stretch vibration at approximately 3422 and 3424 cm^{-1} , respectively, while di(acylamino)triazines **5** and **6** show their N–H stretch vibration band at lower wavenumbers, at 3384 and 3395 cm^{-1} , respectively.

Complex formation of compounds **2**, **5**, and **18–21** with *N*-propylthymine (**17**) in chloroform solution was also studied by means of infrared spectroscopy. Wavenumbers of the N–H stretch vibrations of these compounds in the complexes are also given in Table 2.3.

Table 2.3: Wavenumbers of N–H stretch vibrations of diaminopyridines, diaminotriazines and their acylated derivatives as free molecules and in their complexes with *N*-propylthymine **17.**

Compound	$\nu_{\text{N-H}}$ (cm^{-1})	$\nu_{\text{N-H}}$ (cm^{-1}) in complex with 17	$\nu_{\text{N-H}}$ (cm^{-1}) of 17 in complex ^a
diaminotriazine 2	3424; 3540 ^b	3328; 3497 ^c	3216
di(acetylamino)triazine 5	3384	– ^d	– ^d
di(hexanoylamino)triazine 6	3395	– ^d	– ^d
di(pivaloylamino)triazine 7	3424	– ^d	– ^d
diaminopyridine 18	3408; 3508 ^b	3339; 3493 ^c	3219
2-amino-6-hexanoylamino-pyridine 19	3418, 3511 ^b	3319; 3492 ^c	3218
	3418 ^c	3271	
di(hexanoylamino)pyridine 20	3422	3275	3215
di(acetylamino)pyridine 21	3422	3275	3211

^a $\nu_{\text{N-H}}$ of free **17**: 3395 cm^{-1} ; ^b Symmetric and asymmetric stretch vibrations, respectively; ^c $\nu_{\text{N-H}}$ of hydrogen bonded N–H and of free N–H, respectively; ^d Bands due to complex were not observed; ^e N–H stretch vibration of amide coincides with the symmetric NH_2 stretch vibration.

2.2.3 Complexation in the solid state; X-ray single crystal structures

Cocrystallization. To study the complexation between uracils and (acylated) derivatives of diaminotriazines, cocrystallization of complementary pairs of triazine and uracil derivatives was investigated. No complexes were obtained upon attempts to cocrystallize di(acylamino)triazines **5–7** and *N*-propylthymine from ethyl acetate or hexane; rather, separate crystals of the individual components crystallized. However, complexes were obtained if parent diaminotriazines were cocrystallized with uracils. To study the specificity of the triple hydrogen bond in complexes of these derivatives, derivatives with additional functionalities capable of hydrogen bonding were used, such as hydroxymethyl substituted derivatives, and *N*-1 non-methylated uracils. We prepared a range of crystalline complexes of various diaminotriazines with complementary uracil derivatives, summarized below:

- 6-methyl-triazine **1** with 6-methyl-uracil **12**,
- 6-methyl-triazine **1** with 6-hydroxymethyluracils **15** and **16**,
- 6-hydroxymethyl-triazine **4** with 6-hydroxymethyluracil derivatives **15** and **16**,
- 6-hydroxymethyl-triazine **4** with 6-methyluracil **10**,
- 6-dodecyl-triazine **2** with 6-tridecyluracil derivatives **11** and **13**.

Water or ethanol proved to be the most suitable solvents for cocrystallization. In these solvents, the nicest and largest crystals were formed. This may be ascribed to favorable hydrophobic interactions in these solvents, and to similar solubility of the compounds. The preference for the formation of crystalline 1:1 complexes was very pronounced. Even when a stoichiometry considerably different from 1:1 was used, formation of 1:1 cocrystals was observed, sometimes accompanied by crystals of the compound present in excess. The only exception to the formation of 1:1 cocrystals we observed, was the crystallization of a 1:2 complex of 2,4-diamino-6-methyl-*s*-triazine **1** with 1-*N*-methyl-6-methyluracil **12**. This 1:2 crystalline complex was even formed when an equimolar aqueous solution was used. However, these 1:2 crystals gradually redissolved on prolonged standing, while crystals of a 1:1 complex were formed. The formation of cocrystals with two different stoichiometries is remarkable for multiple hydrogen-bonded complexes, but has been reported previously.²¹

Crystal structures of Diaminotriazine – Uracil Complexes. Unambiguous information about the hydrogen bonding patterns in the cocrystals was obtained by single crystal X-ray diffraction. In some of the crystalline complexes, crystal water is present forming complex hydrogen bonding structures (which we will not discuss in detail). PLUTON²² drawings of the hydrogen bonding patterns between diaminotriazine and uracil of several cocrystals are reported in figures 2.2a–g.

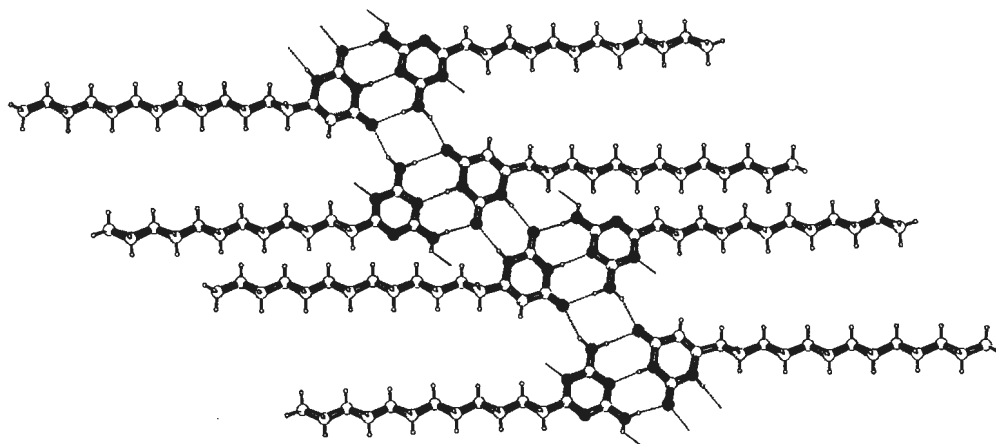


Figure 2.2a: PLUTON representation of the hydrogen bonding pattern between diaminotriazine and uracil in the 6-dodecyl-diaminotriazine•6-tridecyluracil complex **2•11**.

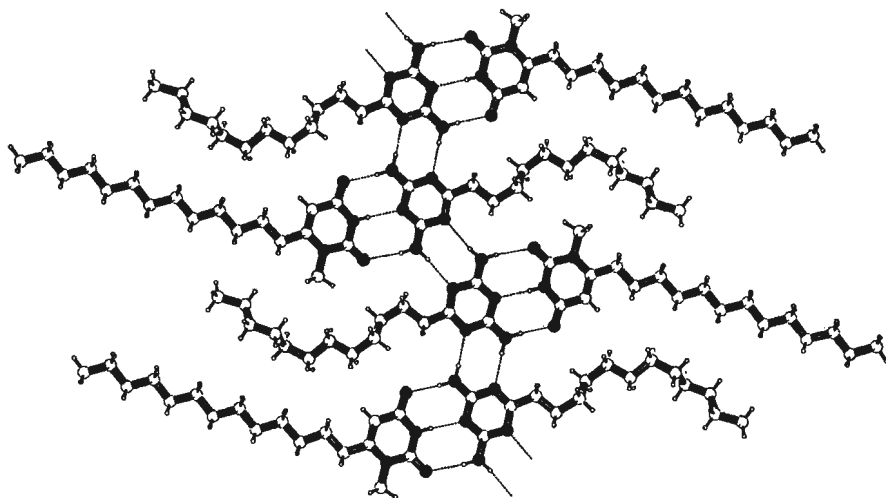


Figure 2.2b: PLUTON representation of the hydrogen bonding pattern between diamino-*s*-triazine and uracil in the 6-dodecyl-diaminotriazine•1-*N*-methyl-6-tridecyluracil complex **2•13**.

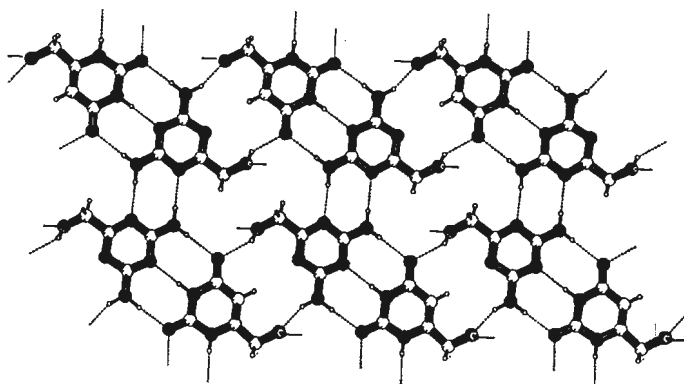


Figure 2.2c: PLUTON representation of the hydrogen bonding pattern between diamino-*s*-triazine and uracil in the 6-hydroxymethyldiaminotriazine•6-hydroxymethyluracil complex **4•15**.

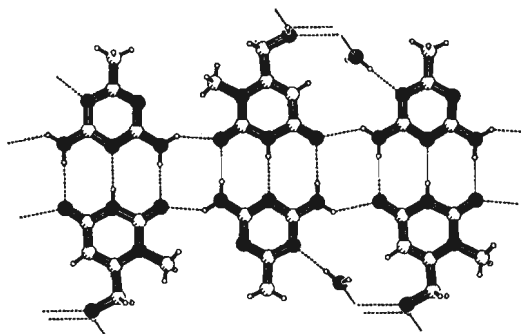


Figure 2.2d: PLUTON representation of the hydrogen bonding pattern between diamino-*s*-triazine and uracil in the 6-methyl-diaminotriazine•1-*N*-methyl-6-hydroxymethyl-uracil complex **1•16**.

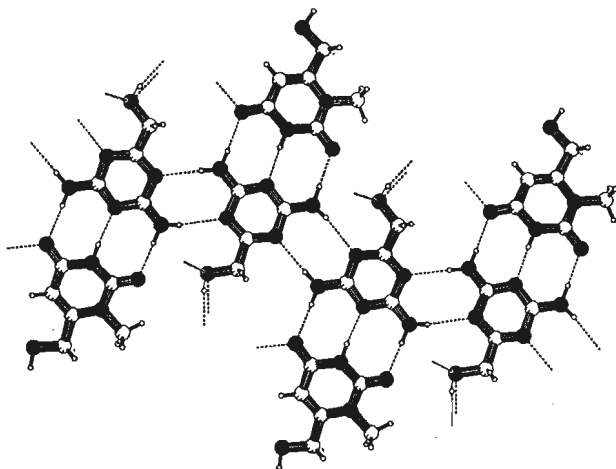
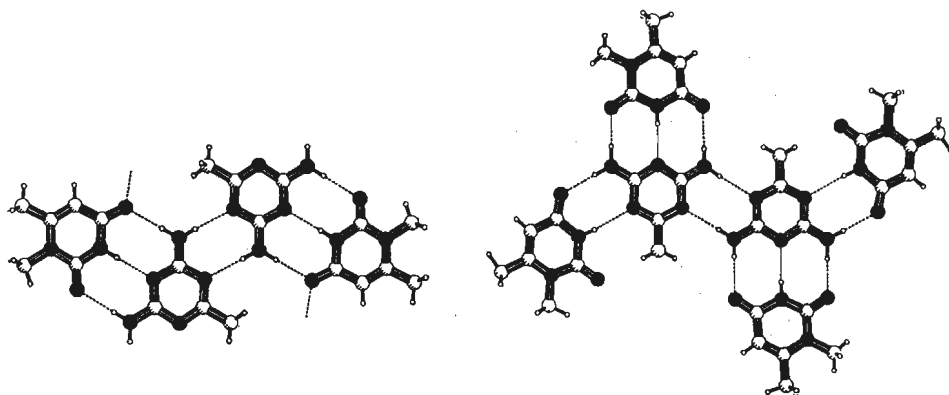


Figure 2.2e: PLUTON representation of the hydrogen bonding pattern between diamino-s-triazine and uracil in the 6-hydroxymethyl-diaminotriazine•1-*N*-methyl-6-hydroxymethyl-uracil complex **4•16**.



Figures 2.2f and g: PLUTON representation of the hydrogen bonding pattern between diamino-s-triazine and uracil in the:
 1:1 6-methyl-diaminotriazine•1-*N*-methyl-6-methyl-uracil complex **1•12** (left),
 1:2 6-methyl-diaminotriazine•1-*N*-methyl-6-methyl-uracil complex **1•12** (right).

X-Ray diffraction of di(acylamino)triazine 5. The crystal structure of di(acetylamino)triazine **5** was determined in order to gain a better insight into the conformational differences between di(acylamino)triazines and di(acylamino)pyridines. A PLUTON drawing of the crystal structure of **5** is shown in figure 2.3. This drawing shows two crystallographically independent molecules, of which three amides are in *cis*-conformation, and one amide in *trans*-conformation. The *trans*-amide deviates 8.97(8) degrees from coplanarity with the triazine ring, presumably to reduce electrostatic repulsion between the carbonyl group and the ring nitrogen atom.

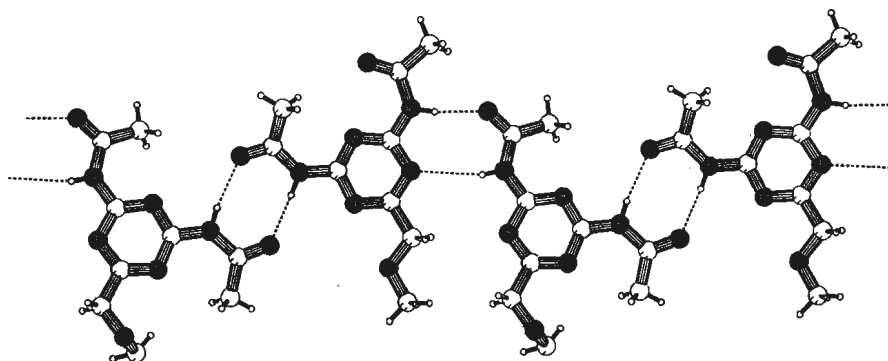


Figure 2.3: PLUTON representation of the hydrogen bonding pattern in the crystal structure of 2,4-di(acetylamino)-6-methoxymethyl-s-triazine (**5**).

2.3 Discussion

2.3.1 Dimerization of uracil derivatives

Non-methylated uracil derivatives possess a lactam-like DA array, and an imide-like ADA array. These compounds can dimerize via hydrogen bonding in five different geometries.²³ Oligomers or polymers can be formed if the two arrays are simultaneously involved in hydrogen bonding. The latter fact is undoubtedly responsible for the low solubility of non-substituted uracil derivatives in chloroform. *N*-1-Methyl-6-tridecyluracil **13** can dimerize via its ADA array in three geometries. However, for the *N*-3-alkyl derivative **14**, only one dimer geometry remains possible.

N-3-Methyl-uracil **14** has a much higher dimerization constant than *N*-1-methyl-uracil **13** (Table 2.1, entries 8 and 9). This observation is in complete agreement with the difference in dimerization constants of imides and lactams reported by Jorgensen⁸ and Burrows.²⁴ These effects were explained through repulsive electrostatic interactions between carbonyl oxygen atoms. We propose that similar effects are contributing to the difference in dimerization constants of **13** and **14**. In the centrosymmetric dimer of **14** (figure 2.4a), there are two repulsive secondary interactions, whereas in all three possible dimer geometries of **13**, due to two spectator oxygens, there are two *additional* repulsive interactions (depicted by double-headed arrows in figure 2.4b). Consequently, the dimerization of **14** is more favorable than the dimerization of **13**. The low dimerization constant of *N*-propylthymine (4.3 M^{-1}) can be explained similar as for uracil **13**.

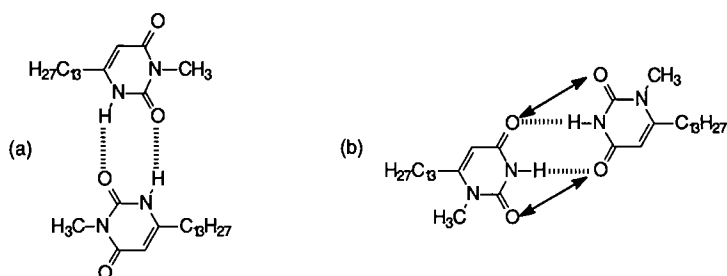


Figure 2.4: (a) Centrosymmetric dimer geometry of 3-*N*-methyl-6-tridecyluracil (**14**).
 (b) One of three possible dimer geometries of 3-*N*-methyl-6-tridecyluracil (**13**).
 Additional repulsive electrostatic interactions are indicated by double-headed arrows.

2.3.2 Comparison of Diaminotriazines and (acylated) Diaminopyridines. Dimerization and complexation with *N*-propylthymine and uracil derivatives

The $^1\text{H-NMR}$ data in table 2.1 show that dimerization constants are low for diaminotriazine **2** and for the mono- and di(hexanoylamino)pyridines **19** and **20**. The dimerization constants of 2,6-diaminopyridine **18** and di(acetylamino)pyridine **21** could not be determined by $^1\text{H-NMR}$ dilution due to low solubility, but these are estimated also to be very low based on infrared spectra of these compounds in dilute chloroform solution.²⁵ The low dimerization constants of compounds **2** and **18–21** can be explained by destabilization of the dimer geometry of a DAD-array by additional repulsive secondary interactions, analogous as for the ADA-array of uracils. Remarkably, the dimerization constants of di(acylamino)triazines, except that of the sterically hindered di(pivaloylamino) derivative **7**, are higher by one order of magnitude.

2,6-Diaminopyridine (**18**) forms a 1:1 complex with *N*-propylthymine (**17**) which has an association constant of 84 M^{-1} . Upon acylation of one of the amino groups, the association constant of the complex increases to 230 M^{-1} , while if both amino groups are acylated with hexanoyl groups, the association constant increases further to 460 M^{-1} . This stepwise increase upon acylation presumably results from the increased acidity of the amide protons as compared to the amino protons in **18**. The association constant of the complex of *N*-propylthymine **17** with di(acetylamino)pyridine **21** ($K_a = 920\text{ M}^{-1}$) is significantly higher than of **17** with di(hexanoylamino)pyridine **20** ($K_a = 460\text{ M}^{-1}$). This difference is remarkable in view that the only difference between **20** and **21** is the chain-length of the alkanoyl substituents, and the difference is likely caused by entropic factors of the alkanoyl chains.

Due to the electron withdrawing nature of the triazine ring, the amino protons of diaminotriazines are expected to be considerably more acidic than the amino protons of aminopyridines. This is indeed the case, since the wavenumbers of the asymmetric and

symmetric NH_2 stretch vibrations—which are known to occur at higher wavenumbers if the amino group is substituted with an electron-withdrawing group²⁶—in diaminotriazine **2** are found at higher wavenumbers than in diaminopyridine **18**. Consequently, the amino protons in diaminotriazines are expected also to be better hydrogen bond donors. Inspection of table 2.2 indeed shows that *N*-propylthymine (**17**) forms a complex with triazine **2** which has a much higher association constant ($K_a = 890 \text{ M}^{-1}$) than the complex with diaminopyridine ($K_a = 84 \text{ M}^{-1}$), while the former complex is of comparable strength as the complex of 2,6-di(acetylamino)pyridine (**21**) with *N*-propylthymine **17** ($K_a = 920 \text{ M}^{-1}$).

Inspection of the IR-data in table 2.3 shows that diaminotriazine **2**, 2,6-diaminopyridine (**18**), 2-amino-6-hexanoylaminopyridine **19**, and di(acetylamino)pyridines **20** and **21** all form complexes with *N*-propylthymine (**17**) in chloroform solution. Complexation induces a decrease of the wavenumber of the N–H stretch vibration of *N*-propylthymine (**17**) of 179, 176, 177, 180 and 184 cm^{-1} , respectively. In the complex with *N*-propylthymine (**17**), the asymmetric and symmetric NH_2 stretch vibrations in diaminotriazine **2** are shifted to lower wavenumbers by approximately 43 and 96 cm^{-1} , respectively, whereas the corresponding shift of vibrations upon complexation is only 15 and 69 cm^{-1} in diaminopyridine **18**. Upon complexation, the wavenumbers of the (single) N–H stretch of di(acetylamino)pyridine **20** and **21** decrease by 147 and 149 cm^{-1} , respectively. From these data, it is evident that *N*-propylthymine (**17**) forms stronger hydrogen bonds with **20**, **21** and **2** than with **18**, in line with the association constants determined by ^1H -NMR titrations.

The lack of association of **2** with **14** ($K_a < 2 \text{ M}^{-1}$) is not unexpected, because a triply hydrogen bonded complex cannot be formed, and steric interactions with the alkyl substituent of **14** cannot be avoided in a complex involving two hydrogen bonds. Complexation of **2** with thiouracil **9** is weaker than with uracil **13**, because the sulfur atom is a weaker hydrogen bond acceptor.

2.3.3 Persistence of the triazine–uracil triple hydrogen bonding motif in the solid state

In all crystal structures of studied diaminotriazine–uracil complexes, the diaminotriazine is paired via its DAD array with the ADA array of a uracil derivative.²⁷ This confirms our observation from complexation experiments in chloroform solution that the DAD–ADA triple hydrogen bond is the dominant interaction between diaminotriazines and uracils. In all the determined crystal structures, except the 1:2 cocrystal **1**•**12**, networks are formed by additional hydrogen bonding interactions between the triply hydrogen bonded complexes. The additional hydrogen bonding interactions we observe in the crystalline diaminotriazine–uracil complexes are the following:

- (i) uracil dimerization (*N*-1-non-methylated uracils **2•11**, and **4•15**),
- (ii) formation of base quadruplets (**2•11**, and **1•16**),
- (iii) triazine dimerization via double hydrogen bonds (1:1 and 1:2 cocrystal **1•12**, **4•15**, and **2•11**),
- (iv) formation of an infinite chain of triazines by dimerization on both sides via double hydrogen bonds (**2•13**, and **4•16**),
- (v) formation of cooperative hydrogen bonding ring-like networks, in cocrystals with crystal water or hydroxymethyl groups (1:1 complex **1•12**, and complex **4•16**).

These additional hydrogen bonding interactions are quite common in nucleobase pairing,²⁷ and seem not to interfere with the triple hydrogen bonding motif.²⁸

In the crystal structure of the 1:2 complex of 2,4-diamino-6-methyl-*s*-triazine **1** with 1-*N*-methyl-6-methyluracil **12**—the only exception to the general formation of 1:1 cocrystals we observed—(figure 2.2g), one of the two uracil molecules is triply hydrogen bonded to the triazine DAD array. However, the second uracil molecule is not triply hydrogen bonded, but forms, with its (central) N–H and one carbonyl, a double hydrogen bond to a triazine N–H and a non central triazine ring nitrogen atom. The other carbonyl group of this uracil molecule points towards one of the hydrogen atoms of the triazine CH₃. The remaining triazine N–H and non central nitrogen atom dimerize in a centrosymmetrical fashion, and sheets are formed of these complexes without further hydrogen bonding interactions.

The hydrogen bond distances of the triple hydrogen bonds in the diaminotriazine–uracil complexes are typically 2.8–3.1 Å, and the angles 159–178 degrees. These values are general for nucleobase pairing, and are comparable to those in cocrystals of di(acylamino)pyridine derivatives with imides.²⁹ They fall in the region of intermediate hydrogen bonding strength.²⁷ The bond distances of the outer N–H[⋯]O=C hydrogen bonds are comparable to the inner N–H[⋯]N distances; the lines through the three nitrogens of diaminotriazine, and through the central nitrogen and two oxygens of uracil, are virtually linear.

2.3.4 Opposite effect of acylation on the stability of diaminopyridine and diaminotriazine complexes. Dimerization and complexation with *N*-propylthymine

The association constant of the complex of diaminopyridine (**18**) with *N*-propylthymine (**17**) increases approximately tenfold upon acetylation of the amino groups. A corresponding increase in association constant upon acetylation of diaminotriazines was expected. However, when the amino groups of a diaminotriazine were acetylated, the association constant of the complexes with *N*-propylthymine dramatically dropped to

approximately 6 M^{-1} (Table 2.2, entries 5, 7 and 8). Infrared spectroscopy also shows that *N*-propylthymine and 2,4-di(acetylamino)triazine **5** do not form a stable complex in chloroform (Table 2.3).

Initially, these unexpected results seemed rather strange. In acylated triazines, the reduced basicity of the ring nitrogen atoms alone fails to explain the differences, because this effect is not observed for di(acylamino)pyridines, where a similar reduction in basicity is expected. The spectroscopic and X-ray data discussed below led us to believe that the differences result from the formation of a linear ADADA array of five hydrogen bonding sites when the amides in di(acylamino)triazines are in a *cis* conformation (figure 2.5).

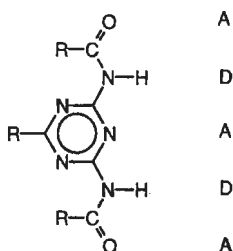


Figure 2.5: Linear ADADA array of a di(acylamino)triazine with *cis*-amide groups.

Whereas in di(acylamino)pyridines the *trans* conformation is the most stable conformation,³⁰ in di(acylamino)triazines the *cis* conformation might predominate, due to electrostatic repulsion between the amide oxygen atom and one of the nitrogen atoms in the triazine ring that cannot be avoided when the amide is *trans*. In both types of molecules, it is expected that the amide group is more or less coplanar with the aromatic ring because of resonance stabilization. A search of the Cambridge structural database for acylaminopyridines, -pyrimidines and -triazines confirmed this hypothesis. The search yielded 8 structures of di(acylamino)pyridines,³¹ all having amides exclusively in the *trans* conformation, with the carbonyl *anti* to the ring nitrogen atom. In the only two structures of 2-acylaminopyrimidines in the database, the amide has a *cis* conformation.³² Remarkably, one of these crystal structures features a linear array of four alternating donor and acceptor groups, incorporated in a quadruply hydrogen bonded centrosymmetric dimer.

Although the crystallographic data suggest a preference for *cis* amides in the non sterically hindered di(acetylamino)triazine **5** and in a 2-acetylamino-4-aminopyrimidine derivative in the solid state,³⁵ they do not give information on the occurrence of this conformation in solution. Therefore, we decided to record infrared spectra of di(acylamino)triazines and di(acylamino)pyridines in dilute chloroform solution.

In the IR spectra of *N*-aryl amides in dilute CHCl_3 or CCl_4 solution, in which the amides are predominantly in *trans*-conformation, the N–H stretch vibration of the *trans*-

amide appears at higher wavenumbers than that of the *cis*-amide.³³ In the infrared spectrum of di(acetylamino)- or di(hexanoylamino)pyridine at 50 mM in dry CHCl_3 , we find a single band at 3422 cm^{-1} , strongly suggesting that the amide groups are predominantly in the *trans* conformation.³⁰

In di(acylamino)triazines **5** and **6**, however, bands at 3383 and 3395 cm^{-1} , respectively, are found for the N–H stretch vibration in dilute chloroform solution (5 mM³⁴). In di(pivaloylamino)triazine **7**, in which the conformation of the amide groups is *trans* for steric reasons, this band is found at 3424 cm^{-1} .³⁵ Comparison of these wavenumbers with the N–H stretch vibration wavenumbers of *cis* and *trans* conformers of acetanilide in CCl_4 solution (3402 and 3446 cm^{-1} respectively)³⁶ strongly suggests that the amide groups in **5** and **6** are predominantly *cis* in solution. Due to the *cis* conformation of the amide groups, these compounds have a linear ADADA array of five hydrogen bonding sites, in noticeable contrast with the DAD array in 2,6-di(acylamino)pyridines. The formation of a linear ADADA array has two important consequences for the complexation behavior of di(acylamino)triazines:

(i) The amide oxygen atoms in di(acylamino)triazines create additional repulsive secondary interactions in complexes with ADA systems, and thus decrease the binding strength with uracil derivatives (see figure 2.6a).³⁶

(ii) Dimerization constants of di(acylamino)triazines are much higher than dimerization constants of di(acylamino)pyridines. The ADADA array of di(acylamino)triazines allows for dimerization to a complex that is held together by four hydrogen bonds, with the geometry depicted in figure 2.6b.³⁷

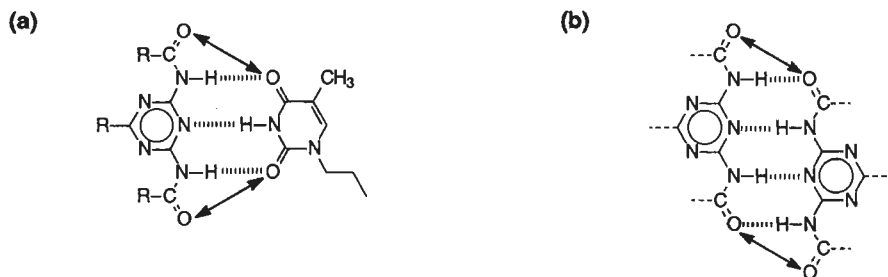


Figure 2.6: (a) Proposed geometry of the complex of *N*-propylthymine (**17**) and di(acetylamino)triazine **5**.

(b) Proposed dimer geometry of di(acylamino)triazines with quadruple hydrogen bonding. Additional repulsive electrostatic interactions are indicated by double-headed arrows.

2.4 Conclusion

2,4-Diamino-*s*-triazines form complexes with uracil derivatives that are as strongly associated as complexes of di(acylamino)pyridines with uracils. Because 6-substituted triazines are synthetically more accessible than 4-substituted di(acylamino)pyridine derivatives, 2,4-diamino-*s*-triazine and uracil represent a convenient couple for supramolecular chemistry. Both units are synthesized in a comparable fashion by simple condensation reactions of nitriles or esters, and β -keto esters, respectively. Furthermore, both units are functionalized in the same fashion with a substituent at the 6-position. The reliability of the triple hydrogen bond as the dominant organizing interaction between diaminotriazines and uracils has been shown by the persistence of the triple hydrogen bonding motif in cocrystals, in the presence of groups capable of additional hydrogen bonding interactions.

The linear ADADA array we propose for acylated diaminotriazines, possible due to the preference for *cis*-amides in these compounds, is not suitable for the formation of complexes with imides. However, acylaminotriazines may be used for the construction of self-complementary complexes via four hydrogen bonds. The interesting possibility to achieve very strong dimerization of self-complementary groups via quadruple hydrogen bonding is explored in the following chapters of this thesis.

2.5 Experimental Section

General methods. Chemicals were purchased from Acros Chimica, Fluka or Aldrich and used as received unless otherwise stated. Compounds **1**, **8**, **10**, **12** and **15** were synthesized analogous to the described methods, and compounds **4**,¹⁰ **16**,¹⁵ and **17**¹⁶ according to literature procedures; all compounds gave satisfactory analyses. All reactions were carried out under an atmosphere of dry nitrogen and solvents were of technical grade, unless otherwise stated. Anhydrous THF and diethyl ether were obtained by distillation from sodium/potassium/benzophenone, analytical grade pyridine, ethanol and iso-propanol were dried over 4 Å molecular sieves. NMR-spectra were recorded on a Varian Gemini 300 or a Bruker AM400. Chemical shifts are given in ppm relative to TMS for proton and carbon spectra. For the ¹H-NMR titrations, deuteriochloroform was used as received. IR-spectra were recorded on a Perkin-Elmer 1600 FT-IR spectrometer. Melting points were determined on a Jenaval THMS 600 melting point microscope and are uncorrected.

Binding experiments. For the ¹H-NMR titrations, CDCl₃ (Cambridge Isotope Laboratories) was used as received, since the chloroform was found to be of sufficient quality: (i) Upon saturation of CDCl₃ from a freshly-opened bottle with water, the association constant of the complexes of di(hexanoylamino)pyridine **20** with uracils **17** and **13** dropped by maximal 20%, (ii) Filtration of CDCl₃ through alumina before the titration did not change the association constant of the complex **2**•**17** significantly (<10%).³⁸ ¹H-NMR titration experiments were performed following the guidelines of Connors,³⁹ Derenleau⁴⁰ and Carta *et al.*⁴¹ Dimerization and association constants were evaluated by fitting the data to the appropriate equation using a nonlinear least squares fitting procedure. When one of the components in a complex showed significant dimerization, the binding model for fitting the

complexation data to obtain the association constant was adopted to a model taking dimerization into account, using the previously determined dimerization constant and its CIS value as fixed parameters.

IR-experiments in chloroform. Dry chloroform for the infrared experiments was obtained by purification of analytical grade chloroform (stabilized with ethanol) by several extractions with water, followed by drying over calcium chloride for two hours, and distillation under an atmosphere of dry nitrogen. Spectra were taken in a 0.1 mm NaCl cell for concentrations higher than 5 mM, and in a 1 mm. cell for lower concentrations (typically 1–5 mM). Solvent contributions were removed by subtraction.

Preparation of diaminotriazine–uracil cocrystals. Unless otherwise stated, cocrystals were obtained by crystallization from excess hot water by slow cooling, followed by slow evaporation in air. Cocrystals of 2,4-diamino-6-dodecyl-s-triazine and 6-tridecyluracil were obtained by slow evaporation of an ethanol/water/dichloromethane 8:1:1 v/v/v solution. Cocrystals of 2,4-diamino-6-dodecyl-s-triazine and 1-*N*-methyl-6-tridecyluracil were obtained by dissolving both components in warm aqueous ethanol, followed by slow cooling and evaporation of solvent in air.

X-ray single crystal structure analyses. Crystals suitable for X-ray structure determination were mounted on a Lindemann-glass capillary, and transferred to an Enraf-Nonius CAD4-T diffractometer on rotating anode (MoK α radiation, graphite monochromator, $\lambda = 0.71073$ Å, $T = 150$ K). Data were corrected for Lorentz-polarization effects and for linear instability in the periodically measured reference reflections, but not for absorption. The unit-cell parameters were checked for the presence of higher lattice symmetry.⁴² The structures were solved by automated direct methods (SHELXS-86⁴³). Refinement on F^2 was carried out by full-matrix least-squares techniques (unless otherwise stated: SHELXL-93⁴⁴). No observance criterion was applied during refinement. All hydrogen atoms were located on different Fourier maps; their coordinates were included as parameters in the refinement. All non-hydrogen atoms were refined with anisotropic thermal parameters. Hydrogen atoms were refined with a fixed isotropic thermal parameter related to the value of the equivalent isotropic displacement parameter of their carrier atoms.

Crystal data for compound 5: C₉H₁₃N₅O₃, $M_r = 239.23$, colourless, plate-shaped crystal (0.05 x 0.2 x 0.7 mm), triclinic, space group $P\bar{1}$ (no. 2) with $a = 8.7289$ (8), $b = 10.9012$ (7), $c = 11.5137$ (7) Å, $\alpha = 95.915$ (5), $\beta = 93.588$ (6), $\gamma = 93.153$ (6)°, $V = 1085.54$ (14) Å³, $Z = 4$, $D_c = 1.464$ g.cm⁻³, $F(000) = 504$, $\mu(\text{Mo K}\alpha) = 1.1$ cm⁻¹. 8465 Reflections measured, 4985 independent reflections, $R_{\text{int}} = 0.033$ ($1.78^\circ < \theta < 27.50^\circ$), and 385 parameters. Final $wR2 = 0.106$, $w = 1/[\sigma^2(F^2) + (0.004P)^2 + 0.28P]$, $R1 = 0.043$ (for 3791 $I > 2\sigma(I)$), $S = 1.04$, $-0.26 < \Delta\rho < 0.24$ e Å⁻³.

Crystal data for complex 2•11: C₁₅H₂₉N₅•C₁₇H₃₀N₂O₂, $M_r = 573.87$, colourless plate-shaped crystal (0.02 x 0.6 x 1.0 mm), triclinic, space group $P\bar{1}$ (no. 2), with $a = 6.7134$ (13), $b = 7.7297$ (7), $c = 31.988$ (3) Å, $\alpha = 93.917$ (7), $\beta = 91.894$ (11), $\gamma = 93.704$ (12)°, $V = 1651.4$ (4) Å³, $Z = 2$, $D_c = 1.154$ g.cm⁻³, $F(000) = 632$, $\mu(\text{Mo K}\alpha) = 0.7$ cm⁻¹. 12414 Reflections measured, 7576 independent reflections, $R_{\text{int}} = 0.064$ ($0.64^\circ < \theta < 27.50^\circ$), 547 parameters. Final $wR2 = 0.174$, $w = 1/[\sigma^2(F^2) + (0.0567P)^2]$, $R1 = 0.071$ (for 3332 $I > 2\sigma(I)$), $S = 1.02$, $-0.25 < \Delta\rho < 0.24$ e Å⁻³.

Crystal data for complex 2•13: C₁₅H₂₉N₅•C₁₈H₃₂N₂O₂, $M_r = 587.90$, colourless, needle-shaped crystal (0.05 x 0.05 x 0.3 mm), triclinic, space group $P\bar{1}$ (no. 2), with $a = 11.779$ (6), $b = 12.319$ (8), $c = 13.782$ (6) Å, $\alpha = 66.71$ (4), $\beta = 75.94$ (4), $\gamma = 73.97$ (4)°, $V = 1745.1$ (19) Å³, $Z = 2$, $D_c = 1.119$ g.cm⁻³, $F(000) = 648$, $\mu(\text{Mo K}\alpha) = 0.7$ cm⁻¹. 6432 Reflections measured, 5494 independent reflections, $R_{\text{int}} = 0.0918$ ($1.63^\circ < \theta < 25.0^\circ$), and 392 parameters. Hydrogen atoms were included on calculated positions. The atoms C(117) through C(120) of the dodecyl group are disordered over two positions. Final $wR2 = 0.2104$, $w = 1/[\sigma^2(F^2) + (0.01P)^2 + 4.0P]$, $R1 = 0.0974$ (for 2696 $I > 2\sigma(I)$), $S = 1.299$, $-0.33 < \Delta\rho < 0.40$ e Å⁻³.

Crystal data for complex 4•15: $C_4H_7N_5O \cdot C_5H_8N_2O_3$, $M_r = 283.24$, colourless, block-shaped crystal (0.3 x 0.5 x 0.7 mm), triclinic, space group $P\bar{1}$ (no. 2) with $a = 6.9057$ (6), $b = 9.0323$ (8), $c = 10.0639$ (8) Å, $\alpha = 73.793$ (7), $\beta = 72.431$ (7), $\gamma = 80.202$ (7)°, $V = 572.13$ (10) Å³, $Z = 2$, $D_c = 1.644$ g.cm⁻³, $F(000) = 296$, $\mu(Mo K\alpha) = 1.3$ cm⁻¹. 5391 Reflections measured, 2610 independent reflections, $R_{int} = 0.078$ ($2.19^\circ < \theta < 27.50^\circ$), and 220 parameters. Final $wR2 = 0.137$, $w = 1/[\sigma^2(F^2) + (0.0466P)^2 + 0.06P]$, $R1 = 0.052$ (for 1479 $I > 2\sigma(I)$), $S = 1.01$, for $-0.27 < \Delta\rho < 0.32$ e Å⁻³.

Crystal data for complex 1•16: $C_4H_7N_5 \cdot C_6H_8N_2O_3 \cdot H_2O$, $M_r = 299.29$, colourless, block-shaped crystal (0.1 x 0.2 x 0.4 mm), triclinic, space group $P\bar{1}$ (no. 2), with $a = 6.9536$ (4), $b = 7.3103$ (6), $c = 13.2804$ (7) Å, $\alpha = 94.337$ (5), $\beta = 102.548$ (5), $\gamma = 96.874$ (5)°, $V = 650.61$ (8) Å³, $Z = 2$, $D_c = 1.528$ g.cm⁻³, $F(000) = 316$, $\mu(Mo K\alpha) = 1.2$ cm⁻¹. 4839 Reflections measured, 2977 independent reflections, $R_{int} = 0.0275$, ($1.58^\circ < \theta < 27.5^\circ$), and 241 parameters. Positional parameters of the hydrogen atoms were refined. Final $wR2 = 0.1134$, $w = 1/[\sigma^2(F^2) + (0.0528P)^2 + 0.15P]$, $R1 = 0.0425$ (for 2055 $I > 2\sigma(I)$), $S = 1.036$, $-0.22 < \Delta\rho < 0.33$ e Å⁻³.

Crystal data for 1:1 complex 1•12: $C_4H_7N_5 \cdot C_6H_8N_2O_2 \cdot 3H_2O$, $M_r = 319.33$, colourless, needle-shaped crystal (0.1 x 0.1 x 0.4 mm), triclinic, space group $P\bar{1}$ (no. 2) with $a = 7.2290$ (6), $b = 9.1350$ (9), $c = 12.2020$ (9) Å, $\alpha = 107.15$ (7), $\beta = 103.27$ (6), $\gamma = 94.52$ (7)°, $V = 740.0$ (4) Å³, $Z = 2$, $D_c = 1.433$ g.cm⁻³, $F(000) = 340$, $\mu(Mo K\alpha) = 1.2$ cm⁻¹. 6999 Reflections measured, 3388 independent reflections, $R_{int} = 0.0456$, ($1.82^\circ < \theta < 27.5^\circ$), and 262 parameters. Positional parameters of the hydrogen atoms were refined. Final $wR2 = 0.1406$, $w = 1/[\sigma^2(F^2) + (0.0800P)^2 + 0.05P]$, $R1 = 0.0495$ (for 2391 $I > 2\sigma(I)$), $S = 1.011$, $-0.32 < \Delta\rho < 0.25$ e Å⁻³.

Crystal data for complex 4•16: $C_4H_7N_5O \cdot C_6H_8N_2O_3 \cdot 2H_2O$, $M_r = 333.31$, colourless, needle-shaped crystal (0.05 x 0.05 x 0.8 mm), monoclinic, space group $P2_1/c$ (no.14), with $a = 6.8342$ (10), $b = 17.246$ (2), $c = 12.3853$ (12) Å, $\alpha = 90$, $\beta = 95.194$ (10), $\gamma = 90^\circ$, $V = 1453.8$ (3) Å³, $Z = 4$, $D_c = 1.523$ g.cm⁻³, $F(000) = 704$, $\mu(Mo K\alpha) = 1.3$ cm⁻¹. 5589 Reflections measured, 3302 independent reflections, $R_{int} = 0.0808$, ($1.18^\circ < \theta < 27.5^\circ$), and 260 parameters. Positional parameters of the hydrogen atoms were refined, except for the disordered hydrogen atoms of water, which were included in a rigid group. Final $wR2 = 0.1819$, $w = 1/[\sigma^2(F^2) + (0.0488P)^2]$, $R1 = 0.0808$ (for 1445 $I > 2\sigma(I)$), $S = 1.038$, $-0.38 < \Delta\rho < 0.34$ e Å⁻³.

Crystal data for 1:2 complex 1•12: $C_4H_7N_5 \cdot 2C_6H_8N_2O_2$, $M_r = 405.41$, colourless, plate-shaped crystal (0.05 x 0.5 x 0.5 mm), triclinic, space group $P\bar{1}$ (no. 2) with $a = 8.8253$ (9), $b = 9.4084$ (15), $c = 12.377$ (2) Å, $\alpha = 107.271$ (12), $\beta = 98.762$ (9), $\gamma = 105.526$ (11)°, $V = 915.0$ (3) Å³, $Z = 2$, $D_c = 1.472$ g.cm⁻³, $F(000) = 428$, $\mu(Mo K\alpha) = 1.1$ cm⁻¹. 4900 Reflections measured, 4174 independent reflections, $R_{int} = 0.0556$, ($1.78^\circ < \theta < 27.5^\circ$), and 331 parameters. The structure was solved with SIR-88, and refined using SHELXL-93. Positional parameters of the hydrogen atoms were refined. Final $wR2 = 0.1968$, $w = 1/[\sigma^2(F^2) + (0.0976P)^2 + 0.22P]$, $R1 = 0.0667$ (for 2539 $I > 2\sigma(I)$), $S = 1.039$, $-0.27 < \Delta\rho < 0.50$ e Å⁻³.

2,4-Diamino-6-dodecyl-s-triazine (2). Tridecanitril (20.3 g, 0.104 mol) was heated under reflux overnight with dicyanodiamide (9.18 g, 0.109 mol), and potassium hydroxide (1.77 g, 0.031 mol) in dry *i*-propanol (120 mL). After cooling to ambient temperature, ice-water was added. The resultant white precipitate was filtered, and was crystallized from water/ethanol 1:1 v/v yielding large colourless plates (70%). These crystals appeared to contain the product and starting material in a 1:1 ratio.⁴⁵ Dissolving the solid in warm methanol and subsequent addition of a large amount of hexane caused 2 to precipitate as tiny needles. Repeating this procedure gave pure 2 (8.72 g, 30%, mp 121.5°C). ¹H-NMR (CDCl₃) δ : 5.12 (br, 4H), 2.48 (t, 3H), 1.69 (m, 2 H), 1.26 (m, 18 H), 0.88 (t, 3H). ¹³C-NMR (CDCl₃) δ : 179.7, 167.1, 38.8, 31.9, 29.6, 29.6, 29.5, 29.4, 29.3, 27.9, 22.7, 14.1. IR (KBr) ν : 3493,

3452, 3394, 3315, 3144, 2916, 2850, 1628, 1550, 1433 cm^{-1} . Anal. calcd for $\text{C}_{15}\text{H}_{29}\text{N}_5$: C, 64.48; H, 10.46; N, 25.06. Found: C, 64.09; H, 10.59; N, 24.88.

2,4-Diamino-6-methoxymethyl-*s*-triazine (3). A mixture of dicyanodiamide (31.0 g, 0.37 mol), methoxyacetonitrile⁴⁶ (29.2 mL, 0.34 mol) and potassium hydroxide (5.70 g, 84 mmol) in dry *iso*-propanol (240 mL) was heated under reflux overnight. After cooling to 0°C, the resulting white precipitate was filtered off, and washed with cold water (50.5 g, 88%). An analytical sample was prepared by crystallization from hot water, giving colourless plates. Only after thoroughly drying at 50°C *in vacuo*, satisfactory elemental analysis of **3** was obtained, mp 258–260°C (with decomposition and sublimation; solid phase transition at 244–250°C). ¹H-NMR (DMSO-*d*₆) δ : 6.95, 6.75 (br, 4H), 4.05 (s, 2H), 3.29 (s, 3H). ¹³C-NMR (DMSO-*d*₆) δ : 174.6, 167.3, 74.2, 58.5. IR (KBr) ν : 3385, 3333, 3231, 3146, 1667, 1638, 1546, 1469 cm^{-1} . Anal. calcd for $\text{C}_5\text{H}_9\text{N}_5\text{O}$: C, 38.71; H, 5.85; N, 45.14. Found: C, 39.06; H, 5.77; N, 45.50.

2,4-Di(acetylamino)-6-methoxymethyl-*s*-triazine (5). To 2,4-diamino-6-methoxymethyl-*s*-triazine **3** (8.55 g, 50 mmol), acetic anhydride (50 mL) was added (no reaction occurred). After boiling for 15 min under reflux, the suspension had turned into a clear solution, and reflux was continued for 2 h. After cooling, most of the acetic anhydride was removed *in vacuo*. Then, diethyl ether was added, and the resultant suspension was filtered and washed thoroughly with diethyl ether. After drying at 50°C *in vacuo*, crude **5** was obtained (8.14 g, 68%). An analytical sample of **5**, as suitable X-ray quality crystals, was prepared by crystallization from hot ethyl acetate after treatment with active charcoal, mp 165–166°C (solid phase transition at 158–160°C). ¹H-NMR (CDCl_3) δ : 9.67 (br, 2H), 4.54 (s, 2H), 3.53 (s, 3H), 2.56 (s, 6H). ¹³C-NMR (CDCl_3) δ : 178.8, 172.6, 164.4, 74.4, 60.0, 26.5. IR (KBr) ν : 3477, 3294, 3162, 2932, 1737, 1688, 1589, 1496, 1298 cm^{-1} . Anal. calcd for $\text{C}_9\text{H}_{13}\text{N}_5\text{O}_3$: C, 45.19; H, 5.48; N, 29.27. Found: C, 45.24; H, 5.31; N, 29.16.

2,4-Di(hexanoylamino)-6-methoxymethyl-*s*-triazine (6). To a suspension of 2,4-diamino-6-methoxymethyl-*s*-triazine (8.55 g, 50 mmol) in boiling dry pyridine (35 mL), hexanoyl chloride (14 mL, 0.102 mol) was added slowly. After 20 min refluxing, a clear solution had formed, which was then cooled to ambient temperature. Addition of ethyl acetate (100 mL) gave a suspension which was filtered. The filtrate was evaporated and the residue was dissolved in dichloromethane. The solution was washed with dilute sodium bicarbonate solution and with water, dried over sodium sulfate, filtered and concentrated to ca. 50 mL. Addition of a large amount of hexane caused **6** to precipitate slowly. The product was filtered and washed with hexane, and the precipitation procedure was repeated once more. Drying *in vacuo* gave pure **6** (12.91 g, 74%). An analytical sample was prepared by dissolving in hot ethyl acetate, treatment with active charcoal and filtration. Adding hexane caused the product to precipitate as white grains, mp 82–83°C. ¹H-NMR (CDCl_3) δ : 9.91 (br, 2H), 4.50 (s, 2H), 3.50 (s, 3H), 2.83 (t, 4H), 1.68 (m, 4H), 1.30 (m, 8H), 0.88 (t, 6H). ¹³C-NMR (CDCl_3) δ : 178.8, 175.5, 164.4, 74.4, 59.9, 38.4, 31.9, 24.9, 22.9, 14.4. IR (KBr) ν : 3252, 3201, 3145, 2955, 2928, 2871, 1736, 1891, 1583, 1485, 1381, 1322 cm^{-1} . Anal. calcd for $\text{C}_{17}\text{H}_{29}\text{N}_5\text{O}_3$: C, 58.10; H, 8.32; N, 19.93. Found: C, 57.89; H, 8.40; N, 19.70.

2,4-Di(pivaloylamino)-6-methyl-*s*-triazine (7). To a suspension of 2,4-diamino-6-methyl-*s*-triazine (6.26 g, 50 mmol) in boiling dry pyridine (110 mL), pivaloyl chloride (2.6 mL, 0.102 mol) was added slowly via a syringe. After boiling under reflux for 75 min, the clear solution was poured into ice-water. The resultant precipitate was filtered, and dissolved in dichloromethane. The dichloromethane phase was extracted with water, dried over sodium sulfate, filtered and partially evaporated. Addition of a large amount of hexane caused the product to precipitate as off-white crystals (9.65 g, 66%). Recrystallization from hot ethanol/water 1:3 v/v yielded crystals of the hydrate of **7**, mp (of the anhydrate) 221–222°C (loss of crystal water and sublimation to anhydrous crystals from 151–213°C;

sublimation to liquid 213–221°C). $^1\text{H-NMR}$ (CDCl_3) δ : 8.35 (br, 2 H), 2.58 (s, 3H), 1.32 (s, 18 H). $^{13}\text{C-NMR}$ (CDCl_3) δ : 179.2, 176.3, 163.9, 40.5, 27.1, 25.8. IR (KBr) ν : 3477, 3263, 2975, 1708, 1588, 1487, 1397, 1360 cm^{-1} . Anal. calcd. for $\text{C}_{14}\text{H}_{23}\text{N}_5\text{O}_2 \cdot 0.5 \text{H}_2\text{O}$: C, 55.61; H, 8.00; N, 23.16. Found: C, 55.56; H, 7.83; N, 23.24.

6-Tridecyl-thiouracil (9). Ethyl 3-oxopalmitoate was prepared first, using the method described by Huckin.⁴⁷ To 60% sodium hydride (4.42 g, 0.11 mol) in dry THF (250 mL), was added at 0 °C ethyl acetoacetate (13.0 g, 0.10 mol). After stirring at this temperature for 15 min, 1.6 M *n*-butyllithium in hexane (65.6 mL, 0.105 mol) was added dropwise with a syringe at the same temperature. After stirring for 15 min at 0°C, dodecyl bromide (27.6 g, 0.11 mol) was added. Then the temperature was allowed to rise to room temperature during 30 min, whereupon the mixture was poured into acidified ice-water and extracted several times with diethyl ether. The combined diethyl ether layers were copiously washed with water, dried over sodium sulfate and evaporated to dryness to yield a yellow oil (33.77 g). NMR showed the oil to consist of ethyl 3-oxopalmitoate and unreacted dodecyl bromide in a ~ 3:2 ratio (yield 67%). This crude product was used without purification.

The condensation reaction of the keto-ester with thiourea to yield the thiouracil was performed analogous to the method of Gershon.⁴⁸ Freshly cut sodium (2.17 g, 0.094 mol) was dissolved in dry ethanol (94 mL). To the solution were added subsequently thiourea (5.0 g, 0.066 mol) and crude ethyl 3-oxo-palmitoate (23.7 g, ca. 0.047 mol) at once. After refluxing overnight, the solution was cooled to ambient temperature and acidified with dilute hydrochloric acid. After removal of most of the solvent in vacuo, the product was filtered off. Crystallization from ethanol gave pure **9** (8.39 g, 57%). An analytical sample was prepared by recrystallization from water:ethanol 4/1 v/v, mp 154–155°C. $^1\text{H-NMR}$ ($\text{DMSO}-d_6$) δ : 12.34 and 12.00 (br, 2 H), 5.66 (s, 1H), 2.32 (t, 2H), 1.31 (m, 2H), 1.21 (m, 20 H), 0.82 (t, 3H). $^{13}\text{C-NMR}$ ($\text{DMSO}-d_6$) δ : 176.4, 161.4, 103.2, 31.7, 29.4, 29.3, 29.1 (overlapping peaks), 29.0, 28.7, 27.6, 22.5, 14.3. IR (KBr) ν : 3058, 2955, 2918, 2849, 1662, 1639, 1585 cm^{-1} . Anal. calcd for $\text{C}_{17}\text{H}_{30}\text{N}_2\text{OS}$: C, 65.76; H, 9.74; N, 9.02. Found: C, 65.89; H, 9.78; N, 9.06.

6-Tridecyluracil (11). 6-Tridecylthiouracil (4.10 g, 13 mmol) and chloroacetic acid (2.49 g, 26 mmol) were heated under reflux in water (26 mL) in air during 6 h, whereafter a clear water-layer with a floating pasty oil was obtained. After adding concentrated hydrochloric acid (6.5 mL), refluxing was continued overnight to yield a clear liquid containing crystals. After cooling in an ice bath, the crystals were filtered off and recrystallized from chloroform, then from ethanol/water 4:1 v/v to yield **11** as tiny white needles (3.25 g, 85%), mp 172–173.5°C. $^1\text{H-NMR}$ ($\text{DMSO}-d_6$) δ : 10.88 and 10.78 (br, 2H), 5.30 (s, 1H), 2.24 (t, 2H), 1.51 (m, 2 H), 1.22 (m, 20H), 0.83 (t, 3H). $^{13}\text{C-NMR}$ ($\text{DMSO}-d_6$) δ : 165.0, 157.2, 152.0, 98.2, 32.0, 31.8, 29 (overlapping peaks), 27.6, 22.1, 13.9. IR (KBr) ν : 2954, 2920, 2847, 1740, 1650 cm^{-1} . Anal. calcd for $\text{C}_{17}\text{H}_{30}\text{N}_2\text{O}_2$: C, 69.35; H, 10.27; N, 9.51. Found: C, 69.60; H, 10.44; N, 9.22.

1-*N*-methyl-6-tridecyluracil (13). 2,4-Bis(trimethylsilyloxy)-6-tridecylpyrimidine was prepared as described for 2,4-bis(trimethylsilyloxy)-6-trimethylsilyloxymethyl-pyrimidine (vide infra). The crude product was distilled quickly with the aid of a burner (79%, bp 205°C, 0.8 mm Hg). $^1\text{H-NMR}$ (CDCl_3) δ : 6.09 (s, 1H), 2.48 (t, 2H), 1.59 (m, 2H), 1.21–1.18 (m, 20 H), 0.81 (t, 3 H), 0.31 (s, 18 H). $^{13}\text{C-NMR}$ (CDCl_3) δ : 174.5, 170.1, 163.1, 102.2, 32.6, 31.7, 29.6, 29.5, 29.4 (overlapping peaks), 29.3, 28.5, 22.7, 14.1, 0.4.

The distilled 2,4-bis(trimethylsilyloxy)-6-tridecylpyrimidine (3.79 g, 86.4 mmol) was set aside with freshly distilled methyl iodide (10 mL) under nitrogen in the dark. After a period of two weeks, ethanol was added, and the methyl iodide evaporated in vacuo into a cold trap. Dilute hydrochloric acid was added, and the product was filtered. The product was dissolved in chloroform, and the chloroform solution was successively extracted with dilute hydrochloric acid, dilute potassium permanganate

solution in dilute acid, sodium sulfite solution, dilute hydrochloric acid and water. The chloroform layer was dried over sodium sulfate, filtered and diluted with hexane. Partial evaporation of the solvent gave a white precipitate, which was filtered off. Crystallization from water/ethanol 1:1 v/v, then from ethanol gave analytically pure **13** as tiny white needles (1.84 g, 54% based on uracil **11**, mp 138.6–139.8°C). $^1\text{H-NMR}$ (CDCl_3) δ : 10.19 (br, 1H), 5.50 (s, 2H), 3.31 (s, 3H), 2.40 (t, 2H), 1.52 (m, 2H), 1.33 (m, 2H), 1.19 (m, 8 H), 0.81 (t, 3H). $^{13}\text{C-NMR}$ (CDCl_3) δ : 163.3, 157.6, 152.2, 100.6, 32.6, 31.8, 30.3, 29.5 (overlapping peaks), 29.4, 29.3, 29.2, 29.1, 28.9, 27.0, 22.5, 14.0. IR (KBr) ν : 3176, 3044, 2953, 2922, 2848, 1717, 1679 cm^{-1} . Anal. calcd for $\text{C}_{18}\text{H}_{32}\text{N}_2\text{O}_2$: C, 70.09; H, 10.46; N, 9.08. Found: C, 70.38; H, 10.78; N, 8.99.

Column chromatography (silica, CHCl_3 :MeOH 200:3 v/v) of the mother liquor from the recrystallization of **13** afforded another fraction of pure **13** (0.31 g, 9% based on uracil **11**) ($R_f = 0.20$), and a small amount of 3-*N*-methyl-6-tridecyluracil (**14**) (0.25 g, 7% based on uracil **11**, mp 147.0–147.4°C) ($R_f = 0.30$). $^1\text{H-NMR}$ (CDCl_3) δ : 10.61 (br, 1H), 5.59 (s, 2H), 3.30 (s, 3H), 2.39 (t, 2H), 1.64 (m, 2H), 1.32 (m, 2H), 1.25 (m, 18H), 0.87 (t, 3H). $^{13}\text{C-NMR}$ (CDCl_3) δ : 163.7, 153.8, 153.5, 99.2, 32.6, 31.8, 29.6 (overlapping peaks), 29.5, 29.4, 29.3, 29.1, 28.9, 27.0, 26.8, 22.6, 14.0. IR (KBr) ν : 3420, 2919, 2850, 1738, 1637, 1598 cm^{-1} . Anal. calcd for $\text{C}_{18}\text{H}_{32}\text{N}_2\text{O}_2$: C, 70.09; H, 10.46; N, 9.08. Found: C, 70.92; H, 10.41; N, 8.68. MS: m/e 308.30 (M^+ , 4.6%).

1-*N*-Methyl-6-hydroxymethyluracil (16). To a suspension of 6-hydroxymethyluracil¹⁵ (9.95 g, 70 mmol) in dry THF (500 mL) were added trimethylsilyl chloride (28 mL, 0.22 mol) at once, and dry triethylamine (22 mL, 0.22 mol) in THF (200 mL) dropwise (analogous to the method of Nishimura).⁴⁹ After stirring overnight, the suspension was filtered (under nitrogen). The white cake was thoroughly extracted with dry THF. The combined filtrates were evaporated to dryness. The residual yellow oil was distilled (23.72 g, 95%, bp 109°C, 0.05 mmHg). The product, 2,4-bis(trimethylsilyloxy)-6-trimethylsilyloxymethylpyrimidine, is extremely sensitive to moisture. $^1\text{H-NMR}$ (CDCl_3) δ : 6.21 (s, 1H), 4.23 (s, 2H), 0.25 (s, 18H), 0.02 (s, 9H). $^{13}\text{C-NMR}$ (CDCl_3) δ : 174.1, 171.2, 163.1, 100.2, 64.9, 0.8, 0.8, 0.2.

To the distilled 2,4-bis(trimethylsilyloxy)-6-trimethylsilyloxymethylpyrimidine (23.7 g, 66 mmol) was added freshly distilled methyl iodide (ca. 100 mL), under an atmosphere of dry nitrogen. After standing in the dark for two weeks, 1 M hydrochloric acid (300 mL) was added. After stirring for 1 h, methyl iodide was distilled off under reduced pressure into a cold trap. The water layer was extracted repeatedly with diethyl ether which removed the yellow colour. The water layer was then neutralized to pH = 7 and evaporated to ca. 200 mL. Cooling to 0°C gave pure **16** as nice crystals (5.49 g, 53%, mp 235–237°C, slight dec. starting at 230°C). Another 20% yield of **16** was obtained by evaporation of the mother liquor to dryness, extraction of the residual solid with hot DMSO, evaporation of this DMSO solution to dryness, and finally crystallization from water. $^1\text{H-NMR}$ ($\text{DMSO}-d_6$) δ : 5.70 (br, 1H), 5.60 (s, 1H), 4.33 (s, 2H), 3.19 (s, 3H) ppm. $^{13}\text{C-NMR}$ ($\text{DMSO}-d_6$) δ : 163.2, 158.1, 152.2, 98.3, 59.3, 29.3 ppm. IR (KBr) ν : 3286, 3174, 3045, 1714, 1674 cm^{-1} . Anal. calcd for $\text{C}_6\text{H}_8\text{N}_2\text{O}_3$: C, 46.15; H, 5.16; N, 17.94. Found: C, 46.43; H, 5.41; N, 17.95.

2-Amino-6-hexanoylamino-6-pyridine (19). To a well-stirred solution of 2,6-diaminopyridine (2.18 g, 20 mmol) in dry THF (40 mL) and triethylamine (2.9 mL, 20.5 mmol) was added dropwise hexanoyl chloride (2.69 g, 20 mmol) at 0°C. After 10 min, the precipitate was filtered and the filtrate evaporated to dryness. The product mixture was dissolved in chloroform and extracted 5 times with water, which removed 2,6-diaminopyridine **18** quantitatively (**19** is insoluble in water). Column chromatography with 3% methanol in chloroform (product: $R_f = 0.21$; bis derivative: $R_f = 0.44$) followed by crystallization from hexane/dichloromethane afforded pure **19** as tiny needles (1.39 g, 57%, mp 81.8–82.4°C). A 13% yield fraction of bis derivative **20** was also obtained. $^1\text{H-NMR}$ (CDCl_3) δ : 7.76 (br,

1H), 7.54 (d, 1H), 7.44 (t, 1H), 6.24 (d, 1H), 4.33 (br, 2H), 2.32 (t, 2H), 1.70 (m, 2H), 1.32 (m, 4H), 0.89 (t, 3H). ¹³C-NMR (CDCl₃) δ: 171.9, 157.1, 149.9, 139.9, 104.0, 103.1, 37.3, 31.1, 24.9, 22.1, 13.7. IR (KBr) ν: 3477, 3362, 3235, 2954, 2927, 2857, 1673, 1622 cm⁻¹. Anal. calcd. for C₁₁H₁₇N₃O: C, 63.74; H, 8.27; N, 20.27. Found: C, 64.10; H, 8.39; N, 20.29.

2,6-Di(hexanoylamino)pyridine (20). In an attempt to synthesize the mono(hexanoylamino)pyridine **19**, to a solution of 2,6-diaminopyridine **18** (1.09 g, 0.01 mol) in dry pyridine (20 mL) was added hexanoyl chloride (1.54 mL, 0.011 mol) at 0°C. After stirring at ambient temperature overnight, the solution was evaporated to dryness, and the residue dissolved in chloroform. The chloroform solution was extracted with water three times, dried over sodium sulfate, and evaporated to dryness. Analytically pure **20** was obtained in 42% yield by crystallization from hexane/ethyl acetate 1:2 v/v with norit treatment, mp 127–128°C. No trace of mono-acylated compound could be found in the mother liquor. ¹H-NMR **20** (CDCl₃) δ: 8.24 (br, 2H), 7.93 (d, br, 2H), 7.64 (t, 1H), 2.34 (tr, 4H), 1.66 (m, 4H), 1.30 (m, 8H), 0.88 (t, 6H). ¹³C-NMR (CDCl₃) δ: 171.8, 149.5, 140.3, 109.3, 37.3, 31.1, 24.8, 22.1, 13.6. IR (KBr) ν: 3246, 3040, 2960, 2931, 2858, 1661, 1585, 1526, 1447 cm⁻¹. Anal. calcd. for C₁₇H₂₇N₃O₂: C, 66.85; H, 8.91; N, 13.76. Found: C, 66.73; H, 8.96; N, 13.67.

2,6-Di(acetylamino)pyridine (21). To a solution of 2,6-diaminopyridine **18** (1.09 g, 10 mmol) in dry pyridine (7 mL) was added acetic anhydride (2.4 mL, 25 mmol). After stirring at ambient temperature overnight, the solution was evaporated to dryness. Recrystallization of the residue from water afforded 1.83 g of pure **21** (95% yield), mp 210–210.5°C. ¹H-NMR (CDCl₃) δ: 7.90 (d, br, 2H), 7.74 (tr, 1H), 7.57 (br, 2H), 2.20 (s, 6H). ¹³C-NMR (DMSO-*d*₆) δ: 169.6, 150.7, 140.2, 109.2, 24.4. IR (KBr) ν: 3292, 3252, 3194, 3150, 3048, 1678, 1584, 1529, 1450, 1300, 1244 cm⁻¹. Anal. calcd. for C₉H₁₁N₃O₂: C, 55.69; H, 5.71; N, 21.65. Found: C, 55.68; H, 5.71; N, 21.71.

References and Footnotes

- 1) (a) J.-M. Lehn, *Makromol. Chem., Macromol. Symp.*, **1993**, *69*, **1**, (b) J.-M. Lehn, M. Mascal, A. DeCian, J. Fischer, *J. Chem. Soc., Perkin Trans. 2*, **1992**, 461, (c) T.M. Bohano, S. Denzinger, R. Fink, W. Paulus, H. Ringsdorf, M. Weck, *Angew. Chem. Int. Ed. Eng.*, **1995**, *34*, 58, (d) M. Mascal, P.S. Fallon, A.S. Batsanov, B.R. Heywood, S. Champ, M. Coldough, *J. Chem. Soc., Chem. Commun.*, **1995**, 805.
- 2) R.F.M. Lange, E.W. Meijer, *Macromolecules*, **1995**, *28*, 782.
- 3) (a) B. Feibush, A. Figueroa, R. Charles, K.D. Onan, P. Feibush, B.L. Karger, *J. Am. Chem. Soc.*, **1986**, *108*, 3310, (b) A. D. Hamilton, D. van Engen, *J. Am. Chem. Soc.*, **1987**, *109*, 5035, (c) A.D. Hamilton, N. Pant, A.V. Muehldorf, *Pure & Appl. Chem.*, **1988**, *60*, 533, (d) A. V. Muehldorf, D. van Engen, J.C. Warner, A.D. Hamilton, *J. Am. Chem. Soc.*, **1988**, *110*, 6561, (e) M.-J. Brienne, J. Gabard, J.-M. Lehn, I. Stibor, *J. Chem. Soc., Chem. Comm.*, **1989**, 1868, (f) A.D. Hamilton, A. Muehldorf, S.-K. Chang, N. Pant, S. Goswam, D. Van Engen, *J. Incl. Phenom. Molec. Reco. Chem.*, **1989**, *7*, 27, (g) A.D. Hamilton, D. Little, *J. Chem. Soc., Chem. Commun.*, **1990**, 297, (h) S.J. Geib, S.C. Hirst, C. Vicent, A.D. Hamilton, *J. Chem. Soc., Chem. Commun.*, **1991**, 1283, (i) S.-K. Chang, D. Van Engen, E. Fan, A.D. Hamilton, *J. Am. Chem. Soc.*, **1991**, *113*, 7640, (j) M. S. Goodman, S.D. Rose, *J. Am. Chem. Soc.*, **1991**, *113*, 9380, (k) T. Gulik-Krzywicki, C. Fouquey, J.-M. Lehn, *Proc. Natl. Acad. Scie. USA*, **1993**, *90*, 163, (l) C. Fouquey, J.-M. Lehn, A.-M. Levelut, *Adv. Mat.*, **1990**, *2*, 254, (m) M. Kotera, J.-M. Lehn, J.-P. Vigneron, *J. Chem. Soc., Chem. Commun.*, **1994**, 197, (n) N. Tamura, K. Mitsui, T.

- Nabeshima, Y. Yano, *J. Chem. Soc., Perkin Trans. 2*, **1994**, 2229, (o) P. Tecilla, V. Jubian, A.D. Hamilton, *Tetrahedron*, **1995**, 51, 435.
- 4) (a) G. M. Whitesides, E.E. Simanek, J.P. Mathias, C.T. Seto, D.N. Chin, M. Mammen, D.M. Gordon, *Acc. Chem. Res.*, **1995**, 28, 37, (b) C.T. Seto, G.M. Whitesides, *J. Am. Chem. Soc.*, **1990**, 112, 6409, (c) J. A. Zerkowski, C.T. Seto, D.A. Wierda, G.M. Whitesides, *J. Am. Chem. Soc.*, **1990**, 112, 9025, (d) C.T. Seto, G.M. Whitesides, *J. Am. Chem. Soc.*, **1991**, 113, 712, (e) J.A. Zerkowski, C.T. Seto, G.M. Whitesides, *J. Am. Chem. Soc.*, **1992**, 114, 5473, (f) C.T. Seto, G.M. Whitesides, *J. Am. Chem. Soc.*, **1993**, 115, 905, (g) J.P. Mathias, C.T. Seto, E.E. Simanek, G. M. Whitesides, *J. Am. Chem. Soc.*, **1994**, 116, 1725, (h) J.A. Zerkowski, J.C. MacDonald, C.T. Seto, D.A. Wierda, G. M. Whitesides, *J. Am. Chem. Soc.*, **1994**, 116, 2383, (i) J.A. Zerkowski, G.M. Whitesides, *J. Am. Chem. Soc.*, **1994**, 116, 4298, (j) J.P. Mathias, E.E. Simanek, J.A. Zerkowski, C.T. Seto, G. M. Whitesides, *J. Am. Chem. Soc.*, **1994**, 116, 4316, (k) J.P. Mathias, E.E. Simanek, G.M. Whitesides, *J. Am. Chem. Soc.*, **1994**, 116, 4326, (l) J.C. MacDonald, G.M. Whitesides, *Chem. Rev.*, **1994**, 2383, (m) E.E. Simanek, M. Mammen, D.M. Gordon, D. Chin, J.P. Mathias, C.T. Seto, G.M. Whitesides, *Tetrahedron*, **1995**, 51, 607, (n) E.E. Simanek, M.I.M. Wazeer, J.P. Mathias, G.M. Whitesides, *J. Org. Chem.*, **1994**, 59, 4904, (o) J.S. Lindsey, P.C. Kearney, *J. Am. Chem. Soc.*, **1988**, 110, 6575, (p) N. Kimizuka, T. Kawasaki, T. Kunitake, *J. Am. Chem. Soc.*, **1993**, 115, 4387, (q) N. Tamura, K. Kajiki, T. Nabeshima, Y. Yano, *J. Chem. Soc., Chem. Commun.*, **1994**, 2583, (r) K.C. Russell, E. Leeze, A. Van Dorsselaer, J.-M. Lehn, *Angew. Chem.*, **1995**, 107, 244, (s) N. Kimizuka, T. Kawasaki, K. Hirata, T. Kunitake, *J. Am. Chem. Soc.*, **1995**, 117, 6360.
- 5) (a) R. Ahuja, P.-L. Caruso, D. Möbius, W. Paulus, H. Ringsdorf, G. Wildburg, *Angew. Chem.*, **1993**, 105, 1082, (b) T.M. Bohanon, S. Denzinger, R. Fink, W. Paulus, H. Ringsdorf, M. Weck, *Angew. Chem. Int. Ed. Eng.*, **1995**, 34, 58.
- 6) I. Willner, J. Rosengaus, S. Biali, *Tetrahedron Lett.*, **1992**, 33, 3805.
- 7) (a) Y. Honda, K. Kurihara, T. Kunitake, *Chem. Lett.*, **1991**, 681, (b) T.K. Park, J. Schroeder, J. Rebek Jr., *J. Am. Chem. Soc.*, **1991**, 113, 5125, (c) T. K. Park, Q. Feng, J. Rebek Jr., *J. Am. Chem. Soc.*, **1992**, 114, 4529, (d) R.F.M. Lange, E.W. Meijer, *Macromolecules*, **1995**, 28, 782.
- 8) (a) W.L. Jorgensen, J. Pranata, *J. Am. Chem. Soc.*, **1990**, 112, 2008, (b) J. Pranata, S. G. Wierschke, W.L. Jorgensen, *J. Am. Chem. Soc.*, **1991**, 113, 2810.
- 9) (a) E.M. Smolin, L. Rapoport, *The Chemistry of Heterocyclic Compounds*, Vol. 13, s-Triazines, Ed. A. Weissberg, John Wiley & Sons, New York, **1959**.
- 10) H.J. Sims, H.B. Parseghian, P.L. de Benneville, *J. Org. Chem.*, **1958**, 23, 724.
- 11) R. Gaudry, *Org. Syntheses Coll. Vol. 3*, Ed. E.C. Horning, New York, **1955**, 436.
- 12) (a) A. Ostrogovich, G. Gheorghiu, *Gazz. Chim. Ital.* **1930**, 60, 648, (b) A. Ostrogovich, G. Gheorghiu, *Gazz. Chim. Ital.*, **1932**, 62, 317, (c) C. Grundmann, E. Beyer, *Chem. Ber.*, **1950**, 83, 452.
- 13) (a) D.J. Brown, *The Chemistry of Heterocyclic Compounds*, vol. 16, *The Pyrimidines*, Ed. A. Weissberger, John Wiley & Sons, New York, **1962**, (b) D.J. Brown, *Chemistry of Heterocyclic Compounds*, vol. 16 *Supplement I, The Pyrimidines*, Ed. E.C. Taylor, and A. Weissberger, John Wiley & Sons, New York, **1970**.
- 14) (a) D.J. Brown, *Chemistry of Heterocyclic Compounds*, vol. 52, *The Pyrimidines*, Ed. E.C. Taylor and A. Weissberger, John Wiley & Sons, New York, **1994**, 533, (b) J. Pliml, M. Prystaš, *The Hilbert-Johnson Reaction of 2,4-Dialkoxy-pyrimidines with Halogenoses*, in *Advances in Heterocyclic Chemistry*, volume 8, Ed. A.R. Katritzky, A.J. Boulton, Academic Press, New York, **1967**.

- 15) (a) K.L. Nagpal, *J. Med. Chem.*, **1972**, *15*, 121, (b) L.O. Ross., L. Goodman., B.R. Baker, *J. Org. Chem.*, **1960**, *25*, 1950.
- 16) D.T. Browne in *Synthetic Procedures in Nucleic Acid Chemistry*, vol. 1, Ed. W. Zorbach, Werner & Tipson, R. Stuart, John Wiley & Sons, New York, **1968**, p. 98; b) D.T. Browne, J. Eisinger, N.J. Leonard, *J. Am. Chem. Soc.*, **1968**, *90*, 7302.
- 17) (a) J. Bernstein, B. Stearns, E. Shaw, W.A. Lott, *J. Am. Chem. Soc.*, **1947**, *69*, 1151, (b) B. Feibush, A. Figueroa, R. Charles, K.D. Onan, P. Feibush, B.L. Karger, *J. Am. Chem. Soc.*, **1986**, *108*, 3310, (c) A. D. Hamilton, D. van Engen., *J. Am. Chem. Soc.*, **1987**, *109*, 5035.
- 18) For the equation, see R. Deans, G. Cooke, V.M. Rotello, *J. Org. Chem.*, **1997**, *62*, 836.
- 19) K. A. Connors, *Binding Constants*, John Wiley & Sons, New York, **1987**, 24.
- 20) R. Deans, G. Cooke, V.M. Rotello, *J. Org. Chem.*, **1997**, *62*, 836.
- 21) J. Bernstein, M.C. Etter, L. Leiserowitz in *Structure Correlation*, vol. 2, Ed. H.-B. Burgi, J.D. Dunitz, VCH, Weinheim, Germany, **1994**, 431.
- 22) A.L. Spek, *PLUTON*, Utrecht University, Utrecht, The Netherlands, **1993**.
- 23) G.A. Jeffrey, W. Saenger, *Hydrogen Bonding in Biological Structures*, Springer Verlag, Berlin, **1991**, p. 248.
- 24) A.D. Burrows, C.W. Chan, M.M. Chowdry, J.E. McGrady, D.M.P. Mingos, *Chem. Soc. Rev.*, **1995**, 329.
- 25) A 50 mM solution of **18** and **21** does not show any sign of dimerization (< 5% dimer).
- 26) L.J. Bellamy, *The Infrared Spectra of Complex Molecules*, 3rd Edn., Chapman and Hall Ltd., London, **1975**, p. 279 & 314.
- 27) Two other complexes of which no crystal structure was determined (**1•15**, **4•10**), also had a 1:1 triazine uracil ratio as indicated by NMR.
- 28) G.R. Desiraju, *Angew. Chem. Int. Ed. Eng.*, **1995**, *34*, 2311.
- 29) (a) B. Feibush, A. Figueroa, R. Charles, K.D. Onan, P. Feibush, B.L. Karger, *J. Am. Chem. Soc.*, **1986**, *108*, 3310, (b) A. D. Hamilton, D. van Engen, *J. Am. Chem. Soc.*, **1987**, *109*, 5035, (c) A.D. Hamilton, N. Pant, A.V. Muehldorf, *Pure & Appl. Chem.*, **1988**, *60*, 533, (d) A. V. Muehldorf, D. van Engen, J.C. Warner, A.D. Hamilton, *J. Am. Chem. Soc.*, **1988**, *110*, 6561, (e) S.J. Geib, S.C. Hirst, C. Vicent, A.D. Hamilton, *J. Chem. Soc., Chem. Commun.*, **1991**, 1283, (f) S.-K. Chang, D. Van Engen, E. Fan, A.D. Hamilton, *J. Am. Chem. Soc.*, **1991**, *113*, 7640, (g) N. Shimizu, S. Nishagaki, Y. Nakai, K. Osaki, *Acta Cryst. B*, **1982**, *B38*, 2309.
- 30) A.R. Katritzky, I. Ghiviraga, *J. Chem. Soc., Perkin Trans. 2*, **1995**, 1651.
- 31) (a) refs. 29, and a) S.S. Flack, J.-L. Chaumette, J.D. Kilburn, G.J. Langley, M. Webster, *J. Chem. Soc., Chem. Commun.*, **1993**, 399, (b) R.P. Dixon, S.J. Geib, A.D. Hamilton, *J. Am. Chem. Soc.*, **1992**, *114*, 365.
- 32) R.J. Griffin; P.R. Lowe, *J. Chem. Soc., Perkin Trans. 2*, **1994**, 1811.
- 33) (a) L.J. Bellamy, *The Infrared Spectra of Complex Molecules*, 3rd Edn., Chapman and Hall Ltd., London, **1975**, p. 233, (b) H.E. Hallam, C.M. Jones, *J. Mol. Struct.*, **1970**, *5*, 1, (c) R.A. Russell, H.W. Thompson, *Spectrochim. Acta*, **1956**, *8*, 138.
- 34) It is essential to record at this low concentration, as at higher concentrations dimerization is observed (seen by the appearance of broad peaks at 3251 and 3192 cm⁻¹).
- 35) The (50 mM) solution of compound **7** contained (crystal) water (seen in the infrared spectrum at 3667 cm⁻¹), but this could be removed by rigorously drying the solution over calcium chloride. The wavenumber of the N-H stretch of the dried solution is used (3424 cm⁻¹); the value for the solution containing water is 3433 cm⁻¹.

- 36) Although the amide groups of **7** are in a *trans* amide conformation, complexation with *N*-propylthymine is weak ($K_a = 4.7 \text{ M}^{-1}$). This observation is in accordance with the observation of Feibush^{3a} that di(pivaloylamino)pyridines do not form complexes with imides, presumably due to steric hindrance.
- 37) An alternative dimer geometry, which is found in the crystal structure of **5**, is expected to be significantly less stable in solution because it is held together by two instead of four hydrogen bonds.
- 38) A similar relatively low influence of the water content of the CDCl_3 on association constants was reported by: J.C. Adrian, C.S. Wilcox, *J. Am. Chem. Soc.*, **1991**, *113*, 678.
- 39) K. A. Connors, *Binding Constants*, John Wiley & Sons, New York, **1987**.
- 40) D.A. Derenleau, *J. Am. Chem. Soc.*, **1969**, *91*, 4044.
- 41) (a) G. Carta, G. Crisponi, V. Nurchi, *Tetrahedron*, **1981**, *37*, 2115, (b) G. Carta, G. Crisponi, *J. Chem. Soc., Perkin Trans. 2*, **1982**, 53.
- 42) A.L. Spek, *J. Appl. Crystallogr.*, **1988**, *21*, 578.
- 43) G.M. Sheldrick, SHELXS-86, Program for crystal structure determination, University of Göttingen, Germany, **1986**.
- 44) G.M. Sheldrick, SHELXL-93, Program for crystal structure refinement, University of Göttingen, Germany, **1993**.
- 45) Addition of acetonitrile to a deuteriochloroform solution of pure 2,4-diamino-6-dodecyl-s-triazine does not result in any proton shifts.
- 46) (a) C.S. Marvel, P.K. Porter, in: *Org. Syn., Coll. Vol. 1*, Ed. H. Gilman, John Wiley & Sons, New York, **1941**, 377, (b) H.R. Henze, N.E. Rigler, *J. Am. Chem. Soc.*, **1934**, *56*, 1350.
- 47) S. N. Huckin, L. Weiler, *J. Am. Chem. Soc.*, **1974**, *96*, 1082.
- 48) H. Gershon, R. Braun, Scala, A. *J. Med. Chem.*, **1963**, *6*, 87.
- 49) T. Nishimura, I. Iwai, *Chem. Pharm. Bull.*, **1964**, *12*, 352.

Chapter 3

The DADA Motif in Quadruply Hydrogen Bonded Dimers of Triazines and Pyrimidines

Abstract:

Dimerization via quadruple hydrogen bonding in a Donor–Acceptor–Donor–Acceptor (DADA) array in acylated diaminotriazine and diaminopyrimidine derivatives is studied in detail using ^1H -NMR spectroscopy, FT-IR spectroscopy and X-ray diffraction.

2,4-Di(acylamino)triazines are capable of dimerization via quadruple hydrogen bonding ($K_{\text{dim}} = 37\text{--}130\text{ M}^{-1}$), because these compounds can form an ADADA array due to the preference for cis-amide conformations. These ADADA dimers are destabilized relative to DADA dimers by two additional repulsive secondary interactions caused by the terminal acceptor functionalities. Removal of these two spectator repulsions —by using mono-acylated diaminotriazine derivatives— effects an increase in the dimerization constant to 530 M^{-1} .

An increase in the stability of the dimers is also achieved by replacing the cis-amide group by a (butyl)ureido group; the ureido group forms an intramolecular hydrogen bond pre-organizing the array. Hence, the dimerization constants of di(ureido)triazines are $180\text{--}440\text{ M}^{-1}$, despite destabilization of these dimers by two spectator repulsions. The highest dimerization constant of the triazine derivatives studied is observed for a mono-ureido derivative ($K_{\text{dim}} = 2.0 \times 10^4\text{ M}^{-1}$). These dimers are not destabilized by spectator repulsions, and the DADA array is pre-organized. The value is more than one order of magnitude higher than for mono-acylated diaminotriazines, and almost two orders higher than for di(ureido)triazines.

Dimerization of self-complementary DADA arrays is also observed for acylated derivatives of 2,4-diaminopyrimidine. In di(acylamino)pyrimidines, a DADA array is formed because the acylamino group between the two ring nitrogens prefers the cis-conformation, while the acylamino group adjacent to only one ring-nitrogen is in a trans-conformation. The dimerization constants of di(acylamino)pyrimidines are between 200 and 1000 M^{-1} . Pre-organization by an intramolecular hydrogen bond also increases the stability of dimers of pyrimidine derivatives. The dimerization constant of 2-butylureido-4-acetylamino-pyrimidine is too large to be measured directly in pure chloroform. By extrapolation of dimerization constants of this compound in chloroform/methanol solvent mixtures, the value in pure CDCl_3 was estimated to lie between 2×10^5 and $1 \times 10^6\text{ M}^{-1}$.

3.1 Introduction

In molecular recognition, arrays of multiple parallel or near-parallel hydrogen bonds are a commonly used motif,¹ since strength, specificity and directionality are increased compared to single hydrogen bonds. The strength of multiple hydrogen bonded complexes has been found to depend not only on the number of hydrogen bonds—and the donor acidity and acceptor basicity of the individual hydrogen bonds²—but also strongly on the particular arrangement of the donor and acceptor functional groups.³ Linear arrays of three hydrogen bonds have been studied in detail, and the strength of triple hydrogen bonds was found to vary from moderate ($K_a = 10^2$ – 10^3 M⁻¹ for the DAD–ADA couple in chloroform),⁴ to strong ($K_a = 10^5$ – 10^6 M⁻¹ for the DDD–AAA couple in chloroform).⁵ Despite its moderate strength, the DAD–ADA couple is by far the most frequently encountered couple in supramolecular engineering, because of its ease of synthesis. The synthesis of the components of the much stronger bonding DDA–AAD, and especially of the DDD–AAA couple, requires much more effort. Several strongly bonded hetero-complexes held together by more than three hydrogen bonds have also been described, of which a few examples are given in figure 3.1.^{6–9}

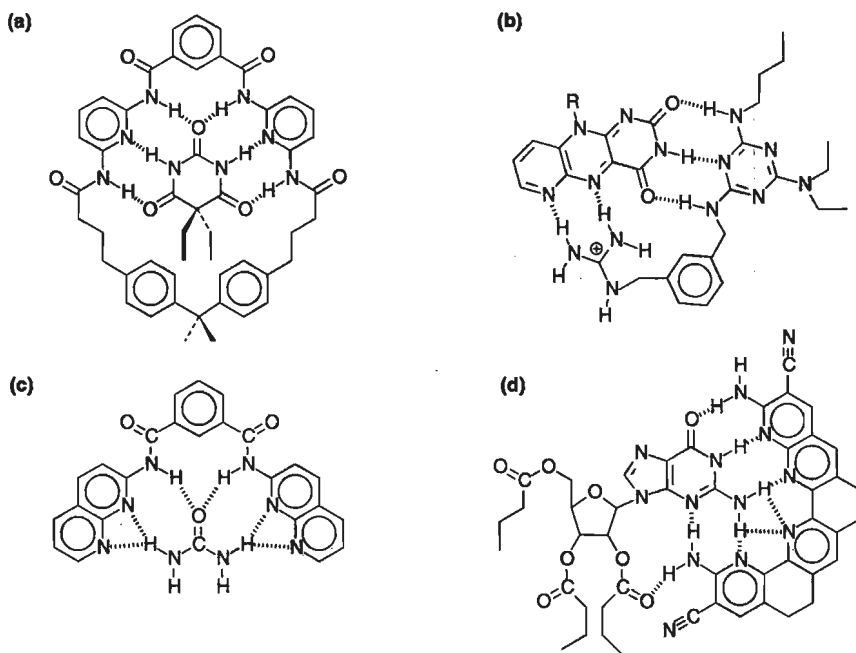


Figure 3.1: Host–guest complexes with a very high binding strength:

- (a) complex of a barbiturate with an artificial receptor, held together by 6 hydrogen bonds of two cooperative triple hydrogen bonding arrays, $K_a = 1.4 \times 10^6$ M⁻¹ in chloroform,⁶
- (b) flavin–receptor complex, $K_a = 1.4 \times 10^5$ M⁻¹ in chloroform,⁷
- (c) urea–receptor complex, $K_a = 6.6 \times 10^3$ M⁻¹ in chloroform,⁸
- (d) guanine–receptor complex, $K_a > 1.9 \times 10^5$ M⁻¹ in CDCl₃/DMSO 4:1 v/v.⁹

In these cases, however, the array of hydrogen bonding groups is not linear. All these strongly bonded complexes, and other examples,¹⁰ are usually obtained by elaborate synthesis.

For a number of applications —such as self-assembling container molecules¹¹ and supramolecular tubes¹²— self-complementarity is used. Self-complementarity, combined with strong association of the functional groups, is also advantageous for the assembly of linear hydrogen bonded polymers.¹³ Evidently, self-complementarity is found only in arrays with an even number of hydrogen bonds. Several examples of self-complementary DA-arrays have been described,¹⁴ but the strength of two hydrogen bonds is only moderate. In principle, the strength could be increased by using linear arrays of four cooperative hydrogen bonds, but such arrays are notably absent in the field of supramolecular chemistry.¹⁵

In the previous chapter, dimerization of di(acylamino)triazines via four cooperative hydrogen bonds was proposed to explain their higher dimerization constants ($K_{\text{dim}} = 37 \text{ M}^{-1}$) with respect to di(acylamino)pyridines ($K_{\text{dim}} < 1 \text{ M}^{-1}$). Since the amides in di(acylamino)triazines prefer a *cis*-conformation —as was shown by IR-studies in dilute chloroform solution— a linear ADADA-array can be formed. This ADADA array can dimerize via four hydrogen bonds as depicted in figure 3.2a. However, this dimer geometry is destabilized by two additional repulsive secondary interactions, indicated by the double-headed arrows. Since these repulsive interactions result from a superfluous carbonyl group in the ADADA array that itself is not involved in hydrogen bonding, we will refer to these interactions as spectator repulsions.

Because of the potential of dimerization via four hydrogen bonds, it was decided to investigate the possibility of obtaining significantly stronger bonded dimers than the dimer of di(acetylamino)triazine **1**. As a first approach to stronger dimerization, the two spectator repulsions destabilizing the di(acetylamino)triazine dimer are eliminated. This can be achieved by using mono-acylated diaminotriazines (figure 3.2b).

In a second approach to stronger dimers, the carbonyl groups are fixed into a pre-organized and coplanar array. This is achieved by an intramolecular hydrogen bond (figures 3.2c and d) of a ureido functionality, which can be obtained by reacting the amine(s) of the diaminotriazine with an isocyanate. To obtain a full comparison of effects, the dimerization of di(ureido)triazine derivatives (figure 3.2c) —dimers with two spectator repulsions— is investigated as well as dimerization of mono(ureido) derivatives (figure 3.2d) —dimers without two spectator repulsions.

1: $R = -CH_2-O-CH_3$; $R' = -CH_3$

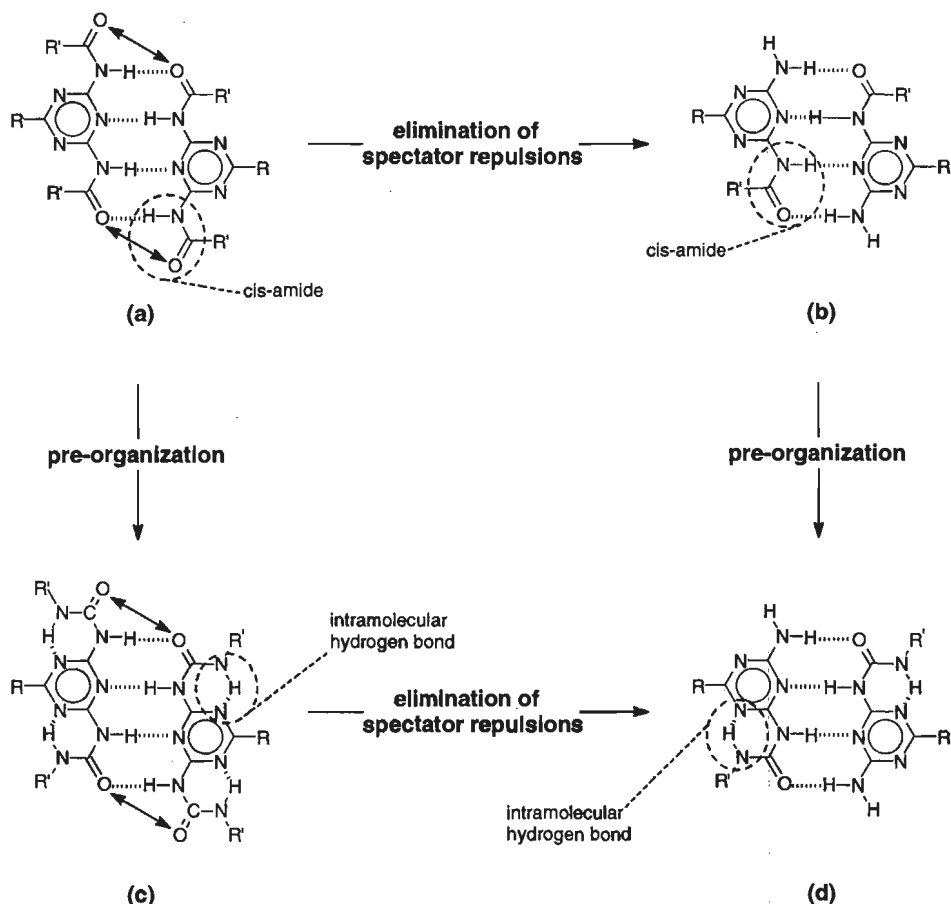


Figure 3.2: Quadruple hydrogen bonding in acylamino- and ureidotriazines:

- (a) The dimers of di(acylamino)triazine are destabilized by two spectator repulsions.
- (b) Dimers of monoacylated diaminotriazines are not destabilized by two spectator repulsions.
- (c and d) In ureidotriazines, the array is pre-organized by an intramolecular hydrogen bond.
- (c) Di(ureido)triazine dimers are destabilized by two spectator repulsions.
- (d) Mono(ureido)triazine dimers are not destabilized by spectator repulsions.

The concept of quadruple hydrogen bonding via DADA arrays is extended to diacylated derivatives of 2,4-diaminopyrimidine: the amide group between the two aromatic ring nitrogens is expected to be in a *cis*-conformation, just like in acylaminotriazines, while the other amide, adjacent to only one ring nitrogen, is expected to be in *trans*-conformation, like in acylaminopyridines (figure 3.3a). Furthermore, the concept of pre-organization by an intramolecular hydrogen bond is also applied here (figure 3.3b).

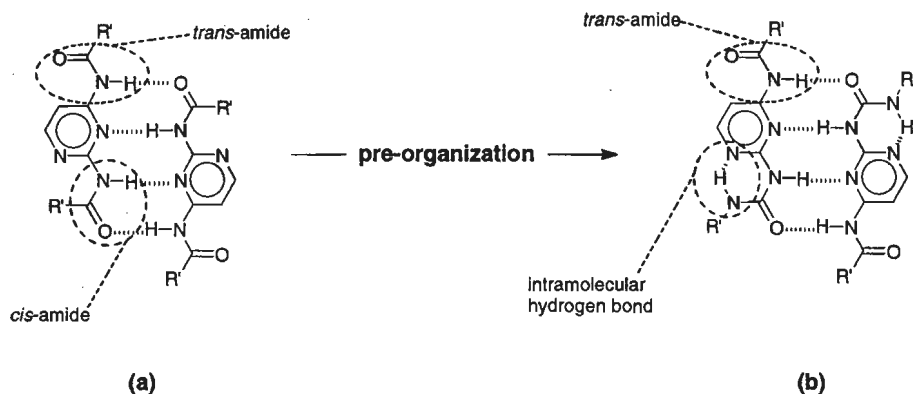


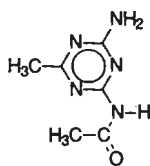
Figure 3.3: Quadruple hydrogen bonding in:
 (a) dimers of di(acylamino)pyrimidine,
 (b) dimers of 2-ureido-4-acylamino pyrimidine.

We studied in detail the effect of the modifications as described above on the hydrogen bonding properties of acylated derivatives—both with acylamino groups as well as with a ureido group—of 2,4-diaminotriazine and 2,4-diaminopyrimidine. X-ray diffraction studies on single crystals were used to elucidate the hydrogen bonding pattern in the solid state, furthermore affording detailed information on the bonding geometry. In solution, the formation of quadruply hydrogen bonded dimers was studied by $^1\text{H-NMR}$ and FT-IR spectroscopy. Furthermore, dilution studies in chloroform solution afforded dimerization constants. The results of these studies are discussed in the framework of the model of Jorgensen.²

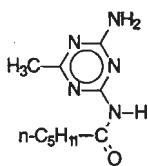
3.2 Quadruple Hydrogen Bonding in Acylated Diaminotriazine Derivatives

3.2.1 Synthesis

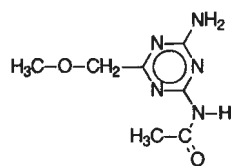
Amido derivatives of diaminotriazines. Mono-acylated diamino-*s*-triazines **2–4** were prepared by heating a suspension of the corresponding diaminotriazine in a mixture of the corresponding anhydride and pyridine as solvent, at reflux temperature for a short period (15–30 min).¹⁶ The formation of the bis-derivative was minimized by stopping the reaction as soon as the diaminotriazine had dissolved completely. Derivatives **2–4** were obtained in good to excellent yields by merely cooling of the reaction mixture in an ice-water bath: the mono-acylated product crystallized, while the trace of di(acylated) derivative remained in solution. Derivatives **2–4** have low solubilities in chloroform—the solvent in which association via hydrogen bonding is generally studied—obstructing detailed NMR/IR studies in this solvent.



2

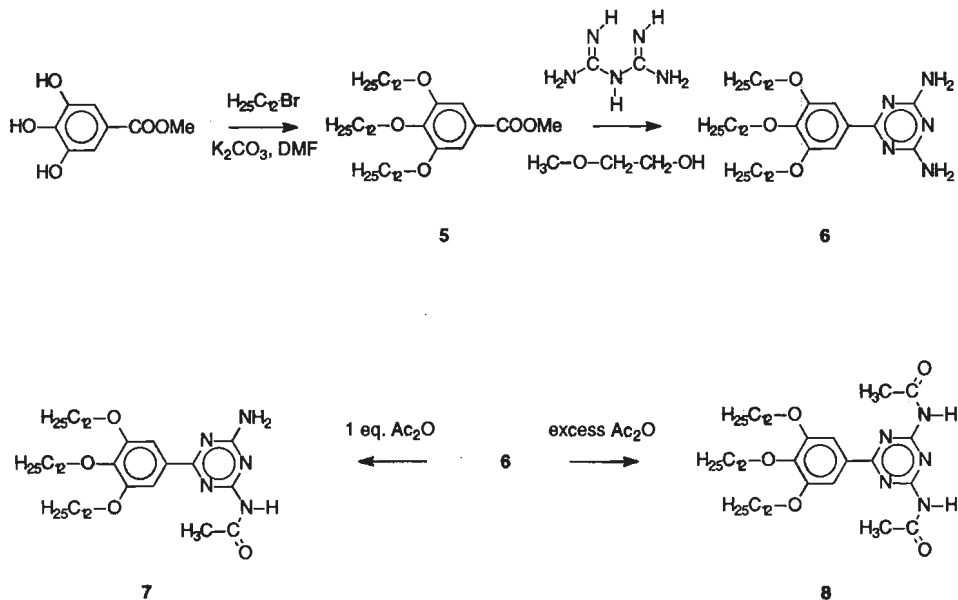


3



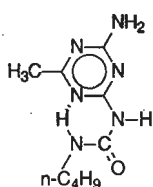
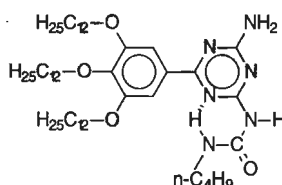
4

Due to the low solubility of derivatives 2–4, mono-acetylated diaminotriazine 7—having three solubilizing alkyl chains—was prepared (scheme 3.1). Methyl 3,4,5-trihydroxybenzoate was alkylated in DMF with dodecyl bromide and potassium carbonate at 70°C, to afford methyl 3,4,5-tri(dodecyloxy)benzoate 5.¹⁷ A condensation reaction¹⁸ of this ester 5 with biguanide¹⁹ afforded the corresponding diaminotriazine 6. Mono-acetylated derivative 7 was predominantly formed by refluxing triazine 6 with one equivalent of acetic anhydride in dry pyridine for two hours, although the crude product of the reaction was contaminated with 6 and 8. The diaminotriazine 6 was easily removed by crystallization from ethyl acetate. However, the desired mono(acetyl) derivative 7 could not be purified completely from di(acetyl) derivative 8 by either column chromatography or crystallization. Finally, a fraction containing 5% bis-acetylated compound 8 was the purest batch obtained. For a complete comparison, bis(acetylamino)triazine 8 was synthesized by refluxing 6 in excess acetic anhydride.

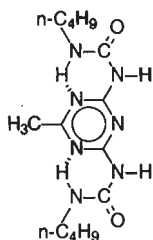
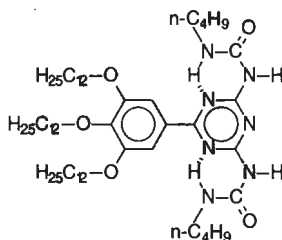


Scheme 3.1: Synthesis of 6-[3,4,5-tri(dodecyloxy)phenyl] substituted diaminotriazines.

Ureido derivatives of diaminotriazines. To obtain the ureido derivatives of diaminotriazines, acylation reactions with isocyanates were performed. Heating a solution of 2,4-diamino-6-methyl-s-triazine in pyridine with butyl isocyanate²⁰ under reflux for two hours primarily gave rise to mono-acylation. By cooling of the solution, the mono-butylureido derivative **9** crystallized in a 95% yield. Only a trace amount of the bis-ureido derivative **11** was present in the mother liquor. Compound **9** was obtained pure by crystallization from chloroform. The limited solubility of **9** in chloroform prompted the preparation of **10**, with a similar solubilizing group as in the case of the acetyl derivative. This compound **10** was prepared in a similar way as described for **9**, but purification to remove traces of bis-derivative **12** was performed by column chromatography.

**9****10**

In addition, to perform a full study of hydrogen bonding properties in ureidotriazines, bis-ureido derivatives **11** and **12** were prepared. These well-soluble compounds were obtained by prolonged heating of the appropriate diaminotriazine with tenfold excess of butyl isocyanate in pyridine at reflux.

**11****12**

3.2.2 Hydrogen bonding pattern in the solid state

To elucidate the hydrogen bonding pattern in the solid state, crystal structures were determined by single crystal X-ray diffraction. The crystal structures of mono(acetylamino)- and mono(ureido)aminotriazines **2** and **9** feature quadruply hydrogen bonded, planar, centrosymmetrical dimers of DADA arrays (figure 3.4a–b). The carbonyl group of both the acetylamino derivative **2** (figure 3.4a), as well as of the ureido derivative **9** (figure 3.4b), are *cis* with respect to the N–H on the ring, giving rise to a DADA array. An intramolecular

hydrogen bond of the ureido group to a non-central triazine ring nitrogen atom is present in ureido derivative **9**. The N to N distance is 2.658 (4) Å, with an angle of 139 (2) degrees in the hydrogen bond.

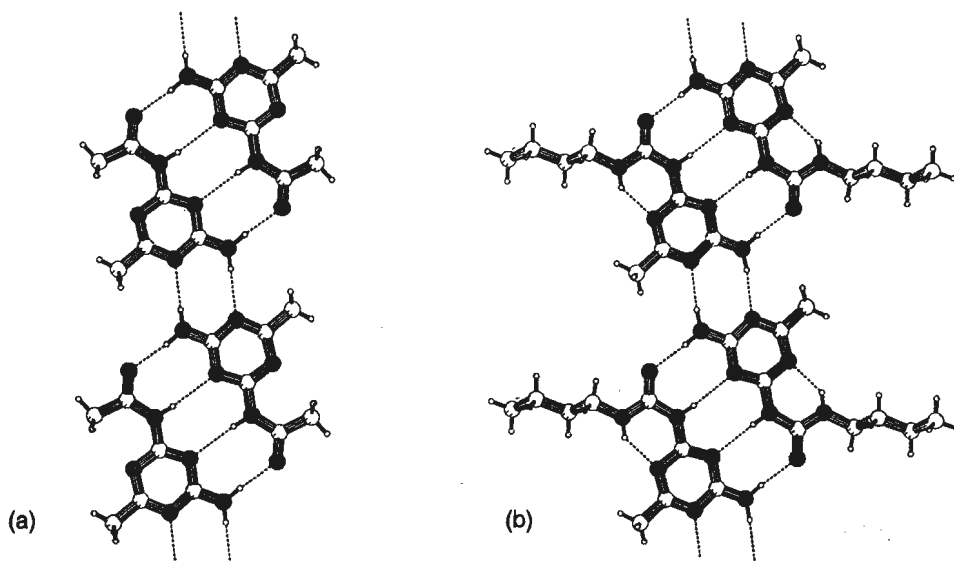


Figure 3.4 : PLUTON representation of the hydrogen bonding patterns in the crystal structures of:
 (a) 2-(acetylamino)-4-amino-6-methyl-*s*-triazine **2**,
 (b) 2-butylureido-4-amino-6-methyl-*s*-triazine **9**.

In both crystal structures, infinite chains are formed by additional dimerization via double hydrogen bonds of the remaining triazine amine with a non-central triazine ring nitrogen atom. Thus, in the solid state, all potential donor atoms of **2** and **9** are involved in hydrogen bonding. Bond lengths and angles of the quadruply hydrogen bonded dimers are reported in Table 3.1.

Table 3.1: Hydrogen bond distances [Å] and X–H···X bond angles [°] in the crystal structures of **2 and **9**.**

	N–H···N distance	N–H···N angle	N–H···O=C distance	N–H···O=C angle	Hydrogen bond length difference
2	3.195 (2)	174.5 (1.9)	2.839(2)	175(2)	0.356
9	3.101(4)	176(3)	2.797(4)	176(3)	0.304

A striking difference in bond length between the inner (N–H···N) and the outer hydrogen bond (N–H···O=C) is present: the inner N–H···N hydrogen bonds are 0.30 Å to 0.36 Å longer than the outer N–H···O=C hydrogen bonds. The DADA arrays in both crystal

structures deviate significantly from linearity; the oxygen atom does not fall on the line connecting the three nitrogen atoms in the array of one molecule, but is protruding. The enforced bond length difference between $\text{N-H}\cdots\text{O}=\text{C}$ and $\text{N-H}\cdots\text{N}$ hydrogen bonds—which have in general similar equilibrium lengths²¹—apparently does not prevent the formation of dimers. Bond lengths are slightly shorter in ureido derivative **9** than in acetyl derivative **2**.²²

In the crystal structure of di(butylureido)triazine derivative **11**, both butylureido substituents are in a *cis*, *trans* conformation, and intramolecularly hydrogen bonded (figure 3.5). These intramolecular hydrogen bonds have distances of 2.655 (6) and 2.684 (6) Å with angles of 132.6 (1.6) and 131.5 (1.6) degrees, respectively. These values are similar to those in **9**. Formation of a quadruply hydrogen bonded dimer is not observed in the crystals of **11** studied, because one of the intramolecular hydrogen bonds is directed to the central triazine ring nitrogen between the two ureido substituents. As a result, dimerization via quadruple hydrogen bonding is impossible, and a two-dimensional hydrogen bonding network is present, formed by one double hydrogen bonding and two single hydrogen bonding interactions per molecule.

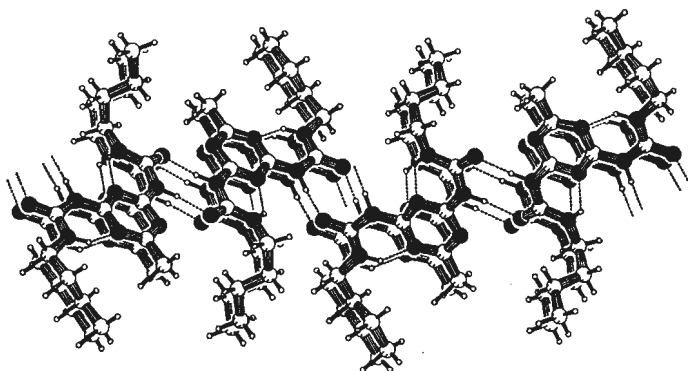


Figure 3.5: PLUTON representation of the hydrogen bonding pattern in the crystal structure of **11**.

3.2.3 Association studies in chloroform solution

Formation of Hydrogen Bonded Complexes. The formation of hydrogen bonded complexes in solution was substantiated by FT-IR and ¹H-NMR spectroscopy. By measuring IR-spectra in chloroform at various concentrations, N-H and NH₂ stretch vibrations of monomer and dimer could be assigned (table 3.2).²³ These IR-studies show that the molecules exist in the tautomeric forms as shown in the structural formulas; other tautomeric forms have not been observed. The antisymmetric and symmetric NH₂ stretch vibrations in the monomers of compounds **7** and **10** are found at similar positions as for parent diaminotriazines (see chapter 2). Upon dimerization, a shift to lower wavenumbers occurs similar to, but somewhat larger than for, diaminotriazines upon complexation with uracils (see chapter 2). For the monomers of di(acetylamino)triazines **1** and **8**, and of

mono(acetyl) diaminotriazine **7**, the amide N–H absorption is found between 3380 and 3390 cm^{-1} , a position characteristic for a *cis*-amide conformer (see chapter 2). Upon dimerization, a shift of the acetylamino N–H stretch vibration to lower wavenumbers is observed, similar as for *N*-propylthymine upon complexation with a diaminotriazine; again, the shift is somewhat larger. The ureido N–H stretch vibration in the monomers is found between 3424 and 3415 cm^{-1} , and shifts upon dimerization also to lower wavenumbers by comparable numbers as the amido N–H protons (see table 3.2).

Table 3.2: N–H stretch vibrations (ν in cm^{-1}) in monomers and dimers of diaminotriazine derivatives, most likely assignment of vibrations (in parentheses), and complexation induced shifts ($\Delta\nu$).

Compound	ν N–H in monomer	ν N–H in dimer	$\Delta\nu^a$
di(acetylamino)- triazine 1	3384 (<i>cis</i> -amide)	3251 (N–H \cdots O=C)	133
		3192 (N–H \cdots N)	192
di(acetylamino)- triazine 8	3390 (<i>cis</i> -amide) ^b	3252 (N–H \cdots O=C)	138
		3192 (N–H \cdots N)	198
mono(acetyl)- diaminotriazine 7	3542 (antisymmetric NH ₂)	3494 (non-bonded NH ₂)	^c
	3424 (symmetric NH ₂)	3304 (NH ₂ \cdots O=C)	168
	3392 (<i>cis</i> -amide)	3219 (N–H \cdots N)	173
mono(ureido)- triazine 10	3542 (antisymmetric NH ₂)	3490 (non-bonded NH ₂)	^c
	3424 (symmetric NH ₂)	3295 (NH ₂ \cdots O=C)	181
	3424 (ureido N–H)	3203/3223 (N–H \cdots N)	221/201
	3284 (intramolecular HB)	3223/3203 (intramolecular HB)	
di(butylureido)- triazine 11	3415 (ureido N–H)	3285 (N–H \cdots O=C)	130
		3252 (N–H \cdots N)	163
		3287 (intramolecular HB)	^d

^a $\Delta\nu = \nu$ N–H in dimer – ν N–H in monomer; ^b A shoulder at 3419 is also observed, which is ascribed to a trace of *trans*-amide; ^c The stretch vibrations of both N–H functionalities of a NH₂ are coupled, resulting in antisymmetric and symmetric NH₂ stretch vibrations. The average of these corresponds to the non-bonded N–H stretch vibration in the dimer, where coupling is not present. Hence, the sum of observed $\Delta\nu$'s corresponds to the $\Delta\nu$ upon dimerization; ^d The vibration of the intramolecular hydrogen bond coincides.

The presence of hydrogen bonded complexes was further substantiated with ¹H-NMR. At high concentrations in chloroform, the N–H signals of most compounds in this study have positions at very low field, indicating that the N–H protons are involved in hydrogen bonding. Dilution effects a gradual upfield shift, indicating dissociation of the hydrogen bonded complex, and a fast exchange between monomer and dimer on the NMR timescale.

Dimerization Constants. For most compounds, dimerization constants were obtained by monitoring the N–H resonances in $^1\text{H-NMR}$ in chloroform at 298 K as a function of concentration. The concentration dependence of the N–H resonances could be fitted well to a model assuming dimerization only (see Experimental Section for procedure). The fitting procedure afforded both dimerization constants, as well as Chemically Induced Shift values (CIS), given in table 3.3. In many cases, dimerization constants could also be determined by monitoring other protons, such as the acetyl CH_3 , butyl CH_2 , or aromatic protons where appropriate, despite a small CIS value. The dimerization constants of monoureido-aminotriazine **10** and di(ureido)derivative **11** could not be determined reliably by $^1\text{H-NMR}$.²⁴ These dimerization constants were therefore determined by fitting the monomer and dimer peak intensities of N–H vibrations in the FT-IR spectrum at different concentrations. This technique afforded values of $2.0 (\pm 0.3) \times 10^4 \text{ M}^{-1}$ and $440 (\pm 60) \text{ M}^{-1}$ for derivatives **10** and **11**, respectively (see Experimental Section for details).

Table 3.3: Dimerization Constants (K_{dim}) in CDCl_3 , and CIS values of N–H protons of triazine derivatives at 298 K.

Compound	$K_{\text{dim}} (\text{M}^{-1})^a$	CIS (ppm) ^a	$\Delta G_{\text{dim}} (\text{kJ} \cdot \text{mol}^{-1})$
diaminotriazine 6	1.3 (0.05)	2.85 (0.05)	−0.65
di(acetylamino)triazine 1	35 (5)	2.35 (0.03)	−8.81
di(acetylamino)triazine 8	130 (20)	3.0 (0.1)	−12.2
di(butylureido)triazine 11	440 (60) ^b	–	−15.5
di(butylureido)triazine 12	180 (20) ^c	–	−12.9
mono(acetyl)-diaminotriazine 7	530 (40) ^d	2.9 (0.05)	−15.5
mono(ureido)triazine 10	$2.0 (0.3) \times 10^4$ ^b	–	−24.5

^a Estimated error in parentheses; ^b determined by IR in CHCl_3 ; ^c Fitted from shift of phenyl protons and CH_2 protons of butyl group; ^d Compound contaminated with 5% of bis-derivative; dimerization constants determined for batches with 5 and 20% of bis-derivative were 530 and 730 M^{-1} , respectively.

Substituents exert a large influence on the dimerization constants. The dimerization constants differ substantially for analogues **1** and **8**—di(acetylamino)triazines only differing in the 6-position substituent—, and for analogues **11** and **12**—di(butylureido)triazines also differing only in the 6-position substituent. In a recent paper with related di(acylamino)triazine derivatives,²⁵ it was proposed that electron donating groups on a phenyl group at the 6-position enhance binding, while electron withdrawing groups diminish binding. This trend is consistent with our observations for di(acetylamino)triazines **1** and **8**. However, the opposite is observed for di(butylureido)triazines **11** and **12**, which may be related to steric hindrance of the phenyl group at the 6-position on forming the intramolecular hydrogen bond in these ureido derivatives. As a result of the strong opposite effect of

substituents, a fair comparison of di(acetylamino)triazines and di(butylureido)triazines to show the effect of pre-organization of the intramolecular hydrogen bond cannot be made.

As a consequence of the strong substituent effects on dimerization constants in di(acetylamino)triazines **1** and **8**, the dimerization constant of mono-acetyl diaminotriazine **7** is 15 times higher than K_{dim} of di(acetylamino)triazine **1**, but only three times higher than K_{dim} of di(acetylamino)triazine **8**. This substituent effect interferes with the effect of removing two spectator repulsions, but the results still clearly indicate that DADA arrays dimerize stronger than ADADA arrays of analogous compounds. The effect of elimination of two spectator repulsions is more pronounced in ureido derivatives. K_{dim} of mono-ureido triazine **10**, having a DADA array without spectator repulsion, is almost two orders of magnitude higher than K_{dim} of diureido-triazines **11** and **12** that have ADADA arrays. The largest dimerization constant is observed for monoureido triazine derivative **10**, having a pre-organized DADA-array.

Variable temperature ^1H -NMR studies with di(acetylamino)- and di(butylureido)triazine derivatives. Di(acetylamino)- and di(butylureido) triazines **1** and **11** do not form quadruply hydrogen bonded dimers in the solid state. The dimerization constants of these compounds are also lower than of their corresponding mono-acylated derivatives, which do feature quadruply hydrogen bonded dimers in the solid state. To gain more information on the association mode for the di(acylated) compounds in solution, variable temperature ^1H -NMR studies were performed.

Cooling of chloroform solution of **1** resulted in decoalescence of the N-H signal and of the acetyl signal in the ^1H -NMR spectrum (figure 3.6). At 230 K in CDCl_3 , the N-H and the acetyl peaks of **1** have both split in two equally intense peaks. The N-H signals have downfield shifts, 10.5 and 11.4 ppm, indicating involvement in hydrogen bonding. The decoalescence behavior observed is completely in line with dimerization via quadruple hydrogen bonding. Formation of polymeric aggregates via two kinds of double hydrogen bonds (figures 3.7a and 3.7b) is considered unlikely for the following reasons: (i) in solution, formation of polymeric aggregates is entropically less favorable than formation of dimers, (ii) the ratio of hydrogen bonds to spectator repulsions is lower in the polymeric aggregates than in the dimers. Consequently, the former association mode is less favorable, (iii) the slow exchange of dimers—decoalescence at low temperatures—should have resulted in separate signals for the end-groups.

Coalescence upon cooling is also observed in the ^1H -NMR spectrum of **12** for all the N-H signals, as well as for the N- CH_2 protons of the butyl group. Furthermore, a second set of signals is observed at 280 K and below (figure 3.8, indicated by asterices). The ratio of the two sets of signals is concentration dependent at 260 K; the amount of least-abundant form increases upon dilution from less than 10% at 35 mM to 30% at 1 mM.

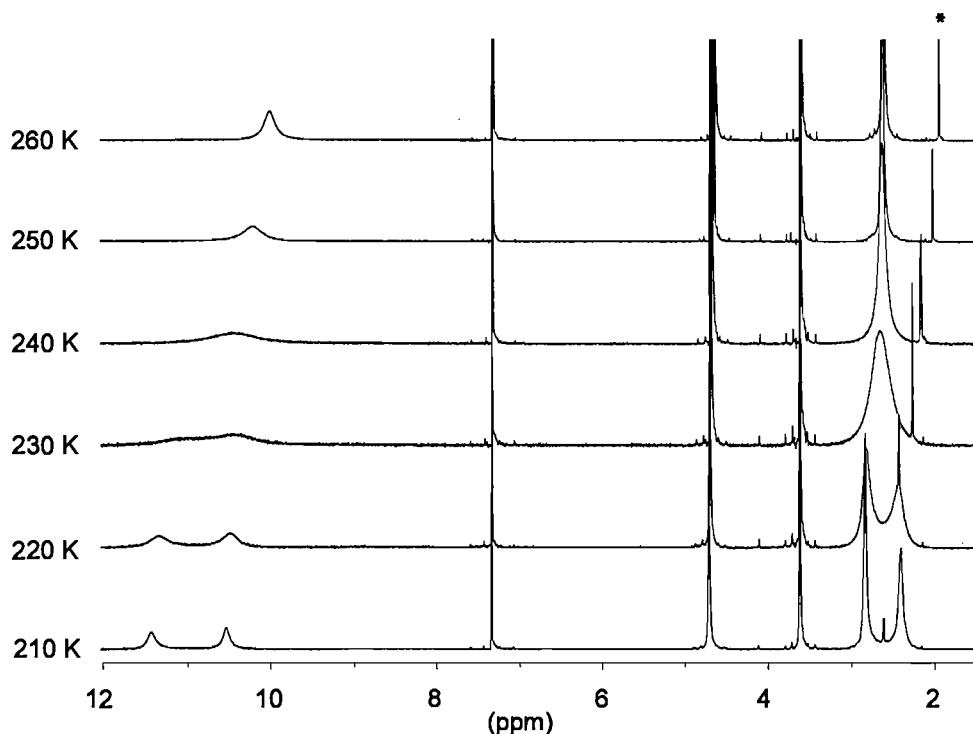


Figure 3.6: Variable temperature NMR experiment of a 20 mM CDCl_3 solution of di(acetylamino)-triazine **1**. The asterisk indicates a minor impurity.

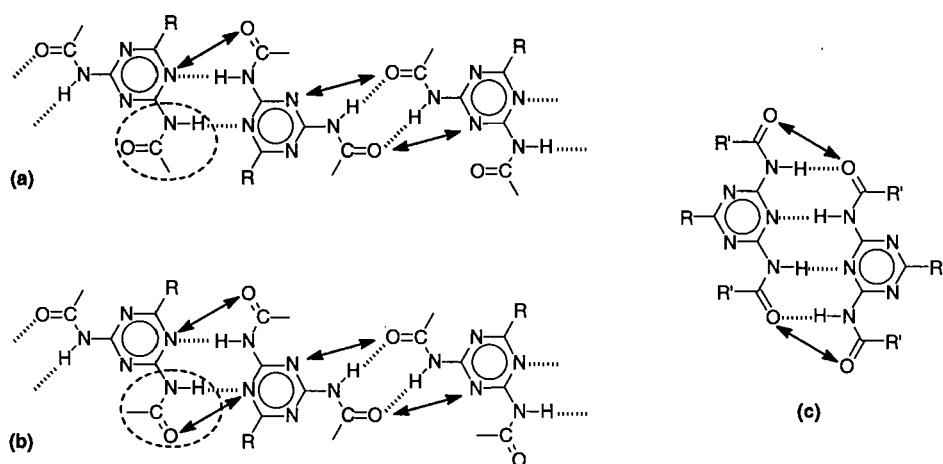


Figure 3.7: Two possible association modes of di(acylamino)triazines via two kinds of double hydrogen bonds, leading to polymeric aggregates: **(a)** with one out of four amides in a *trans*-conformation, as observed in the crystal structure, **(b)** with all amides in *cis*-conformation, having more symmetry. **(c)** Formation of a quadruply hydrogen bonded dimer. Spectator repulsions are indicated by double-headed arrows.

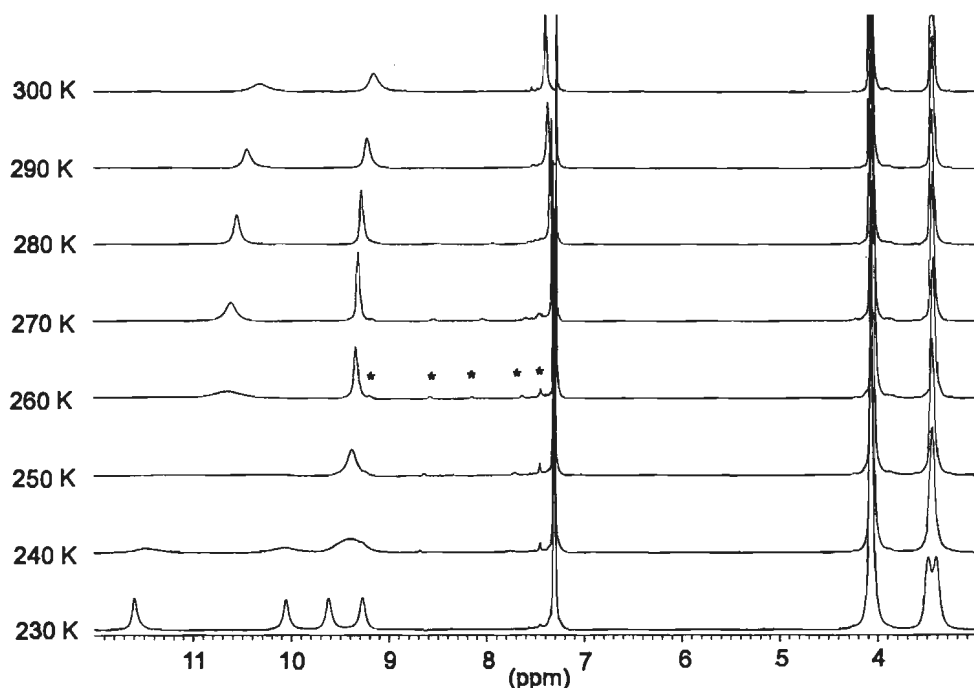


Figure 3.8: Variable temperature NMR-experiment of a 35 mM solution of **12** in CDCl_3 . The asterisks indicate a minor amount of another conformer (see below).

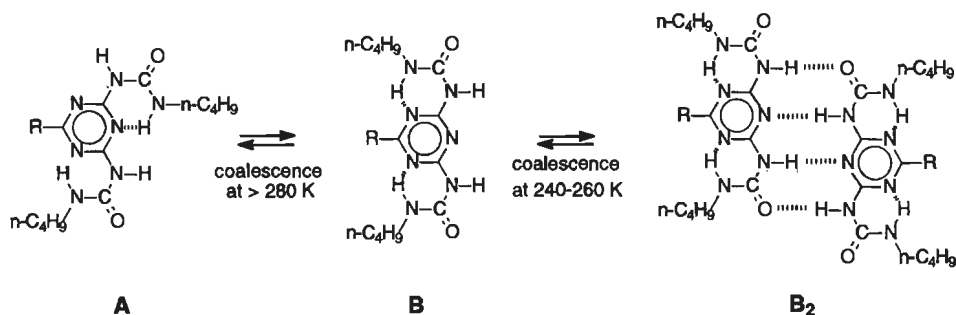


Figure 3.9: Temperature dependent equilibria in chloroform solutions of **12**.

The observed behavior is explained by the equilibria shown in figure 3.9. Four separate signals with equal intensity are observed for the N–H protons at low temperatures, indicating slow exchange on the NMR-timescale of quadruply hydrogen bonded dimers (**B₂** in figure 3.9). Coalescence occurs upon heating in the region 240–260 K. Above 260 K, dimers **B₂** exchange fast with their monomer **B**. A second set of four N–H resonances, and an aromatic C–H signal, is observed in the range 240–280 K, which increases in intensity upon heating. This second set is assigned to conformer **A**, which does not dimerize via quadruple

hydrogen bonding, and exchanges slowly with conformer **B**. The positions of the N–H signals of form **A** indicate that two of these N–H protons are not involved in hydrogen bonding.

In conclusion, in contrast to what is observed in the solid state, formation of polymeric aggregates through double hydrogen bonds is negligible in solution for di(acylamino)- and di(ureido) triazines. The results clearly indicate that in solution, di(acylamino)- and di(ureido) triazines form dimers held together by four hydrogen bonds as depicted in figures 3.2a and 3.2c.

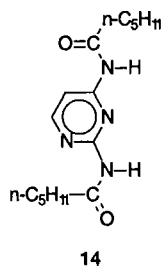
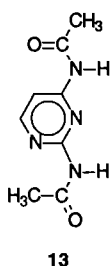
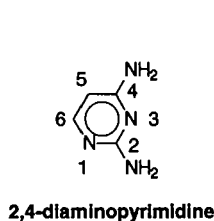
3.3 Quadruple Hydrogen Bonding in Acylated Diaminopyrimidine Derivatives

3.3.1 Introduction

In the triazine derivatives discussed above, additional hydrogen bonds are present between the remaining NH₂ donor and a ring nitrogen acceptor. In view of the desirability of unidirectional interactions for supramolecular applications,²⁶ —and to show the generality of the concept— the scope was extended to acylated derivatives of 2,4-diaminopyrimidine. A unidirectional interaction with respect to hydrogen bonding was expected to be feasible in these compounds, because the additional hydrogen bonding sites as present in mono-acylated diaminotriazines are not present in di-acylated diaminopyrimidines.

3.3.2 Synthesis

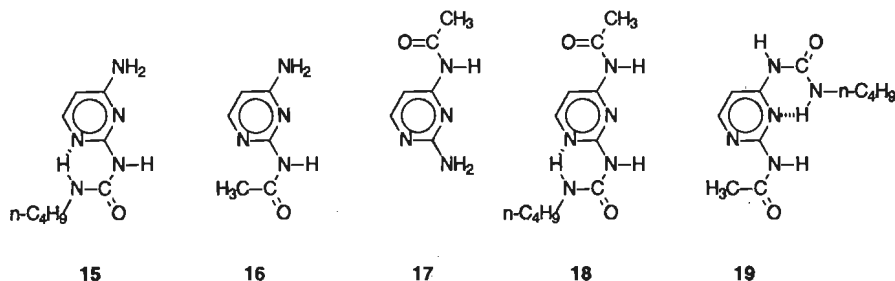
Acyl derivatives. Di(acylamino)pyrimidines **13** and **14** were prepared by reacting 2,4-diaminopyrimidine with an excess of the corresponding anhydrides in boiling pyridine.



Ureido derivatives. The first acylation of 2,4-diaminopyrimidine with one equivalent butyl isocyanate occurred with high selectivity at predominantly the 2-position, resulting in 2-butylureido-4-aminopyrimidine **15**. The desired compound **15** could be isolated pure by one crystallization of the crude product from ethanol. Also acylation with one

equivalent acetic anhydride afforded predominantly the 2-isomer **16**. The 2-acetyl-2,4-diaminopyrimidine isomer **16** was separated by column chromatography from minor amounts of starting material, the 4-acetyl isomer **17**, and the di(acetyl) derivative **13**. The solubility in chloroform of compounds **15–17** was too low to perform association studies.

Acylation of **15** with acetyl chloride yielded the well-soluble compound **18**, the identity of which was confirmed by single crystal X-ray diffraction (see below). Reaction of pure **16** with one equivalent butyl isocyanate gave the other isomer, 2-acetyl-4-butylureidopyrimidine **19**. Again, solubility of this compound in chloroform was not sufficient for association studies.



3.3.3 Hydrogen bonding pattern in the solid state

In their crystal structure, the molecules of 2,4-di(hexanoylamino)pyrimidine **14** and 2-butylureido-4-acetylaminopyrimidine **18** form centrosymmetric, quadruply hydrogen bonded dimers of DADA arrays (see figure 3.10a–b).

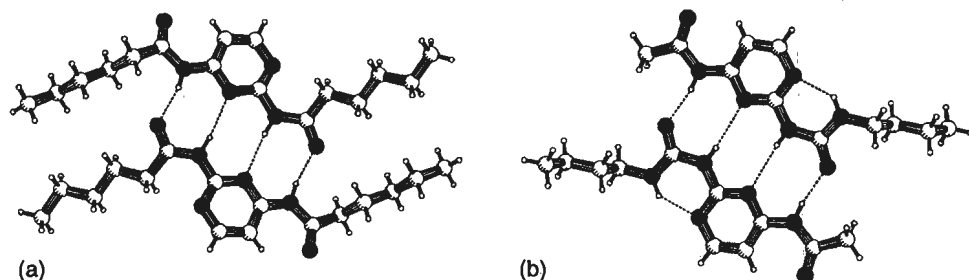


Figure 3.10: PLUTON representation of the hydrogen bonding patterns in the crystal structures of:
 (a) 2,4-di(hexanoylamino)pyrimidine **14**,
 (b) 2-butylureido-4-acetylaminopyrimidine **18**.

In the crystal structure of di(hexanoylamino)pyrimidine **14**, the amide between the two ring nitrogens is in a *cis*-conformation, resulting in a DADA array. The other amide of di(hexanoylamino)pyrimidine **14**, adjacent to only one ring nitrogen, is in a *trans*-

conformation, and coplanar with the pyrimidine ring. A short contact between the hydrogen atom on C5 and the carbonyl oxygen atom of this *trans*-amide is present; the distance from C5 to the carbonyl oxygen is 2.851(2) Å, under an angle of 125(2) degrees. In the crystal structure of ureido derivative **18**, a DADA array is formed by the carbonyl functionality of the butylureido group that is in *cis*-conformation. Furthermore, an intramolecular hydrogen bond from the ureido N–H to the non-central pyrimidine ring nitrogen N1 is present. The N–N distance is 2.671(3) Å with an angle of 136(2) degrees. The 4-acetylamino group in this pyrimidine derivative is also in a *trans*-conformation, and coplanar with the pyrimidine ring. A comparable short distance between the carbonyl of the 2-acylamino substituent and the hydrogen atom on C5 is present in the crystal structure of **18** as in the crystal structure of **14**; the distance is 2.834(4) Å and the angle is 118(2) degrees.

Bond lengths and angles of the quadruply hydrogen bonded dimers are reported in Table 3.4, illustrating an even larger difference in bond length between the inner (N–H \cdots N) and the outer hydrogen bond (N–H \cdots O=C) than observed for the triazine derivatives. Like for the triazines, bond lengths in the ureido derivative (**18**) are slightly shorter than in the diamide derivative (**14**).

Table 3.4: Hydrogen bond distances [Å] and X–H–X bond angles [°] in the crystal structures of **14 and **18**.**

	N–H \cdots N distance	N–H \cdots N angle	N–H \cdots O=C distance	N–H \cdots O=C angle	Hydrogen bond length difference
14	3.245(2)	166(2)	2.789(2)	162(2)	0.456
18	3.239(4)	171(2)	2.748(3)	169(2)	0.491

In contrast to the triazine derivatives **2** and **11**, pyrimidine derivatives **14** and **18** do not form hydrogen bond networks in the solid state via additional hydrogen bonding interactions. The only hydrogen bonding interactions in the crystal structures of both these pyrimidine derivatives are those needed for the formation of the dimer, including the intramolecular hydrogen bond in **18**. The absence of additional hydrogen bonding interactions between the pyrimidine dimers allows for several supramolecular applications in which unidirectionality is a conceptual prerequisite.²⁷

Crystal structure of di(acetylamino)pyrimidine **13.** Remarkably, the molecules of di(acetylamino)pyrimidine **13** (figure 3.11) are not dimerized via quadruple hydrogen bonding in the crystal. Although the amides of molecules of **13** have the required conformation for formation of a quadruply hydrogen bonded dimer in the crystal structure (one amide is *cis*, one is *trans*), the *cis*-amide does not have the appropriate orientation to form a quadruply hydrogen bonded dimer. The *cis*-amide dimerizes via two hydrogen bonds,

and two additional attractive interactions between the *cis*-amide carbonyl and an aromatic C–H are present. These ‘dimeric’ structures are connected via single hydrogen bonds of the *trans*-amide via an infinite chain (see figure 3.11). In this way, a pleated plane is formed by a two-dimensional hydrogen bonding network.

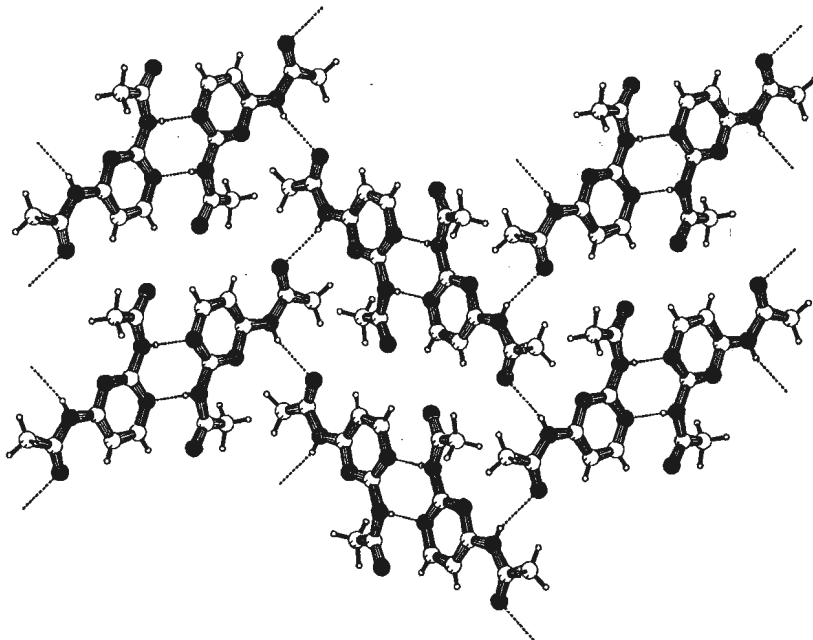


Figure 3.11: PLUTON representation of the hydrogen bonding pattern in the crystal structure of **13**.

The absence of the quadruple hydrogen bonding motif in the crystal structure of di(acetylamino)pyrimidine **13** is remarkable. A more precise analysis shows that the same number of hydrogen bonds per molecule is present in the crystal structure of **13** as in the crystal structure of derivative **14**, which does form quadruply hydrogen bonded dimers. Apparently, favorable packing interactions stabilize the observed structure observed for **13**. This explanation is supported by the high density of the crystal of **13** of 1.5 g.cm^{-3} .

3.3.4 Association in Chloroform Solution; Dimerization Constants

Mode of Association. IR spectra in (concentrated) chloroform solution and in the solid state show strong similarity for derivatives **14** and **18**, both in the N–H region ($3500\text{--}3170 \text{ cm}^{-1}$) as well as in the double bond region ($1750\text{--}1400 \text{ cm}^{-1}$). This similarity is a strong argument that the complexation mode is the same in the solid state and in solution: dimerization via quadruple hydrogen bonding.²⁸ N–H stretch vibrations of monomer and dimer in chloroform solution, reported in table 3.5, as well as ^1H -NMR and ^{13}C -NMR spectra

taken both in CDCl_3 and in $\text{DMSO}-d_6$ are only in agreement with the tautomeric forms of the structural formulas.²⁹ Like for the triazines, ^1H -NMR indicates association via hydrogen bonding.

Table 3.5: N–H stretch vibrations (ν in cm^{-1}) in monomers and dimers of diamino-pyrimidine derivatives, most likely assignment of vibrations (in parentheses), and complexation induced shifts ($\Delta\nu$).

Compound	ν N–H in monomer	ν N–H in dimer	$\Delta\nu$
di(acylamino)-pyrimidines 13 , 14	3417 (<i>trans</i> -amide N–H)	3250 (N–H \cdots O=C)	167
2-butylureido-4-acetylamino-pyrimidine 18	3408 (<i>cis</i> -amide N–H)	3172 (N–H \cdots N)	236
	3426 (ureido N–H) ^b	3170 (ureido N–H \cdots N)	256
	3415 (<i>trans</i> -amide N–H) ^c	3257 (amide N–H \cdots O=C)	158
		3286 (intramolecular HB)	

^a $\Delta\nu = \nu$ N–H in dimer – ν N–H in monomer; ^b Measured at 0.3 mM and 0.09 mM in a 5 mm cell, a small and split peak is observed that can be ascribed to monomer; ³⁰ ^b The N–H stretch vibration of the intramolecular hydrogen bonded N–H in the monomer could not be determined.

Dimerization constants in CDCl_3 . By fitting the concentration dependence of the N–H resonances as described in section 3.2,³¹ dimerization constants and chemically induced shift values (CIS) of pyrimidine derivatives **13** and **14** in pure CDCl_3 were obtained (table 3.6). The dimerization constant of **18** in pure chloroform is beyond the range measurable by ^1H -NMR: the resonances only start to shift at the lowest measurable concentrations. With IR spectroscopy, which allows for higher dilutions, the dimerization constant of **18** in pure chloroform could also not be determined, because only a small percentage of dissociation is observed at the lowest measurable concentration.

Table 3.6: Dimerization Constants (K_{dim}) in CDCl_3 , and CIS values of N–H protons of pyrimidine derivatives at 298 K.

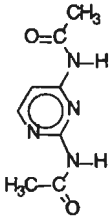
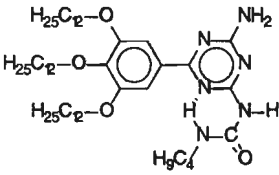
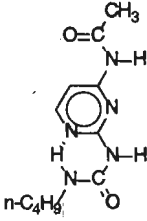
Compound	K_{dim} (M^{-1}) ^a	CIS (ppm) ^a	ΔG_{dim} ($\text{kJ}\cdot\text{mol}^{-1}$)
di(acetylamino)pyrimidine 13	890 (60)	2.95 (0.02)	–16.8
		2.47 (0.02)	
di(hexanoylamino)pyrimidine 14	170 (30)	2.73 (0.01)	–12.7
		2.35 (0.01)	
2-butylureido-4-acetylamino-pyrimidine 18	– ^b	–	–

^a estimated error in parentheses; ^b too large to measure.

The dimerization constants of di(acylamino)pyrimidines **13** and **14** ($K_{\text{dim}} = 890$ and 170 M^{-1} , respectively) are remarkably different for analogues that only differ in the length of the alkanoyl substituent. These differences are likely to be caused by entropic factors of the alkanoyl groups, since the shifts of the wavenumbers of the two N–H stretch vibrations of the amides of **13** and **14** upon complexation are the same.

Dimerization Constants in CDCl_3 / CH_3OH mixtures. Because the dimerization constant of **18** in pure chloroform was too large to determine directly by ^1H -NMR or IR, dimerization constants were measured in mixtures of chloroform with methanol. It was expected that the co-solvent methanol would compete in hydrogen bonding, resulting in a decrease of dimerization constants. We anticipated that dimerization constants would come into the measurable range, and that it might even be possible to extrapolate to K_{dim} values in pure CDCl_3 . To check the reliability of this technique, the dimerization constants of mono-ureidotriazine **10** and di(acetylamino)pyrimidine **13** were also determined in the solvent mixtures (Table 3.7).³²

Table 3.7: Dimerization Constants (M^{-1}) of Triazine and Pyrimidine derivatives in solvent mixtures of CDCl_3 and CH_3OH at 298 K.

<div style="display: flex; justify-content: space-around; align-items: center;"> <div style="text-align: center;">  <p>13</p> </div> <div style="text-align: center;">  <p>10</p> </div> <div style="text-align: center;">  <p>18</p> </div> </div>									
com- pound	Volume percentage CH_3OH in CDCl_3 (%)								
	0	0.5	1	2	3	4	5	7	10
13	890	195	67	21	- ^d	6	- ^c	- ^c	- ^c
10	2.0×10^4 ^a	- ^b	6800	4800	2070	1920	1100	700	- ^d
18	- ^b	- ^b	5.0×10^4	2.2×10^4	8000	5800	3200	1500	800

^a IR value; ^b Too large to determine directly; ^c K_{dim} too low to determine due to low solubility; ^d not determined.

The dimerization constant of **18** in pure chloroform was estimated to lie between 2×10^5 and $1 \times 10^6 \text{ M}^{-1}$, based on three different methods of extrapolation.

(i) Monomer and dimer shifts in the mixtures were plotted versus solvent composition, and extrapolated to pure CDCl_3 . A good extrapolation was obtained for the proton next to the acetylamino substituent, because monomer and dimer shifts for this proton are very similar in the applied mixed solvent systems. Thus, an estimate for the dimerization constant in pure CDCl_3 of $1.9 (\pm 0.5) \times 10^5 \text{ M}^{-1}$ was obtained.³³

(ii) $\log K_{\text{dim}}$ was plotted versus solvent composition (figure 3.12). Although it has been presumed that a linear relation between energy of association and solvent mixture composition is present,³⁴ we find a non-linear relation between $\log K_{\text{dim}}$ and solvent composition. A similar non-linear relation has recently been reported for other hydrogen bonded complexes in toluene/ethanol mixtures by Hayashi.³⁵ This non-linear relation hampers extrapolation to pure CDCl_3 . A relation between observed dimerization constants in the mixtures and solvent composition may be derived from a simple model that uses only additional competitive equilibria between monomer and co-solvent (see Experimental Section). Fitting of the points does give lines that go nicely through the points (solid lines), but we do not obtain a reliable combination of parameters, and hence no reliable value in pure CDCl_3 . Fitting of the datapoints for compounds **10** and **13**, omitting the measured point in pure CDCl_3 (dotted lines), affords extrapolated values higher than the measured values.

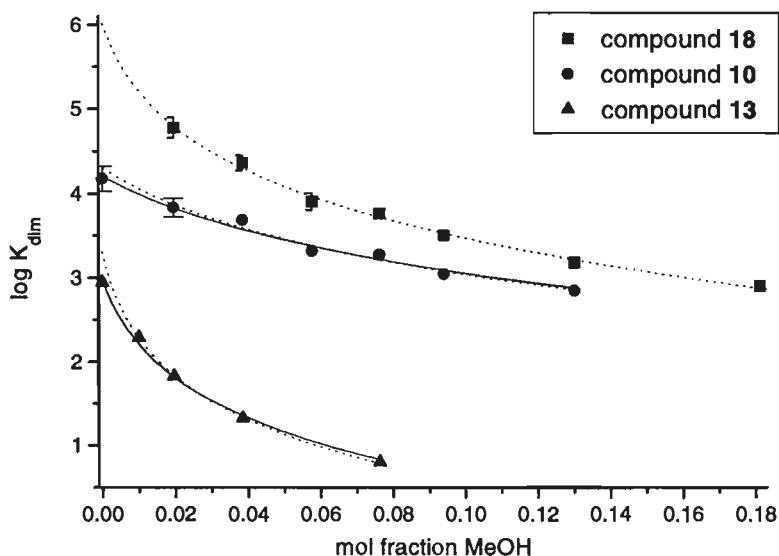


Figure 3.12: Plot of $\log K_{\text{dim}}$ versus solvent composition. Solid lines represent fits including the datapoint in pure CDCl_3 ; dotted lines represent fits without the datapoint in pure CDCl_3 . Error bars are only given when errors are larger than the size of the point.

(iii) Because the energies of many processes have been shown to be linearly related to solvent polarity, $\log K_{\text{dim}}$ was plotted versus $\text{ET}(30)$, one of the most widely used empirical parameters for solvent polarity (figure 3.13).³⁶ A strikingly linear relation between $\log K_{\text{dim}}$ and $\text{ET}(30)$ is obtained.³⁷ Extrapolation affords a value of roughly $5 \times 10^5 \text{ M}^{-1}$ for the dimerization constant of **18** in pure CDCl_3 .³⁸

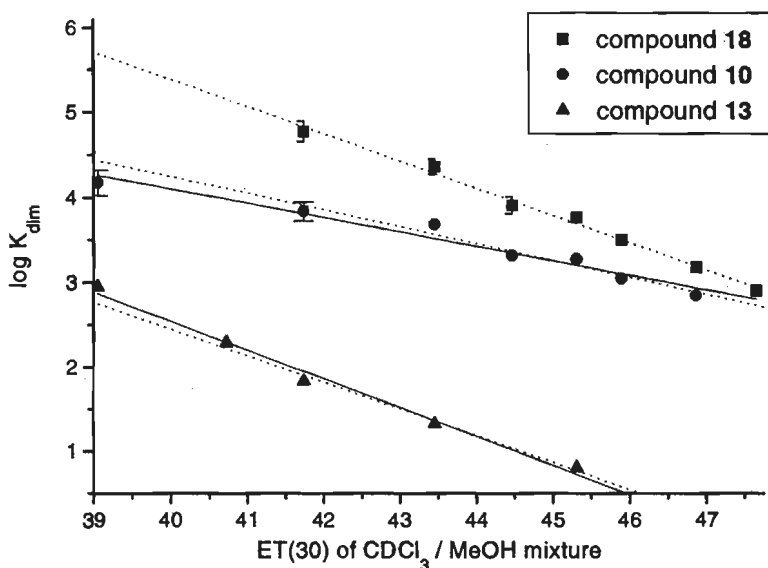


Figure 3.13: Plot of $\log K_{\text{dim}}$ versus $\text{ET}(30)$ value, and linear fitted lines. Solid lines represent fits including the datapoint in pure CDCl_3 ; dotted lines represent fits without the datapoint in pure CDCl_3 . Error bars are only given when errors are larger than the size of the point. The $\text{ET}(30)$ value of CDCl_3 equals 39.00.

3.4 Evaluation of Relative Strength of Dimerization

Although the dimers of compounds **2–4**, **7–14**, and **18** are all stabilized by four intermolecular hydrogen bonds, the strength of the dimers differs remarkably by as much as $21.3 \text{ kJ}\cdot\text{mol}^{-1}$. The dimerization constants of complexes destabilized by spectator repulsions²—present in di(acylated) derivatives of diaminotriazines and resulting from the spectator carbonyl groups in their ADADA-array—are lower than of corresponding mono-acylated derivatives with a DADA-array without these repulsive interactions. That di(acetylamino)triazine derivative **1** (see chapter 2) and di(butylureido)triazine **11** do not form quadruply hydrogen bonded dimers in the solid state is also likely to be related to the relative low stability of dimers of a ADADA array. A fair comparison of di(ureido)triazines with

respect to di(acylamino)triazines to show the effect of pre-organization could not be made, because of the strong opposite effect of substituents on the association constants.

The dimerization constants of compounds with DADA arrays differ significantly, ranging from $K_{\text{dim}} = 170 \text{ M}^{-1}$ ($\Delta G_{\text{dim}} = -12.7 \text{ kJ.mol}^{-1}$) to $K_{\text{dim}} = 1.9 \times 10^5 \text{ M}^{-1}$ ($\Delta G_{\text{dim}} = -30.1 \text{ kJ.mol}^{-1}$).³⁹ Sartorius and Schneider have recently proposed a simple free energy relationship for the stability of multiple hydrogen bonded complexes in chloroform.⁴⁰ This model predicts a dimerization constant of 310 M^{-1} ($\Delta G_{\text{dim}} = -14.2 \text{ kJ.mol}^{-1}$) for DADA arrays. The dimerization constants of amide derivatives **7**, **13** and **14** agree reasonably well with the calculated value ($K_{\text{dim}} = 530$, 890 and 170 M^{-1} , respectively). However, the dimerization constants of ureido-substituted derivatives **10** and **18** are anomalously high ($K_{\text{dim}} = 2.0 \times 10^4$ and $1.9 \times 10^5 \text{ M}^{-1}$, respectively), exceeding the calculated values by 10.3 and 15.9 kJ.mol^{-1} . Clearly, the strength of these quadruply hydrogen bonded complexes is determined by more factors than just the number and order of hydrogen bonds.

The most striking difference in dimerization constants is observed between compounds with a butylureido substituent on one hand and compounds with an acetylamino substituent on the other hand. The DADA array in ureido derivatives **10** and **18** is stabilized by pre-organization by the intramolecular hydrogen bond. In dimers of amido-compounds **7**, **13** and **14**, the amide is in an enthalpically unfavorable *cis*-conformation, and it is coplanar with the aromatic ring. In ureido-derivatives **10** and **18**, formation of an energetically favorable intramolecular hydrogen bond fixes the carbonyl in the enthalpically unfavorable *cis*-conformation required for dimerization. Furthermore, two rotations are freezed by pre-organization: rotation over the C–N bond from the aromatic ring to the N–H substituent, as well as rotation of the amide bond itself. We believe that these are the main effects responsible for the larger dimerization strength of ureido derivatives in comparison with amido derivatives.

The differences may also be related to different enthalpies of the individual hydrogen bonds themselves. A rough idea of the enthalpy of hydrogen bond formation may be obtained from shifts in the N–H stretch vibrations upon dimerization ($\Delta\nu$). These shifts are similar for **13** and **18** ($\Delta\nu$ N–H values are 167 and 235 cm^{-1} for **13**, and 158 and 256 cm^{-1} for **18**). For mono(acetyl)- and monoureido-amino triazines **7** and **10**, a larger shift of wavenumbers upon complexation is present in the ureido than in the amido compound ($\Delta\nu$ N–H values are 168 and 173 cm^{-1} for **7**, and 181 and 221/201 cm^{-1} for **10**).

The dimerization constant of ureido-pyrimidine **18** ($K_{\text{dim}} = 1.9 \times 10^5 \text{ M}^{-1}$) is approximately one order of magnitude higher than that of ureidotriazine **10** ($K_{\text{dim}} = 2.0 \times 10^4 \text{ M}^{-1}$). A less pronounced difference in the same direction is observed for acetylated derivatives of pyrimidines and triazines ($K_{\text{dim}} = 890 \text{ M}^{-1}$ for di(acetylamino)pyrimidine **13**, and 530 M^{-1} for acetylaminotriazine **7**, respectively). These differences are partly related to a larger enthalpy of hydrogen bond formation. Shifts of wavenumbers of N–H stretch

vibrations in IR upon complexation (tables 3.2 and 3.5) are significantly larger in pyrimidines than in corresponding triazines, both for the *cis*-amide as well as the ureido substituent. The larger enthalpy upon hydrogen bond formation in the pyrimidines is likely to be caused by the higher basicity of the pyrimidine ring nitrogens. However, also a steric effect of the 6-phenyl substituent on the formation of the intramolecular hydrogen bond in ureido-triazine **10** may account for the lower dimerization constant of the triazine **10** with respect to pyrimidine **18**.

3.5 Conclusion

Self-complementary DADA arrays are obtained in one step by acylation of 2,4-diaminopyrimidine or 2,4-diaminotriazine with an acid chloride or anhydride. Because of the favored *cis*-amide conformation of an amide between two aromatic ring nitrogens, the DAD array of parent diamino-derivative is extended to a DADA array. The stability of dimers is increased significantly by replacing the *cis*-amide group by a ureido substituent. The ureido substituent forms an intramolecular hydrogen bond to a non-central ring nitrogen, pre-organizing the array. These ureido compounds are conveniently synthesized by an acylation reaction with an isocyanate.

The concept of dimerization via quadruple hydrogen bonding opens a wide range of possibilities for several supramolecular applications, because of the unique combination of ease of synthesis of the units, the conceptual advantage of self-complementarity, and the strength of the four-point interaction. The absence of additional hydrogen bonding interactions between dimers of pyrimidine derivatives is useful for several supramolecular applications where unidirectionality is required.

3.6 Experimental Section

General methods. Chemicals were purchased from Acros Chimica, Fluka or Aldrich and used as received unless otherwise stated. All reactions were carried out under an atmosphere of dry nitrogen unless otherwise stated. Solvents were of technical grade unless otherwise stated. Anhydrous THF and diethyl ether were obtained by distillation from sodium/potassium/benzophenone; analytical grade pyridine, ethanol and *iso*-propanol were dried over 4 Å molecular sieves. NMR-spectra were recorded on a Varian Gemini 300 or a Bruker AM400. Chemical shifts are given in ppm relative to TMS for proton and carbon spectra. For the ¹H-NMR titrations, CDCl₃ was used as received. For the IR-experiments in solution, analytical grade chloroform (stabilized with ethanol) was purified by extractions with water, followed by drying over calcium chloride for two hours and distillation under an atmosphere of dry nitrogen. IR-spectra were recorded on a Perkin-Elmer 1600 FT-IR spectrometer. For determination of the dimerization constants with IR, spectra were recorded on a Perkin-Elmer 2000 FT-IR spectrometer. Spectra at concentrations above 5 mM were taken in a 0.1 mm NaCl cell,

and in a 1 mm cell (or 5 mm cell) for lower concentrations. UV/VIS spectra for determination of ET(30) solvent polarity were measured on a Perkin Elmer Lambda 2B spectrophotometer. Melting points were determined on a Jenaval THMS 600 melting point microscope and are uncorrected.

Binding experiments. For the $^1\text{H-NMR}$ titrations, CDCl_3 (Cambridge Isotope Laboratories) was used as received from a recently purchased, newly opened bottle which was kept in the dark and had a clear silver blade. At least 10 datapoints in the 20–80% saturation range were measured. The dimerization constants were evaluated by non-linear least-squares computer fitting of the concentration dependence of the chemical shifts of N–H protons (and also of aromatic and CH_3 protons were appropriate) to the appropriate equation, following the guidelines of Connors.⁴¹

Determination of dimerization constants from IR-spectra. IR spectra of 7 samples of dissolved compound in dry chloroform were taken at varying concentrations. The spectra were corrected for solvent, dissolved water and water vapour. Concentrations ranged from 1×10^{-3} to 2×10^{-5} M for compound 10, and from 3×10^{-2} to 8×10^{-4} M for compound 11. Spectra of monomer-dimer mixtures were regarded as a fraction-weighted sum of the spectra of the pure monomer and of the pure dimer. Measured spectra, spectral range $3560\text{--}3390\text{ cm}^{-1}$, were fitted affording the pure monomer and dimer spectra, as well as the fractions of monomer and dimer at each concentration, which gives the dimerization constant. No trend with the concentration was found in the fitted dimerization constants, and the values at different concentrations had only a small relative error (<5%), indicating this technique is very reliable.

Derivation of relation between $\log K_{\text{dim}}$ and solvent mixture composition. A monomer molecule (designated as M) associates with a single methanol molecule of the cosolvent (S) to a monomer-methanol complex (M-S), with corresponding equation for the competitive complexation (K_{comp}) with methanol.



The equation for the dimerization (K_{dim}) is as follows:



The dimerization constant in the solvent mixture (K_{obs}) is then expressed as:

$$K_{\text{obs}} = \frac{[\text{D}]}{(\text{total } [\text{M}])^2} = \frac{[\text{D}]}{([\text{M}] + [\text{M-S}])^2}$$

Substitution and rearrangement gives the following equation:

$$\log K_{\text{obs}} = \log K_{\text{dim}} - 2 * \log (1 + K_{\text{comp}} * [\text{S}])$$

Taking into account the possibility of higher order association, i.e. for example two molecules of methanol per monomer molecule, it can be deduced that the formula then becomes an array:

$$\begin{aligned} \log K_{\text{obs}} = \log K_{\text{dim}} - 2 * \log (1 + K_{\text{comp}1} * [\text{S}] + \\ K_{\text{comp}2} * [\text{S}]^2 + \\ K_{\text{comp}3} * [\text{S}]^3 + \dots) \end{aligned}$$

As $[\text{S}]$ is the concentration of free competing solvent, the equation only holds if $K_{\text{comp}} * [\text{S}] \ll 1$. The observed relation between $\log K_{\text{obs}}$ and solvent composition could be fitted reasonably well with the

equation without higher order terms (lines in figure 3.13). The combination of parameters from the fits is however not reliable; exclusion of the point at 0% gives a significant change in the values of the parameters.

X-ray single crystal structure analyses. Crystals suitable for X-ray analysis were mounted on a Lindemann glass capillary and transferred onto an Enraf-Nonius CAD4T diffractometer, and were irradiated with Mo K α irradiation with graphite monochromator, $\lambda = 0.71073$ Å, ω scan, at $T = 150$ K, on rotating anode. Data were corrected for Lp effects, and for linear instability of three reference reflections, but not for absorption. The structure was solved by automated direct methods (SHELXS-96). Refinement on F^2 was carried out by full-matrix least-squares techniques (SHELXL-96); no observance criterion was applied during refinement. Positional parameters for hydrogen atoms were included in the refinement; initial values were obtained from a difference Fourier map. All non-hydrogen atoms were refined with anisotropic thermal parameters; hydrogen atoms were refined with a fixed thermal isotropic related to the value of the equivalent isotropic of their carrier-atoms by a factor of 1.5 for the CH₃ and NH₂ hydrogen atoms, and 1.2 for the other hydrogen atoms.

Crystal data for 2: C₆H₉N₅O, $M_r = 167.17$, colourless needle-shaped crystal (0.05 x 0.10 x 0.45 mm), triclinic, space group $P\bar{1}$ (no. 2) with $a = 4.0732$ (3), $b = 8.6054$ (9), $c = 11.1902$ (14) Å, $\alpha = 75.348$ (9), $\beta = 83.461$ (8), $\gamma = 78.752$ (8)°, $V = 371.33$ (7) Å³, $Z = 2$, $D_c = 1.4951$ (3) g.cm⁻³, $F(000) = 176$, $\mu(\text{Mo K}\alpha) = 1.1$ cm⁻¹. 3882 Reflections measured, 1703 independent reflections, $R_{\text{int}} = 0.047$ ($1.9^\circ < \theta < 27.5^\circ$), and 136 parameters. Refinement converged at $wR2 = [\sum[w(F_o^2 - F_c^2)^2] / \sum[w(F_o^2)^2]]^{0.5} = 0.1170$, $w = 1/[\sigma^2(F^2) + (0.0592P)^2 + 0.13P]$, where $P = (\max(F_o^2, 0) + 2F_c^2)/3$, $R1 = \sum |F_o| - F_c / \sum |F_o| = 0.0426$ (for 1343 reflections with $I > 2\sigma(I)$), $S = 1.041$, $-0.30 < \Delta\rho < 0.28$ e Å⁻³.

Crystal data for 9: C₉H₁₆N₆O, $M_r = 224.27$, colourless, needle-shaped crystal (0.05 x 0.10 x 0.50 mm), triclinic, space group $P\bar{1}$ (no. 2) with $a = 4.703$ (2), $b = 7.924$ (6), $c = 15.833$ (18) Å, $\alpha = 78.69$ (9), $\beta = 86.18$ (6), $\gamma = 74.43$ (6)°, $V = 557.3$ (8) Å³, $Z = 2$, $D_c = 1.3365$ (19) g.cm⁻³, $F(000) = 240$, $\mu(\text{Mo K}\alpha) = 0.9$ cm⁻¹. 4350 Reflections measured, 2567 independent reflections, $R_{\text{int}} = 0.059$, ($1.3^\circ < \theta < 27.5^\circ$), and 193 parameters. Refinement converged at $wR2 = 0.1323$, $w = 1/[\sigma^2(F^2) + (0.0465P)^2 + 0.07P]$, $R1 = 0.0553$ (for 1474 reflections with $I > 2\sigma(I)$), $S = 1.021$, $-0.22 < \Delta\rho < 0.27$ e Å⁻³.

Crystal data for 11: C₁₄H₂₅N₇O₂, $M_r = 323.4$, colourless plate-shaped crystal (0.05 x 0.2 x 0.6 mm), monoclinic, space group $C2/c$ (no. 15) with $a = 29.54$ (2), $b = 4.613$ (5), $c = 26.89$ (2) Å, $\alpha = 90$, $\beta = 109.34$ (7), $\gamma = 90^\circ$, $V = 3457$ (5) Å³, $Z = 8$, $D_c = 1.2427$ (18) g.cm⁻³, $F(000) = 1392$, $\mu(\text{Mo K}\alpha) = 0.9$ cm⁻¹. 20434 Reflections measured, 3191 independent reflections, $R_{\text{int}} = 0.4191$, ($0.80^\circ < \theta < 25.1^\circ$), and 226 parameters. Hydrogen atoms were included on calculated positions. The atoms C112 through C115 of the butyl group are disordered over two positions. Final $wR2 = 0.1990$, $w = 1/[\sigma^2(F^2) + (0.0403P)^2]$, $R1 = 0.0682$ (for 1136 $I > 2\sigma(I)$), $S = 0.954$, $-0.35 < \Delta\rho < 0.23$ e Å⁻³.

Crystal data for 13: C₈H₄N₄O₂, $M_r = 194.19$, colourless needle-shaped crystal (0.05 x 0.1 x 0.4 mm), monoclinic, space group $P2_1/c$ (no. 14) with $a = 5.4141$ (5), $b = 19.552$ (2), $c = 9.1558$ (15) Å, $\alpha = 90$, $\beta = 116.886$ (9), $\gamma = 90^\circ$, $V = 864.4$ (2) Å³, $Z = 4$, $D_c = 1.4922$ (3) g.cm⁻³, $F(000) = 408$, $\mu(\text{Mo K}\alpha) = 1.1$ cm⁻¹. 4496 Reflections measured, 1973 independent reflections, $R_{\text{int}} = 0.0865$, ($1.04^\circ < \theta < 27.5^\circ$), and 157 parameters. Positional parameters of the hydrogen atoms were refined. Final $wR2 = 0.1222$, $w = 1/[\sigma^2(F^2) + (0.0399P)^2]$, $R1 = 0.0543$ (for 1116 $I > 2\sigma(I)$), $S = 0.970$, $-0.24 < \Delta\rho < 0.31$ e Å⁻³.

Crystal data for 14: C₁₆H₂₈N₄O₂, $M_r = 306.41$, colourless block-shaped crystal (0.2 x 0.3 x 0.5 mm), triclinic, space group $P\bar{1}$ (no. 2) with $a = 4.9675$ (11), $b = 8.1236$ (7), $c = 20.911$ (3) Å, $\alpha = 100.663$ (9), $\beta = 93.080$ (15), $\gamma = 91.680$ (12)°, $V = 827.4$ (2) Å³, $Z = 2$, $D_c = 1.2299$ (3) g.cm⁻³, $F(000) = 332$, $\mu(\text{Mo K}\alpha) = 0.8$ cm⁻¹. 4552 Reflections measured, 3814 independent reflections, $R_{\text{int}} = 0.055$, ($1.0^\circ < \theta < 27.5^\circ$), and 277 parameters. Refinement converged at $wR2 = 0.1567$, $w = 1/[\sigma^2(F^2) +$

$(0.0880\text{P})^2 + 0.31\text{P}$, $R_1 = 0.0553$ (for 2963 reflections with $I > 2\sigma(I)$), $S = 1.015$, $-0.27 < \Delta\rho < 0.34 \text{ e } \text{\AA}^{-3}$.

Crystal data for 18: $\text{C}_{11}\text{H}_{17}\text{N}_5\text{O}_2$, $M_r = 251.29$, colourless, needle-shaped crystal ($0.1 \times 0.1 \times 0.7 \text{ mm}$), monoclinic, space group C2/c (no. 15) with $a = 20.119$ (18), $b = 5.194$ (2), $c = 25.186$ (16) \AA , $\alpha = 90$, $\beta = 94.55$ (4) $^\circ$, $\gamma = 90$, $V = 2624$ (3) \AA^3 , $Z = 8$, $D_c = 1.2722$ (15) g.cm^{-3} , $F(000) = 1072$, $\mu(\text{Mo K}\alpha) = 0.9 \text{ cm}^{-1}$. 8860 Reflections measured, 3007 independent reflections, $R_{\text{int}} = 0.075$, ($1.0^\circ < \theta < 27.3^\circ$), and 214 parameters, measured on an Enraf-Nonius FAST area detector on rotating anode. Refinement converged at $wR_2 = 0.1332$, $w = 1/[\sigma^2(F^2) + (0.0300\text{P})^2 + 4.33\text{P}]$, $R_1 = 0.0644$ (for 2305 reflections with $I > 2\sigma(I)$), $S = 1.16$, $-0.25 < \Delta\rho < 0.25 \text{ e } \text{\AA}^{-3}$.

2-Amino-4-acetylamino-6-methyl-s-triazine (2). A suspension of 2,4-diamino-6-methyl-s-triazine (2.50 g, 20 mmol) in a mixture of dry pyridine (30 mL) and acetic anhydride (20 mL) was boiled under reflux for 15 min, and a much thicker suspension was obtained. After quick cooling to ambient temperature, the suspension was filtered, and the residue was washed thoroughly with acetone, giving almost pure **2** (3.30 g, 99%). Crystallization from DMF gave analytical pure product as X-ray quality crystals, mp $> 300^\circ\text{C}$ (sublimation). $^1\text{H-NMR}$ ($\text{DMSO-}d_6$) δ : 10.12 (s, 1H), 7.30 and 7.24 (br, 2H), 2.22 and 2.21 (2 s, 6H). $^{13}\text{C-NMR}$ ($\text{DMSO-}d_6$) δ : 175.8, 169.9, 167.0, 163.5, 25.2, 24.8. IR (KBr) ν : 3301, 3215, 3133, 3036, 1676, 1611, 1535, 1486, 1370, 1305 cm^{-1} . Anal. calcd. for $\text{C}_8\text{H}_9\text{N}_5\text{O}$: C, 43.11; H, 5.43; N, 41.89. Found: C, 43.27; H, 5.43; N, 41.89.

2-Amino-4-hexanoylamino-6-methyl-s-triazine (3). In a similar procedure as for **2**, reaction of 2,4-diamino-6-methyl-s-triazine (2.50 g, 20 mmol) with hexanoic anhydride (19 mL, 80 mmol) in dry pyridine (60 mL) gave compound **3** (2.80 g, 65%), with continuing reflux for 15 min after dissolution. Crystallization from DMF gave an analytically pure sample, mp $234\text{--}235^\circ\text{C}$. $^1\text{H-NMR}$ ($\text{DMSO-}d_6$) δ : 10.09 (s, 1H), 7.27 (br, 1H), 7.21 (br, 1H), 2.52 (t, 2H), 2.22 (s, 3H), 1.54 (m, 2H), 1.26 (m, 4H), 0.87 (t, 3H). $^{13}\text{C-NMR}$ ($\text{DMSO-}d_6$) δ : 175.8, 172.4, 167.1, 163.4, 36.6, 30.8, 24.7, 24.3, 21.6, 13.8. IR (KBr) ν : 3305, 3236, 3138, 2954, 2930, 2870, 1691, 1673, 1612, 1535, 1367, 1330, 1267, 1211 cm^{-1} . Anal. calcd. for $\text{C}_{10}\text{H}_{17}\text{N}_5\text{O}$: C, 53.79; H, 7.67; N, 31.37. Found: C, 53.94; H, 7.53; N, 31.87.

2-Amino-4-acetylamino-6-methoxymethyl-s-triazine (4). In a similar procedure as for **2**, 2,4-diamino-6-methoxymethyl-s-triazine (3.40 g, 20 mmol) was reacted with acetic anhydride (20 mL) in dry pyridine, resulting in a crude yield of **4** in 61%. An analytical sample was prepared by crystallization from DMF, mp 252°C . $^1\text{H-NMR}$ ($\text{DMSO-}d_6$) δ : 10.25 (s, 1H), 7.49 (br, 1H), 7.39 (br, 1H), 4.22 (s, 2H), 3.35 (s, 3H), 2.24 (s, 3H). $^{13}\text{C-NMR}$ ($\text{DMSO-}d_6$) δ : 175.5, 170.0, 167.1, 163.6, 73.6, 58.3, 25.2. IR (KBr) ν : 3303, 3229, 3145, 2935, 1672, 1608, 1540, 1374, 1310 cm^{-1} . Anal. calcd. for $\text{C}_7\text{H}_{11}\text{N}_5\text{O}_2$: C, 42.64; H, 5.62; N, 35.51. Found: C, 42.49; H, 5.49; N, 36.05.

Methyl 3,4,5-tri(dodecyloxy)-benzoate (5). A 500 mL flask, charged with methyl 3,4,5-trihydroxybenzoate (gallic acid methyl ester) (11.04 g, 0.06 mol) was brought under nitrogen atmosphere. Subsequently added were dry DMF (280 mL), anhydrous potassium carbonate (66.34 g, 0.48 mol), and, after a few minutes, 1-bromododecane (59.8 g, 0.24 mol). The suspension was stirred overnight at 65°C with a large magnetic stirring egg grinding the potassium carbonate. The suspension was filtered, and the residue was washed with hexane. The filtrate was extracted with water (300 mL). The aqueous phase was extracted three times with hexane (300 mL). The combined organic phases were subsequently extracted with water, twice with 1 M hydrochloric acid and twice with water. The organic phase was dried over sodium sulfate, treated with active carbon, filtered and evaporated to dryness. The product thus obtained was NMR pure, however TLC showed an impurity (hexane/ethyl acetate 4/1 v/v: product $R_f = 0.58$; impurities at $R_f = 0.29$ and 0). These impurities were removed by recrystallizing twice from ethanol (2 L) with filtering lukewarm, yielding TLC pure product

as tiny microneedles (38.34 g, 93%), mp 43.8°C. $^1\text{H-NMR}$ (CDCl_3) δ : 7.23 (s, 2H), 4.01 (t, 6H), 3.88 (s, 3H), 1.8–1.6 (m, 6H), 1.5–1.4 (m, 6H), 1.3 (br, 48H), 0.89 (t, 9H). $^{13}\text{C-NMR}$ (CDCl_3) δ : 167.4, 153.4, 142.8, 125.2, 108.6, 74.0, 69.7, 32.5, 30.9, 30.3, 30.2, 30.1, 30.0, 29.9, 26.6, 23.2, 14.6. IR (KBr) ν : 2919, 2848, 1716, 1589 cm^{-1} . Anal. calcd. for $\text{C}_{44}\text{H}_{80}\text{O}_5$: C, 76.69; H, 11.70. Found: C, 77.43; H, 11.65.

2,4-Diamino-6-[3,4,5-tri(dodecyloxy)phenyl]-s-triazine (6). Sodium (7.65 g, 0.33 mol) was dissolved in dry ethoxyethanol (400 mL). Biguanide sulfate¹⁶ (31.5 g, 0.158 mol) was added, and the mixture was stirred under reflux for 2 h. To the suspension was added methyl 3,4,5-tri(dodecyloxy)phenylbenzoate (72.4 g, 0.106 mol), and reflux was continued overnight. The solvent was removed, and the resulting sticky brown gum was dissolved in dichloromethane. The suspension was treated with active carbon. The insoluble material was removed by filtration through celite. Impurities with R_f (5% methanol in dichloromethane) = 0 and R_f = 0.49 (black) were removed from the product (R_f = 0.46, fluorescing blue) by crystallization from dilute ethanolic sodium hydroxide solution (2L). The product was further purified by simple column chromatography (first elution with dichloromethane: product R_f = 0, impurity R_f = 0.74), then elution with 5% methanol in dichloromethane. A second crystallization from slightly basic ethanol (2 L, containing 0.4g KOH/L) gave the pure product as tiny microneedles (26.4 g, 34%), mp 98–100°C. $^1\text{H-NMR}$ (CDCl_3) δ : 7.55 (s, 2H), 5.51 (br, 4H), 4.2 (m, 6H), 1.9–1.7 (m, 6H), 1.5–1.4 (m, 6H), 1.3–1.2 (br, 38 H), 0.88 (t, 9H). $^{13}\text{C-NMR}$ (CDCl_3) δ : 172.5, 168.1, 153.5, 142.0, 131.7, 107.3, 74.0, 69.6, 32.5, 30.9, 30.2 (overlapping peaks), 30.0, 29.9, 26.7, 23.2, 19.0, 14.7. IR (KBr) ν : 3475, 3401, 3170, 2930, 2852, 1627, 1568, 1545, 1511, 1467, 1417, 1377 cm^{-1} . Anal. calcd. for $\text{C}_{45}\text{H}_{81}\text{N}_5\text{O}_3$: C, 73.02; H, 11.03; N, 9.46. Found: C, 73.00; H, 11.51; N, 9.55.

2-Amino-4-(acetylamino)-6-[3,4,5-tri(dodecyloxy)phenyl]-s-triazine (7). A solution of 2,4-diamino-6-[3,4,5-tri(dodecyloxy)phenyl]-s-triazine (1.60 g, 2.2 mmol) **5** and acetic anhydride (0.22 g, 2.2 mmol) in dry pyridine (15 mL) were heated under reflux for 1 h. After cooling, solvent was evaporated under reduced pressure aided by co-distillation with toluene. The product was dissolved in hot ethyl acetate, treated with active carbon, and filtered hot. After cooling, the white precipitate (containing a mixture of **7** and **8**) was filtered (the mother liquor contained almost only the diamino-s-triazine **6**) and crystallized subsequently from dichloromethane, and from ether/THF 10:1 v/v, gave product (0.34 g, 20%) which was 95% pure, mp 60°C (liquid crystalline), change to other LC-phase at 148°C, isotropization at 158°C. $^1\text{H-NMR}$ (CDCl_3) δ : 10.49 (br, 1H), 8.40 (br, 1H), 7.60 (br, 2H), 5.47 (br, 1H), 4.0 (m, 6H), 2.80 (s, 3H), 1.83 (m, 4H), 1.74 (m, 2H), 1.47 (m, 6H), 1.27 (br, 54H), 0.88 (6H). $^{13}\text{C-NMR}$ (CDCl_3) δ : 175.4, 171.5, 167.8, 163.7, 152.9, 142.0, 130.2, 106.9, 73.5, 67.0, 31.9, 30.4, 29.7 (overlapping peaks), 29.6, 29.5, 29.4, 26.8, 26.1, 26.1, 22.7, 14.1. IR (KBr) ν : 3500, 3297, 3220, 2920, 2850, 1678, 1837, 1582, 1540 cm^{-1} . Anal. calcd. for $\text{C}_{47}\text{H}_{83}\text{N}_5\text{O}_4$: C, 72.17; H, 10.69; N, 8.95. Found: C, 72.44; H, 11.02; N, 8.98.

2,4-Di(acetylamino)-6-[3,4,5-tri(dodecyloxy)phenyl]-s-triazine (8). A solution of diaminotriazine **6** (3.12 g, 42.2 mmol) was boiled under reflux in acetic anhydride (50 mL) for 4 h. After cooling, the acetic anhydride was distilled off in vacuo, aided by co-distillation of toluene. The brown gum was then dissolved in hot hexane, treated with active carbon, and filtered. A small amount of ether was added to the solution, and after cooling, the white precipitate was filtered (2.97 g, 85%). Analytically pure product was obtained by crystallization from dichloromethane giving tiny microneedles (1.66 g, 48%), mp 97°C, clearance point 186.5–187.4°C. $^1\text{H-NMR}$ (CDCl_3) δ : 10.24 (br., 2H), 7.51 (s, 2H), 3.97–3.92 (m, 6H), 2.61 (s, 6H), 1.79–1.72 (m, 6H), 1.46 (br, 6H), 1.28 (br, 42H), 0.89 (t, 9H). $^{13}\text{C-NMR}$ (CDCl_3) δ : 172.9, 172.1, 163.8, 152.7, 142.7, 129.0, 106.8, 73.3, 68.7, 31.9, 30.4, 29.8, 29.7, 29.6, 29.5, 29.4, 29.3 (twice), 26.5, 26.2, 26.1, 22.6, 14.0. IR (KBr) ν : 3252, 2918,

2850, 1739, 1681, 1554, 1423 cm^{-1} . Anal. calcd. for $\text{C}_{49}\text{H}_{85}\text{N}_5\text{O}_5$: C, 71.40; H, 10.39; N, 8.50. Found: C, 71.66; H, 10.53; N, 8.71.

2-Amino-4-(butylureido)-6-methyl-*s*-triazine (9). A suspension of 2,4-diamino-6-methyl-*s*-triazine (1.25 g, 10 mmol) and butyl isocyanate (2.4 mL, 21 mmol) in dry pyridine (50 mL) was heated under reflux for 2 h. After this period, the solvent was removed under reduced pressure. The resulting solid was suspended in hexane, filtered and washed thoroughly with hexane. The product was crystallized from chloroform to give a white powder (2.0 g, 95%). An analytical sample was prepared by recrystallization from ethanol giving thin plates, mp 141–142°C. X-ray quality crystals were obtained by crystallization from DMF. $^1\text{H-NMR}$ ($\text{DMSO}-d_6$, 120°C): δ : 8.96 (br, 1H), 8.47 (br, 1H), 6.88 (br, 2H), 3.24 (q, 2H), 2.24 (s, 3H), 1.54 (p, 2H), 1.38 (m, 2H), 0.92 (t, 3H). $^{13}\text{C-NMR}$ ($\text{DMSO}-d_6$, 120°C) δ : 174.8, 165.9, 162.7, 153.1, 38.4, 30.7, 23.8, 18.8, 12.5. IR (KBr) ν : 3212, 2956, 2950, 2861, 1683, 1617, 1587, 1533, 1481 cm^{-1} . Anal. calcd. for $\text{C}_9\text{H}_{16}\text{N}_5\text{O}$: C, 48.20; H, 7.19; N, 37.47. Found: C, 48.13; H, 7.29; N, 37.54.

2-Amino-4-(butylureido)-6-[3,4,5-tri(dodecyloxy)phenyl]-*s*-triazine (10). A solution of 2,4-diamino-6-[3,4,5-tri(dodecyloxy)phenyl]-*s*-triazine **6** (0.74 g, 1.0 mmol) and butyl isocyanate (0.23 mL, 2.0 mmol) in dry pyridine (10 mL) was heated under reflux for 2 h. The solvent was evaporated in vacuo leaving a yellow gum. Column chromatography (silica gel, dichloromethane/methanol 97:3 v/v) afforded 0.35 g (42%) of product **10**. Crystallization from toluene gave analytically pure product as tiny needles, mp 85°C (liquid crystalline), clearance point 182.9–183.8°C. $^1\text{H-NMR}$ (CDCl_3) δ : 10.16 (br, 1H), 9.78 (t, 1H), 9.29 (br, 1H), 7.37 (s, 2H), 5.49 (br, 1H), 3.96 (m, 6H), 3.30 (m, 2H), 1.75 (m, 6H), 1.66 (m, 2H), 1.57 (m, 2H), 1.5–1.1 (m, 42H), 0.87 (t, 3H), 0.80 (t, 9H). $^{13}\text{C-NMR}$ (CDCl_3) δ : 170.3, 167.2, 163.7, 155.9, 153.0, 142.1, 130.2, 106.9, 73.5, 69.2, 40.0, 32.2, 31.9, 30.4, 29.7, 29.7, 29.7, 29.6, 29.5, 29.4, 26.1, 26.1, 22.7, 20.3, 14.1, 13.8. IR (KBr) ν : 3492, 3419, 3212, 3132, 2921, 2849, 1684, 1638, 1578, 1528 cm^{-1} . Anal. calcd. for $\text{C}_{50}\text{H}_{90}\text{N}_6\text{O}_4$: C, 71.52; H, 10.80; N, 10.05. Found: C, 71.52; H, 11.26; N, 9.89.

2,4-Di(butylureido)-6-methyl-*s*-triazine (11). A suspension of 2,4-diamino-6-methyl-*s*-triazine (1.25 g, 10 mmol) and butyl isocyanate (11.3 mL, 100 mmol) in dry pyridine (50 mL) were heated under reflux for 16 h. After this period, water was added to the resultant solution to hydrolyse the excess of butyl isocyanate. After removal of the solvent, the resulting solid was crystallized from ethanol/ water 2:1 v/v. Column chromatography (6% THF in chloroform), followed by crystallization from ethyl acetate and treatment with active carbon, gave analytically pure sample (0.53 g, 16%), mp 229°C. $^1\text{H-NMR}$ (CDCl_3) δ : 10.17 (br), 9.05 (br), 3.32 (q, 4H), 2.42 (s, 3H), 1.52 (m, 4H), 1.34 (m, 4H), 0.89 (t, 6H). $^{13}\text{C-NMR}$ (CDCl_3) δ : 175.1, 162.8, 153.6, 39.4, 31.1, 25.2, 19.8, 13.3. IR (KBr) ν : 3407, 3266, 3203, 2956, 2930, 2918, 2871, 1704, 1684, 1593, 1526, 1478 cm^{-1} . Anal. calcd. for $\text{C}_{14}\text{H}_{25}\text{N}_7\text{O}_2$: C, 52.00; H, 7.79; N, 30.32. Found: C, 51.93; H, 7.70; N, 30.47.

2,4-Di(butylureido)-6-[3,4,5-tri(dodecyloxy)phenyl]-*s*-triazine (12). A solution of 2,4-diamino-6-[3,4,5-tri(dodecyloxy)phenyl]-*s*-triazine (**6**) (1.48 g, 2.0 mmol) and butyl isocyanate (2.3 mL, 20 mmol) was heated under reflux in dry pyridine (20 mL) for three days. After quenching with water, the solvent was evaporated in vacuo leaving a dark yellow gum. The product was crystallized from ethanol after treatment with active carbon, treated with active carbon in hot hexane to remove coloration, and finally crystallized from a ethanol/dichloromethane mixture by slow evaporation of solvent to air to yield pure **12** (1.16 g, 61%), mp 40°C, and clearance point 177°C. $^1\text{H-NMR}$ (CDCl_3) δ : 10.45 (br, 2H), 9.19 (br, 2H), 7.37 (s, 2H), 4.1 (m, 6H), 3.44 (q, 4H), 1.85 (m, 4H), 1.77 (m, 4H), 1.63 (m, 4H), 1.44 (m, 6H), 1.39–1.26 (m, 42H), 0.95 (t, 6H), 0.88 (t, 6H). $^{13}\text{C-NMR}$ (CDCl_3) δ : 170.1, 163.5, 154.2, 153.3, 143.2, 129.3, 107.2, 73.7, 69.4, 40.1, 32.2, 31.9, 30.3, 29.7, 29.6, 29.4 (several), 29.3,

26.1, 26.0, 22.7, 20.3, 14.1, 13.8. IR (KBr) ν : 3299, 3251, 2923, 2853, 1715, 1684, 1597, 1535 cm^{-1} . Anal. calcd. for $\text{C}_{55}\text{H}_{99}\text{N}_7\text{O}_5$: C, 70.39; H, 10.63; N, 10.45. Found: C, 70.20; H, 10.97; N, 10.36.

2,4-Di(acetylamino)pyrimidine (13). A suspension of 2,4-diaminopyrimidine (1.10 g, 10 mmol) and acetic anhydride (4 mL, 40 mmol) in dry pyridine (20 mL) was heated under reflux for 3 h. After cooling, the suspension was diluted with hexane, and filtered. The crude product was crystallized from ethyl acetate with treatment with active carbon, giving white powder. Subsequent crystallization from ethanol gave analytically pure product (0.34 g, 18%), mp 250°C. $^1\text{H-NMR}$ (CDCl_3) δ : 10.86 (br, 1H), 10.01 (br, 1H), 8.44 (d, 1H), 8.00 (d, 1H), 2.65 (s, 3H), 2.30 (s, 3H). $^{13}\text{C-NMR}$ (CDCl_3) δ : 175.0, 170.9, 159.5, 159.1, 157.0, 105.9, 25.5, 24.5. $^1\text{H-NMR}$ ($\text{DMSO}-d_6$) δ : 10.67 (br, 1H), 10.30 (br, 1H), 8.46 (d, 1H), 7.71 (d, 1H), 2.15 (s, 3H), 2.12 (s, 3H). $^{13}\text{C-NMR}$ ($\text{DMSO}-d_6$) δ : 170.7, 169.3, 159.3, 158.4, 157.3, 104.6, 24.7, 24.2. IR (KBr) ν : 3270, 3155, 3106, 2976, 2930, 1685, 1587, 1499, 1420, 1380, 1288, 1241 cm^{-1} . Anal. calcd. for $\text{C}_8\text{H}_{10}\text{N}_4\text{O}_2$: C, 49.48; H, 5.19; N, 28.85. Found: C, 47.79; H, 5.53; N, 27.72.

2,4-Di(hexanoylamino)pyrimidine (14). A suspension of 2,4-diaminopyrimidine (1.10 g, 10 mmol) and hexanoic anhydride (7 mL, 30 mmol) in dry pyridine (20 mL) was heated under reflux for 3 h. After cooling, the suspension was diluted with hexane, and filtered. The crude product was crystallized from hexane/ethyl acetate 1:1 v/v with active carbon treatment, giving white crystals (1.10 g, 36%), mp 180–180.5°C. $^1\text{H-NMR}$ (CDCl_3) δ : 10.77 (br, 1H), 9.89 (br, 1H), 8.42 (d, 1H), 8.00 (d, 1H), 3.04 (tr, 2H), 2.54 (tr, 2H), 1.71 (m, 4H), 1.38 (m, 8H), 0.92 (m, 6H). $^{13}\text{C-NMR}$ (CDCl_3) δ : 178.0, 174.3, 159.5, 158.9, 156.9, 105.8, 37.3, 37.0, 31.5, 31.4, 24.9, 24.4, 22.5, 22.4, 13.9. IR (KBr) ν : 3270, 3166, 2955, 2871, 1699, 1674, 1452 cm^{-1} . Anal. calcd. for $\text{C}_{18}\text{H}_{26}\text{N}_4\text{O}_2$: C, 62.72; H, 8.55; N, 18.29. Found: C, 62.36; H, 8.51; N, 18.66.

2-Butylureido-4-amino-pyrimidine (15). To a solution of 2,4-diaminopyrimidine (1.10 g, 10 mmol) in warm dry THF (50 mL) was added via a syringe butyl isocyanate (1.13 mL, 10 mmol). After boiling under reflux for 1 h, the suspension was cooled, and diluted with water (200 mL). Upon reduction of the volume to approx. 100 mL, white powder precipitated. This white powder was filtered, and crystallization from ethanol gave analytically pure **15** as crystals (0.30 g, 15%), mp 264.5°C with decomposition. $^1\text{H-NMR}$ ($\text{DMSO}-d_6$) δ : 9.43 (t, 1H), 9.09 (s, 1H), 7.88 (d, 1H), 7.09 (br, 2H), 6.03 (d, 1H), 3.18 (q, 2H), 1.46 (m, 2H), 1.31 (m, 2H), 0.90 (t, 3H). $^{13}\text{C-NMR}$ ($\text{DMSO}-d_6$) δ : 163.9, 158.0, 155.0, 154.6, 99.1, 38.6, 31.7, 19.7, 13.7. IR (KBr) ν : 3378, 3243, 3168, 3067, 2954, 2926, 2869, 1655, 1610, 1555, 1467, 1352, 1273 cm^{-1} . Anal. calcd. for $\text{C}_9\text{H}_{14}\text{N}_5\text{O}$: C, 51.91; H, 6.78; N, 33.63. Found: C, 51.47; H, 7.28; N, 33.39.

2-Acetylamino-4-amino-pyrimidine (16), and a minor amount 4-Acetylamino-2-amino-pyrimidine (17). To a solution of 2,4-diaminopyrimidine (1.69 g, 15 mmol) in warm dry THF (70 mL) was added via a syringe acetic anhydride (1.45 mL, 15 mmol). After boiling under reflux for 5 h, the solution was cooled, and evaporated to dryness. Column chromatography (flash silica, 10% MeOH in chloroform) afforded 0.10 g of di(acetylamino)pyrimidine **13** (3%), 0.38 g of 2-amino-4-acetylamino-pyrimidine (17%, compound **17**, mp 165–167°C), and 1.19 g of 2-acetylamino-4-amino-pyrimidine (52%, compound **16**). Analytical sample of **16** was prepared by crystallization from chloroform/ethanol 4:1 v/v, mp 205.5–206.5°C. $^1\text{H-NMR}$ of **16** ($\text{DMSO}-d_6$) δ : 9.87 (s, 1H), 7.93 (d, 1H), 6.64 (br, 2H), 6.13 (d, 1H), 2.20 (s, 3H). $^{13}\text{C-NMR}$ ($\text{DMSO}-d_6$) δ : 169.7, 164.1, 157.5, 155.5, 100.4, 24.8. IR of **16** (KBr) ν : 3408, 3340, 3261, 3206, 1656, 1642, 1613, 1561, 1472, 1316 cm^{-1} . Anal. calcd. for $\text{C}_8\text{H}_8\text{N}_4\text{O}$: C, 47.36; H, 5.30; N, 36.82. Found: C, 47.04; H, 5.37; N, 36.86.

$^1\text{H-NMR}$ of **17** ($\text{DMSO}-d_6$) δ : 10.32 (s, 1H), 8.13 (d, 1H), 7.26 (d, 1H), 6.42 (br, 2H), 2.10 (s, 3H). $^{13}\text{C-NMR}$ ($\text{DMSO}-d_6$) δ : 170.4, 163.2, 159.3, 158.4, 99.0, 24.2. IR of **17** (KBr) ν : 3468, 3439,

3341, 3205, 3158, 3015, 1719, 1657, 1607, 1581, 1526, 1452, 1304, 1247 cm^{-1} . Anal. calcd. for $\text{C}_6\text{H}_8\text{N}_4\text{O}$: C, 47.36; H, 5.30; N, 36.82. Found: C, 41.24; H, 6.01; N, 29.77.

2-Butylureido-4-acetylaminopyrimidine (18). To a warm solution of 2-butylureido-4-aminopyrimidine **15** (0.42 g, 2 mmol) in dry pyridine (30 mL) was added acetyl chloride (0.16 g, 2.1 mmol) in dry THF (10 mL). Immediately, the solution turned yellow. After a few minutes, the solution was evaporated to dryness, and the residue was dissolved partially in hot acetone (100 mL), with some added triethylamine. Water (300 mL) was added to give a clear solution. Evaporation of solvent to 100 mL resulted in a white precipitate, which was filtered and washed with water. Column chromatography (flash silica, ethanol/chloroform 97:3 v/v) gave pure product (0.20 g, 40%). Analytical sample as fine white crystals was obtained by dissolving in hot ethyl acetate, treatment with active carbon, and crystallization, mp 211.5–212°C. X-ray quality crystals were obtained by slow evaporation to air of a dichloromethane/hexane 10:1 v/v solution. $^1\text{H-NMR}$ (CDCl_3) δ : 12.04 (s, 1H), 9.66 (t, 1H), 9.38 (s, 1H), 8.27 (d, 1H), 7.93 (d, 1H), 3.36 (q, 4H), 2.30 (s, 3H), 1.61 (m, 2H), 1.42 (m, 2H), 0.97 (m, 3H). $^{13}\text{C-NMR}$ (CDCl_3) δ : 171.6, 160.1, 157.6, 156.9, 156.0, 104.6, 39.7, 31.6, 24.4, 20.2, 13.8. $^1\text{H-NMR}$ ($\text{DMSO}-d_6$) δ : 10.73 (s, 1H), 9.47 (s, 1H), 9.09 (t, 1H), 8.38 (d, 1H), 7.44 (d, 1H), 3.22 (q, 2H), 2.16 (s, 3H), 1.49 (m, 2H), 1.31 (m, 2H), 0.90 (t, 3H). $^{13}\text{C-NMR}$ ($\text{DMSO}-d_6$) δ : 170.2, 159.2, 157.7, 157.5, 153.9, 102.2, signal missing lying under DMSO-peak, 31.9, 24.5, 19.6, 13.7 ppm. IR (KBr) ν : 3290 (s), 3205, 3172, 2953, 2910, 1711, 1673, 1594, 1564, 1448, 1330, 1313 cm^{-1} . Anal. calcd. for $\text{C}_{11}\text{H}_{17}\text{N}_5\text{O}_2$: C, 52.58; H, 6.82; N, 27.87. Found: C, 52.74; H, 6.90; N, 27.78.

2-Acetyl-amino-4-butylureidopyrimidine (19). 2-Acetyl-amino-4-aminopyrimidine **16** (0.39 g, 2.6 mmol) was dissolved in dry pyridine (5 mL) by heating. To this warm solution was added butyl isocyanate (0.32 g, 2.8 mmol). The mixture was boiled under reflux for 1 h, resulting in a clear red solution. The solution was evaporated to dryness, and the residue was crystallized from methanol/water 1:2 v/v with treatment with active carbon and the product isolated at 4°C to give pure **19** (0.20 g, 31%), mp 241–242°C. $^1\text{H-NMR}$ ($\text{DMSO}-d_6$) δ : 10.73 (s, 1H), 9.77 (s, 2H), 8.25 (d, 1H), 8.55 (d, 1H), 3.21 (q, 2H), 2.13 (s, 3H), 1.52 (m, 2H), 1.30 (m, 2H), 0.90 (t, 3H). $^{13}\text{C-NMR}$ ($\text{DMSO}-d_6$) δ : 169.1, 158.9, 157.8, 155.7, 154.0, 102.2, 39.2, 31.5, 24.6, 19.6, 13.7. IR (KBr) ν : 3192, 2956, 1710, 1687, 1605, 1563, 1514, 1414, 1328, 1208 cm^{-1} . Anal. calcd. for $\text{C}_{11}\text{H}_{17}\text{N}_5\text{O}_2$: C, 52.58; H, 6.82; N, 27.87. Found: C, 52.65; H, 6.85; N, 28.15.

References and Footnotes

- 1) (a) A.D. Hamilton, A. Muehldorf, S.-K. Chang, N. Pant, S. Goswami, D. Van Engen, *J. Inclus. Phenom. Mol. Recog. Chem.*, **1989**, 7, 27, (b) A.D. Hamilton, N. Pant, A. Muehldorf, *Pure Appl. Chem.*, **1988**, 60, 553, (c) F. Vögtle, *Supramolecular Chemistry*, J. Wiley & Sons, Chichester, **1991**, (d) J.-M. Lehn, *Supramolecular Chemistry, Concepts and Perspectives*, VCH, Weinheim, **1995**.
- 2) (a) M.H. Abraham, *J. Phys. Org. Chem.*, **1993**, 6, 660, (b) M.H. Abraham, *Chem. Soc. Rev.*, **1993**, 22, 73.
- 3) (a) W.L. Jorgensen, J. Pranata, *J. Am. Chem. Soc.*, **1990**, 112, 2008, (b) J. Pranata, S. G. Wierschke, W.L. Jorgensen, *J. Am. Chem. Soc.*, **1991**, 113, 2810.
- 4) see refs. 3, 4 and 5 in chapter 2, and: (a) I. Willner, J. Rosengaus, S. Biali, *Tetrahedron Lett.*, **1992**, 33, 3805, (b) Y. Honda, K. Kurihara, T. Kunitake, *Chem. Lett.*, **1991**, 681, (c) T.K. Park, J. Schroeder, J. Rebek Jr., *J. Am. Chem. Soc.*, **1991**, 113, 5125, (d) T. K. Park, Q. Feng, J. Rebek Jr., *J. Am. Chem. Soc.*, **1992**, 114, 4529.

- 5) (a) T. J. Murray, S.C. Zimmerman, *J. Am. Chem. Soc.*, **1992**, *114*, 4010, (b) E.E. Fenlon, T.J. Murray, M.H. Baloga, S.C. Zimmerman, *J. Org. Chem.*, **1993**, *58*, 6625, (c) S.C. Zimmerman, T.J. Murray, *Tetrahedron Lett.*, **1994**, *35*, 4077.
- 6) Receptors for barbiturates: (a) A. D. Hamilton, D. van Engen, *J. Am. Chem. Soc.*, **1987**, *109*, 5035, (b) A.D. Hamilton, N. Pant, A.V. Muehldorf, *Pure & Appl. Chem.*, **1988**, *60*, 533, (c) A.D. Hamilton, A. Muehldorf, S.-K. Chang, N. Pant, S. Goswami, D. Van Engen, *J. Incl. Phenom. Molec. Reco. Chem.*, **1989**, *7*, 27, (d) S.-K. Chang, D. Van Engen, E. Fan, A.D. Hamilton, *J. Am. Chem. Soc.*, **1991**, *113*, 7640.
- 7) Receptors for flavin: (a) N. Tamura, T. Kajiki, T. Nabeshima, Y. Yano, *J. Chem. Soc., Chem. Comm.*, **1994**, 2583, (b) N. Tamura, K. Mitsui, T. Nabeshima, Y. Yano, *J. Chem. Soc., Perkin Trans. 2*, **1994**, 2229.
- 8) Receptor for urea: S. Goswami, R. Mukherjee, *Tet. Lett.*, **1997**, *38*, 1619; other examples: (a) T.W. Bell, J. Liu, *J. Am. Chem. Soc.*, **1988**, *110*, 3673, (b) T.W. Bell, Z. Hou, *Angew. Chem. Int. Ed. Engl.*, **1997**, *36*, 1536.
- 9) Receptor for guanine: T.W. Bell, Z. Hou, S.C. Zimmerman, P.A. Thiesen, *Angew. Chem.*, **1995**, *107*, 2321.
- 10) Other examples include: (a) T.R. Kelly, C. Zhao, G.J. Bridger, *J. Am. Chem. Soc.*, **1989**, *111*, 3744, (b) A.D. Hamilton, D. Little, *J. Chem. Soc., Chem. Commun.*, **1990**, 297, (c) S.C. Hirst, A.D. Hamilton, *Tetrahedron. Lett.*, **1990**, *31*, 2401, (d) M.S. Goodman, S.D. Rose, *J. Am. Chem. Soc.*, **1991**, *113*, 9380, (e) S.J. Geib, S.C. Hirst, C. Vicent, A.D. Hamilton, *J. Chem. Soc., Chem. Commun.*, **1991**, 1283, (f) J.S. Lindsey, P.C. Kearney, R.J. Duff, P.J. Tjivikua, J. Rebek Jr., *J. Am. Chem. Soc.*, **1988**, *110*, 6575.
- 11) R. Wyler, J. de Mendoza, J. Rebek, *Angew. Chem. Int. Ed. Engl.*, **1993**, *32*, 1699.
- 12) M.R. Ghadiri, J.R. Granja, R.A. Milligan, D.E. McRee, N. Khazanovich, *Nature*, **1993**, *366*, 324.
- 13) J.-M. Lehn, *Makromol. Chem., Macromol. Symp.*, **1993**, *69*, 1.
- 14) (a) Y. Ducharme, J.D. Wuest, *J. Org. Chem.* **1988**, *53*, 5787, (b) F. Persico, J.D. Wuest, *J. Org. Chem.*, **1993**, *58*, 95, (c) E. Boucher, M. Simard, J.D. Wuest, *J. Org. Chem.*, **1995**, *60*, 1408.
- 15) The only example was reported by R.J. Griffin, P.R. Lowe, *J. Chem. Soc., Perkin Trans 1*, **1992**, 1811.
- 16) In the initial reports, the reaction is performed in the corresponding anhydride as solvent: (a) A. Ostrogovich, G. Gheorghiu, *Gazz. Chim. Ital.* **1930**, *60*, 648, (b) *ibid.*, **1932**, *62*, 317.
- 17) The original procedure of (a) J. Malthête, A.M. Levelut, N.H. Tihn, *J. Phys. Lett.*, **1985**, *46*, L875, (b) H. Meier, E. Praß, G. Zerban, F. Kosteyen, *Z. Naturforsch.*, **1988**, *43B*, 889 was adapted according to A.R.A. Palmans, J.A.J.M. Vekemans, H. Fischer, R.A. Hikmet, E.W. Meijer, *Chem. Eur. J.*, **1997**, *3*, 300.
- 18) E.M. Smolin, L. Rapoport, *The Chemistry of Heterocyclic Compounds*, Vol. 13, s-Triazines, A. Weissberg Edn., John Wiley & Sons, New York, **1959**.
- 19) (a) D. Karipides, W.C. Fernelius, *Inorg. Syn.*, **1963**, *7*, 56, (b) *ibid.*, p. 58.
- 20) An excess of 2.2 equivalents was used, as this was an attempt to synthesize the di(ureido)derivative.
- 21) The mean effective equilibrium bond length of a series of N-H \cdots O=C and N-H \cdots N hydrogen bonds in crystal structures of purines and pyrimidines are 1.88 Å and 1.90 Å, respectively; G.A. Jeffrey, W. Saenger, *Hydrogen Bonding in Biological Structures*, Springer, Berlin, **1994**.

- 22) Although it seems axiomatic that shorter hydrogen bonds mean stronger hydrogen bonding (see reference 21), a thorough analysis of bonding distances has shown that packing factors effect a 20% distortion from the equilibrium length. However, especially since the geometry of the dimers are virtually the same, the shorter distances in ureido derivatives may well point to stronger bonding, although the shorter distances may not be considered as proof.
- 23) The formation of dimers is concluded from the fact that upon dilution, the intensity of all bands assigned to complexed N–H groups diminishes simultaneously, while the intensity of all bands assigned to uncomplexed N–H functionalities (in the monomer) increases simultaneously. The shifts upon dimerization that can be derived are all characteristic for hydrogen bonds of intermediate strength.
- 24) For compound **10**, the ^1H -NMR dilution technique gave no reliable value because the N–H signals became too broad to monitor at low concentrations. Monitoring of the phenyl signals was hampered by the fact that the monomer shift coincided with a ^{13}C -satellite of CDCl_3 , obstructing reliable determination of peak positions at low concentrations. For compound **11**, the NMR-dilution technique was hampered by the occurrence of a second process, which leads to a decrease of δ -values at higher concentrations, probably stacking of dimers.
- 25) R. Daens, G. Cooke, V.M. Rotello, *J. Org. Chem.*, **1997**, *62*, 836.
- 26) Non-unidirectional interactions may result in the formation of polymeric aggregates, as observed in the crystal structure.
- 27) Of course, other and weaker interactions are present in the crystals of these derivatives, such as π -stacking.
- 28) In accordance with the fact that the molecules of di(acetylamino)pyrimidine **13** do not dimerize via quadruple hydrogen bonding in the crystal, there are significant differences between the IR-spectra in the solid state and chloroform solution for derivative **13**.
- 29) Differences in the chemical shift of non-N–H protons in the ^1H -NMR spectrum in CDCl_3 and the spectrum in $\text{DMSO}-d_6$ are < 0.4 ppm, while resonances in ^{13}C -spectra in chloroform and $\text{DMSO}-d_6$ do not differ more than 5 ppm for compounds **13** and **18** (see Experimental Section). This indicates no change in tautomeric form upon dissociation of the dimer.
- 30) At the lowest concentration at which an IR spectrum in chloroform could be measured (0.09 mM in a 5 mm cell), a weak and split absorption band at 3420 cm^{-1} is present. This band reaches less than 20% of the dimer absorption band, and is assigned to two overlapping bands: the N–H stretch vibration of the *trans*-amide N–H and of the ureido N–H. The absorption of the intramolecular hydrogen bond in the monomer could not be determined because only few dissociation is reached and this band appears in the same region as the dimer bands.
- 31) Dimerization constants could again also be determined by monitoring acetyl CH_3 , butyl CH_2 , or aromatic protons were appropriate, despite a small CIS value.
- 32) The dimerization constant of ureido-triazine **10** in all the mixtures was determined using the phenyl proton (the N–H resonances became too broad in all mixtures). Of 2-butylureido-4-acetylamino-pyrimidine **18**, the acetyl CH_3 and the proton adjacent to the acetylamino substituent were monitored. For compound **13**, all proton resonances (both N–H and other) gave the same dimerization constants in all the mixtures.
- 33) Several samples were measured in pure CDCl_3 at as low as reasonably possible concentrations (approx. 0.015 mM). Using the extrapolated monomer and dimer shift values, the percentage of monomer can be calculated using the position of the resonance of H5 in

pure CDCl_3 : 34% monomer at 0.015 mM. Hence, the dimerization constant follows: $1.9 (\pm 0.5) \times 10^5 \text{ M}^{-1}$. The error in the value was estimated from averaging multiple samples.

- 34) M. Mammen, E.E. Simanek, G.M. Whitesides, *J. Am. Chem. Soc.*, **1996**, *118*, 12614.
- 35) T. Hayashi, T. Miyahara, N. Koide, Y. Kato, H. Masuda, H. Ogoshi, *J. Am. Chem. Soc.*, **1997**, *119*, 7281.
- 36) For an excellent review on solvent polarity and ET(30) see: (a) C. Reichardt, *Solvents and Solvent Effects in Organic Chemistry*, 2nd Edn., VCH Weinheim, **1990**, (b) C. Reichardt, *Chem. Rev.*, **1994**, *94*, 2319, further (c) J.G. Dawber, J. Ward, R.A. Williams, *J. Chem. Soc., Faraday Trans. I*, **1988**, *84*, 713, (d) E. Bosch, M. Roses, *J. Chem. Soc., Faraday Trans.*, **1992**, *88*, 3541.
- ET(30) is one of the most widely used empirical solvent polarity parameters, and is defined as $28590/\lambda_{\text{max}}$ of Reichardt's Dye, 2,6-diphenyl-4-(2,4,6-triphenylpyridinio)phenolate. ET(30) values in mixed solvent systems do not measure the bulk solvent polarity, but they rather reflect the polarity of the solvation shell surrounding the dye. The deviation from linearity of experimental ET(30) values and solvent composition is in fact a nice measurement for preferential solvation of the dye by the more polar component in a solvent mixture. In mixed solvent systems with one polar hydrogen bonding donor component, such as methanol, it has been shown that ET(30) is a measure for specific hydrogen bonding interactions between hydrogen bonding donor cosolvent and Reichardt's Dye [C.A. Coleman, C.J. Murray, *J. Org. Chem.*, **1997**, *57*, 3578].
- 37) The linear relation between ET(30) and $\log K_{\text{dim}}$ suggests that preferential solvation of the monomer occurs in a similar way as for Reichardt's Dye.
- 38) The error is estimated to be relatively large ($\pm 4 \times 10^5 \text{ M}^{-1}$), since a large extrapolation is made, and linear extrapolating for **10** and **13** affords similar errors.
- 39) We will arbitrarily use the value of $1.9 \times 10^5 \text{ M}^{-1}$ for the dimerization constant of **18**. That the real value may actually be larger does not alter the line of the discussion.
- 40) J.Sartorius, H.-J. Schneider, *Chem. Eur. J.* **1996**, *2*, 1446.
- 41) K. A. Connors, *Binding Constants*, John Wiley & Sons, New York, **1987**, (b) For the equation for fitting the dimerization, see R. Deans, G. Cooke, V.M. Rotello, *J. Org. Chem.*, **1997**, *62*, 836.

Chapter 4

The DDAA Quadruple Hydrogen Bonding Motif in 2-Ureido-4-Pyrimidinones

Abstract:

Both in the solid state and in chloroform solution, 6-methyl-2-butylureido-4-pyrimidinone 3a dimerizes via four hydrogen bonds. This occurs via a linear Donor–Donor–Acceptor–Acceptor (DDAA) array of hydrogen bonding sites in the 4[1H]-pyrimidinone tautomer. The DDAA array is pre-organized by an intramolecular hydrogen bond from the non-central pyrimidine N–H group to the oxygen atom of the urea functionality.

Dimerization via quadruple hydrogen bonding is general for ureidopyrimidinones 3a–l. However, compounds with other substituents than 3a can form dimers with a DADA array—which is also pre-organized by an intramolecular hydrogen bond—of an aromatic pyrimidin-4-ol tautomer. The tautomeric equilibrium between the 4[1H]-pyrimidinone and pyrimidin-4-ol tautomers is strongly influenced by electronic substituent effects. Electronegative 6-substituents favor the pyrimidin-4-ol form. In dimers with a DDAA-array, as well as in dimers with a DADA-array, all donors are involved in the construction of the dimer. The interaction is unidirectional with respect to hydrogen bonding. The dimerization strength of both quadruply hydrogen bonded dimers in apolar solvents is very large; in CDCl₃, no sign of dissociation is observed upon dilution down to 10^{−4} M.

*In polar solvents, like DMSO, ureidopyrimidinones exist predominantly as a monomeric 6[1H]-pyrimidinone tautomer. In mixed solvent systems of CDCl₃ and DMSO-*d*₆, dimers of 4[1H]-pyrimidinone and pyrimidin-4-ol tautomer are in equilibrium with this monomeric 6[1H]-pyrimidinone tautomer; these equilibria are slow on the NMR-timescale. Solvent and concentration effects on these tautomeric equilibria are rationalized by the monomer–dimer relationship. Complex dimerization constants in chloroform, which include a tautomerization between dimeric and monomeric form, exceed 10⁶ M^{−1} for compound 3a—with a DDAA array of the 4[1H]-pyrimidinone tautomer—and 4.5 × 10⁵ M^{−1} for compound 3l—with a DADA array of the pyrimidin-4-ol tautomer. In a mixture of two compounds at low concentrations in CDCl₃, slowly exchanging hetero-dimers—formed in an (almost statistical) ratio—are observed. The lifetime of the dimers in CDCl₃ is estimated between 0.1 seconds and 3 minutes.*

4.1 Introduction

In many synthetic self-assembling structures, the components are held together by arrays of multiple hydrogen bonds.¹ Due to their strength, directionality and specificity, arrays of multiple hydrogen bonds are useful building blocks for the reliable construction of complex supramolecular structures. This combination of advantageous properties is expected to be particularly pronounced in large arrays of hydrogen bonds. That large arrays of hydrogen bonds form very stable complexes has been shown in many occasions, such as reports on synthetic receptors for barbiturates,² urea,³ flavin,⁴ guanines,⁵ and melamine⁶ (see chapter 3 for some examples), reports of self-assembled receptors,⁷ and nanotubes formed from cyclic peptides,⁸ and also in other examples.⁹ However, the use of these multipoint hydrogen bonding groups is limited by the synthetic efforts required for their preparation.

In the previous chapter, it was shown that strongly bonded dimers of self-complementary, linear arrays of Donor–Acceptor–Donor–Acceptor (DADA) hydrogen bonding sites could easily be obtained.¹⁰ Based on differences in secondary interactions from the Jorgensen model,¹¹ stronger dimerization is expected when the order of the hydrogen bonding functional groups in the array is changed from DADA to DDAA (see figure 4.1). The empirical evaluation of Schneider¹² has predicted association constants for DADA and DDAA arrays of 3.1×10^2 and $3.6 \times 10^6 \text{ M}^{-1}$ in chloroform, respectively.

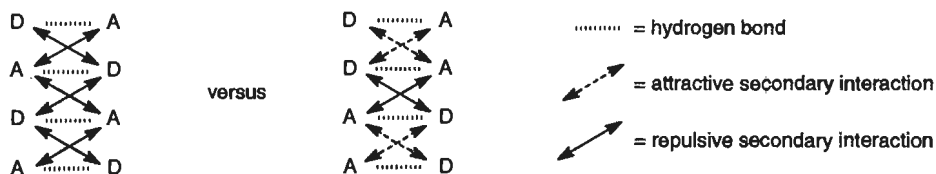


Figure 4.1: Interactions in DADA and DDAA dimers. While both quadruply hydrogen bonded dimers have 4 attractive primary hydrogen bonds, the DADA dimer has 6 repulsive secondary interactions, whereas the DDAA dimer has 2 repulsive and 4 attractive secondary interactions.

The expected very strong dimerization of self-complementary DDAA arrays of hydrogen bonding sites is interesting, for example for the construction of linear supramolecular polymers. Therefore, it was decided to investigate the binding properties of 2-ureido-4-pyrimidinone derivatives, which can be easily synthesized in one step by reaction of an isocytosine with an isocyanate.¹³ Based on the experimentally observed^{14,15,16} and quantum mechanically calculated¹⁷ relative stabilities of the tautomeric forms of the parent isocytosine, 2-ureido-4-pyrimidinone is expected to exist in one of the forms depicted in figure 4.2.

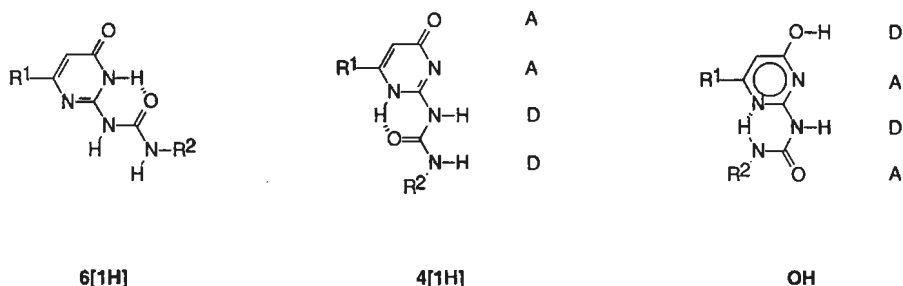


Figure 4.2: Three possible tautomeric forms of 2-ureido-4-pyrimidinone:

6[1H] 6[1H]-pyrimidinone tautomer,

4[1H] 4[1H]-pyrimidinone tautomer having a DDAA array of hydrogen bonding sites,

OH pyrimidin-4-ol tautomer having a DADA array of hydrogen bonding sites.

In analogy to the parent isocytosines, the 6[1H]-pyrimidinone tautomer is expected to be the most stable tautomeric form of an isolated 2-ureido-4-pyrimidinone molecule.¹⁸ However, ureidopyrimidinones may actually exist as dimers of tautomeric forms **4[1H]** and **OH**, since considerable stabilization is expected by dimerization of the linear array of four hydrogen bonds. Noticeable, both dimerization via a DDAA array, as well as dimerization via a DADA array is possible. In both cases, the linear array of the four hydrogen bonds is pre-organized by an intramolecular hydrogen bond, a concept shown in the previous chapter to enhance the stability of the dimers considerably.⁴

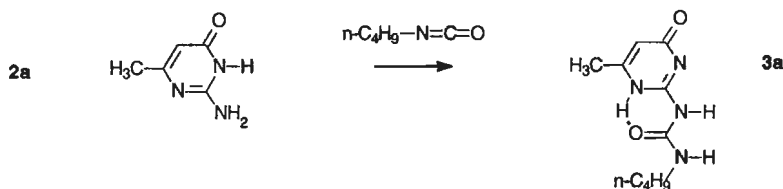
In this chapter, the formation of exceptionally stable DDAA dimers of 6-methyl-2-butylureido-4-pyrimidinone **3a**—synthesized in one step from commercially available and inexpensive starting materials—is reported first. The full scope of dimerization of ureidopyrimidinones was investigated in a range of ureidopyrimidinones **3a–l**, bearing different substituents on C6, and at the terminal ureido nitrogen.¹⁹ As we show by X-ray crystallographic and FT-IR studies in the solid state, and FT-IR and various NMR techniques in solution, these derivatives can dimerize via DDAA arrays of the 4[1H]-pyrimidinone tautomer, as well as via DADA arrays of the pyrimidin-4-ol tautomer. The dimerization strength was studied by experiments in mixed solvent systems of CDCl₃ and DMSO-*d*₆.

4.2 Results and Discussion

4.2.1 The DDAA motif in dimers of 2-butylureido-6-methyl-4[1H]-pyrimidinone

2-Butylureido-6-methyl-4-pyrimidinone (or *N*-butylaminocarbonyl 6-methyl-isocytosine) **3a** was readily prepared by reaction of commercially available 6-methyl-isocytosine **2a** with butyl isocyanate in boiling pyridine (scheme 4.1). Compound **3a** indeed

forms quadruply hydrogen bonded DDAA-dimers, both in the solid state as well in chloroform solution, as is evident from single X-ray diffraction on suitable crystals, FT-IR in the solid state and solution, and NMR-spectroscopy.



Scheme 4.1: Synthesis of 2-butylureido-6-methyl-4-pyrimidinone 3a.

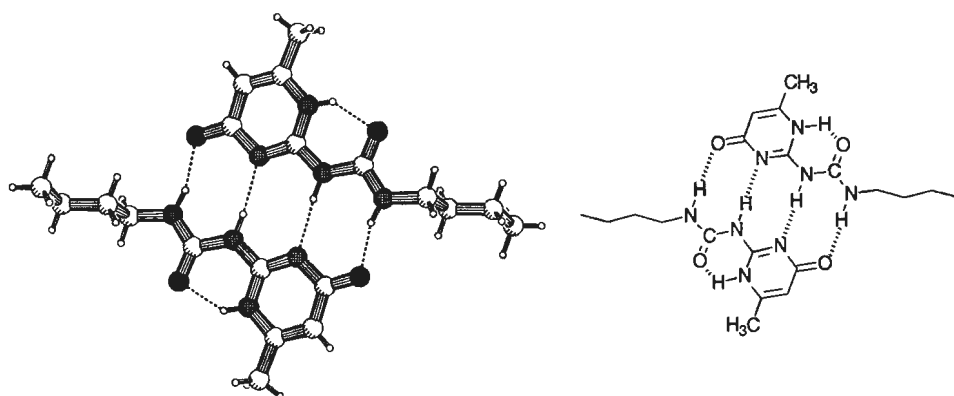


Figure 4.3: PLUTON representation of the dimer geometry of 3a in the crystal.

The crystal structure of 3a (figure 4.3) shows that the molecules are in the 4[1H]-pyrimidinone form. The urea functionality is in a *trans-trans* conformation, and an intramolecular hydrogen bond is present from the non-central pyrimidine N–H to the carbonyl group of the *trans-trans* urea functionality. This results in a pre-organized DDAA array of hydrogen bonding sites, which forms a centrosymmetrical dimer. All the three potential hydrogen bonding donors of one molecule are involved in the construction of the dimer. The intramolecular hydrogen bond is not part of the recognition site, but very important for the stability of a dimer as we showed in chapter 3, and will show later. The bonding distances are reported and discussed later in section 4.2.2.

Formation of hydrogen bonds is evident from the FT-IR spectrum of 3a in KBr. The N–H region features an absorption at 3212 cm^{-1} , which is assigned to the outer $\text{N-H}\cdots\text{O}=\text{C}$ hydrogen bond from the terminal ureido N–H group to the pyrimidine carbonyl atom at C4. Another absorption is present at 3147 cm^{-1} , assigned to the inner $\text{N-H}\cdots\text{N}$ hydrogen bond from the ureido N–H to the central pyrimidine ring nitrogen atom. The absorption of the intramolecular hydrogen bonded N–H in the pyrimidinone dimer is not observed separately, and probably lies under the large peak of C–H absorptions.

Strong similarity between IR-spectra in the solid state and in chloroform indicates that the DDAA dimers persist in chloroform solution. In the ^1H -NMR-spectrum of **3a** in CDCl_3 (figure 4.4), the N–H proton resonances are found at 13.15, 11.86, and 10.15 ppm; the large downfield shifts for the N–H protons are indicative for involvement in strong hydrogen bonding. Since the ^1H -NMR spectrum shows only one form, and IR-spectra of **3a** in the solid state and in chloroform solution are very similar, it is concluded that **3a** exists in chloroform solution exclusively as 4[1H]-pyrimidinone dimers. Dilution in CDCl_3 of **3a** to 10^{-4} M^{-1} does not result in significant dissociation,²⁰ which puts a lower limit on the dimerization constant of $4.5 \times 10^5 \text{ M}^{-1}$ (for determination of dimerization constants, vide infra).

The DDAA dimer geometry of the 4[1H]-pyrimidinone tautomer of **3a** in solution was confirmed by nuclear Overhauser effect (NOE) spectroscopy, used to assign the N–H proton signals. A strong NOE-effect for the resonance at 13.15 ppm was observed when the CH_3 signal was irradiated. The resonance at 13.15 ppm therefore corresponds to H_a . Analogous reasoning led to the assignment as given in figure 4.4. The protons at 13.15 and 11.86 (in figure 4.4, H_a and H_b , respectively) exchange within 4 seconds, the applied irradiation time. Quick exchange is also observed with D_2O exchange experiments, which indicate that the N–H proton of the ureido-substituent adjacent to the CH_2 exchanges slowly, whereas the other N–H groups are exchanged directly after addition and mixing of D_2O .

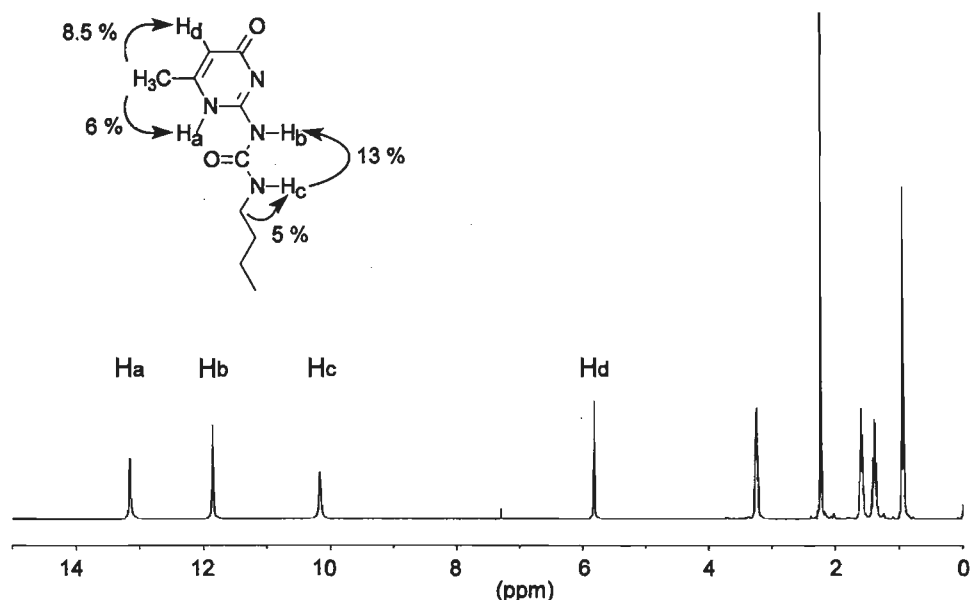
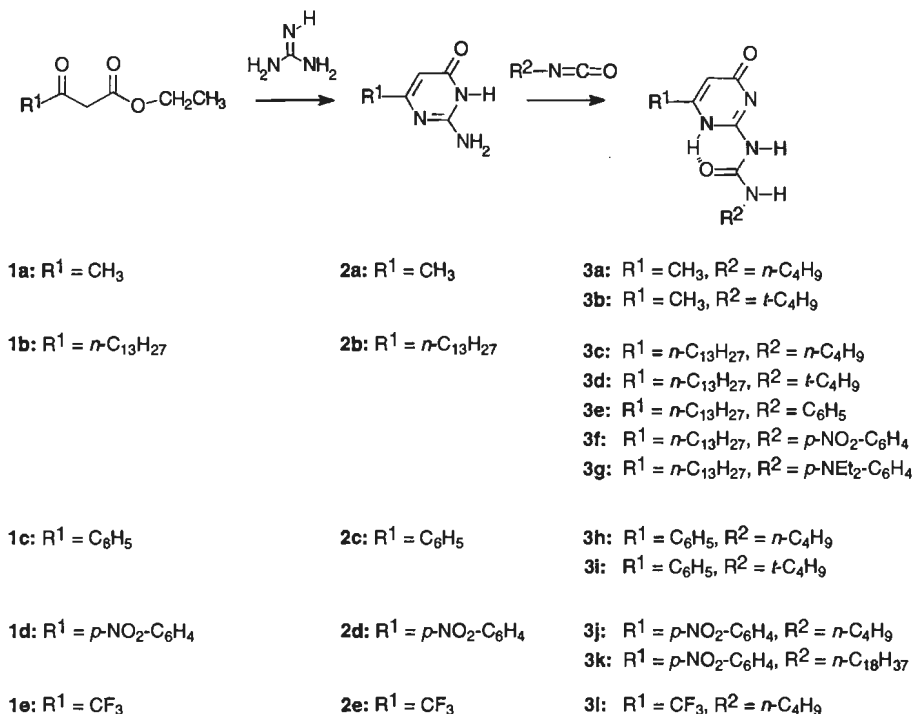


Figure 4.4: ^1H -NMR-spectrum of compound **3a** in CDCl_3 , and geometry of dimerized molecule. Nuclear Overhauser effects between protons (in%) are indicated with arrows.

4.2.2 Tautomeric equilibrium between dimeric 2-ureido-4[1H]-pyrimidinone and 2-ureido-pyrimidin-4-ol tautomers

Synthesis. The scope of dimerization of the ureido-4-pyrimidinone functionality was investigated in a range of derivatives (compounds **3a–l**), bearing different substituents at C-6 and at the terminal ureido nitrogen. These compounds were synthesized by a two-step sequence as depicted in scheme 4.2.

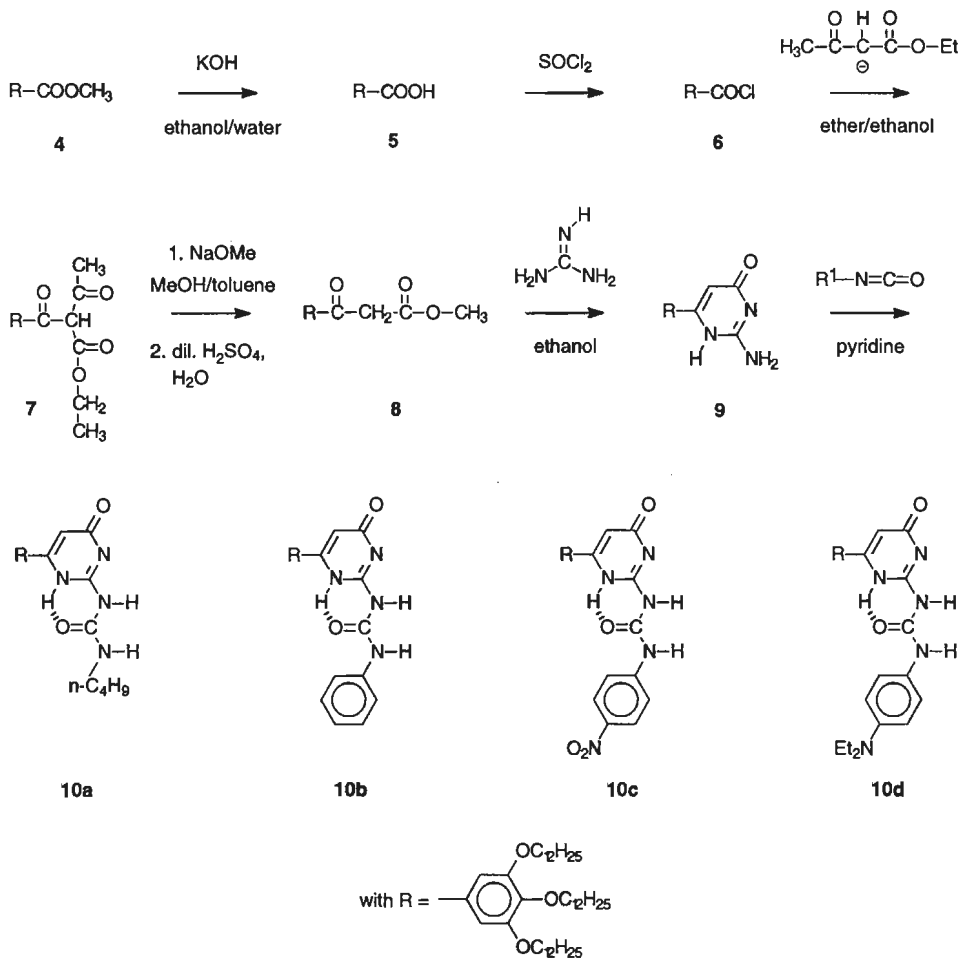


Scheme 4.2: Route to the ureidopyrimidinones **3a–3l**.

Condensation of the appropriate β-keto-ester (**1a–e**) with guanidine (added as guanidinium carbonate) afforded 6-substituted isocytosines **2a–e**. Keto-esters **1a** and **1c–1e** were commercially available; the synthesis of **1b** has been described in chapter 2. In the subsequent step, the isocytosine was reacted with the appropriate isocyanate to give the target compounds **3a–k**. The isocyanates were also commercially available, except *p*-diethylaminophenyl isocyanate, which was synthesized analogous to a literature procedure by reaction of *p*-diethylamino-aniline with phosgene.²¹ These *N*-acylation reactions were generally performed in boiling pyridine with reaction times of 2 to 4 hours. In all cases, except for compound **3l**, cooling resulted in crystallization of the crude ureidopyrimidinones. The crude products could be purified well by recrystallization. Some derivatives are thermally

instable; heating of **3f** in DMSO solution results in decomposition, and the parent isocytosine was detected by NMR.

The solubility of 6-phenyl substituted compounds was enhanced considerably by attaching three dodecyloxy chains on the phenyl group, as in compounds **10a–d** (scheme 4.3).



Scheme 4.3: Route to ureidopyrimidinone derivatives **10a–d** with the 3,4,5-tri(dodecyloxy)-phenyl group at the 6-position.

Ester **4**, of which the synthesis is described in chapter 3, was hydrolysed to the acid **5**, and then converted to acid chloride **6** by refluxing in thionyl chloride. The acid chloride was then converted to β -keto-ester **8** via a two-step synthesis analogous to literature procedures.²² First, in an ether/ethanol mixture, the mono-anion of ethyl acetoacetate was condensed with acid chloride **6** to give **7**. In the next step, an acetyl group of **7**—crude **7** was used without purification—was preferentially eliminated as methyl acetate by reaction with methoxide in a

methanol / toluene mixture. The resulting β -keto-ester **8** in turn was reacted with guanidinium carbonate to afford isocytosine **9**. Subsequent *N*-acylation with the appropriate isocyanates afforded the target molecules **10a–d**.

Crystal structure evidence for tautomerism in the solid state. Compound **3h** crystallized either as needles or as plates upon slow evaporation of a chloroform solution in air. As revealed by X-ray diffraction, the molecules of **3h** in the needles are present as dimers of the 4[1H]-pyrimidinone tautomer (figure 4.5), like for compound **3a**. Four independent molecules form two independent dimers, without internal crystallographic symmetry. One molecule of CHCl_3 —which is also present in the crystal— is hydrogen bonded to the ureido carbonyl group of one molecule of a dimer. Two crystallographically independent and non-centrosymmetrical dimers are formed, one of which is depicted in figure 4.5.

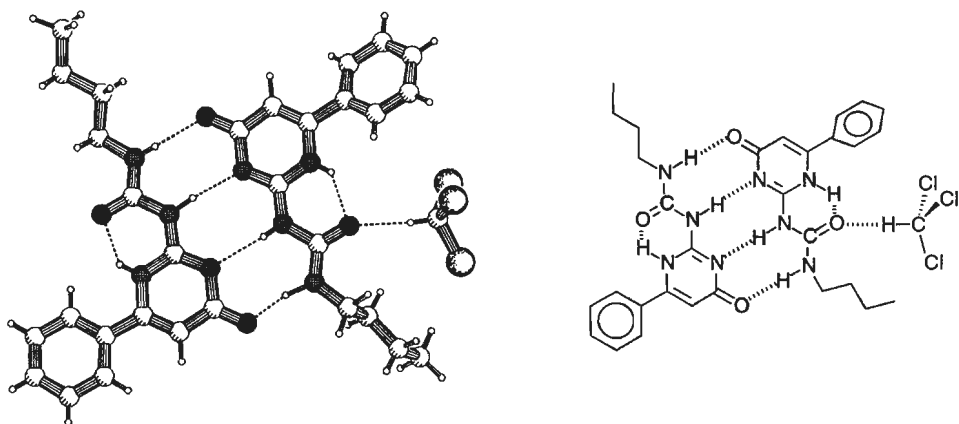


Figure 4.5: PLUTON representation of the dimer geometry of the molecules of **3h** in the 4[1H]-pyrimidinone tautomer in the needle-shaped crystals.

In contrast, the molecules in the plate-like crystals of **3h** exist as dimers of the pyrimidin-4-ol tautomer, bearing a hydroxyl functionality as proton donor (figure 4.6). The butylureido functionality is in the *cis-trans* conformation, and forms an intramolecular hydrogen bond to the non-central pyrimidine ring nitrogen atom. In this manner, a DADA array originates, forming a quadruply hydrogen bonded dimer.

X-ray diffraction on several crystals revealed that at least three crystal modifications had formed, all in which the dimers have a similar geometry. In all modifications, the dimers are packed in layers; the main difference between the modifications is the relative position of these layers with respect to each other. Like in the crystal structure with DDAA dimers of the 4[1H]-pyrimidinone tautomer, all six hydrogen bonds are involved in the build-up of the dimeric structure in the pyrimidin-4-ol dimers.

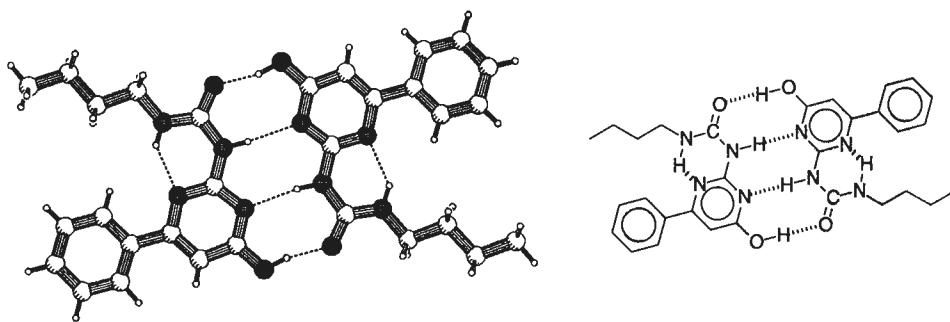


Figure 4.6: PLUTON representation of the dimer geometry of the molecules of **3h** in the pyrimidin-4-ol tautomer in the plate-shaped crystals.

Bonding distances in Pyrimidin-4-ol and 4[1H]-Pyrimidinone dimers.

First, the difference in directionality of the intramolecular hydrogen bonds is addressed. The intramolecular hydrogen bond in dimers of the pyrimidin-4-ol tautomer is directed from the ureido N–H group—which is in *cis-trans* conformation—to the non-central pyrimidine nitrogen N1 atom. In all three crystal modifications of **3h** with pyrimidin-4-ol dimers, the intramolecular hydrogen bonds have very similar N–N distances between 2.67 and 2.68 Å, with angles of approximately 136 degrees. These values are comparable to the values found for ureido-triazine and 2-butylureido-4-acetylamino-pyrimidine described in chapter 3.

In dimers of the 4[1H]-pyrimidinone tautomer, the intramolecular hydrogen bond is directed from the N–H group on the non-central pyrimidine ring nitrogen atom N1 to the oxygen atom of the urea functionality, which is in *trans-trans* conformation. The bond lengths and angles of the intramolecular hydrogen bond in the crystal structure of **3a** (with only one crystallographically independent intramolecular hydrogen bond) and in the crystal structure of 4[1H]-pyrimidinone tautomer of **3h** (with four crystallographically independent intramolecular hydrogen bonds because of pseudo-symmetry) are very similar; the N–N distance is 2.56 Å with an angle of 134–140 degrees. Compared to the distance in the pyrimidin-4-ol dimers, the bond distances are significantly shorter; the angles are comparable.

The arrays of the quadruple hydrogen bonds are virtually planar—the r.m.s. deviation from planarity is in the range 0.05 to 0.10 Å—both in the crystal structures of 4[1H]-pyrimidinone tautomers (compounds **3a** and **3h**), as well as of pyrimidin-4-ol tautomers (compound **3h**, 3 modifications). Bond lengths and angles of the quadruple hydrogen bonds are collected in table 4.1.

Table 4.1: Bond distances [Å] and X–H–X angles [°] in the crystal structures of 3a, and of the 4[1H]-pyrimidinone and pyrimidin-4-ol tautomer of 3h.

compound	N–H···N distance	N–H···N angle	X–H···O ^a distance	X–H···O angle	Hydrogen bond length difference
3a	2.966(3)	175(3)	2.757(3)	163(3)	0.209
4[1H]-pyrimidinone 3h^b	2.95(1)	172(6)	2.78(5)	166(3)	~ 0.17
pyrimidin-4-ol 3h^c	2.98(1)	173(4)	2.58(1)	169(3)	~ 0.40

^a X = N in 3a and 4[1H]-pyrimidinone tautomer of 3h; X = O in pyrimidin-4-ol tautomer of 3h; ^b Average of four sets, since four independent molecules are present that form two crystallographically non-centrosymmetrical dimers; ^c Average of 6 sets, since there are three pyrimidin-4-ol polymorphs with each two crystallographically non-equivalent molecules forming non centrosymmetric dimers.

The quadruple arrays of donor and acceptor functional groups are not linear in pyrimidin-4-ol nor in 4[1H]-pyrimidinone tautomer. As observed for the molecules in chapter 3, the outer hydrogen bonds are longer than the inner ones: the carbonyl is protruding from the line through the three nitrogen atoms involved in hydrogen bonding. In DDAA dimers of the 4[1H]-pyrimidinone tautomer, the difference between inner and outer hydrogen bonding lengths is however strikingly smaller (difference only 0.13–0.21 Å) than in DADA dimers of the 2-ureido-4-pyrimidin-4-ol form (difference 0.40 Å). Table 4.2. gives a comparison of the hydrogen bonding distances of inner and outer hydrogen bonds of 4[1H]-pyrimidinone dimers, pyrimidin-4-ol dimers, and of 2-butylureido-4-acetylamino-pyrimidine dimers (see chapter 3).

Table 4.2: Comparison of bond distances [Å] in the crystal structures of 4[1H]-pyrimidinone dimers, pyrimidin-4-ol dimers, and of 2-butylureido-4-acetylamino-pyrimidine 11.

system	N–H···N distance (inner HB)	X–H···O distance ^a (outer HB)	Hydrogen bond length difference
DDAA of 4[1H]-pyrimidinone	2.95–2.97	2.76–2.78	0.17–0.21
DADA of pyrimidin-4-ol	2.98	2.58	0.40
DADA of 4-acetylamino-pyrimidine 11	3.24	2.75	0.49

^a X = N in DDAA of 4[1H]-pyrimidinone and DADA of 2-butylureido-4-acetylamino-pyrimidine 11; X = O in DADA of pyrimidin-4-ol.

Noticeable are the short outer $\text{O}-\text{H}\cdots\text{O}=\text{C}$ hydrogen bonds in the pyrimidin-4-ol dimers (2.58 Å in all three crystal modifications);²³ the corresponding distance in related 2-butylureido-4-acetylamino-pyrimidine discussed in chapter 3 is 2.75 Å. Also, the inner hydrogen bonds in the pyrimidin-4-ol dimers are significantly shorter than in the related DADA dimer of 2-butylureido-4-acetylamino-pyrimidine **11** (2.96 Å versus 3.24 Å). In the DDAA systems, the hydrogen bonds have a normal length (2.95–2.97 Å for the inner, and 2.76–2.80 Å for the outer hydrogen bond). The inner hydrogen bonds of DDAA systems are of similar length as for the DADA dimers of pyrimidin-4-ol, while the inner hydrogen bonds of 2-butylureido-4-acetylamino-pyrimidine **11** are significantly longer. The outer hydrogen bonds of DDAA systems are of similar length as for the DADA dimers of 2-butylureido-4-acetylamino-pyrimidine **11**, while pyrimidin-4-ol has significantly shorter outer hydrogen bonds.

Comparison of IR of Pyrimidin-4-ol and 4[1H]-Pyrimidinone tautomers.

The FT-IR spectra in the solid state of dimers of **3h** in the 4[1H]-pyrimidinone and the pyrimidin-4-ol tautomer (figures 4.7 and 4.8) show very pronounced differences.

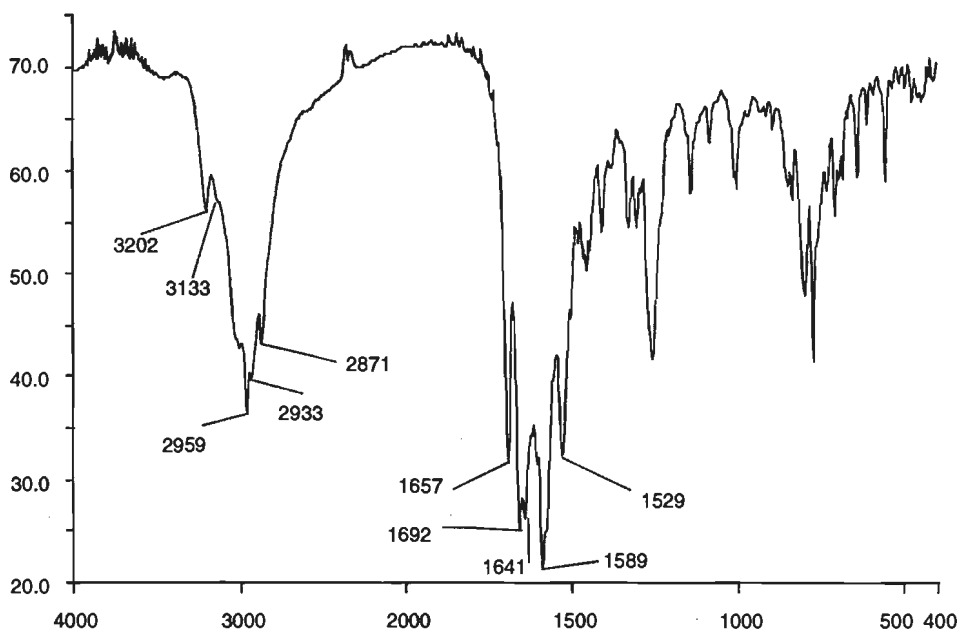


Figure 4.7: IR spectrum in KBr of crystals of compound **3h** in the 4[1H]-pyrimidinone form.

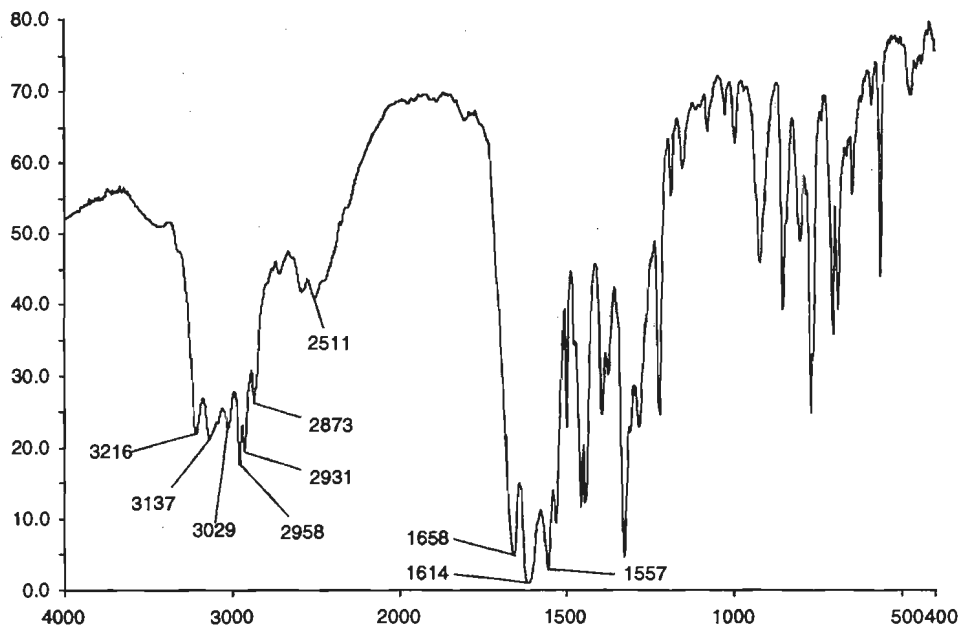


Figure 4.8: IR spectrum in KBr of crystals of compound **3h** in the pyrimidin-4-ol form.

The two tautomeric forms have characteristic bands. Therefore, IR is a powerful tool for a quick analysis to define the tautomeric form present. Dimers of the pyrimidin-4-ol tautomer feature a very indicative absorption at approximately 2500 cm^{-1} . This band is characteristic for a strong $\text{O}-\text{H}\cdots\text{O}=\text{C}$ hydrogen bond, like in an acid dimer. The inner $\text{N}-\text{H}\cdots\text{N}$ hydrogen bond—from the ureido $\text{N}-\text{H}$ to the central pyrimidine ring nitrogen—is found in the region $3155\text{--}3130\text{ cm}^{-1}$, at a similar position as for dimers of the 4[1H]-pyrimidinone tautomer. The absorption of the intramolecular $\text{N}-\text{H}\cdots\text{N}$ hydrogen bond in the pyrimidin-4-ol dimers is present between 3200 and 3260 cm^{-1} .

Pyrimidin-4-ol and 4[1H]-Pyrimidinone tautomers in solution. The ^1H -NMR spectrum in CDCl_3 of 6-phenyl substituted compound **3h** shows two sets of signals (figure 4.9a). The most-abundant set of $\text{N}-\text{H}$ signals (87%) is found at $\delta = 13.95, 12.06, 10.23\text{ ppm}$, and is assigned to the 4[1H]-pyrimidinone tautomer.²⁴ A second set of signals, ascribed to dimers of the pyrimidin-4-ol tautomer, is observed at $13.6, 11.3$ and 10.0 ppm (13% in abundance). Double sets of signals in the same ratio are also observed for the alkylidene signal and $\text{NH}-\text{CH}_2$ signals. Noticeable is the approx. 0.5 ppm downfield shift of the alkylidene proton of the pyrimidin-4-ol tautomer relative to the 4[1H]-pyrimidinone tautomer. This is assigned to an aromatic shift. The ratio between the dimers of the two tautomeric forms is solvent dependent; dimers of 4[1H]-pyrimidinone tautomer and pyrimidin-4-ol

tautomer of compound **3h** are present in approximately equal amounts in toluene (figure 4.9b).

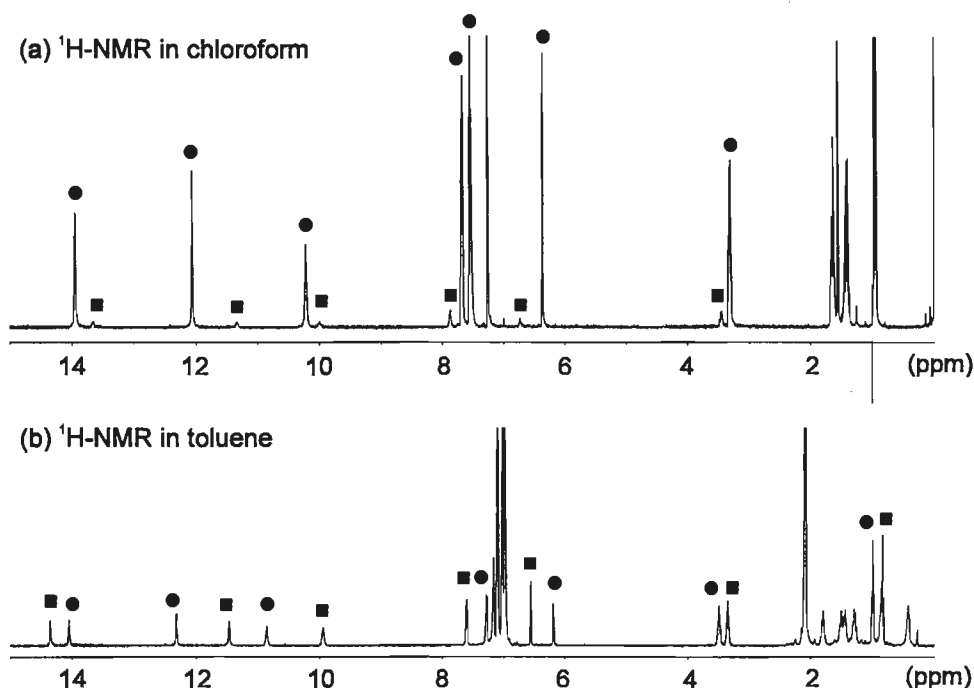
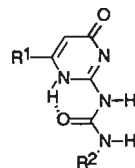


Figure 4.9: ¹H-NMR spectra of **3h**. (a) in CDCl₃, (b) in toluene-*d*₈; ● = signals of 4[1H]-pyrimidinone tautomer, ■ = signals of pyrimidin-4-ol tautomer.

The ratio of pyrimidin-4-ol and 4[1H]-pyrimidinone dimers differs enormously for molecules with different substituents. The ratio is obtained by integration of the two sets in ¹H-NMR. Thus, dimers of pyrimidin-4-ol and 4[1H]-pyrimidinone are present in a roughly 1:1 ratio in CDCl₃ for compounds **3i** and **3k**. 6-Trifluoromethyl derivative **3l** is present in CDCl₃ exclusively as the pyrimidin-4-ol dimeric form.²⁵ The O–H resonance in dimers of this compound is assigned to the signal at $\delta = 14.30$ ppm. The intramolecularly hydrogen bonded terminal N–H of the butylureido chain corresponds to the signal at 9.30 ppm, because this signal is a triplet and exchanges slowly with D₂O. The ureido N–H resonance is found at $\delta = 11.14$ ppm. Relative amounts of both tautomers in the solvents CDCl₃, toluene-*d*₈ and THF-*d*₈ are reported in table 4.3 for several ureidopyrimidinones.

Table 4.3: Relative amounts of dimers of 4[1H]-pyrimidinone and pyrimidin-4-ol tautomers for different compounds in various solvents.^a

Com- pound	R ¹	R ²	% 4[1H]- pyrimidinone in CDCl ₃	% 4[1H]- pyrimidinone in toluene- <i>d</i> ₈	% 4[1H]- pyrimidinone in THF- <i>d</i> ₈
3a	CH ₃	<i>n</i> -C ₄ H ₉	> 99	insoluble	insoluble
3b	CH ₃	<i>t</i> -C ₄ H ₉	97	-	-
3c	C ₁₃ H ₂₇	<i>n</i> -C ₄ H ₉	> 99	87	79
3d	C ₁₃ H ₂₇	<i>t</i> -C ₄ H ₉	96.5	76	-
3e	C ₁₃ H ₂₇	C ₆ H ₅	> 99	98	-
3f	C ₁₃ H ₂₇	<i>p</i> -NO ₂ -C ₆ H ₅	> 99	insoluble	insoluble
3g	C ₁₃ H ₂₇	<i>p</i> -NEt ₂ -C ₆ H ₅	> 99	97	-
3h	C ₆ H ₅	<i>n</i> -C ₄ H ₉	86	42	-
3i	C ₆ H ₅	<i>t</i> -C ₄ H ₉	50	44	-
3k	<i>p</i> -NO ₂ -C ₆ H ₅	<i>n</i> -C ₁₈ H ₃₇	40	insoluble	insoluble
3l	CF ₃	<i>n</i> -C ₄ H ₉	< 1	-	-
10a	C ₆ H ₂ (OC ₁₂ H ₂₅) ₃	<i>n</i> -C ₄ H ₉	87	56	31
10b	C ₆ H ₂ (OC ₁₂ H ₂₅) ₃	C ₆ H ₅	93	77	-
10c	C ₆ H ₂ (OC ₁₂ H ₂₅) ₃	<i>p</i> -NO ₂ -C ₆ H ₅	> 99	> 99	-
10d	C ₆ H ₂ (OC ₁₂ H ₂₅) ₃	<i>p</i> -NEt ₂ -C ₆ H ₅	85	51	-

^a Only dimers of the 4[1H]-pyrimidinone and pyrimidin-4-ol tautomer were observed in these solvents.

4.2.3 Dilution studies to obtain dimerization constants

Studies in chloroform. As was mentioned in section 4.2.1, dilution of **3a** in CDCl₃ did not result in perceivable dissociation. Upon dilution of a CDCl₃ solution of compound **3l**—which exists exclusively as dimers of the pyrimidin-4-ol tautomer in chloroform— or of a CDCl₃ solution of compound **3i**—which is present as a 1:1 mixture of 4[1H]-pyrimidinone and pyrimidin-4-ol dimers—to 10⁻⁴ M, dissociation was also not observed,²⁰ nor did the ratio 4[1H]-pyrimidinone/pyrimidin-4-ol dimers change for **3i**. In view of the noise in the spectrum at these low concentrations, a conservative estimate of the percentage of dissociation is made that lies below 10%. This estimate results in a lower limit of 4.5 × 10⁵ M⁻¹ for the dimerization constant of both pyrimidin-4-ol and 4[1H]-pyrimidinone tautomers of **3a**, **3i** and **3l**.

Studies in THF. More quantitative data on the size of dimerization constants were desired than that they exceed $4.5 \times 10^5 \text{ M}^{-1}$ in pure CDCl_3 . Therefore, we measured ^1H -NMR spectra in more polar solvents—in which dimerization due to hydrogen bonding is expected to be weaker—and diluted to observe dissociation effects. Dilution of **10a** in $\text{THF-}d_8$ showed that the ratio between dimers²⁶ of the 4[1H]-pyrimidinone and pyrimidin-4-ol tautomer tautomers is strongly concentration dependent at low concentrations (see figure 4.10).

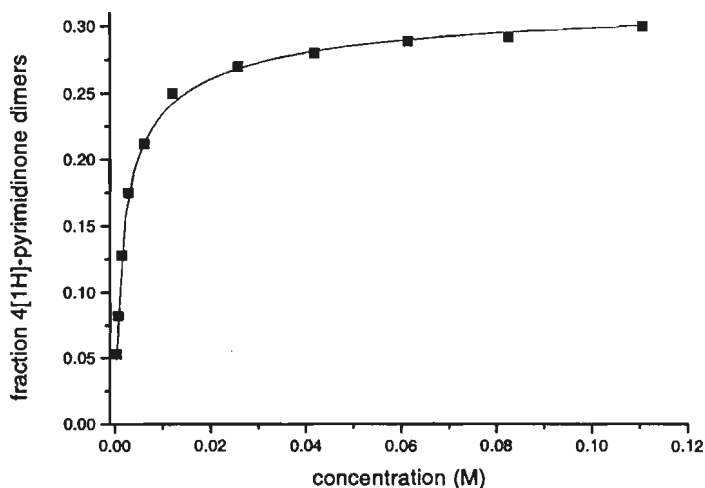


Figure 4.10: Plot of the fraction of 4[1H]-pyrimidinone tautomer versus the concentration in solutions of **10a** in $\text{THF-}d_8$; the solid line serves to guide the eye.

Furthermore, the position of the N–H and O–H signals of the pyrimidin-4-ol tautomer showed a concentration dependence, while the signals of the 4[1H]-pyrimidinone tautomer did not shift in the measured concentration range. These observations indicate that the 4[1H]-pyrimidinone tautomer is dimeric throughout the whole concentration range studied, whereas the pyrimidin-4-ol dimers dissociate at lower concentrations. Because only a small dissociation range could be covered, a dimerization constant could not be fitted to the concentration dependence of the N–H (O–H) protons of the pyrimidin-4-ol dimers. The equilibrium between dimers of 4[1H]-pyrimidinone and pyrimidin-4-ol tautomers was found also to be concentration dependent for compound **3c** in $\text{THF-}d_8$, and for **10a** in pyridine- d_5 . No concentration dependence within the measurable range was observed in CDCl_3 , toluene- d_8 and *o*-dichlorobenzene- d_4 .

Studies in mixed solvent systems, in particular DMSO/ CDCl_3 mixtures.

As another option to explore the strength of dimerization, studies were performed in solvent mixtures of CDCl_3 with methanol and DMSO. Addition of up to 10% MeOH to CDCl_3

solutions of **3a** did not result in significant dissociation,²⁷ and addition of more methanol led to strong line broadening of the N–H resonances to such extent that a quantitative analysis was impossible. Addition of DMSO-*d*₆ —a strong hydrogen bond acceptor solvent— to CDCl₃ solutions of compound **3a** resulted in only slight line-broadening of the N–H resonances of dimers (at fixed positions at δ = 13.95, 12.06, and 10.23 ppm). However, with increasing amounts of DMSO added, a second set of (broader) N–H peaks emerged at 11.4, 9.4 and 7.2 ppm, respectively. In pure DMSO, the latter set of signals is the only one observed. Separate signals are also observed for the alkylidene proton, and for the protons of the butyl CH₂ and the 6-methyl substituent.

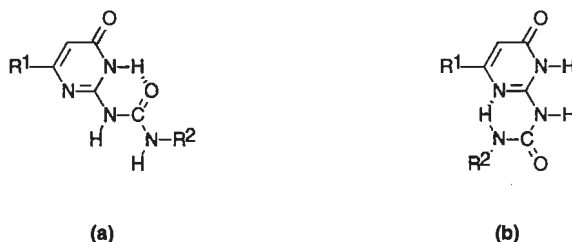


Figure 4.11: Two possible geometries of the monomeric 6[1H]-pyrimidinone tautomer, as observed for compounds **3a**, **3l** and **3l** in DMSO solution. Geometry (a) is found in solution.

This new set of signals is attributed to a monomeric 6[1H]-pyrimidinone tautomer. The N–H peak positions (at 11.4, 9.4 and 7.2 ppm for compound **3a**) agree best with the conformation **a** in figure 4.11, with an intramolecularly hydrogen bonded pyrimidinone N1–H group, and two non-hydrogen bonded ureido N–H groups.

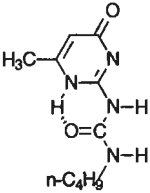
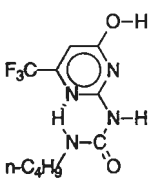
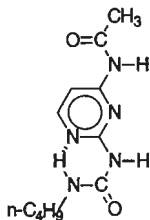
This assignment is confirmed by the observation that for **3l** (R^1 = phenyl; R^2 = *t*-butyl) —of which in CDCl₃ dimers of the 4[1H]-pyrimidinone and pyrimidin-4-ol tautomers coexist in a 1:1 ratio—a third tautomer is observed in CDCl₃/DMSO-*d*₆ mixtures, which is also ascribed to the 6[1H]-tautomer. The 6[1H]-pyrimidinone tautomer is also the monomeric form in CDCl₃/DMSO-*d*₆ mixtures of 6-trifluoromethyl derivative **3l**, which is present entirely in the pyrimidin-4-ol dimeric form in pure chloroform. Notably, the alkylidene proton of the 6[1H]-pyrimidinone tautomer for **3l** is 0.4 ppm upfield (at 6.3 ppm) with respect to the alkylidene signal of the dimeric pyrimidin-4-ol form (at 6.7 ppm). Additional proof for the assignment of this new tautomer was obtained from ¹³C-NMR spectra of **3a** and **3l** in CDCl₃ and DMSO-*d*₆. Whereas the ¹³C-NMR spectra of **3a** in CDCl₃ and DMSO-*d*₆ are very similar—but not identical—the ¹³C-NMR spectra of **3l** in CDCl₃ and DMSO-*d*₆ show significant differences. The spectra indicate that **3a** exists as pyrimidinone tautomer in both solvents, whereas **3l** changes of tautomeric form from CDCl₃ to DMSO-*d*₆.

In a given solvent mixture, the ratio (K_{dim^*}) of dimeric tautomer (either the 4[1H]-pyrimidinone tautomer for **3a**, or the pyrimidin-4-ol tautomer for **3l**) to the square of the concentration of 6[1H]-pyrimidinone tautomer has a constant value within experimental

error.²⁸ This implies a dimer–monomer relationship, with the 6[1H]-pyrimidinone tautomer as the most stable form of monomeric molecules of **3a** or **3l** in CDCl₃/DMSO-*d*₆ solvent mixtures. The constant ratio of dimeric tautomer (either 4[1H]-pyrimidinone or pyrimidin-4-ol) over the squared concentration of 6[1H]-pyrimidinone tautomer may then be considered as a *complex dimerization* constant (K_{dim}^*), based on dimerization and simultaneous tautomerization (see discussion). With the expectation that extrapolation to pure chloroform would be feasible, the complex dimerization constants of compounds **3a** and **3l** were determined in several CDCl₃/DMSO-*d*₆ solvent mixtures (Table 4.4). In the solvent mixtures used, only the 6[1H]-pyrimidinone tautomer was observed as the monomeric species.

The dimerization constant of 2-butylureido-4-acetylamino-pyrimidine **11** (see chapter 3) was also determined in several of these mixtures, since dissociation of dimers of this compound is not accompanied by tautomerization. For this compound, a quick exchange between monomers and dimers was observed,²⁹ and dimerization constants were determined by fitting the concentration dependence of the CH₃ and aromatic H5 proton signal (see chapter 3). We also determined the ET(30) solvent polarity of the solvent mixtures.

Table 4.4: Complex dimerization constants K_{dim}^* of ureidopyrimidinones **3a and **3l**, and dimerization constants K_{dim} of **11** in several CDCl₃/DMSO-*d*₆ mixtures.^{a, b}**

<div style="display: flex; justify-content: space-around; align-items: center;"> <div style="text-align: center;">  <p>3a</p> </div> <div style="text-align: center;">  <p>3l</p> </div> <div style="text-align: center;">  <p>11</p> </div> </div>										
Com- pound	solvent composition: volume% DMSO- <i>d</i> ₆ in CDCl ₃ , and ET(30) values									
	0.3%	0.5%	1%	2%	3%	4%	6%	8%	10%	15%
3a	39.00	39.33	39.37	39.76	39.87	40.21	40.55	41.02	41.26	41.98
3a	1.2*10 ⁶	2.0*10 ⁵	5.0*10 ⁴	1.2*10 ⁴	3.9*10 ³	2200	750	370	170	51
3l	160	53	14	2.8	1.3	0.52	0.24	- ^c	- ^c	- ^c
11	-	-	-	2.6*10 ⁴	-	1.2*10 ⁴	5600	-	-	-

^a Estimated error <20% for **3a**, <40% for **3l**, and <30 % for **11**; ^b In pure CDCl₃, no dimerization constants could be determined, ^c Too low to determine.

We tried to evaluate the dimerization constants in pure CDCl₃ with the same three methods as described in chapter 3. Extrapolation of the monomer and dimer shift is not

applicable in slowly exchanging systems like **3a** and **3l**, while for **11**, a good extrapolation could not be obtained.³⁰

Log K_{dim}^* of ureidopyrimidinones **3a** and **3l** is strongly dependent on solvent composition, especially when small amounts of DMSO- d_6 are present in the solvent mixtures (figure 4.12). Because of this, extrapolation to a K_{dim}^* value in pure chloroform is impossible without a quantitative model for the relation between dimerization constant and solvent composition. The procedure used in chapter 3 for fitting dimerization constants in MeOH/ CDCl_3 mixtures —based on a model taking competitive complexation of monomers by the cosolvent into account³¹— did not give a reliable combination of parameters, rendering extrapolation to a value for the dimerization constant in pure CDCl_3 impossible.

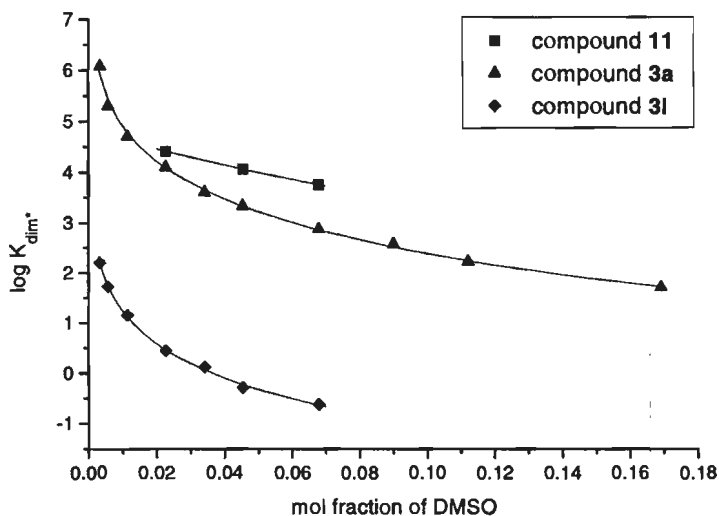


Figure 4.12: Plot of $\log K_{\text{dim}}^*$ versus solvent composition for compounds **3a**, **3l** and **11** in $\text{CDCl}_3/\text{DMSO}-d_6$ mixtures; the lines only serve to guide the eye.

A third method of extrapolation involved plotting $\log K_{\text{dim}}^*$ versus the experimental ET(30) solvent polarity (figure 4.13). We had expected (and hoped for) a linear relation between $\log K_{\text{dim}}^*$ and ET(30) solvent polarity, because $\log K_{\text{dim}}^*$ is a sum of $\log K_{\text{dim}}$ and $2 \times \log K_{\text{taut}}$ (see discussion). Both values are expected to be linearly related to ET(30), because:

(i) The energies of many equilibria have been found to be linearly related to ET(30) solvent polarity (see chapter 3). Furthermore, we have established a linear relationship between $\log K_{\text{dim}}$ and ET(30) solvent polarity for the systems described in the chapter 3, which were measured in $\text{CDCl}_3/\text{MeOH}$ mixtures and dealt with compounds not undergoing tautomerization upon dissociation. To test the generality of this linear relation, we measured the dimerization constants of compound **11** in the $\text{CDCl}_3/\text{DMSO}-d_6$ solvent mixtures.

(ii) Tautomeric equilibria are known to be dependent on solvent polarity, and their log K values have often been found to be linearly related to solvent polarity.¹⁴ However, the tautomeric equilibria themselves cannot be determined for **3a** and **3l**, because of the simultaneous effect of dimerization.³²

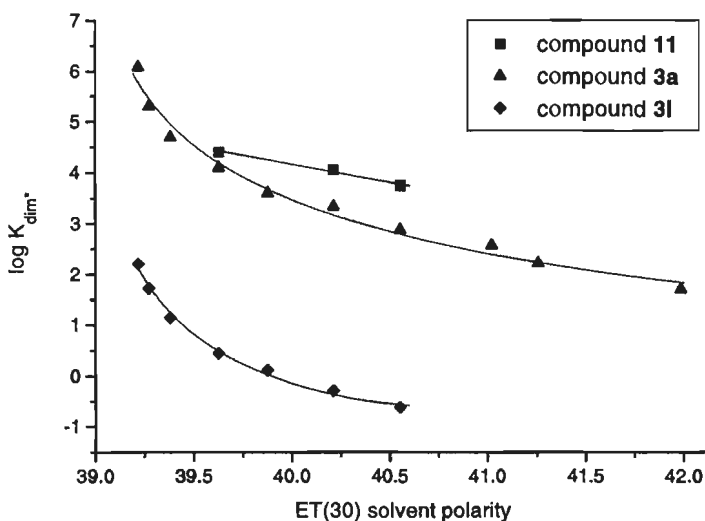


Figure 4.13: Plot of $\log K_{dim}^*$ versus the ET(30) solvent polarity of the $CDCl_3/DMSO-d_6$ mixtures; the lines serve to guide the eye. The ET(30) value of $CDCl_3$ equals 39.00.

In contrast to the systems described in chapter 3, the relation between $\log K_{dim}^*$ and the ET(30) solvent polarity is strongly non-linear for compounds **3a** and **3l**, especially at relatively low amounts of cosolvent $DMSO-d_6$ (figure 4.13). Despite the limited number of data points, the results clearly indicate that $\log K_{dim}^*$ of compound **11** is less dependent on ET(30) than the $\log K_{dim}^*$ of **3a** and **3l**.³³ This difference is probably related to a solvent dependent contribution of K_{taut} to K_{dim}^* for compounds **3a** and **3l**.

As a result of the strong solvent composition dependence at low amounts of DMSO, we cannot give a reliable extrapolation for the value in pure $CDCl_3$. The strong solvent composition dependence indicates that the complex dimerization constant K_{dim}^* of 6-methyl derivative **3a** in pure chloroform significantly exceeds $10^6 M^{-1}$. Especially when $\log K_{dim}^*$ is plotted versus ET(30), it is clear that a large gap is present between the measured range and pure $CDCl_3$. Furthermore, the data clearly indicate that the complex dimerization constant K_{dim}^* of 6-trifluoromethyl derivative **3l**—present as a DADA dimer of a pyrimidin-4-ol tautomer—is lower than that of **3a**—present as a DDAA dimer of a 4[1H]-pyrimidinone tautomer—by roughly 4 orders of magnitude in the $CDCl_3/DMSO-d_6$ mixtures.

4.2.4 Exchange of dimers: heterodimers

Exchange between monomer and dimer in hydrogen bonded complexes is generally fast on the NMR-timescale, and a time-averaged peak position is observed. At lower temperatures, exchange rates may become slow on the NMR timescale. This was observed for quadruply hydrogen bonded dimers of di(amido)- or di(ureido)triazines (see chapter 3). Exchange at room temperature is expected to be slower for the more strongly hydrogen bonded dimers of ureidopyrimidinones. Slow exchange between monomer and dimer of ureidopyrimidinone, even at high concentrations (0.5 M), was described in the previous section, and is probably related to a slow tautomerization step.³⁴ The exchange rate of dimers is even more interesting, as the life-time of a dimer is the important factor that determines physical properties related to dynamic exchange. Exchange of dimers may be much faster than monomer–dimer exchange if dimers exchange without the slow tautomerization to the most stable form of the monomer.

The ¹H-NMR spectrum of mixtures of two ureidopyrimidinone derivatives at low concentrations indeed shows slowly exchanging hetero-dimers: the spectrum at 298 K of an equimolar 1 mM solution of **3c** and **10c** (figure 4.14) shows splitting of the signals attributed to N–H protons, but also of the signals of phenyl and alkylidene protons.³⁵ The process of exchange leads to an almost statistical mixture of dimers, as in equimolar mixtures of **3c** and **10c**, a 1:1 ratio of heterodimers and homodimers is observed.³⁶

The lifetime of the dimers is estimated to lie between 0.01 seconds (the lifetime for which coalescence is expected) and 3 minutes (the time needed to prepare a sample and measure its spectrum). In an attempt to analyse the exchange between the dimers, temperature and concentration dependent spectra were taken. A concentration experiment performed with the couple **3e** and **3h** (figure 4.15) cannot be explained by a simple coalescence process. A concentration dependent upfield shift, possibly due to stacking, is also observed.

Because of the ambiguity, the exchange rate was studied by EXSY, a 2D-NMR measurement. This type of measurement is more reliable, because exchange is observed unambiguously, and the ratios between molecules that do and do not exchange is integrated. Preliminary results of these experiments performed by Michel Pepers indicated that there is indeed exchange between the dimers, of which the life-time is below 0.2–0.4 s.

The exchange rate of the dimers is much higher than the tautomeric equilibration of the monomer. Hence, if the dimer exchange occurs via monomers, these do not tautomerize before exchange. Other explanations are that the 4[1H]-pyrimidinone tautomer instead of the 6[1H]-pyrimidinone tautomer is the most stable form of the monomer in pure chloroform, or that two dimers exchange in a sort of concerted process without dissociation.

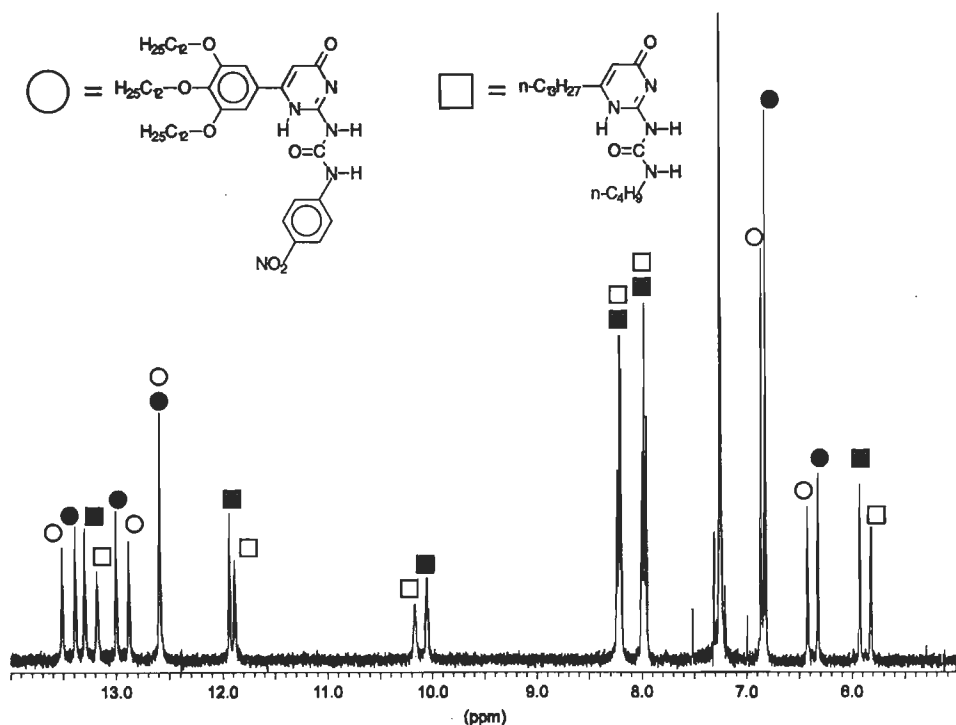


Figure 4.14: ^1H -NMR spectrum of a 1 mM equimolar CDCl_3 solution of **3c** and **10c** at 298 K; open figures belong to homo-dimers, filled figures to hetero-dimers.

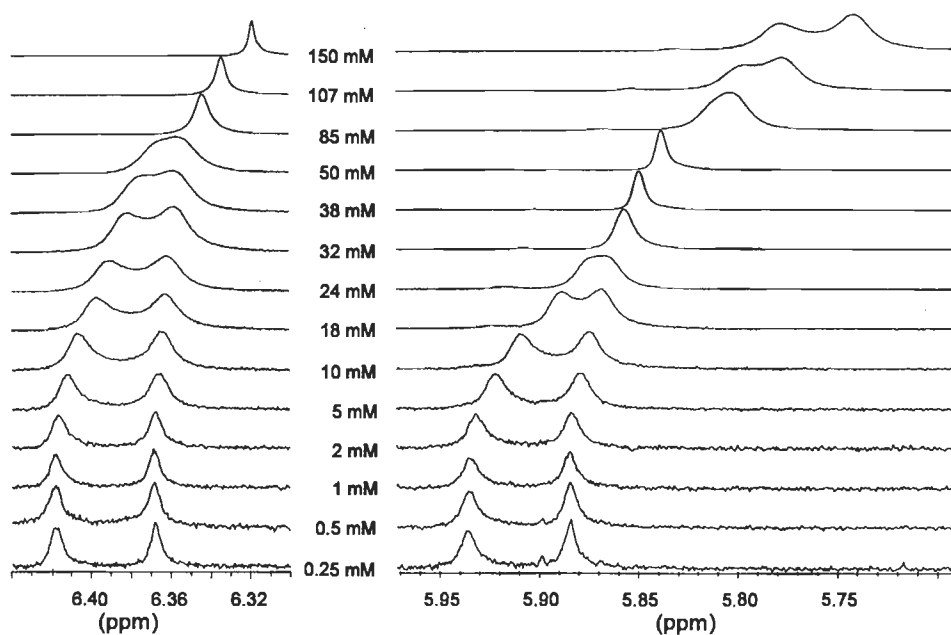


Figure 4.15: Dilution experiment with an equimolar CDCl_3 solution of **3e** and **3h** at 298 K.

4.3 Evaluation

4.3.1 Monomer–Dimer, and Tautomeric Equilibria in Solution

In solution, three different tautomeric forms of 2-ureido-4-pyrimidinones are observed. These are proposed to be related by the equilibria depicted in figure 4.16.

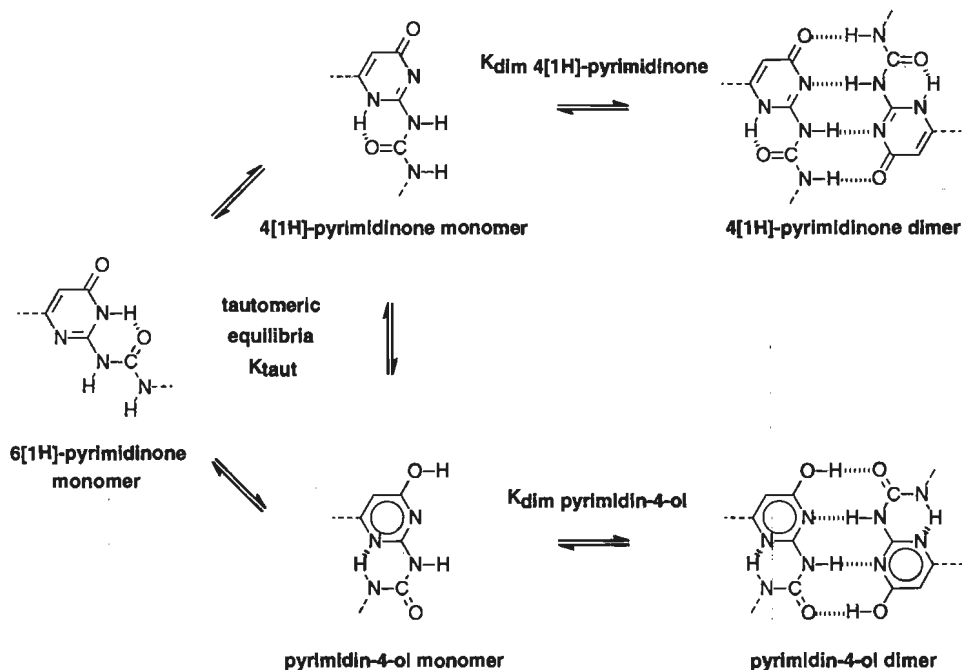


Figure 4.16: Equilibria in solution between tautomeric forms, and between monomer and dimer of ureidopyrimidinones 3.

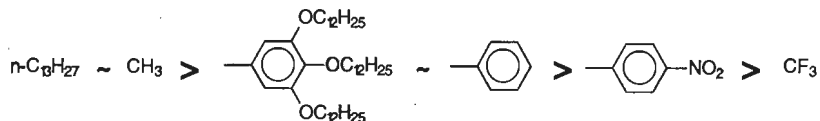
The complex dimerization constant K_{dim^*} is thus related to the dimerization constant K_{dim} of a single tautomer, and the tautomerization constant K_{taut} of that tautomer. Within the simplified scheme proposed in figure 4.16 for the complex process, the following equations describe the relation of K_{dim^*} , K_{dim} and K_{taut} for derivatives with 4[1H]-pyrimidinone dimers; a similar relation can be derived for derivatives with pyrimidin-4-ol dimers.

$$K_{\text{dim}} = \frac{\text{concentration 4[1H]-pyrimidinone dimers}}{[\text{concentration 4[1H]-pyrimidinone monomers}]^2}$$

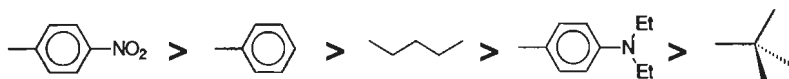
$$K_{\text{taut}} = \frac{\text{concentration 4[1H]-pyrimidinone monomer}}{\text{concentration 6[1H]-pyrimidinone monomer}}$$

$$K_{\text{dim}^*} = \frac{\text{concentration 4[1H]-pyrimidinone dimers}}{[\text{concentration 6[1H]-pyrimidinone monomers}]^2}$$

Substituent effects on tautomeric equilibria. As is evident from inspection of Table 4.2, a very large influence on the 4[1H]-pyrimidinone/pyrimidin-4-ol equilibrium is exerted by the substituents. The following relative preference for the 4[1]-pyrimidinone form over the pyrimidin-4-ol form in dimers was deduced for the 6-substituent,



while for the ureido substituent, the following relative order was deduced:



Clearly, the effects of both substituents are predominantly electronic. An electron-withdrawing group at the 6-position, for example a 6-trifluoromethyl substituent, favors the pyrimidin-4-ol tautomer. This effect can be understood by applying an explanation given by Gordon and Katritzky for the analogous 4-pyridone system to the 2-ureido-4-pyrimidinone unit (figure 4.17).^{14,18} Both the 4[1H]-pyrimidinone (**4[1H]**) and the pyrimidin-4-ol (**OH**) tautomer are in (hypothetical) equilibrium with the same protonated species (the two structures in the middle of figure 4.17 are mesomers). The position of the tautomeric equilibrium is then determined by the relative acidities of the O—H and N—H protons: if the O—H proton is more acidic than the N—H, then this proton will be abstracted most easily, and the 4[1H]-pyrimidinone tautomer results; if the N—H proton is more acidic, then pyrimidin-4-ol tautomer results. The effect of the 6-position substituent X can now be understood. An electron withdrawing group X renders the *ortho* N—H more acidic, and thus results in a preference for the pyrimidin-4-ol tautomer. Although the effect of a substituent Y was not studied due to limited synthetic accessibility, an electron withdrawing substituent Y is similarly expected to stabilize the 4[1H]-pyrimidinone tautomer.

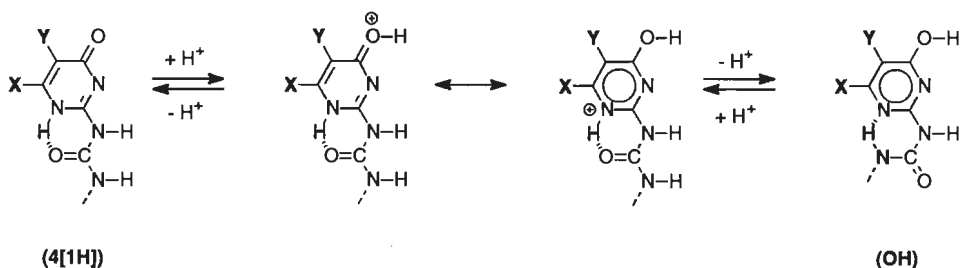


Figure 4.17: Explanation for the preference for the pyrimidin-4-ol tautomer (**OH**) over the 4[1H]-pyrimidinone tautomer (**4[1H]**) with electron withdrawing 6-position substituents.

There is also a distinct electronic effect of the ureido substituent. Electron withdrawing groups on the ureido group favor the 4[1H]-pyrimidinone tautomer. The cause of this effect is rather unclear to us. Obviously, an electron-withdrawing group renders the adjacent N–H more acidic, and consequently, this N–H becomes a better hydrogen bond donor. The different acidities of the N–H groups adjacent to the ureido substituents are also reflected in the relative exchange rates of N–H signals with D₂O. The N–H protons adjacent to the butyl substituent in **3a** or the *p*-di(ethylamino)phenyl substituent in **3g** exchange slower than corresponding protons adjacent to a phenyl or *p*-nitrophenyl substituents in compounds **3e** and **3f**. However, it is unclear to us why the increase of donor strength of the ureido N–H has a larger stabilizing effect on 4[1H]-pyrimidinone dimers than on pyrimidin-4-ol dimers.

Solvent and concentration effects. The solvent composition was found to have a strong effect on the complex dimerization constants K_{dim}^* in CDCl₃/DMSO-*d*₆ mixtures. Since K_{dim}^* is equivalent to the product of K_{dim} of a single tautomer times the square of a tautomeric equilibrium constant K_{taut} , this can be explained very well: the solvent is expected to have an effect on K_{dim} as well as on K_{taut} .

The observation of the 6[1H]-pyrimidinone tautomer as the monomeric form in DMSO, or in its mixtures with chloroform, is in line with generally accepted knowledge. For related uracils and parent isocytosine, it has been well documented that a 6[1H]-pyrimidinone tautomer is more stable than a 4[1H]-pyrimidinone tautomer.^{14,18} In relatively non-polar solvents favorable for hydrogen bonding, and also in the solid state, dimers of the 4[1H]-pyrimidinone tautomer and of the pyrimidin-4-ol tautomer are observed. These normally less stable tautomeric forms are stabilized significantly by the strong dimerization via quadruple hydrogen bonding.

The largest relative amount of 4[1H]-pyrimidinone dimers was observed in chloroform. In other solvents, such as THF, *o*-dichlorobenzene and pyridine, but also the very apolar solvent toluene, a higher fraction of the molecules is present in the pyrimidin-4-ol dimeric form. The observed high relative amount of 4[1H]-pyrimidinone dimers in chloroform may be due to stabilization of the keto-groups by interactions of the hydrogen donor of chloroform. Aromatic solvents, such as toluene, pyridine and *o*-dichlorobenzene, seem to favor the aromatic pyrimidin-4-ol tautomer. Dilution in THF resulted in an increase of the amount of the pyrimidin-4-ol tautomer, reaching approximately 100% at high dilutions, and the observed concentration dependence of the pyrimidin-4-ol tautomer N–H and O–H signals suggested dissociation of the dimers of this tautomer. These observations suggest that the pyrimidin-4-ol tautomer is the most stable form of monomeric **10a** in THF-*d*₈. This is in sharp contrast to the situation in CDCl₃/DMSO-*d*₆ mixtures, and may be explained by stabilization of keto-groups by the weak hydrogen bonding donor interactions of chloroform.

4.3.2 Relative strength of dimerization

In an evaluation of the dimerization strength, it should be kept well in mind that we determined complex dimerization constants K_{dim}^* . These complex dimerization constants K_{dim}^* give the ratio between dimerized and non-dimerized molecules that actually will occur in solution at a given concentration, and reflect the difference in energy between the dimer and the most stable form of the monomer. The dimerization constants K_{dim} of a single tautomer in the $\text{CDCl}_3/\text{DMSO}-d_6$ mixtures are higher than the complex dimerization constants K_{dim}^* , because K_{dim}^* is the product of K_{dim} and K_{taut}^2 , and K_{taut} is smaller than 1 (nearly all the monomer is in the 6[1H]-pyrimidinone form). Because 4[1H]-pyrimidinone or pyrimidin-4-ol monomers were not observed, we could not determine K_{dim} and K_{taut} separately.

The complex dimerization constant in chloroform of 6-trifluoromethyl ureido-pyrimidinone **31**—which exists in chloroform as the pyrimidin-4-ol tautomer dimerized in a DADA array—($K_{\text{dim}}^* > 4.5 \times 10^5 \text{ M}^{-1}$) exceeds the value predicted by Schneider (310 M^{-1} for DADA arrays) by at least three orders of magnitude, or $32 \text{ kJ}\cdot\text{mol}^{-1}$. The anomalously high stability of pyrimidin-4-ol dimers may be attributed to a combination of two effects:

(i) The DADA array is pre-organized by an intramolecular hydrogen bond. Pre-organization was shown in chapter 3 to increase the dimerization constants of multiple hydrogen bonded dimers strongly.

(ii) The dimers of the pyrimidin-4-ol tautomer contain an $\text{O}-\text{H}\cdots\text{O}=\text{C}$ hydrogen bond, which are known to be stronger than $\text{N}-\text{H}\cdots\text{O}=\text{C}$ hydrogen bonds.³⁷ The empirical free energy relationship of Schneider is entirely based on systems with weaker $\text{N}-\text{H}\cdots\text{O}=\text{C}$ and $\text{N}-\text{H}\cdots\text{N}$ hydrogen bonds; also the compounds in chapter 3 had this kind of hydrogen bonds.

The complex dimerization constants of DDAA systems of this study in chloroform could not be determined exactly, because the complex dimerization constants K_{dim}^* measured in the mixed solvent systems could not be extrapolated to pure chloroform. The results show that the value for **3a** in pure CDCl_3 is at least of the same order of magnitude as predicted by Schneider ($3.6 \times 10^6 \text{ M}^{-1}$). The actual values of K_{dim}^* are probably even larger, because:

(i) The complex dimerization constant K_{dim}^* of **3a** is already $1.2 \times 10^6 \text{ M}^{-1}$ in CDCl_3 with 0.3% v/v $\text{DMSO}-d_6$, while it is strongly dependent on the presence of small amounts of DMSO.

(ii) The DDAA-array is pre-organized by an intramolecular hydrogen bond, which was shown in the previous chapter to result in anomalously high association constants for DADA-arrays.

(iii) IR indicates stronger hydrogen bonding in the DDAA dimers than in the DADA dimers discussed in the previous chapter.

4.4 Conclusion

A novel building block for self-assembly, ureido-pyrimidinone, is synthesized from readily available isocytosines and isocyanate derivatives. This building block forms exceptionally stable dimers via a pre-organized array of four hydrogen bonds, with effective dimerization constants significantly exceeding 10^6 M^{-1} in chloroform. Furthermore, no additional hydrogen bonding interactions are present between ureido-pyrimidinone dimers; the unidirectionality with respect to hydrogen bonding is advantageous for several supramolecular purposes.

Although the association behavior is complicated by tautomeric equilibria, —both dimerization via a DADA or a DDAA array is possible— these tautomeric equilibria can be steered by the predictable substituent effects. Hence, two discrete self-complementary hydrogen bonding units with DDAA and DADA arrays, respectively, are obtained. As a fortunate coincidence, derivatives with *n*-alkyl substituents at both the ureido-group and at the 6-position —which are the easiest accessible, have the largest possibility for structural variation, and have good solubility characteristics— are exclusively present in chloroform as 4[1H]-pyrimidinone dimers, the tautomeric form with the highest association constant. The ready availability of compounds with the self-complementary DDAA motif of the 4[1H]-pyrimidinone tautomer opens the way to special supramolecular architectures, because of the unique and unprecedented combination of strength and ease of synthesis.

4.5 Experimental Section

General methods. Chemicals were purchased from Acros Chimica, Fluka or Aldrich and used as received unless otherwise stated. All reactions were carried out under an atmosphere of dry nitrogen unless otherwise stated. Solvents were of technical grade unless otherwise stated. Anhydrous THF was obtained by distillation from sodium/potassium/benzophenone; analytical grade pyridine, ethanol and *iso*-propanol were dried over 4 Å molecular sieves. NMR-spectra were recorded on a Varian Gemini 300 or a Bruker AM400 spectrometer. Chemical shifts are given in ppm relative to TMS. For the ^1H -NMR titrations, deuteriochloroform was used as received. IR-spectra were recorded on a Perkin-Elmer 1600 FT-IR spectrometer. Dry chloroform for the infrared experiments in solution was obtained by purification of analytical grade chloroform by several extractions with water, followed by drying over calcium chloride for two hours, and distillation under an atmosphere of dry nitrogen. Spectra at concentrations higher than 5 mM were taken in a 0.1 mm NaCl cell, and for lower concentrations in a 1 mm cell. Melting points were determined on a Jenaval THMS 600 melting point microscope and are uncorrected.

Binding experiments. Dimerization constants were determined from integrated peak areas of appropriate signals. For compound **3a**, the sharp and intense CH_3 signals were used, allowing reliable integration down to 10^{-5} M with an estimated relative error of 20% in the 10–90% saturation range. For

compound **3I**, the broader N–H signals had to be used, resulting in a larger relative error of 40% in the 20–80% saturation range.

X-ray single crystal structure analyses. Data were collected on an Enraf-Nonius CAD4T diffractometer on rotating anode (ω scan, $T = 150$ K, Mo $K\alpha$ radiation, graphite monochromator, $\lambda = 0.71073$ Å). Accurate unit-cell parameters and an orientation matrix were determined by least-squares fitting of the setting angles of 25 well-centered reflections.³⁸ The unit cell parameters were checked for the presence of higher order lattice symmetry.³⁹ Data were corrected for L_p effects and for the observed linear decay of the periodically measured reference reflections. Structures were solved with direct methods using SHELXS-96, and refined on F^2 using SHELXL-96. In the weighing scheme, $P = (\max(F_o^2, 0) + 2F_c^2)/3$. No observation criterion was applied during refinement on F^2 . The hydrogen atoms of **3h** (4[1H]-pyrimidinone tautomer) were included in the refinement on calculated positions; the hydrogen atoms of all other structures were located on a difference Fourier map, and their coordinates were included as parameters in the refinement. The non-hydrogen atoms of all structures were refined with anisotropic thermal parameters. The hydrogen atoms were refined with a fixed isotropic displacement parameter related to the value of the equivalent isotropic displacement parameter of their carrier atoms. Neutral atom scattering factors and anomalous dispersion corrections were taken from the International Tables for Crystallography.⁴⁰ Geometrical calculations and illustrations were performed with PLATON.⁴¹

Crystal data for 3a: $C_{10}H_{16}N_4O_2$, $M_r = 224.26$, colourless, plate-shaped crystal ($0.05 \times 0.15 \times 0.60$ mm), triclinic, space group $P\bar{1}$ (no. 2) with $a = 4.5570(2)$, $b = 10.3195(8)$, $c = 12.0901(10)$ Å, $\alpha = 83.525(7)^\circ$, $\beta = 83.602(6)^\circ$, $\gamma = 86.813(5)^\circ$, $V = 560.87(7)$ Å³, $Z = 2$, $D_c = 1.3279(2)$ g.cm⁻³, $F(000) = 240$, $\mu(\text{Mo } K\alpha) = 1.0$ cm⁻¹. 5857 Reflections measured, 2565 independent reflections, $R_{int} = 0.1273$, ($1.7^\circ < \theta < 27.5^\circ$), and 193 parameters. Final $wR2 = 0.1743$, $w = 1/[\sigma^2(F^2) + (0.0711P)^2]$, $R1 = 0.0652$ (for 1473 $I > 2\sigma(I)$), $S = 0.984$, $-0.38 < \Delta\rho < 0.31$ e Å⁻³.

Crystal data for 3h 4[1H]-pyrimidinone tautomer: $(C_{15}H_{18}N_4O_2) \cdot \frac{1}{2} (CHCl_3)$, $M_r = 346.02$, colourless, needle-shaped crystal ($0.1 \times 0.1 \times 0.6$ mm), triclinic, space group $P\bar{1}$ (no. 2) with $a = 13.9838(14)$, $b = 14.431(2)$, $c = 16.9539(15)$ Å, $\alpha = 86.314(11)^\circ$, $\beta = 88.910(8)^\circ$, $\gamma = 71.063(11)^\circ$, $V = 3231.3(7)$ Å³, $Z = 8$, $D_c = 1.4226(3)$ g.cm⁻³, $F(000) = 1448$, $\mu(\text{Mo } K\alpha) = 3.3$ cm⁻¹. 25717 Reflections measured, 11391 independent reflections, $R_{int} = 0.2346$, ($1.2^\circ < \theta < 26.5^\circ$), and 887 parameters. Final $wR2 = 0.1725$, $w = 1/[\sigma^2(F^2) + (0.0401P)^2]$, $R1 = 0.0736$ (for 4061 $I > 2\sigma(I)$), $S = 0.894$, $-0.36 < \Delta\rho < 0.38$ e Å⁻³.

Crystal data for the three modifications of 3h pyrimidin-4-ol tautomer: $M_r = C_{15}H_{18}N_4O_2$, $M_r = 286.33$, colourless, plate-shaped crystal.

modification A) Crystal dimensions $0.05 \times 0.2 \times 1.0$ mm, triclinic, space group $P\bar{1}$ (no. 2) with $a = 10.1040(7)$, $b = 11.2468(10)$, $c = 14.6926(9)$ Å, $\alpha = 77.710(7)^\circ$, $\beta = 70.286(6)^\circ$, $\gamma = 64.667(6)^\circ$, $V = 1416.0(10)$ Å³, $Z = 4$, $D_c = 1.3431(2)$ g.cm⁻³, $F(000) = 608$, $\mu(\text{Mo } K\alpha) = 0.9$ cm⁻¹. 11078 Reflections measured, 6477 independent reflections, $R_{int} = 0.0411$, ($1.5^\circ < \theta < 27.5^\circ$), and 487 parameters. Final $wR2 = 0.1402$, $w = 1/[\sigma^2(F^2) + (0.0655P)^2]$, $R1 = 0.0546$ (for 3612 $I > 2\sigma(I)$), $S = 0.978$, $-0.32 < \Delta\rho < 0.25$ e Å⁻³.

Modification B) Crystal dimensions $0.05 \times 0.20 \times 0.50$ mm, triclinic, space group $P\bar{1}$ (no. 2) with $a = 11.0259(10)$, $b = 11.1756(10)$, $c = 13.2723(10)$ Å, $\alpha = 90.187(6)^\circ$, $\beta = 106.695(7)^\circ$, $\gamma = 112.808(8)^\circ$, $V = 1431.8(2)$ Å³, $Z = 4$, $D_c = 1.3283(2)$ g.cm⁻³, $F(000) = 608$, $\mu(\text{Mo } K\alpha) = 0.9$ cm⁻¹. 7028 Reflections measured, 5050 independent reflections, $R_{int} = 0.2318$ ($1.62^\circ < \theta < 25.0^\circ$), and 487 parameters. Positional parameters for the hydrogen atoms were refined. Final $wR2 = 0.1495$, $w = 1/[\sigma^2(F^2) + (0.020P)^2 + 2.0P]$, $R1 = 0.0692$ (for 2595 $I > 2\sigma(I)$), $S = 1.125$, $-0.35 < \Delta\rho < 0.33$ e Å⁻³.

Modification C) Crystal dimensions 0.03 x 0.20 x 0.30 mm, triclinic, space group $P\bar{1}$ (no. 2) with $a = 8.3975$ (8), $b = 10.4896$ (18), $c = 17.377$ (2) Å, $\alpha = 92.667$ (12), $\beta = 98.049$ (9), $\gamma = 108.196$ (12)°, $V = 1433.2$ (3) Å³, $Z = 4$, $D_c = 1.3270$ (3) g.cm⁻³, $F(000) = 608$, $\mu(\text{Mo K}\alpha) = 0.9$ cm⁻¹. 8025 Reflections measured, 5041 independent reflections, $R_{\text{int}} = 0.0551$ ($1.19^\circ < \theta < 25.0^\circ$) and 487 parameters. Positional parameters for the hydrogen atoms were refined. Final $wR2 = 0.1582$, $w = 1/[\sigma^2(F^2) + (0.0447P)^2]$, $R1 = 0.0757$ (for 2177 $I > 2\sigma(I)$), $S = 1.024$, $-0.31 < \Delta\rho < 0.28$ e Å⁻³.

N-Butylaminocarbonyl-6-methyl-isocytosine (3a). A suspension of 6-methyl-isocytosine, **2a**, (6.20 g, 50 mmol) and butyl isocyanate (10 mL, 90 mmol) in dry pyridine (200 mL) was boiled under reflux for 2 h, giving a clear solution. After cooling, acetone was added (200 mL), and the resulting white micro-crystalline powder was filtered. Recrystallization from ethanol/ chloroform 9:1 v/v gave analytically pure **3a** (3.30 g, 99%), as colourless needles, mp 225°C with sublimation. X-ray quality crystals were obtained by slow evaporation of a dichloromethane solution to air. ¹H-NMR (CDCl₃) δ : 13.15 (s, 1H), 11.85 (s, 1H), 10.16 (s, 1H), 5.81(s, 1H), 3.24 (dd, 2H), 2.23 (s, 3H), 1.58 (m, 2H), 1.37 (m, 2H), 0.94 (tr, 3H). ¹³C-NMR (CDCl₃) δ : 173.0, 156.5, 154.7, 148.1, 106.6, 39.7, 31.5, 20.1, 18.9, 13.7. ¹H-NMR (DMSO-*d*₆) δ : 11.82 (s, br, 1H), 9.75 (s, br, 1H), 7.52 (s, br, 1H), 5.78 (st, 1H), 3.17 (q, 2H), 2.05 (s, 3H), 1.44 (m, 2 H), 1.25 (m, 2H), 0.86 (t, 3H). ¹³C-NMR (DMSO-*d*₆) δ : 164.0 (br), 161.5 (br), 154.8, 151.4, 104.5, 38.8, 31.2, 23.2 (br), 19.4, 13.6. IR (KBr) ν : (dimeric 4[1H]-pyrimidinone tautomer) 3215, 3147, 3036, 2954, 2916, 2870, 1704, 1665, 1583, 1528, 1252 cm⁻¹. Anal. calcd. for C₁₀H₁₆N₄O₂: C, 53.56; H, 7.19; N, 24.98. Found: C, 53.57; H, 7.36; N, 25.18.

N-*t*-Butylaminocarbonyl-6-methyl-isocytosine (3b). A suspension of 6-methyl-isocytosine, **2a**, (1.24 g, 10 mmol) and *t*-butyl isocyanate (1.7 mL, 15 mmol) in dry pyridine (25 mL) was boiled under reflux for 4 h, giving a clear solution. Cooling induced the formation of crystals. Acetone was added (50 mL), and the resulting powder was filtered. Recrystallization from acetone/chloroform 1:1 v/v gave analytically pure **3b** (0.46 g, 21%) as white needles, mp 203–204°C (dec, gas evolves). ¹H-NMR (CDCl₃) δ : (major tautomer > 97%)13.14 (s, 1H), 11.73 (s, 1H), 9.53 (s, 1H), 5.81 (s, 1H), 2.22 (s, 3H), 1.43 (s, 9H). ¹³C-NMR (CDCl₃) δ : 172.8, 155.8, 154.9, 147.9, 106.7, 51.3, 28.8, 18.9. IR (KBr) ν : (dimeric 4[1H]-pyrimidinone tautomer) 3212, 2970, 1698, 1674, 1636, 1586, 1521, 1265 cm⁻¹. Anal. calcd. for C₁₀H₁₆N₄O₂: C, 53.56; H, 7.19; N, 24.98. Found: C, 53.76; H, 7.29; N, 25.04.

6-Tridecyl-isocytosine (2b). Crude β -keto ester **1b** (136.1 g, containing 0.29 mol of keto ester, see chapter 3) in ethanol (220 mL) was boiled with guanidinium carbonate (30.6 g, 0.17 mol) overnight. The resultant clear, yellow solution was partially evaporated to dryness by distillation of ethanol at atmospheric pressure, and then cooled, inducing precipitation of a white powder. Addition of hexane (500 mL) and then water (500 mL) resulted in the precipitation of more white powder, which was filtered off, and washed thoroughly with water, then acetone. Crystallization from ethanol gave pure **2b** as tiny white plates (39.7 g, 36%), mp 181°C. ¹H-NMR (DMSO-*d*₆) δ : 10.57 (s, 1H), 6–7 (br, 2H), 5.36 (s, 1H), 2.24 (t, 2H), 1.55 (t, 2H), 1.26 (m, 20 H), 0.86 (t, 3H). ¹³C-NMR (DMSO-*d*₆) δ : 171.8, 162.7, 155.0, 99.2, 36.1, 30.4, 28.1 (multiple peaks), 26.6 (multiple peaks), 21.1, 12.6. IR (KBr) ν : 3365, 3146, 2920, 2850, 2713, 1662, 1634, 1553, 1468, 1400 cm⁻¹. Anal. calcd. for C₁₇H₃₁N₃O: C, 69.58; H, 10.65; N, 14.32. Found: C, 69.74; H, 10.80; N, 14.00.

N-Butylaminocarbonyl-6-tridecyl-isocytosine (3c). A solution of 6-tridecyl-isocytosine **2b**, (10.22 g, 36 mmol) and butyl isocyanate (6.8 mL, 60 mmol) in dry pyridine (200 mL) was boiled under reflux for 2 h. After cooling, the solution was evaporated to dryness. Treatment of the residue in hot acetone with active carbon, and crystallization afforded analytically pure **3c** as tiny white needles (11.6 g, 82%), mp 118°C. ¹H-NMR (CDCl₃) δ : 13.18 (s, 1H), 11.88 (s, 1H), 10.17 (s, 1H), 5.82 (s, 1H), 3.24 (q, 2H), 2.45 (t, 2H), 1.62 (m, 4H), 1.31 (m, 22 H), 0.90 (m, 6H). ¹³C-NMR (CDCl₃) δ : 174, 157, 155, 152, 106, 41, 33, 32, 30 (multiple peaks), 24, 21, 15, 14. IR (KBr) ν : (dimeric pyrimidin-4-ol tautomer)

3203, 3130, 3012, 2955, 2920, 2849, 2498, 1666, 1610, 1557, 1453, 1318 cm^{-1} . Anal. calcd. for $\text{C}_{22}\text{H}_{41}\text{N}_4\text{O}_2$: C, 67.31; H, 10.27; N, 14.35. Found: C, 67.31; H, 10.41; N, 14.35.

***N*-*t*-Butylaminocarbonyl-6-tridecyl-isocytosine (3d).** A solution of 6-tridecyl-isocytosine, **2b**, (0.56 g, 2 mmol), and *t*-butyl isocyanate (0.3 mL, 2.6 mmol) in dry pyridine (10 mL) was boiled under reflux for 2 h. After cooling, the suspension was diluted with acetone. The precipitated powder was filtered off and recrystallized from acetone to give pure **3d** as white needles (0.55 g, 70%), mp 117.3–117.9°C (recrystallization via liquid at 113–116°C). $^1\text{H-NMR}$ (CDCl_3) δ : 13.22 (s, 1H), 11.72 (s, 1H), 9.57 (s, 1H), 5.81 (s, 1H), 2.45 (t, 2H), 1.63 (m, 2H), 1.42 and 1.31 (m, 29H), 0.88 (t, 3H). Furthermore: 3.5% of pyrimidin-4-ol tautomer: 13.5 (s, 1H), 11.0 (s, 1H), 10.0 (s, 1H), 6.1 (s, 1H), 2.6 (m, 2H), other peaks obscured by peaks of main tautomer. $^{13}\text{C-NMR}$ (CDCl_3) δ : 173.0, 155.9, 155.0, 152.1, 105.7, 51.2, 32.6, 31.7, 29.6, 29.6, 29.4 (multiple peaks), 29.3, 29.2, 29.0, 28.8, 26.9, 22.7, 14.1. IR (KBr) ν : (dimeric pyrimidin-4-ol tautomer) 3224, 3133, 2922, 2850, 2490, 1664, 1612, 1560, 1458, 1330 cm^{-1} . Anal. calcd. for $\text{C}_{22}\text{H}_{41}\text{N}_4\text{O}_2$: C, 67.31; H, 10.27; N, 14.35. Found: C, 67.57; H, 10.36; N, 14.30.

***N*-Phenylaminocarbonyl-6-tridecyl-isocytosine (3e).** A solution of 6-tridecylisocytosine, **2b**, (2.93 g, 10 mmol) and phenyl isocyanate (2.1 mL, 18 mmol) in dry pyridine (50 mL) was boiled under reflux for 2 h. After cooling, the suspension was diluted with acetone and the resulting powder was filtered. Crystallization from acetone/chloroform 2:1 v/v afforded analytically pure **3e** (1.25 g, 30%) as a white microcrystalline powder, mp 155–156°C. $^1\text{H-NMR}$ (CDCl_3) δ : 13.0 (s, 1H), 12.21 (s, 1H), 12.19 (s, 1H), 7.70 (d, 2H), 7.34 (t, 2H), 7.09 (t, 1H), 5.83 (s, 1H), 2.30 (t, 2H), 1.53 (m, 2H), 1.26 (m, br, 20 H), 0.88 (t, 3H). $^{13}\text{C-NMR}$ (CDCl_3) δ : 173.0, 154.6, 152.8, 142.0, 138.2, 128.9, 123.9, 120.6, 106.0, 32.5, 32.0, 29.6, 29.6, (multiple peaks), 29.4, 29.4, 29.2, 28.8, 26.6, 22.7, 14.1. IR (KBr) ν : (dimeric 4[1H]-pyrimidinone tautomer) 3133, 3022, 2910, 2850, 1701, 1660, 1580, 1500 cm^{-1} . Anal. calcd. for $\text{C}_{24}\text{H}_{36}\text{N}_4\text{O}_2$: C, 69.87; H, 8.79; N, 13.58. Found: C, 69.97; H, 8.99; N, 13.49.

***N*-(*p*-Nitrophenyl)aminocarbonyl-6-tridecyl-isocytosine (3f).** A solution of 6-tridecyl-isocytosine **2b**, (0.44 g, 1.5 mmol) and *p*-nitrophenyl isocyanate (0.27 g, 1.6 mmol) in dry pyridine (20 mL) was boiled under reflux overnight. The resultant suspension was evaporated to dryness, and the yellow powder extracted with hot toluene. Crystallization of the residue from acetic acid afforded analytically pure **3f**, mp 234.5–237.5°C. $^1\text{H-NMR}$ (CDCl_3 , 55°C, saturated) δ : 12.83 (s, 1H), 12.7 (s, br, 1H), 12.36 (s, br, 1H), 8.20 (d, 2H), 7.94 (d, 2H), 5.99 (s, 1H), 2.56 (t, 2H), 1.71 (s, 2H), 1.27 (s, br, 20 H), 0.88 (t, 3H). $^{13}\text{C-NMR}$ could not be measured: solubility too low in CDCl_3 even at 55°C, solubility too low in $\text{DMSO}-d_6$ at ambient temperatures, and total decomposition upon heating of sample to 110°C. IR (KBr) ν : (dimeric 4[1H]-pyrimidinone tautomer) 3067, 2920, 2850, 2750, 1712, 1656, 1625, 1574, 1511, 1500, 1334, 1240 cm^{-1} . Anal. calcd. for $\text{C}_{24}\text{H}_{35}\text{N}_5\text{O}_4$: C, 63.00; H, 7.71; N, 15.31. Found: C, 62.65; H, 7.63; N, 15.49.

***N*-(*p*-*N,N*-Diethylaminophenyl)aminocarbonyl-6-tridecyl-isocytosine (3g).** A solution of 6-tridecylisocytosine **2b**, (2.93 g, 10 mmol) and *p*-*N,N*-diethylaminophenyl isocyanate⁴² (3.0 g, 15 mmol) in dry pyridine (20 mL) was boiled under reflux for 4 h. After cooling, water was added, resulting in precipitation of a brown gum. This was crystallized subsequently from acetone/water/ethanol 20:10:1 v/v/v with treatment with active charcoal, and from acetone/ethanol 1:1 v/v to give analytically pure **3g** (1.04 g, 22%), mp 76–90 °C (dec). $^1\text{H-NMR}$ (CDCl_3) δ : 13.09 (s, 1H), 12.12 (s, 1H), 11.97 (s, 1H), 7.49 (d, 2H), 6.67 (d, 2H), 5.75 (s, 1H), 3.32 (m, 4H), 2.19 (m, 2H), 1.48 (m, 2H), 1.24 (m, br, 20 H), 1.14 (tr, 3H), 0.88 (t, 3H). $^{13}\text{C-NMR}$ (CDCl_3) δ : 173.0, 154.6, 152.5, 144.8, 126.8, 122.5, 112.7, 105.6, 44.6, 32.3, 31.7, 29.6–29.2 (multiple peaks), 28.7, 26.5, 22.6, 14.1, 12.5. IR (KBr) ν : (dimeric 4[1H]-pyrimidinone tautomer) 3128, 3030, 2923, 2851, 1698, 1663, 1616, 1587, 1512, 1326, 1243 cm^{-1} . Anal. calcd. for $\text{C}_{28}\text{H}_{45}\text{N}_5\text{O}_2$: C, 69.53; H, 9.38; N, 14.48. Found: C, 69.99; H, 9.56; N, 14.33.

6-Phenyl-isocytosine (2c). A mixture of ethyl benzoylacetate 1c (19.2 g, 0.10 mol) and guanidinium carbonate (9.09 g, 50 mmol) in absolute ethanol (100 mL) was refluxed overnight. After cooling, the precipitated white powder was filtered off, and washed thoroughly with ethanol, water and acetone. Drying gave pure 2c (12.02 g, 64%), mp 312°C. $^1\text{H-NMR}$ (DMSO- d_6 , 90°C) δ : 10.84 (br, 1H), 7.9 (m, 2H), 7.43 (m, 3H), 6.62 (br, 2H), 6.11 (s, 1H). $^{13}\text{C-NMR}$ (DMSO- d_6 , 90°C) δ : 162.8, 162.2, 155.2, 137.1, 128.9, 127.4, 125.9, 97.4. IR (KBr) ν : 3350, 3087, 2956, 1658, 1502, 1476, 1380 cm^{-1} . Anal. calcd. for $\text{C}_{10}\text{H}_9\text{N}_3\text{O}$: C, 64.16; H, 4.85; N, 22.45. Found: C, 64.05; H, 4.85; N, 22.52.

2-Butylaminocarbonyl-6-phenyl-isocytosine (3h). A suspension of 6-phenyl-isocytosine 2c (1.93 g, 10 mmol) and butyl isocyanate (1.7 mL, 15 mmol) in dry pyridine (40 mL) was boiled under reflux for 4 h. After cooling, acetone was added, and the precipitated white powder was filtered off. Crystallization from ethanol/chloroform 1:1 v/v gave analytically pure 3h (2.34 g, 82%), mp 245°C (pyrimidin-4-ol tautomer). $^1\text{H-NMR}$ (CDCl_3) δ : 13.92 (s, 1H), 12.04 (s, 1H), 10.21 (s, 1H), 7.67 (m, 2H), 7.54 (m, 3H), 6.35 (s, 1H), 3.30 (m, 2H), 1.65 (q, 2H), 1.42 (q, 2H), 0.88 (t, 3H); 14% of pyrimidin-4-ol tautomer at 13.6 (2, 1H), 11.3 (s, 1H), 10.0 (s, 1H), 6.7 (m, 2H), 3.5–3.4 (m, 2H), other peaks obscured by those of main tautomer. $^{13}\text{C-NMR}$ (CDCl_3) δ : 173.2, 157.0, 155.4, 148.8, 131.4, 129.6, 125.8, 104.4, 40.0, 31.6, 20.2, 13.9; pyrimidin-4-ol tautomer at 157.0, 137.0, 130.7, 128.9, 126.9, 39.9, 31.8, other peaks obscured by main tautomer. By crystallization from chloroform, plates and needles could be obtained, both as X-ray quality crystals, mp of both tautomers is at 245°C. The needles of the 4[1H]-pyrimidinone tautomer lose chloroform upon heating, and recrystallize. IR of plates (KBr) ν : (dimeric pyrimidin-4-ol tautomer) 3208, 3134, 3025, 2955, 2930, 2870, 2502, 1657, 1612, 1556, 1441, 1328 cm^{-1} . IR of needles (KBr) ν : (dimeric 4[1H]-pyrimidinone tautomer) 3202, 3133, 3010, 2958, 2871, 1692, 1656, 1588, 1528, 1255 cm^{-1} . Anal. (pyrimidin-4-ol tautomer): calcd. for $\text{C}_{15}\text{H}_{18}\text{N}_4\text{O}_2$: C, 62.92; H, 6.34; N, 19.57. Found: C, 63.10; H, 6.41; N, 19.34.

N-*t*-Butylaminocarbonyl-6-phenyl-isocytosine (3i). A suspension of 6-phenylisocytosine 2c (0.98 g, 5 mmol) and *t*-butyl isocyanate (0.86 mL, 7.5 mmol) in dry pyridine (20 mL) was boiled under reflux for 2 h. After cooling, acetone was added. The white crystals were filtered off, washed with acetone, and dried (1.14 g, 80%), mp 259°C (decomposes); sublimation to liquid between 243–259°C. $^1\text{H-NMR}$ (CDCl_3) δ : (equimolar ratio of pyrimidin-4-ol and 4[1H]-pyrimidinone tautomer) 14.03 (br, 0.5H), 13.79 (s, 0.5H), 11.90 (s, 0.5 H) and 11.12 (s, 0.5 H), 10.02 (s, 0.5 H) and 9.60 (br, 0.5H), 7.90 (1H), 7.67 (1H), 7.54 and 7.49 (3H), 6.70 (br, 0.5H), 6.36 (s, 0.5H), 1.47 (s, 9H). $^{13}\text{C-NMR}$ (CDCl_3) δ : 158, 148.6, 136.8, 131.4, 130.7, 129.6, 128.7, 126.9, 125.7, 104.4, 98, 51.4, 51.1, 29.1, 29.8. IR (KBr) ν : (dimeric pyrimidin-4-ol tautomer) 3214, 3138, 3030, 2974, 2502, 1658, 1609, 1560 cm^{-1} . Anal. calcd. for $\text{C}_{15}\text{H}_{18}\text{N}_4\text{O}_2$: C, 62.92; H, 6.34; N, 19.57. Found: C, 63.40; H, 6.46; N, 19.67.

6-*p*-Nitrophenyl-isocytosine (2d). A mixture of ethyl *p*-nitrobenzoyl-acetoacetate, 1d, (11.86 g, 50 mmol) and guanidinium carbonate (4.86 g, 27 mmol) in absolute ethanol (50 mL) was heated under reflux overnight. After cooling, the dark yellow powder was filtered off, and washed thoroughly with acetone, water and ethanol. The dark yellow-brown powder was triturated at reflux temperature with water/ethanol 1:1 v/v (1 L) resulting in partial solution; subsequent cooling afforded yellow microneedles. This procedure was repeated twice, then the nice yellow microneedles in suspension were decanted and filtered from a brown residue sticking on the bottom of the flask. Drying the needles gave pure 2d (3.49 g, 30%), mp > 300°C (dec). $^1\text{H-NMR}$ (DMSO- d_6) δ : 11.05 (s, 1H), 8.28 (d, 2H), 8.21 (d, 2H), 6.78 (br, 2H), 6.30 (s, 1H). $^{13}\text{C-NMR}$ (DMSO- d_6) δ : 163.3, 161.0, 156.0, 148.1, 143.5, 127.9, 123.5, 99.6. IR (KBr) ν : 3440, 3286, 3167, 3116, 2966, 1662, 1611, 1544, 1345 cm^{-1} . Anal. calcd. for $\text{C}_{10}\text{H}_8\text{N}_4\text{O}_3$: C, 51.60; H, 3.71; N, 24.07. Found: C, 51.33; H, 3.91; N, 24.44.

N-Butylaminocarbonyl-6-*p*-nitrophenyl-isocytosine (3j). A suspension of 6-*p*-nitrophenyl-isocytosine 2d, (1.16 g, 5 mmol) and butyl isocyanate (3 mL, 15 mmol) in dry pyridine (15 mL) was

boiled under reflux for 4 h. After cooling, the suspension was filtered, and the residue washed thoroughly with acetone, water, then again acetone. $^1\text{H-NMR}$ ($\text{DMSO-}d_6$, 110°C , with partial decomposition < 20%) δ : 10.5 (very br, 2H), 8.24 (d, 2H), 8.14 (d, 2H), 7.21 (br, 1H), 6.53 (s, 1H), 3.20 (q, 2H), 1.50 (m, 2H), 1.36 (m, 2H), 0.92 (tr, 3H). $^{13}\text{C-NMR}$ ($\text{DMSO-}d_6$, 110°C) δ : 160.9, 158.8, 154.0, 151.6, 148.2, 142.1, 127.3, 122.9, 103.5, 38.4, 30.6, 18.7, 12.6. Insoluble in CDCl_3 .

***N*-Octadecylaminocarbonyl-6-*p*-nitrophenyl-isocytosine (3k).** A suspension of 6-*p*-nitrophenyl-isocytosine **2d**, (0.92 g, 4 mmol) and octadecyl isocyanate (2.36 g, 8 mmol) in dry pyridine (15 mL) was boiled under reflux for 4 h. After cooling, acetone was added. The powder was filtered off (2.16 g, 105%). Analytical sample was prepared by trituration with hot acetic acid, mp $271\text{--}283^\circ\text{C}$ (dec). $^1\text{H-NMR}$ (CDCl_3 , 60°C , low solubility): 4[1H]-pyrimidinone tautomer 40%: 14.35, 12.10, 10.10, 8.4, 8.05 (d), 6.44; pyrimidin-4-ol tautomer 60%: 13.93, 11.32, 9.74, 8.40, 6.80. Peaks coinciding for both tautomers at: 3.5, 3.3, and 3.1 (m), 1.7–1.0 (alkyl), 0.9 (CH_3). $^1\text{H-NMR}$ ($\text{DMSO-}d_6$, 110°C , partial decomposition < 32%, not given) δ : 10.5 (br, 2H), 8.24 (d, 2H), 8.15 (d, 2H), 7.30 (br, 1H), 6.53 (s, 1H), 3.20 (m, 4H), 1.50 (m, 2H), 1.25 (br, 30H), 0.85 (t, 3H). $^{13}\text{C-NMR}$ ($\text{DMSO-}d_6$, 110°C , partial decomposition < 32%, not given): 161.2, 158.7, 154.0, 151.8, 148.2, 142.2, 127.3, 122.8, 103.5, 30.6, 29.4, 28.7 (multiple peaks), 25.7, 21.2, 12.9. IR (KBr) ν : (dimeric pyrimidin-4-ol) 3228, 3136, 3091, 3024, 2953, 2919, 2849, 2516, 1665, 1618, 1567, 1533, 1456, 1348, 1331 cm^{-1} . Anal. calcd. for $\text{C}_{29}\text{H}_{45}\text{N}_5\text{O}_4$: C, 66.00; H, 8.59; N, 13.27. Found: C, 65.94; H, 8.79; N, 12.81.

6-Trifluoromethyl-isocytosine (2e). A mixture of ethyl trifluoroacetoacetate **1e**, (9.2 g, 50 mmol) and guanidinium carbonate (4.68 g, 26 mmol) in absolute ethanol (50 mL) was heated overnight. After cooling, water (100 mL) was added. The volume of the solution was partially reduced, resulting in precipitation of **2e** (5.63 g, 63%), mp 289°C with sublimation at 220°C to 240°C (other crystals form) and at $280\text{--}289^\circ\text{C}$ (liquid condenses). $^1\text{H-NMR}$ ($\text{DMSO-}d_6$): 9–12 (br, 1H), 6.99 (br, 2H), 5.90 (s, 1H). $^{13}\text{C-NMR}$ ($\text{DMSO-}d_6$): 162.9, 157.2, 153.0 (q), 120.8 (q), 98.5. IR (KBr) ν : 3456, 3330, 3166, 2938, 2767, 1678, 1644, 1496, 1446 cm^{-1} . Anal. calcd. for $\text{C}_5\text{H}_4\text{N}_3\text{OF}_3$: C, 33.53; H, 2.25; N, 23.46. Found: C, 32.05; H, 2.73; N, 24.04.

***N*-Butylaminocarbonyl-6-trifluoromethyl-isocytosine (3l).** A solution of 6-trifluoromethyl-isocytosine, **2e**, (1.79 g, 10 mmol) and butyl isocyanate (1.0 mL, 18 mmol) in dry pyridine (25 mL) was boiled under reflux for 4 h. After cooling, the solution was evaporated to dryness. The resultant powder was crystallized from acetone with treatment with active carbon. Cooling to 0°C resulted in the formation of white crystals (0.74 g, 27%), mp $178.3\text{--}185.5^\circ\text{C}$. Melting and recrystallization in that region occurs too. $^1\text{H-NMR}$ (CDCl_3) δ : 14.30 (s, 1H), 11.14 (s, 1H), 9.30 (s, 1H), 6.64 (s, 1H), 3.38 (m, 2H), 1.58 (m, 2H), 1.43 (m, 2H), 0.97 (t, 3H). $^{13}\text{C-NMR}$ (CDCl_3 , 60°C) δ : 172.6, 157.8, 156.4, 155.5 (q), quartet at (124.4, 121.6, 118.9, 116.2), 100.1, 40.0, 31.3, 19.9, 13.5. $^1\text{H-NMR}$ ($\text{DMSO-}d_6$) δ : 12.17 (s, 1H), 10.46 (s, 1H), 6.93 (s, 1H), 6.39 (s, 1H), 3.14 (q, 2H), 1.44 (m, 2H), 1.29 (m, 2H), 0.89 (t, 3H). $^{13}\text{C-NMR}$ ($\text{DMSO-}d_6$) δ : 160.2 (br), 154.6, 153.4, 152.2 (quartet), 120.7 (quartet), 104.9, 38.8, 31.2, 19.4, 13.5. IR (KBr) ν : (dimeric pyrimidin-4-ol tautomer) 3263, 3150, 3115, 3052, 2969, 2937, 2864, (2594, 2529, 2466, 2398), 1673, 1622, 1563, 1477, 1453, 1340, 1268, 1196, 1143 cm^{-1} . Anal. calcd. for $\text{C}_{10}\text{H}_{13}\text{N}_4\text{O}_2\text{F}_3$: C, 43.17; H, 4.71; N, 20.14. Found: C, 43.54; H, 4.89; N, 20.23.

3,4,5-Tri(dodecyloxy)benzoic acid (5). A suspension of methyl 3,4,5-tri(dodecyloxy)-benzoate, **4**, (38.3 g, 55.6 mmol, see chapter 3), KOH (7.8 g) in ethanol (600 mL) and water (30 mL) was boiled under reflux for 4 h. To the hot solution was cautiously added concentrated hydrochloric acid until acidic. Then the solution was cooled, while more water was added (1L). The white precipitate was filtered, and crystallized from ethanol/*i*-propanol mixture containing a trace of hydrochloric acid, to give analytical pure **5** (33.63 g, 90%), mp $58.3\text{--}59.1^\circ\text{C}$. $^1\text{H-NMR}$ (CDCl_3) δ : 7.33 (s, 2H), 4.03 (m, 6H), 1.82 (m, 4H), 1.74 (m, 2H), 1.5 (m, 6H), 1.3 (m, 48H), 0.88 (m, 9H). $^{13}\text{C-NMR}$ (CDCl_3) δ : 172.70,

153.4, 143.8, 124.2, 109.2, 74.1, 69.8, 32.5, 30.9, 30.3, 30.2, 30.1, 30.0, 29.9 (overlapping peaks), 26.7, 26.6, 23.3, 14.7. IR (KBr) ν : 2920, 2850, 2642, 1684, 1587, 1431, 1334, 1122 cm^{-1} . Anal. calcd. for $\text{C}_{43}\text{H}_{78}\text{O}_5$: C, 76.50; H, 11.65. Found: C, 76.67; H, 11.41.

3,4,5-Tri(dodecyloxy)benzoic acid chloride (6). A suspension of 3,4,5-tri(dodecyloxy)-benzoic acid **5** (27.00 g, 40 mmol) in thionyl chloride (100 mL) was boiled under reflux for 4 h. The solution was evaporated to dryness, and the residue was flushed several times with hexane, leaving a yellow gum. $^1\text{H-NMR}$ (CDCl_3): 7.33 (s, 2H), 4.08 (t, 2H), 4.01 (t, 4H), 1.9–1.7 (m, 6H), 1.5 (m, 6H), 1.3 (br, m, 48H), 0.88 (t, 9H). $^{13}\text{C-NMR}$ (CDCl_3) δ : 168.2, 153.4, 145.4, 127.8, 110.6, 74.3, 69.9, 32.5, 30.9, 30.3–29.9 (multiple overlapping peaks), 29.8, 26.6, 26.5, 23.3, 14.7.

Methyl 3,4,5-tri(dodecyloxy)benzoylacetate (8). To a solution of ethyl acetoacetate (10.93 g, 84 mmol) in dry ether (68 mL) was added a solution of sodium ethoxide (80.8 mmol) in absolute ethanol (prepared by dissolving 1.87 g sodium in 40 mL absolute ethanol), whilst the temperature was maintained below 5°C by cooling with an ice-bath. At the same temperature, crude acid chloride **6** (~40 mmol) in dry ether (100 mL) was added dropwise. The resulting thick suspension was stirred overnight at rt. The suspension was poured into dilute sulfuric acid, and dichloromethane was added. The layers were separated, and the aqueous layer was extracted with dichloromethane. Further work-up of the combined organic phases included washing with a diluted sodium hydrogen carbonate solution (twice), diluted hydrochloric acid (twice), and water (three times), drying over sodium sulfate, filtration, and evaporation to dryness. The resulting white solid (crude **7**) was dissolved in dry toluene (20 mL), and a solution of sodium (60 mmol) in dry methanol (prepared by dissolving 1.40 g sodium in 70 mL methanol) was added slowly. The suspension was stirred for several hours, afterwards heated to reflux gently to achieve complete dissolution, and then stirred overnight at rt. The solution was poured into ice-cold dilute sulfuric acid, and the aqueous phase was extracted with ether/hexane. The combined organic phases were consecutively extracted with dilute hydrochloric acid (twice), sodium hydrogen carbonate solution (twice), and finally with water (three times). The organic phase was dried over sodium sulfate, filtered, and evaporated to dryness. Thin layer chromatography (hexane/ethyl acetate 4:1 v/v) showed that the product **8** (R_f = 0.2) contained as a minor contamination methyl 3,4,5-tri(dodecyloxy)benzoate **4** (R_f = 0.36). This minor impurity was mostly removed by two recrystallizations from *i*-propanol (20.58 g, 70%, purity > 98%); the quality of this product is sufficient for further synthesis. An analytical sample was prepared after column chromatography with hexane/ethyl acetate 5:1 v/v, by crystallization from *i*-propanol, mp at 46°C (isotropisation) with LC in the region 41–46 °C. $^1\text{H-NMR}$ (CDCl_3): 7.17 (s, 2H), 4.03 (m, 6H), 3.75 (s, 3H), 1.8–1.7 (m, 6H), 1.47 (m, 6H), 1.28 (m, 48H), 0.88 (t, 9H). $^{13}\text{C-NMR}$ (CDCl_3) δ : 191.0, 167.9, 152.9, 143.4, 130.7, 107.2, 73.5, 69.2, 69.1, 52.3, 45.6, 31.8, 30.3, 29.6–29.2 (multiple peaks), 26.0, 29.95, 22.6, 14.0. IR (KBr) ν : 2919, 2849, 1744, 1725, 1677, 1583, 1468, 1429, 1341, 1121 cm^{-1} . Anal. calcd. for $\text{C}_{46}\text{H}_{80}\text{O}_8$: C, 75.78; H, 11.06. Found: C, 75.63; H, 10.91.

6-[3,4,5-Tri(dodecyloxy)phenyl]-isocytosine (9). A solution of methyl 3,4,5-tri(dodecyloxy)-benzoylacetate, **8**, (5.86 g, 8 mmol), and guanidinium carbonate (0.87 g, 0.0048 mol) in absolute ethanol (30 mL) was boiled under reflux overnight. The solution was evaporated to dryness, and the residue dissolved in dichloromethane (300 mL). The solution was extracted with water several times, and dried over sodium sulfate. Ethanol was added (200 mL), and the solution boiled and treated with active carbon, and filtered. Slow addition of water to the colourless filtrate, and slow reduction of the volume by rotary evaporation resulted in the precipitation of pure **9** (3.2 g, 54%), isotropisation 130°C. $^1\text{H-NMR}$ (CDCl_3): 12.35 (br, 1H), 7.11 (s, 2H), 6.16 (s, 1H), 5.88 (br, 2H), 4.01 (s, 6H), 1.8–1.7 (m, 6H), 1.48 (m, 6H), 1.26 (m, br, 48H), 0.88 (t, 9H). $^{13}\text{C-NMR}$ (CDCl_3) δ : 159.8, 154.0, 153.8, 151.4, 142.7, 123.6, 105.8, 100.4, 73.7, 70.0, 31.9, 30.5, 29.7–29.5 (multiple peaks), 29.3, 26.2, 26.1, 22.6,

13.9 ppm. IR (KBr) ν : 3155, 2922, 2851, 1654, 1467, 1119 cm^{-1} . Anal. calcd. for $\text{C}_{46}\text{H}_{80}\text{N}_3\text{O}_4$: C, 74.75; H, 10.91; N, 5.68. Found: C, 74.67; H, 10.91; N, 5.73.

***N*-Butylaminocarbonyl-6-[3,4,5-tri(dodecyloxy)phenyl]-isocytosine (10a).** A solution of 6-[3,4,5-tri(dodecyloxy)phenyl]-isocytosine (9). (1.70 g, 2.3 mmol), and butyl isocyanate (0.73 mL, 6.5 mmol) in dry pyridine (20 mL) was boiled for 3 h. The solution was evaporated to dryness, and the residue co-distilled with toluene. The resulting dark yellow gum was dissolved in hot hexane. This solution was treated with sodium dihydrogen phosphate with a few drops of water. The solution was dried over sodium sulfate and treated with active carbon, then filtered through celite. Evaporation gave a yellow gum, which was dissolved in hot dichloromethane/acetone 1:1 v/v. Cooling and slow evaporation in air resulted in the precipitation of white microneedles (1.09 g, 56%), mp 131°C (clearing temperature), LC in the range 45–131°C. ^1H -NMR (CDCl_3) δ : 4[1H]-pyrimidinone tautomer) 13.9, (s, 1H), 12.04 (s, 1H), 10.19 (s, 1H), 6.82 (s, 2H), 6.25 (s, 1H), 4.02 (m, 6H), 3.29 (m, 2H), 1.84 (m, 6H), 1.75 (m, 2H), 1.63 (m, 2H), 1.42 (m, 6H), 1.27 (m, br, 48H), 0.94 (m, 3H), 0.88 (m, 9H). Furthermore, 13% pyrimidin-4-ol tautomer at: 13.62 (s, 1H), 11.38 (s, 1H), 10.00 (s, 1H), 7.05 (s, 2H), 6.62 (s, 1H), 3.42 (m, br, 2H), rest of peaks overlap with peaks of main tautomer. ^{13}C -NMR (CDCl_3) δ : (4[1H]-pyrimidinone tautomer) 173.3, 156.7, 155.0, 153.8, 149.1, 140.9, 125.9, 104.1, 103.6, 73.6, 69.3, 39.8, 31.9, 31.5, 30.3, 29.7–29.2 (multiple peaks), 26.0, 22.7, 20.2, 14.1, 13.8. IR (KBr) ν : 3226, 3132, 3020, 2952, 2920, 2850, 1694, 1639, 1608, 1336, 1121 cm^{-1} . Anal. calcd. for $\text{C}_{51}\text{H}_{90}\text{N}_4\text{O}_5$: C, 72.99; H, 10.81; N, 6.68. Found: C, 73.19; H, 11.12; N, 6.94.

A concentrated solution in THF- d_6 , contains approximately 69% pyrimidin-4-ol tautomer. In toluene- d_8 at all measured concentrations, 44% pyrimidin-4-ol is present. ^{13}C -NMR (THF- d_6) δ : aromatic part of 4[1H]-pyrimidinone set: 173.3, 157.7, 155.9, 154.7, 148.7, 141.9, 126.6, 104.6, 103.8; aromatic part of pyrimidin-4-ol set: 172.9 (br), 164.9, 158.5 (br), 157.8, 154.3, 142.0, 132.1, 106.4, 98.2 (br). ^{13}C -NMR (toluene- d_8) δ : aromatic part of 4[1H]-pyrimidinone set: 173.1, 157.5, 155.6, 154.4, 148.5, 141.6, 126.4, 104.2, 103.7; aromatic part of pyrimidin-4-ol set: 172.7, 164.7, 158.2, 157.8, 154.1, 141.8, 132.1, 106.1, 98.0.

***N*-(Phenylaminocarbonyl)-6-[3,4,5-tri(dodecyloxy)phenyl]-isocytosine (10b).** A solution of 6-[3,4,5-tri(dodecyloxy)phenyl]-isocytosine, 9, (0.37 g, 0.50 mmol), and phenyl isocyanate (0.22 mL, 2.0 mmol) in dry pyridine (5 mL) was boiled for 3 h. The solution was cooled to rt, acetone was added, and the white precipitated powder was filtered off. Crystallization from ethanol gave analytically pure 10b as a white powder (0.03 g, 7%), mp 95–105°C (turning liquid crystalline), isotropization in the range 235–240°C. ^1H -NMR (CDCl_3) δ : (4[1H]-pyrimidinone tautomer) 13.77 (s, 1H), 12.39 (s, 1H), 12.24 (s, 1H), 7.72 (d, 2H), 7.28 (d, 2H), 7.06 (t, 1H), 6.60 (s, 2H), 6.32 (s, 1H), 4.0 (m, 6H), 1.84 (m, 4H), 1.73 (m, 2H), 1.47 (m, 6H), 1.26 (m, 48H), 1.15 (t, 4H), 0.88 (t, 9H). Furthermore, 7% of pyrimidin-4-ol tautomer: 13.25 (s, 1H), 12.40 (s, 1H), 11.49 (s, 1H), 7.55 (br, 2H), 6.66 (s, 1H), rest of peaks overlap with peaks of main tautomer. ^{13}C -NMR (CDCl_3) δ : (only 4[1H]-pyrimidinone tautomer given) 173.2, 154.9, 154.7, 153.8, 149.1, 141.1, 138.2, 128.7, 125.5, 123.7, 120.4, 104.0, 103.8, 73.6, 69.3, 31.9, 30.3, 29.8–29.3 (multiple peaks), 26.1, 22.7, 14.1. IR (KBr) ν : 3205, 3128, 3060, 2919, 2050, 1691, 1646, 1590, 1567, 1499, 1329, 1258, 1120 cm^{-1} . Anal. calcd. for $\text{C}_{53}\text{H}_{86}\text{N}_4\text{O}_5$: C, 74.08; H, 10.09; N, 6.52. Found: C, 72.85; H, 10.09; N, 6.18.

***N*-(*p*-Nitrophenylaminocarbonyl)-6-[3,4,5-tri(dodecyloxy)phenyl]-isocytosine (10c).** A solution of 6-[3,4,5-tri(dodecyloxy)phenyl]-isocytosine (9). (0.37 g, 0.50 mmol), and *p*-nitrophenyl isocyanate (0.16 g, 1.0 mmol) in dry pyridine (5 mL) was heated under reflux for 3 h. After cooling, acetone was added. The resultant white powder was filtered, and dissolved in hot chloroform/acetone 1:1 v/v. The solution was treated with active charcoal and filtered hot. Cooling caused pure 10c to precipitate as a white powder, which was filtered off and dried (0.23 g, 51%), mp 132°C (turning liquid

crystalline), phase change at 159°C, isotropisation with decomposition at 261°C. $^1\text{H-NMR}$ (CDCl_3): 4[1H]-pyrimidinone tautomer) 13.51 (s, 1H), 12.85 (s, 1H), 12.46 (s, 1H), 8.09 (d, 2H), 7.88 (d, 2H), 6.74 (d, 2H), 6.29 (s, 1H), 4.00 (m, 6H), 1.83 (m, 4H), 1.78 (m, 2H), 1.49 (m, 6H), 1.27 (m, br, 48H), 0.88 (t, 9H). $^{13}\text{C-NMR}$ (CDCl_3 , 50°C) δ : 172.9, 154.9, 154.5, 154.1, 149.1, 144.5, 143.4, 142.4, 124.5, 124.3, 119.4, 104.3, 103.4, 73.8, 69.8, 32.0, 30.5, 29.8–29.4 (multiple peaks), 26.2, 26.2, 22.7, 14.0. IR (KBr) ν : 3052, 2955, 2920, 2849, 1701, 1649, 1629, 1582, 1567, 1512, 1498, 1332, 1264, 1226 cm^{-1} . 1 . Anal. calcd. for $\text{C}_{53}\text{H}_{85}\text{N}_5\text{O}_7$: C, 70.40; H, 9.47; N, 7.74. Found: C, 70.51; H, 9.50; N, 7.72.

***N*-(*p*-*N,N*-Diethylaminophenylaminocarbonyl)-6-[3,4,5-tri(dodecyloxy)phenyl]-**

isocytosine (10d). A solution of 6-[3,4,5-tri(dodecyloxy)phenyl]-isocytosine (9). (0.37 g, 0.50 mmol), and *p*-*N,N*-diethylaminophenyl isocyanate (0.19 g, 1.0 mmol) in dry pyridine (5 mL) was boiled for 3 h. After cooling the solution to rt, acetone was added. The resulting white powder was filtered off, and dissolved in a hot dichloromethane/acetone mixture. Slow evaporation of the solution resulted in the precipitation of **10d** as a creamy-white powder (0.28 g, 60%), mp 134.5–135°C (isotropisation), LC in the range 110–135°C. $^1\text{H-NMR}$ (CDCl_3) δ : (4[1H]-pyrimidinone tautomer) 13.83 (s, 1H), 12.34 (s, 1H), 11.91 (s, 1H), 7.51 (d, 2H), 6.84 (s, 2H), 6.68 (d, 2H), 6.33 (s, 1H), 4.0 (m, 6H), 3.33 (dd, 4H), 1.84 (m, 4H), 1.73 (m, 2H), 1.47 (m, 6H), 1.26 (m, 48 H), 1.15 (t, 4H), 0.88 (t, 9H). Furthermore, 15% of pyrimidin-4-ol tautomer: 13.45 (s, 1H), 12.04 (s, 1H), 11.49 (s, 1H), 7.38 (d, 2H), 7.13 (s, 2H), 6.65 (s, 1H), rest of peaks overlap with peaks of main tautomer. $^{13}\text{C-NMR}$ (CDCl_3) δ : (set of 4[1H]-pyrimidinone tautomer given only) 173.3, 155.0, 154.6, 153.8, 153.5, 149.1, 144.9, 141.0, 126.8, 125.9, 122.4, 112.7, 112.3, 105.4, 104.1, 103.8, 73.6, 69.3, 44.6, 44.5, 31.9, 30.4, 30.3, 29.7–29.2 (multiple peaks), 26.1, 26.0, 22.7, 14.1, 12.5. IR (KBr) ν : 3215, 3128, 2923, 2852, 2500, 1691, 1643, 1606, 1514, 1332, 1257, 1229, 1118 cm^{-1} . Anal. calcd. for $\text{C}_{57}\text{H}_{95}\text{N}_5\text{O}_5$: C, 73.58; H, 10.29; N, 7.53. Found: C, 73.91; H, 10.39; N, 7.54.

References and Footnotes

- 1) For a review with many examples of hydrogen bonded self-assembling complexes, see: D.S. Lawrence, T. Jiang, M. Levitt, *Chem. Rev.*, **1995**, *95*, 2229.
- 2) (a) A. D. Hamilton, D. van Engen, *J. Am. Chem. Soc.*, **1987**, *109*, 5035, (b) A.D. Hamilton, N. Pant, A.V. Muehldorf, *Pure & Appl. Chem.*, **1988**, *60*, 533, (c) A.D. Hamilton, A. Muehldorf, S.-K. Chang, N. Pant, S. Goswami, D. Van Engen, *J. Incl. Phenom. Molec. Reco. Chem.*, **1989**, *7*, 27, (d) S.-K. Chang, D. Van Engen, E. Fan, A.D. Hamilton, *J. Am. Chem. Soc.*, **1991**, *113*, 7640.
- 3) (a) T.W. Bell, J. Liu, *J. Am. Chem. Soc.*, **1988**, *110*, 3673, (b) S. Goswami, R. Mukherjee, *Tetrahedron Lett.*, **1997**, *38*, 1619, (c) T.W. Bell, Z. Hou, *Angew. Chem. Int. Ed. Engl.*, **1997**, *36*, 1536.
- 4) (a) N. Tamura, T. Kajiki, T. Nabeshima, Y. Yano, *J. Chem. Soc., Chem. Comm.*, **1994**, 2583–2584, (b) N. Tamura, K. Mitsui, T. Nabeshima, Y. Yano, *J. Chem. Soc., Perkin Trans. 2*, **1994**, 2229–2237.
- 5) T.W. Bell, Z. Hou, S.C. Zimmerman, P.A. Thiesen, *Angew. Chem.*, **1995**, *107*, 2321.
- 6) J.S. Lindsey, P.C. Kearney, R.J. Duff, P.J. Tjivikua, J. Rebek Jr., *J. Am. Chem. Soc.*, **1988**, *110*, 6575.
- 7) R. Wyler, J. de Mendoza, J. Rebek Jr., *Angew. Chem.*, **1993**, *105*, 1820.
- 8) M.R. Ghadiri, J.R. Granja, R.A. Milligan, D.E. McRee, N. Khazanovich, *Nature*, **1993**, *366*, 324.

- 9) Other examples of arrays of more than three hydrogen bonds: (a) T.R. Kelly, C. Zhao, G.J. Bridger, *J. Am. Chem. Soc.*, **1989**, *111*, 3744, (b) A.D. Hamilton, D. Little, *J. Chem. Soc., Chem. Comm.*, **1990**, 297, (c) S.C. Hirst, A.D. Hamilton, *Tetrahedron Lett.*, **1990**, *31*, 2401, (d) M.S. Goodman, S.D. Rose, *J. Am. Chem. Soc.*, **1991**, *113*, 9380, (e) S.J. Geib, S.C. Hirst, C. Vicent, A.D. Hamilton, *J. Chem. Soc., Chem. Commun.*, **1991**, 1283.
- 10) Also published as a communication: F.H. Beijer, R.P. Sijbesma, H. Kooijman, A.L. Spek, and E.W. Meijer, *Angew. Chem.*, **1998**, *110*, 79; *Angew. Chem. Int. Ed. Engl.*, **1998**, *37*, 75.
- 11) (a) W.L. Jorgensen, J. Pranata, *J. Am. Chem. Soc.*, **1990**, *112*, 2008, (b) J. Pranata, S. G. Wierschke, W.L. Jorgensen, *J. Am. Chem. Soc.*, **1991**, *113*, 2810.
- 12) J.Sartorius, H.-J. Schneider, *Chem. Eur. J.* **1996**, *2*, 1446.
- 13) The synthesis of several ureidopyrimidinones has been reported: J. Fan, C. C. Cheng, *J. Heterocycl. Chem.* **1993**, *30*, 1273, (b) T. Urbanski, B. Serafin, J. Zylowski, *J. Med. Chem.*, **1967**, *10*, 521, (c) A. Kreutzberger, H. Schimmelpfennig, *Arch. Pharm.*, **1981**, *314*, 34, (d) G. Vasilev, *Dokl. Bolg. Akad. Nauk.* **1990**, *43*, 57.
- 14) (a) *Advances in Heterocyclic Chemistry, the tautomerism of heterocycles*: J. Elguero, C. Marzin, A.R. Katritzky, P. Linda, Academic Press, New York, **1976**, (b) C. Reichardt, *Solvents and Solvent Effects in Organic Chemistry*, 2nd Edn, VCH, Weinheim, **1990**.
- 15) (a) P. Bühlmann, M. Badertscher, W. Simon, *Tetrahedron*, **1993**, *49*, 595, (b) P. Bühlmann, W. Simon, *Tetrahedron*, **1993**, *49*, 7627.
- 16) L.M. Toledo, K. Musa, J.W. Lauher, F.W. Fowler, *Chem. Mater.*, **1995**, *7*, 1639.
- 17) (a) J.S. Kwiatkowski and B. Pullman in *Advances in Heterocyclic Chemistry*, volume 18, Ed. A.R. Katritzky and A.J. Boulton, Academic Press, New York, **1975**, (b) S.G. Stephanian, E.D. Radchenko, G.G. Sheina, Y.P. Blagoi, *J. Mol. Struct.*, **1990**, *216*, 77, (c) G.G. Sheina, S.G. Stephanian, E.D. Radchenko, Y.P. Blagoi, *J. Mol. Struct.*, **1987**, *158*, 275.
- 18) (a) Ref 14, (b) J. Elguero, C. Marzin, A.R. Katritzky, P. Linda, *The tautomerism of heterocycles*, part of: *Advances in Heterocyclic Chemistry*, supplement 1, Academic Press, New York, **1976**.
- 19) As observed in chapters 2 and 3, substituents exert a large influence on dimerization constants. Furthermore, substituent effects may influence the tautomeric equilibria.
- 20) No upfield shift of the N–H signals is observed, nor do any new signals arise.
- 21) M.H. Benn, A.M. Creighton, L.N. Owen, G.R. White, *J. Chem. Soc.*, **1961**, 2365.
- 22) (a) W.H. Perkin, C. Weizmann, *J. Chem. Soc.*, **1906**, *89 II*, 1655, (b) W. Bradley, R. Robinson, *J. Chem. Soc.*, **1928**, 1548, (c) H. Hunsdiecker, *Berichte*, **1942**, *75*, 1190, (d) H.H. Günthard, S.D. Heinemann, V. Prelog, *Helv. Chim. Act.*, **1953**, *36*, 1147.
- 23) G.A. Jeffrey, *An Introduction to Hydrogen Bonding*, Oxford University Press, Oxford, **1997**.
- 24) In IR in chloroform solution, the 4[1H]-tautomer is dominant.
- 25) Existence of **3I** exclusively in the pyrimidin-4-ol tautomeric form is concluded from: (i) the NMR-spectrum has only one set of signals, (ii) its IR-spectrum in chloroform solution features the characteristic O–H \cdots O=C vibration at 2600–2400 cm⁻¹.
- 26) The presence of dimers is concluded from the position of N–H (O–H) resonances in the ¹H-NMR spectrum, which are found at basically the same positions in THF as in CDCl₃.
- 27) Neither a significant shift of the dimer peaks was observed (shifts less than 0.3 ppm), nor the appearance of new signals was observed.
- 28) Every concentration should be read as within the 20 to 80% saturation range, because integration becomes prone to error with exceeding ratios. Because of the sharpness and

intensity of the CH₃-signal of **3a**, integration of that signal is less prone to error, and the 10–90% saturation range gives similar values for the complex dimerization constants.

- 29) The concentration dependence of the N–H signals is indicative for quick exchange of monomers and dimers.
- 30) The main reason for this is the limited number of datapoints measured. However, monomer and dimer shift of H5 do also strongly depend on solvent composition in the CDCl₃/DMSO-*d*₆ mixtures, in sharp contrast to the CDCl₃/MeOH mixtures in chapter 3.
- 31) The equation derived in chapter 3 was used (see below), but the fit is unreliable by lack of convergence, probably because a limited number of datapoints and too many parameters are involved.

$$\log K_{\text{obs}} = \log K_{\text{dim}} - 2 * \log (1 + K_{\text{comp1}} * [\text{S}] + K_{\text{comp2}} * [\text{S}]^2 + K_{\text{comp3}} * [\text{S}]^3 + \dots)$$

- 32) K_{taut} is not a constant in a solvent mixture, but strongly depends on concentration due to the dimerization.
- 33) Comparison with the results in chapter 3 indicates that the relation should deviate in the direction of solvent mixtures with less DMSO than which were measured.
- 34) Tautomerization involves proton shifts, and a conformational change of the ureido substituent.
- 35) Since the resonances of the non-acidic protons also split up, it is concluded that the observed behavior must be ascribed to the formation of heterodimers, and not to exchange of acidic protons.
- 36) A slight preference for the formation of heterodimers is actually observed for mixtures of compounds with a large electronic difference in the substituents, e.g. a nitrophenyl substituent on the one hand, and a butyl or *p*-diethylaminophenyl substituent on the other hand. The largest splitting is also observed in these cases.
- 37) G.A. Jeffrey, W. Saenger, *Hydrogen Bonding in Biological Structures*, Springer, Berlin, 1994.
- 38) J.L. de Boer, A.J.M. Duisenberg, *Acta Crystallogr.*, **1984**, A40, C-410.
- 39) A.L. Spek, *J. Appl. Crystallogr.*, **1988**, 21, 578.
- 40) *International Tables for Crystallography, volume C*, A.J.C. Wilson Ed., Kluwer Academic Publishers, Dordrecht, The Netherlands, 1992.
- 41) A.L. Spek, *Acta Crystallogr.*, **1990**, A46, C-34.
- 42) M.H. Benn, A.M. Creighton, L.N. Owen, G.R. White, *J. Chem. Soc.*, **1961**, 2365.

Chapter 5

Discotic Liquid Crystals from Quadruply Hydrogen Bonded Dimers

Abstract:

A new type of disk-like mesogens has been synthesized. These disk-like mesogens are formed by a quadruply hydrogen bonded dimer, using self-complementary triazine and ureidopyrimidinone units (see chapters 3 and 4), functionalized at the 6-position with a phenyl group with flexible alkoxy chains. The liquid crystalline properties of these materials—studied by polarization microscopy, differential scanning calorimetry, and X-ray diffraction—were compared with those of materials with disk-like mesogens based on complexes of diaminotriazine and uracil.

Whereas the latter triply hydrogen bonded complexes of two different parts display liquid crystalline behavior in temperature ranges of only 30°C, the mesogens formed by dimers of self-complementary quadruple hydrogen bonding units have mesophase temperature ranges of 90–130°C. The mesophases have similar temperature stability for all quadruple hydrogen bonding units applied, of which the binding strength ranges from weak to very strong. The large temperature range of mesogens with quadruply hydrogen bonded dimers in comparison with double or triply hydrogen bonded complexes may be rationalized by assuming that the core is more rigid and better filled.

*As revealed by X-ray diffraction studies, the mesophases of mesogens formed from quadruply hydrogen bonded dimers are discotic and hexagonal, with one dimer as discotic entity. Mono-acetylamino-triazine **1**, however, has two liquid crystalline phases, of which the higher temperature phase is a D_{ho} phase with one dimer in a disk. The X-ray diffraction pattern of the lower temperature phase indicates a sheet-like structure, with infinite chains of dimers formed by dimerization of the triazine dimers via additional hydrogen bonding interactions.*

5.1 Introduction

Since the discovery of the liquid crystalline phase in 1888 by Reinitzer,¹ numerous compounds exhibiting this behavior have been described in literature.² The liquid crystalline state is a meso-phase in between the solid crystal and the isotropic liquid. Hence, it combines characteristics of both, such as anisotropy of the highly ordered crystalline phase, and mobility of the non-ordered liquid phase. The special properties of liquid crystalline materials are used in numerous applications nowadays. The best-known application is in Liquid Crystalline Displays (LCDs), using refractive index anisotropy.

Two classes of liquid crystals can be distinguished: thermotropic and lyotropic. Thermotropic liquid crystalline behavior is present when a single component shows mesomorphic behavior in a certain temperature range, while lyotropic liquid crystalline behavior is present when a compound in solution shows mesomorphic behavior. Thermotropic liquid crystallinity in single organic compounds originates from shape anisotropy in the molecules.³ Two main classes of shape anisotropy of molecules can be distinguished: the molecules may be rod-like (or lath-like), or disk-like. Rod-like molecules have the tendency to order in a parallel fashion (i.e. in the length of the rod). Depending on the degree of order, nematic or smectic phases result. Mesophases resulting from rod-like molecules have been known for more than 100 years.³

Disk-like molecules can give rise to a nematic discotic phase (N_d), in which the only order is parallelity of the normals of the disks (figure 5.1a). Apart from this N_d phase, disk-like molecules can lead to phases in which the molecules are stacked in columns, the so-called columnar mesophases. The disks may have regular or irregular distances (figure 5.1b). The columns may be ordered in several different ways, with a perpendicular or tilted orientation of the column axis and n-director, and different packing (figure 5.1c). Although it had long been realized that mesophases consisting of disk-like molecules should be possible too, the first example was reported only 20 years ago.⁴

The last decades, research of liquid crystalline materials has become a central topic for many research groups at universities and in industry. Consequently, the number of compounds that display liquid crystalline behavior has grown enormously. The use of non-covalent interactions, such as hydrogen bonding⁵ and metal-ion complexation,⁶ has recently been introduced as a powerful tool to facilitate the synthesis of large and rigid central cores. Hydrogen bonding is both used within one molecule (intramolecular), as well as between two or more molecules (intermolecular). Intramolecular hydrogen bonding may be used to obtain large coplanar disks.⁷ Intermolecular hydrogen bonding may be used to assemble the mesogen from two parts in a non-covalent way.

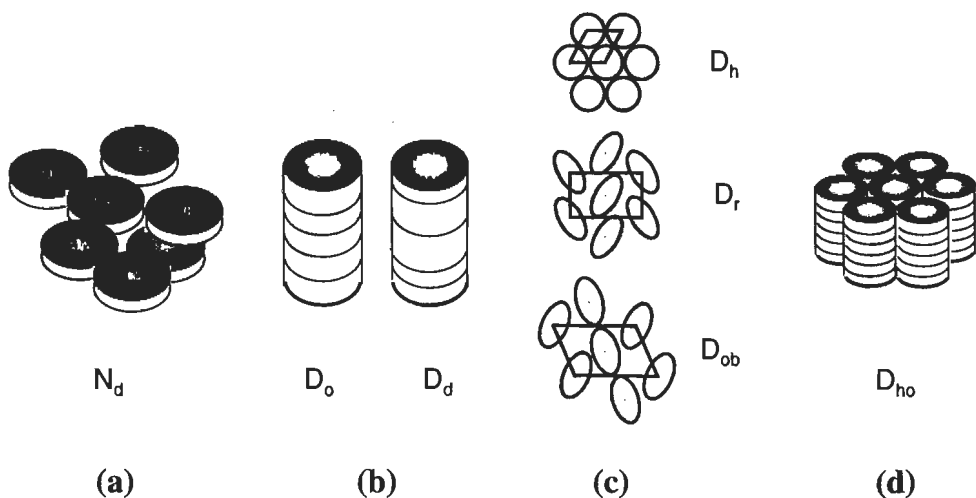


Figure 5.1: Several possible liquid crystalline phases resulting from disk-like molecules:

- (a) In a nematic discotic phase (N_d), the only order is parallelity of the disk-normals.
- (b) Disks can be stacked with a regular distance between the disks (D_o discotic ordered), and with an irregular distance between the discs (D_d discotic disordered).
- (c) The columns of disks can be ordered orthogonally in a hexagonal fashion: D_h , or tilted with several possibilities: D_r : rectangular, D_{ob} : oblique.
- (d) Representation of the D_{ho} phase.

Hydrogen bonding between two different, complementary parts has often been used to form liquid crystals. Lehn showed that 1:1 mixtures of monofunctional molecules with the di(acylamino)pyridine–uracil couple form columnar liquid crystalline phases with hexagonal order (figure 5.2a); the discotic entity contains two complexes.⁸ Furthermore, Lehn has published a thorough study of liquid crystalline materials obtained from equimolar mixtures of bifunctional compounds.⁹ By incorporation of chiral groups, the formation of helical columnar phases was induced. Kato has recently reported on liquid crystals containing the di(acylamino)pyridine–acid combination (figure 5.2b).¹⁰ Many more examples of liquid crystalline materials by hydrogen bonding of two complementary parts, mostly a single hydrogen bond between a pyridine and a carboxylic acid functionality, have been described by Kato and Fréchet,¹¹ and others.¹² Numerous examples of liquid crystalline materials that consist of polymer backbones, functionalized with hydrogen bonding units that are complexed with small molecules, have been reported.¹³

However, only limited use has been made of *self*-complementary units to form discotic phases. Lattermann¹⁴ and Lillya¹⁵ have reported on self-complementary amides forming columnar mesophases (figure 5.2c–d). In these discotic mesophases, the disks are formed by one single dimer. Discotic phases involving carboxyl dimer formation, with two dimers in one disk, have been described by Malthête et al.¹⁶ Lattermann has described the

formation of discotic phases with six *cis*, *cis*-(dihydroxycyclohexyl)-3,4,5-tri(decyloxy)phenyl benzoate molecules in one disk.¹⁷ Generally, the use of hydrogen bonds for construction of the core leads to mesophases with only a limited temperature range.¹⁸

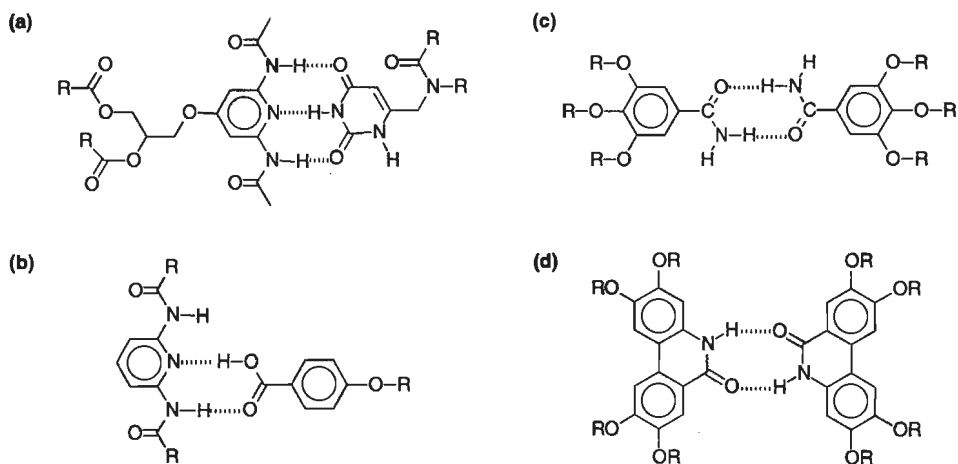


Figure 5.2: (a) the di(acylamino)pyridine-uracil heterocouple used by Lehn.⁸
 (b) the di(acylamino)pyridine-acid heterocouple used by Kato.¹⁰
 (c) self-complementary amide described by Lattermann.¹⁴
 (d) self-complementary amide described by Lillya et al.¹⁵
 R is a long alkyl chain in all cases.

In chapters 3 and 4, we showed several new functional groups capable of dimer formation via self-complementary arrays of four hydrogen bonds, some of which feature very strong bonding. As a result of these investigations, we have modified these hydrogen bonding units with a flexible group, the 3,4,5-tri(dodecyloxy)phenyl group, with the intention to induce liquid crystallinity (see figure 5.3).

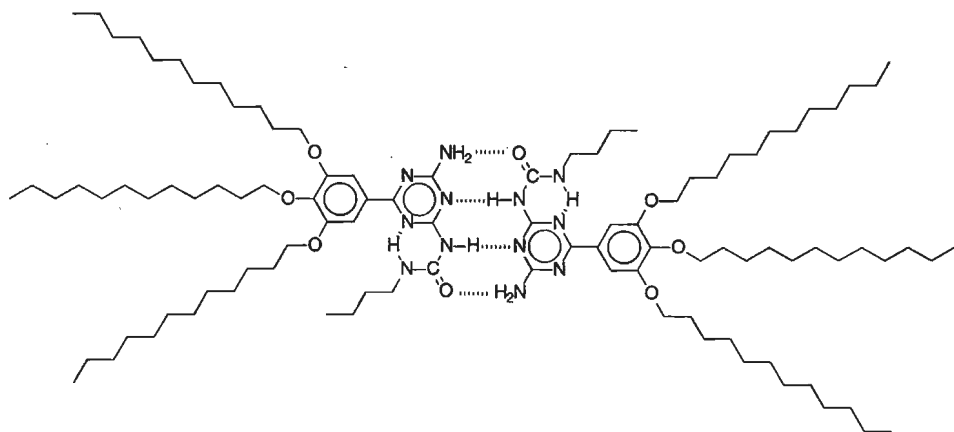


Figure 5.3: Disk-like entity formed by a quadruply hydrogen bonded dimer.

In this chapter, we focus on the thermotropic liquid crystalline behavior of self-complementary compounds **1–4** and **5a–d** (chart 5.1), of which the synthesis has been described in chapters 3 and 4.

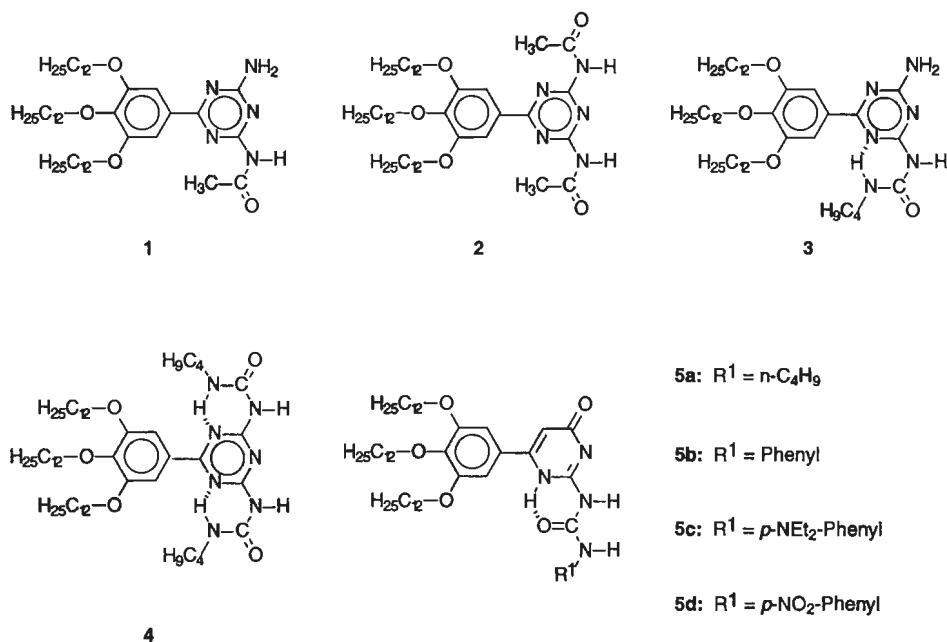


Chart 5.1: Studied derivatives with a self-complementary quadruple hydrogen bonding unit.

To compare the effect of the number of hydrogen bonds on mesophase stability, we have also studied the liquid crystalline properties of complexes with a triply hydrogen bonded core. For that purpose, we have synthesized complexes based on triple hydrogen bonding of the heterocouple diaminotriazine–uracil, with both units substituted with a 3,4,5-tri(dodecyloxy)phenyl group at the 6-position (see chart 5.2). The liquid crystalline properties of most materials were studied by a combination of techniques, such as polarization microscopy, IR, Differential Scanning Calorimetry (DSC) and X-ray diffraction.

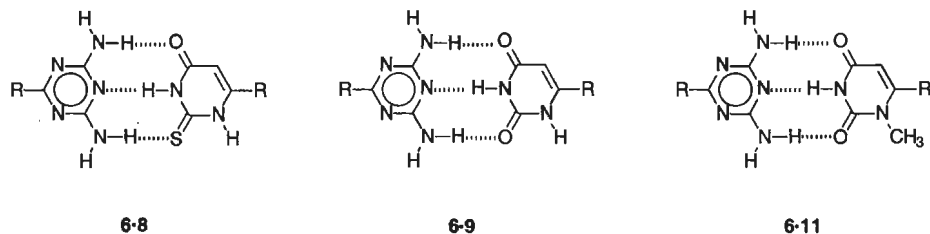


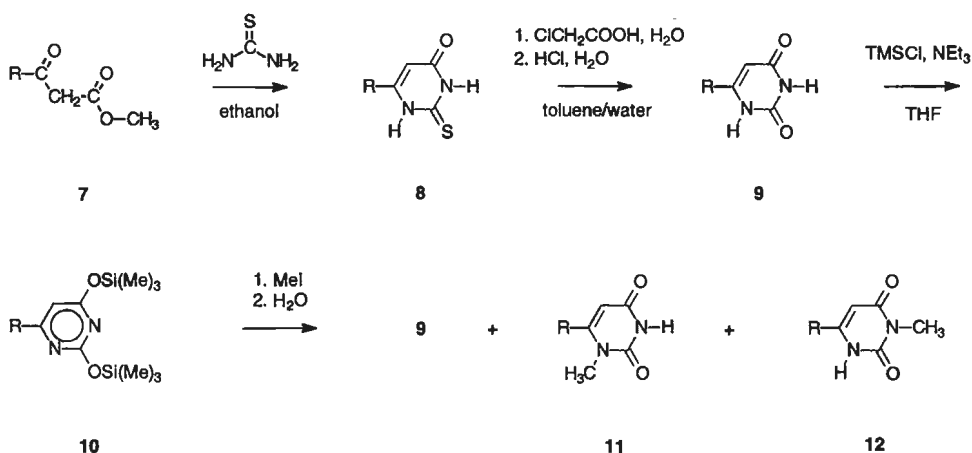
Chart 5.2: Diaminotriazine–uracil hetero-complexes. R is a 3,4,5-tri(dodecyloxy)phenyl group.

5.2 Results

5.2.1 Synthesis

The syntheses of derivatives **1–5d** have been described in chapters 3 and 4, as well as the synthesis of diaminotriazine **6** and keto-ester **7**. Starting from this keto-ester **7**, uracil derivatives **8**, **9**, **11** and **12** were synthesized as depicted in scheme 5.1. Condensation of keto-ester **7** with thiourea gave thiouracil **8**, which was converted to the uracil **9** by acidic hydrolysis after reaction with chloroacetic acid. A two-phase system of water and toluene was used to drive this reaction to completion. Uracil **9** was *N*-1 methylated via the silyl derivative **10**, but in contrast to other uracil molecules described in chapter 2, the conversion to the *N*-1-methylated **11** was low. Only 16% had reacted to the *N*-1-methylated compound after standing for 2 weeks with methyl iodide, while also the *N*-3 methylated compound **12** was formed. The mixture of compounds **9**, **11** and **12** was separated by column chromatography. Since the identity of the fractions was difficult to determine unambiguously based on NMR and IR alone, the identities were ascertained by determination of the association constant of the complex with 2,4-diamino-6-dodecyl-*s*-triazine (see chapter 2). The least polar compound (which was obtained in a yield of only 7%) was identified as the *N*-3-methyl uracil **12**, since the complex of this compound with dodecyl-diaminotriazine had an association constant of only 9 M^{-1} . The second fraction (yield only 16%) was identified as the *N*-1-methyl uracil **11** (K_a of complex with 6-dodecyl-diaminotriazine was 810 M^{-1}).

By co-crystallization from ethanol, 1:1 complexes were obtained of 6-(3,4,5-tri(dodecyloxy)phenyl) substituted diaminotriazine **6** with thiouracil **8**, and with uracils **10** and **11**.



Scheme 5.1: Synthetic route to uracil derivatives used for study; R is a 3,4,5-tri(dodecyloxy)-phenyl group.

5.2.2 Studies of Liquid Crystalline Properties

Polarization Microscopy. The thermotropic properties of compounds **1–4** and **5a–d**, and of the diaminotriazine–uracil complexes **6•8**, **6•9** and **6•11**, were studied with polarization microscopy. Strongly birefringent mesophases were observed for compounds **1–4**, and **5a–d**. The mesophase is present over broad temperature ranges of 90 up to 130°C, and the observed phase transitions were sharp. For these compounds, fan-like textures were obtained upon slowly cooling from the isotropic phase, being typical for D_{ho} phases. The diaminotriazine–uracil complexes feature mesophases with a temperature regime of only approximately 30°C. The liquid crystalline phases appear as viscous fluids, which are slightly birefringent. Upon isotropisation, the viscosity suddenly drops.

IR-spectroscopy. IR-spectra of thin films of the mesophase and melt of compounds **3** and **5a**, taken at elevated temperatures, show only minor differences. The changes do not occur suddenly at melting or isotropisation, but occur gradually (a slight sharpening of peaks is observed, and small changes in intensity). Compound **5a** tautomerizes (partly) to dimers of the pyrimidin-4-ol tautomer upon heating. However, no bands at characteristic positions for free N–H stretch vibrations are observed, even in the isotropic phase, indicating the dimers persist even in the isotropic phase. Similar behavior has been reported for the benzamide derivative with double hydrogen bonding (figure 5.2.c, G. Lattermann, reference 17).

Differential Scanning Calorimetry. DSC-s of compounds **1–4** and **5a** (figure 5.4) feature a large endotherm in the first heating run between 40 and 100°C. This endotherm is ascribed to melting of the crystalline phase to a liquid crystalline mesophase.¹⁹ A second endotherm, with a much smaller enthalpy, is observed between 120 and 200°C. This endotherm corresponds to the transition to the isotropic phase. Crystallization of liquid crystalline samples is generally slow (several hours to a few days); only di(acetylamino)triazine **2** features a quick crystallization in DSC (figure 5.4b).

The thermotropic properties of the studied compounds and complexes are summarized in Table 5.1.

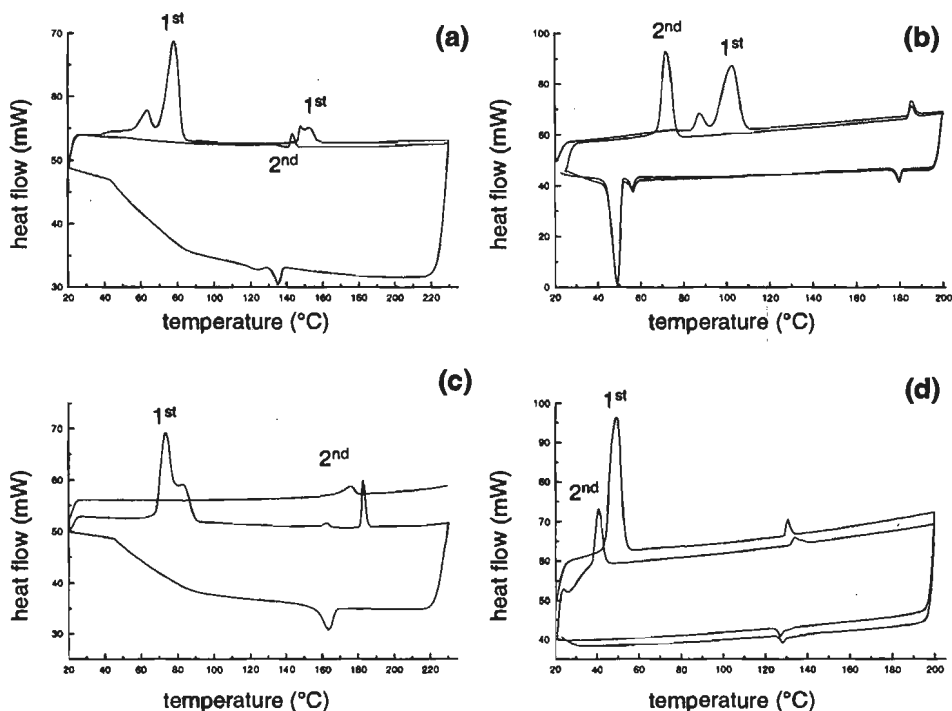


Figure 5.4: First and second heating and cooling run (denoted with 1st and 2nd) in DSC of microcrystalline material of:
 (a) mono(acetyl)diaminotriazine **1**,
 (b) di(acetylamino)triazine **2**,
 (c) mono(butylureido)triazine **3**,
 (d) butylureido-pyrimidinone **5a**.

Mono(acetylamino)triazine **1** has two reversible mesophases (figure 5.4a). The transformation of these two mesophases, at 148°C, occurs very quickly, and was also clearly and repeatedly observed with polarization microscopy. DSCs of monoureidotriazine **3** (figure 5.4c) and di(ureido)triazine **4** feature two transitions in DSC after initial melting of the material and before isotropisation, but only one transition in that region occurs in subsequent runs. This additional transition likely points to the existence a second liquid crystalline phase, which is obtained only in the first heating. However, a clear transition between two mesophases was not observed with polarizing microscopy. The enthalpy of the transition from the crystalline phase to the liquid crystalline phase is much larger than the enthalpy upon isotropization. The values we find are comparable to the systems shown in figure 5.2c and 5.2d, which have melting enthalpies between 40 and 60 J/g, and enthalpies of isotropisation of 2–10 J/g, respectively.

Table 5.1: Thermotropic Properties.^a

Compound	K	T (°C)	ΔH (J/g)	M ₁	T (°C)	ΔH (J/g)	M ₂	T (°C)	ΔH (J/g)	I
1	•	60	80 ^b	•	148	2	•	158	3 ^c	•
2	•	97	50 ^c	-	-	-	•	187	3 ^c	•
3	•	85	117 ^b	• ^d	(162) ^d	(2) ^d	•	183	10 ^c	•
4	•	40	40 ^b	• ^d	(130) ^d	(2) ^d	•	177	2 ^c	•
5a	•	45	50	-	-	-	•	131	2	•
5b	•	95-105	-	-	-	-	•	237	-	•
5c	•	50	-	-	-	-	•	135	-	•
5d	•	131	-	• ^e	(149) ^e	-	•	280 (dec)	-	•
complex 6•8	•	65-70	-	•	105	-	-	-	-	•
complex 6•9	•	95	-	•	115	-	-	-	-	•
complex 6•11	•	82	-	•	105	-	-	-	-	•

• phase observed; ^a Values determined with polarization microscopy; for **1–4** and **5a**, values obtained by DSC are similar to microscopy. The other derivatives, **5b–d** and diaminotriazine-uracil complexes, were studied only with microscopy; ^b First heating run of crystallized sample; only compound **2** crystallized in DSC; ^c Second heating run; ^d Not observed with microscopy, only observed in first heating run with DSC; ^e Transition suspected with microscopy study, observed only in first heating.

X-Ray Diffraction. To elucidate the identity of the mesophases, the mesophases of compounds **1–4** and **5a** were studied by means of X-ray diffraction, focussing in detail on compound **2**. Samples were prepared either by drawing isotropic melts into a glass capillary and cooling back to the liquid crystalline phase, or by shearing the compound between two warm beryllium plates into one direction. Samples were screened to find suitably large monodomains.

At room temperature, a crystallized sample of **2** in a glass capillary features several sharp reflections, characteristic of a highly ordered crystalline phase. The diffraction pattern of a flow-aligned sample of **2** in a glass capillary measured at 137°C, at which temperature **2** is in its mesophase, features a hexagonal arrangement of the small angle reflections at 29.0 Å (see figures 5.5a and b). This pattern is characteristic for a D_{ho} phase, with the X-ray beam in the direction of the column axis. From the small angle reflection, a column distance of 33.5 Å is derived. Superimposed on this diffraction pattern are minor patterns resulting from monodomains with different orientations: one monodomain is also oriented with the X-ray beam parallel with the column axis, but this monodomain is rotated around its length-axis with respect to the first monodomain; another minor monodomain is oriented with the X-ray beam perpendicular to the column axis. The wide angle reflection at 3.7 Å emerges from the monodomain with a perpendicular orientation of the columns and the X-ray beam; this

reflection is assigned to the disk–disk distance. The regular distance of 3.7 Å between the disks indicates this is an ordered phase. The broad reflection at 4.9 Å is assigned to the alkyl halo.

A view perpendicular to the columns of an aligned sample was also obtained for compound **2** (figure 5.5c, measured at 150°C). A sharp reflection is present at 29.0 Å, assigned to the 100 reflection. Weaker reflections with a relative distance to the 100 reflection of $\sqrt{3}$ and $\sqrt{4}$ are present, representing the 110 and 200 reflections. These reflections further substantiate the hexagonal packing of the columns. In the wide angle area, reflections at 3.7 and 4.9 Å are present, the former being oriented perpendicular to the small angle reflection. The perpendicular arrangement indicates that this mesophase is an orthogonal phase. Twenty degrees above the isotropisation temperature, the small angle reflection, the alkyl halo and the disk–disk reflection have not disappeared, but are still present, though broadened. This behavior indicates that the dimers do not break apart at isotropisation, and suggests also that the local stacking of the disks in columns does not disappear suddenly at isotropisation, but rather fades gradually. Lillya^{15b} and Lattermann¹⁷ have reported similar behavior.

Diffraction patterns with the direction of the X-ray beam perpendicular to the columnar axis were also obtained for oriented samples of the mesophases of compounds **5a** (figure 5.5d), and of **3** and **4**. All these diffraction patterns feature a perpendicular orientation of the small-angle reflections and the wide-angle reflections, indicating orthogonal phases. Also the 110 and 200 reflections, with a relative distance to the 100 reflection of $\sqrt{3}$ and $\sqrt{4}$, are present (a circularly integrated intensity distribution showing these reflections is shown for compound **3** in figure 5.5e). For compound **3**, no disk–disk reflection is observed, indicating a disordered D_h phase. The high temperature mesophase of mono-acetyl triazine **1** is a D_h -phase. The observed reflections in the diffraction patterns are summarized in table 5.2.

Table 5.2: Diffraction spacings in Å for the discotic phases of compounds 1–5a.

Compound	1 (high temp. phase) ^a	2 ^b	3 ^c	4 ^d	5a ^e
100 (1)	31.0	29.0	26.4	27.6	28.9
110 ($\sqrt{3}$)	18.4	16.7	15.2	16.7	15.4
200 ($\sqrt{4}$)	15.3	14.4	13.7	14.4	14.1
210 ($\sqrt{7}$)	11.7	-	11.8	12.9	-
alkyl halo	-	4.9	4.7	4.5	4.4
inter disk distance	-	3.7	-	3.5	3.5
inter column distance	35.8	33.5	30.5	31.8	33.4
phase identity	D_h	D_{ho}	D_h	D_{ho}	D_{ho}

^a Measured at 150°C; ^b Measured at 120 and 137°C; ^c Measured at 160, and at 48°C as a supercooled shear-aligned fiber); ^d Measured at 20°C (fiber); ^e Measured at 20°C (supercooled, shear-aligned fiber).

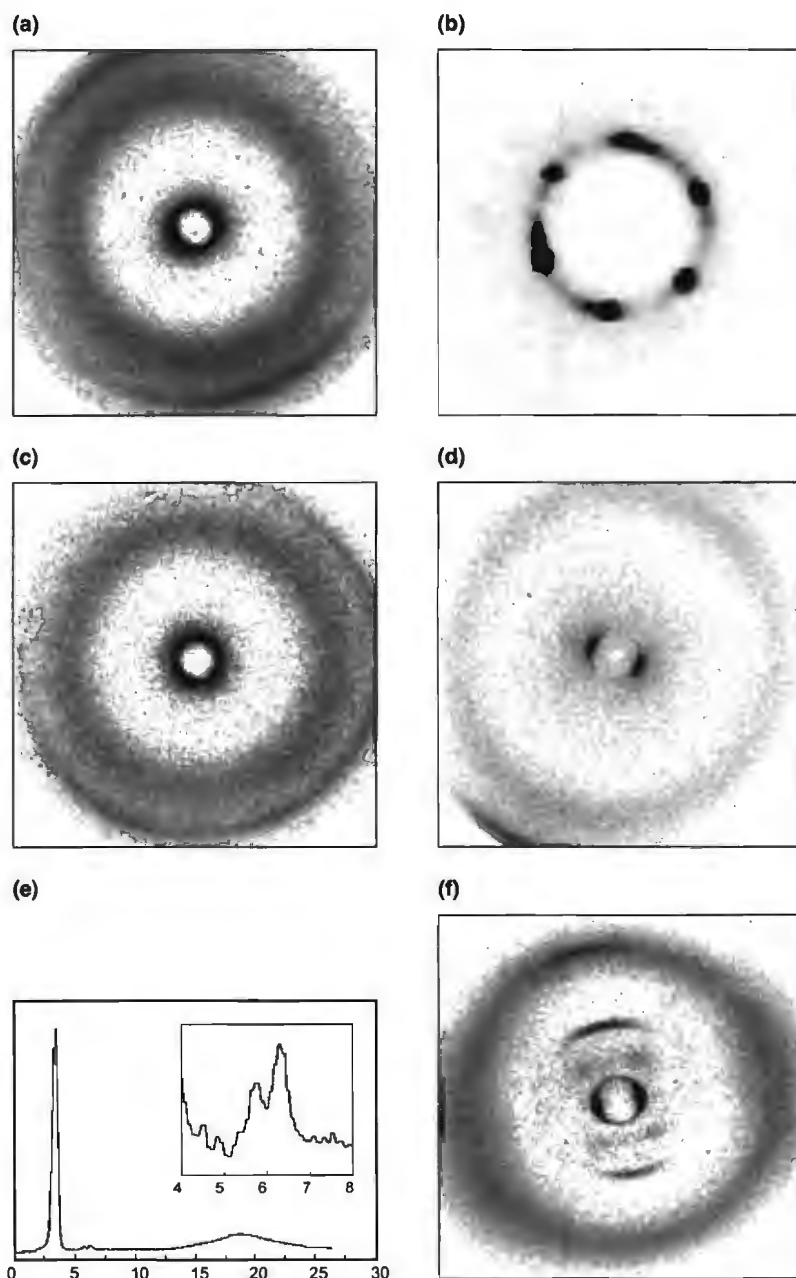


Figure 5.5: X-ray diffraction patterns of the mesophase:
 (a) of compound 2 with a view in the direction of the columns,
 (b) of compound 2; the small angle area enlarged,
 (c) of compound 2 with a view perpendicular to the columns,
 (d) of butylureido-pyrimidinone 5a with a side-view on the columns,
 (e) of compound 3, circularly integrated,
 (f) of the low-temperature phase of compound 1.

The diffraction pattern of a shear-aligned sample of the low temperature mesophase of compound **1**, measured at 42°C (figure 5.5f), features a sharp small angle reflection at 31 Å. Perpendicular to this small angle reflection at 31 Å, sharp reflections are present at 9.4 and 4.6 Å. These reflections indicate that the dimers are repeated at a regular distance in that direction, which probably corresponds to the shearing direction. The observed pattern is a strong argument to propose that the dimers form an infinite, board-like chain by additional triazine dimerization via double hydrogen bonds (see figure 5.6a), similar to the crystal structure of 2-acetyl-amino-4-amino-6-methyl-s-triazine (presented in chapter 3, picture given in figure 5.6b). The repeat-length in the direction of a chain is 10.5 Å in that crystal structure, which corresponds well to the value of 9.4 Å we find for the low temperature mesophase of **1**.

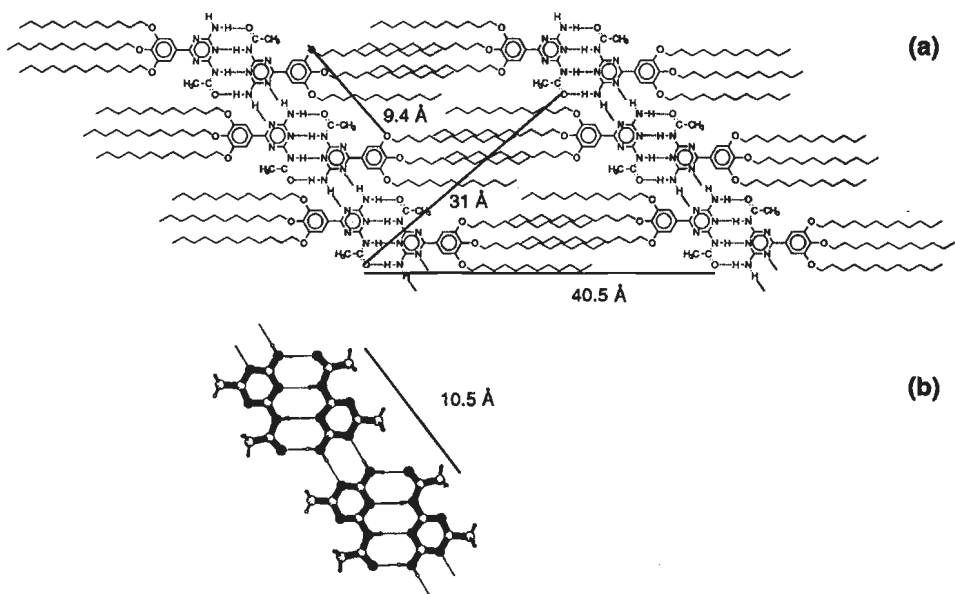


Figure 5.6: (a) Proposed structure of the low temperature mesophase of **1**. The alkyl chains must be partly interdigitated, because the distance of 40.5 Å derived from the 31 Å distance and 40 degrees angle is too short for the alkyl chains to be not interdigitated. (b) X-ray crystal structure of 2-amino-4-acetyl-amino-6-methyl-s-triazine with the relevant distance (see chapter 3).

The 4.6 Å reflection is ascribed to the second order reflection of this 9.4 Å reflection. A broad alkyl halo is present at 4.8 Å, with its main orientation perpendicular to the direction of the infinite chains. The exact origin of the weak and broad reflection at 15.2 Å — split in four equally intense peaks under an angle of 40 degrees — is not fully clear to us. We think that the angle of 40 degrees corresponds to the angle between the shortest distance between the infinite chains (of dimers) and the long distance between two dimers, and that the splitting is caused by the possibility of different orientations in different layers. Obviously, no

reflection due to molecules on top of each other was observed, since the X-ray beam was oriented perpendicularly onto the flat layers.

Hence, the low temperature mesophase of mono-acetylaminotriazine **1** has a sheet-like structure with board-like bands formed by infinite chains of dimers in the sheets. It is a supramolecular analogue of the sanidic phase,²⁰ which has been observed for polymers with disk-like mesogens linked rigidly in the main chain. At elevated temperatures, the relatively weak double hydrogen bonding interactions forming the infinite chains are broken, and a less-ordered columnar D_h-phase results.

5.3 Discussion and Conclusion

5.3.1 Discotic entity

The X-ray diffraction studies clearly indicate that the mesophases of **1–5a** are discotic. It can also be deduced from these data that the discotic entity is a dimer. The small-angle reflection in the discotic phases of **1–5a** corresponds to an inter-column distance of 30.5 to 37 Å. This distance is too large to fit only one molecule per disk: with fully extended alkyl chains, one molecule would be only 26 Å long at most. The value of 30.5 to 37 Å found for the inter-column distance indicates the alkyl chains are not fully extended (a dimer with fully extended alkyl chains would be approximately 52 Å in size), but strongly bent around the central disk.

As a second argument for the presence of one dimer per disk, calculation of the density of the material, using the column diameter and the 3.5–3.7 Å intracolumnar disk–disk spacing, only gives reasonable values if it is assumed that two molecules are present in one disk. Hence, densities of 0.84 and 0.91 g.cm⁻³ are calculated for the discotic phases of **2** (measured in a capillary at 137°C) and **5a** (measured in a fiber at ambient temperature), respectively, while the calculated density of the higher temperature phase of mono(acetylamino)triazine **1a** is 0.67 g.cm⁻³ (measured at 150°C). Unreasonably low densities of 0.33–0.42 g.cm⁻³ would result if the disk contained only one molecule, and unexpectedly high densities > 1 g.cm⁻³ would result if more than two molecules were present in one disk.

The observation that no liquid crystalline mesophase is observed for the di(pivaloylamino)-substituted triazine analogue of **2** is consistent with the concept of a liquid crystalline phase induced by disk-like entities formed by dimers. This compound approximates the shape of monomeric **1–5d**, but the di(pivaloylamino)triazine functionality is not capable of dimerization via quadruple hydrogen bonding, as was shown in chapter 2.

5.3.2 Mesophase temperature stability

Liquid crystalline mesophases are present for all compounds **1–5d** capable of dimerization by way of self-complementary quadruple hydrogen bonding, as well for the complexes studied with the heterocouple diaminotriazine–uracil. The transition to a mesophase occurs generally between 40 and 100°C; only ureidopyrimidinones **5b** and **5d** have higher melting points. The melting temperatures can be assigned to the melting of the dodecyl chains; the very high melting temperatures of **5b** and **5e** are probably caused by very efficient packing in the solid state. Compounds that turn liquid crystalline at high temperatures have also the highest isotropisation temperatures. Thus, the temperature range with liquid crystallinity is 90–130°C for all the compounds **1–5d** with the self-complementary quadruple hydrogen bonding units. These temperature ranges are significantly larger than those reported in literature for double or triply hydrogen bonded complexes, having mesophase temperature ranges of typically a few degrees (the system in figure 5.2c)¹⁴ to 20°C (the system in figure 5.2d).¹⁵ Our triply hydrogen bonded diaminotriazine–uracil complexes also have mesophases in significantly smaller temperature ranges of only 30°C. Although it is very tempting to explain this difference by the association strength of the unit, several observations are not in agreement with the assumption that the mesophase temperature range is related to the association strength in chloroform:

(i) The dimerization strength of di(acetylamino)triazine unit in **2** ($K_{\text{dim}} = 130 \text{ M}^{-1}$) is lower than the association strength of the diaminotriazine–uracil couple ($K_{\text{a}} = 810 \text{ M}^{-1}$ for complex **6•11**), and comparable to the association strength of the pyridone unit applied in the system in figure 5.2d ($K_{\text{dim}} = 95 \text{ M}^{-1}$).¹⁵ However, the mesophase temperature range is 90°C in the former and only 23°C and 20°C in the latter cases.

(ii) The mesophase temperature ranges of compounds **1–5d** are similar, yet the dimerization strength in chloroform of these compounds varies from weak to very strong: all ureidopyrimidinone derivatives **5** dimerize strongly via pre-organized DDAA arrays ($K_{\text{dim}} > 10^6 \text{ M}^{-1}$), derivative **3** dimerizes via a pre-organized DADA array ($K_{\text{dim}} \sim 2.0 \times 10^4 \text{ M}^{-1}$), derivative **1** dimerizes via a DADA array ($K_{\text{dim}} = 530 \text{ M}^{-1}$), and derivatives **2** and **4** dimerize weakly via DADA arrays destabilized by spectator repulsions ($K_{\text{dim}} = 130$ and 180 M^{-1} , respectively). Strikingly, the smallest mesophase temperature range in the quadruply hydrogen bonded dimers is observed for derivative **5a**, which dimerizes very strongly in a DDAA array. The triazine derivatives dimerize less strongly, but have larger mesophase temperature ranges.

(iii) Large differences are observed within the ureidopyrimidinone series, which all have a very large dimerization strength of similar order of magnitude.

(iv) As was indicated by X-ray diffraction experiments, the quadruply hydrogen bonded dimers of compound **2** are not dissociated 20°C above the isotropisation temperature,

while compound **2** has the lowest dimer strength in the range of compounds that can dimerize via quadruple hydrogen bonding we studied.

The relatively large mesophase temperature ranges for the self-complementary quadruple hydrogen bonding units may be explained in several ways. An argument using the difference between dimerization and association of two species fails to explain the differences, since the mesophase temperature ranges for compounds that dimerize by way of double hydrogen bonds are also small. We propose as the most likely argument for the larger mesophase temperature ranges in quadruply hydrogen bonded systems that: (i) the core with a quadruply hydrogen bonded dimer is larger and/or more efficiently filled than with double or triple hydrogen bonding: there is less empty space in the core, (ii) quadruple hydrogen bonding planarizes better than double or triple hydrogen bonds: twisting is more difficult. As a result of these two effects, a more rigid core is present, which results in a larger temperature stability of the columns.

Furthermore, the substituents also have a large influence, as is evident from the ureidopyrimidinone series. Comparison of compound **5a** with **5b** shows that the presence of more aromatic groups in the core induces a larger mesophase temperature range, and higher transition temperatures. This is probably due to the presence of a more rigid and better filled core, with a larger aromatic surface causing stronger π -stacking interactions between the disks. The temperature range and transitions are somewhat lower for diethylaminophenyl-ureidopyrimidinone **5c**, whereas an electron-withdrawing nitrophenyl group in compound **5d** induces an even larger mesophase temperature range.

5.4 Conclusion

Thermotropic discotic liquid crystalline materials with relatively large mesophase temperature ranges are obtained using self-complementary quadruple hydrogen bonding units.

5.5 Experimental Section

General methods. Unless otherwise stated, all reactions were carried out under an atmosphere of dry nitrogen and technical grade solvents were used. Anhydrous THF was obtained by distillation from sodium/potassium/benzophenone. NMR-spectra were recorded on a Varian Gemini 300 or a Bruker AM400. Chemical shifts are given in ppm relative to TMS for proton spectra and carbon spectra. IR-spectra were recorded on a Perkin-Elmer 1600 FT-IR spectrometer. Melting points and liquid crystalline mesophase ranges were determined on a Jenaval THMS 600 polarizing microscope, and are uncorrected. DSC-s were taken on a Perkin-Elmer DSC-7 under a nitrogen atmosphere, with heating and cooling rates of 10 K.min⁻¹.

Wide-Angle X-ray diffraction on liquid crystalline phases. X-ray diffraction patterns of oriented and non-oriented samples were recorded using a multiwire area detector X-1000 coupled with a graphite monochromator. Measurements at elevated temperatures were performed on samples in glass capillaries, and using a Linkam THM 600 hot stage for temperature control (accuracy 0.5 K). Oriented fiber samples were obtained by shearing on a (warm) beryllium plate, and were measured by hanging in the beam at the correct focus point. Samples were screened to find suitable large monodomains.

6-[3,4,5-tri(dodecyloxy)phenyl]-thiouracil (8). Sodium (0.46 g, 20 mmol) was dissolved in dry ethanol (35 mL). Subsequently added were keto-ester **7** (7.29 g, 10 mmol) and thiourea (1.14 g, 15 mmol). The suspension was boiled under reflux overnight; a clear solution was obtained. The ethanol was distilled off gradually, and the resultant gum dissolved in dichloromethane. The solution was extracted with dilute sodium dihydrophosphate solution 5 times. The organic phase was dried over sodium sulfate, filtered, and the filtrate evaporated to dryness. The crude product was purified by column chromatography (3% ethyl acetate in dichloromethane; product: $R_f = 0.15$, impurities with $R_f = 0$ and $R_f = 0.54$), affording 5.0 g pure product (66%). Analytical sample was prepared by dissolution in hot dichloromethane, adding 4 volume parts ethanol and cooling, causing pure **8** to precipitate as a fine white powder (4.12 g, 54%), mp 73.3–75.5°C. $^1\text{H-NMR}$ (CDCl_3) δ : 11.2 (br, 1H), 10.3 (br, 1H), 6.75 (s, 2H), 6.07 (s, 1H), 4.0 (m, 6H), 1.84 (m, 4H), 1.76 (m, 2H), 1.50 (m, 6H), 1.4–1.2 (m, 54H), 0.88 (t, 9H). $^{13}\text{C-NMR}$ (CDCl_3) δ : 175.8, 161.8, 153.6, 153.4, 141.2, 125.3, 104.8, 102.2, 73.6, 69.3, 31.9, 30.2, 29.7–29.2 (multiple peaks), 26.0, 26.0, 22.6, 14.0. IR (KBr) ν : 3480, 3200, 2917, 2851, 1666, 1618, 1556, 1498, 1471, 1452, 1361, 1332, 1172, 1108 cm^{-1} . Anal. calcd. for $\text{C}_{46}\text{H}_{80}\text{N}_2\text{O}_4\text{S}$: C, 72.91; H, 10.64; N, 3.70. Found: C, 71.12; H, 10.70; N, 3.63.

6-[3,4,5-tri(dodecyloxy)phenyl]-uracil (9). A suspension of 6-[3,4,5-tri(dodecyloxy)phenyl]-thiouracil **8** (2.28 g, 3.0 mmol), chloroacetic acid (0.56 g, 6.0 mmol), and water (15 mL) was boiled under reflux for 6 hours in air. The resulting emulsion turned quickly into a solid. Concentrated hydrochloric acid (3 mL) was added, and the emulsion was refluxed overnight. An additional quantity concentrated hydrochloric acid (2 mL) and toluene (6 mL) were added, and reflux was continued for 48 h. Cooling gave a clear waterlayer and a solidified lump. The lump was taken and dissolved in hot chloroform with some ethanol. The hot organic phase was extracted three times with warm water (caution for pressure build-up in the separatory funnel). The chloroform layer was dried over sodium sulfate, and filtered warm. Evaporation gave 2.0 g crude product (purity ~ 95%). This crude product was purified by column chromatography (silica, chloroform 4% ethanol; product: $R_f = 0.40$; impurity $R_f = 0$), affording 1.80 g product. Analytical sample was prepared by dissolving in hot dichloromethane (200 mL), and adding ethanol (1.5 L). The solution was filtered hot, and slow cooling resulted in the precipitation of white powder (1.69 g, 94%), liquid crystalline between 93°C and 154°C. $^1\text{H-NMR}$ (CDCl_3) δ : 9.37 (s, 1H), 8.84 (s, 1H), 6.77 (s, 2H), 5.88 (s, 1H), 4.02 (s, 6H), 1.83 (m, 4H), 1.73 (m, 2H), 1.50 (m, 6H), 1.4–1.2 (m, br, 54H), 0.88 (t, 9H). $^{13}\text{C-NMR}$ (CDCl_3 , 50°C) δ : 164.2, 153.9, 153.0, 152.4, 141.9, 125.9, 105.4, 98.2, 73.7, 69.7, 31.9, 30.4, 29.7–29.3 (multiple peaks), 26.2, 26.1, 22.6, 14.0. IR (KBr) ν : 3180, 2920, 2850, 1728, 1677, 1495, 1468, 1132 cm^{-1} . Anal. calcd. for $\text{C}_{46}\text{H}_{80}\text{N}_2\text{O}_5$: C, 74.55; H, 10.88; N, 3.78. Found: C, 73.27; H, 10.78; N, 3.60.

1-*N*-methyl-6-[3,4,5-tri(dodecyloxy)phenyl]-uracil (11), and 3-*N*-methyl-6-[3,4,5-tri(dodecyloxy)phenyl]-uracil (12). A suspension of uracil **9** (1.48 g, 2 mmol) in dry THF (20 mL), trimethylsilyl chloride (0.54 mL, 4.2 mmol), and dry triethylamine (0.59 mL, 4.2 mmol) was stirred overnight. The suspension was filtered under nitrogen, and the filtrate evaporated to dryness, leaving a yellow gum of (not further characterized) 2,4-bis(trimethylsilyloxy)-6-[3,4,5-tri(dodecyloxy)phenyl]-pyrimidine (**10**). Freshly distilled methyl iodide was added (8 mL), and the mixture was allowed to

stand in the dark for two weeks, with occasional shaking and warming. Ethanol was then added, and the solvent was evaporated in vacuo. The residue was dissolved in chloroform, and the (purple) solution was consecutively extracted with acid, dilute acidic potassium permanganate, 10% sodium sulfite solution (coloration disappeared), dilute acid, and water. Drying of the organic phase over sodium sulfate, filtration, and evaporation to dryness left 1.30 g of a gum. NMR showed this to consist of mainly the starting material, but also of two *N*-1-methyl uracil derivatives. TLC (silica, 5% THF in chloroform) indicates $R_f = 0.44$, $R_f = 0.17$, and $R_f = 0.064$ (starting material). Repeated chromatographic separation afforded three pure fractions. The identity of the first two fractions was ascertained by determination of the association constant with 2,4-diamino-6-dodecyl-*s*-triazine.

fraction 1: $R_f = 0.44$, 0.10 g (7%), 0.0474 g after precipitation in ethanol, mp 109–110°C. *N*-3-methyl derivative **12**, $^1\text{H-NMR}$ (CDCl_3) δ : 10.16 (s, 1H), 6.8 (s, 2H), 5.92 (s, 1H), 4.0 (m, 6H), 3.14 (s, 3H), 1.8–1.7 (m, 6H), 1.5 (m, 6H), 1.4–1.2 (m, br, 54H), 0.88 (tr, 9H). $^{13}\text{C-NMR}$ (CDCl_3) δ : 163.6, 153.6, 153.2, 150.4, 141.1, 126.0, 104.8, 98.0, 75.6, 69.6, 31.9, 30.3, 30.3, 29.7–29.3 (multiple peaks), 27.1, 26.1, 26.0, 22.7, 14.1. IR (KBr) ν : 3263, 3096, 2956, 2918, 2850, 1709, 1639, 1467 cm^{-1} . Anal. calcd. for $\text{C}_{47}\text{H}_{82}\text{N}_2\text{O}_5$: C, 74.75; H, 10.94; N, 3.71. Found: C, 72.15; H, 10.26; N, 3.46.

fraction 2: $R_f = 0.17$, 0.24 g (16%), 0.06 g after precipitation in ethanol, melting at 48°C (liquid crystalline), isotropisation at 58°C. *N*-1-methyl derivative **11**, $^1\text{H-NMR}$ of (CDCl_3) δ : 9.65 (s, 1H), 6.48 (s, 2H), 5.68 (s, 1H), 3.98 (m, 6H), 3.22 (s, 3H), 1.80 (M, 6H), 1.48 (M, 6H), 1.4–1.2 (m, br, 54H), 0.88 (t, 9H). $^{13}\text{C-NMR}$ (CDCl_3) δ : 162.9, 157.3, 153.4, 152.0, 139.6, 127.8, 106.1, 102.8, 73.6, 69.3, 33.7, 31.9, 30.3, 29.7–29.2 (multiple peaks), 26.0, 22.6, 14.1 ppm. IR (KBr) ν : 3168, 3048, 2929, 2850, 1700, 1466, 1330, 1242, 1116 cm^{-1} . Anal. calcd. for $\text{C}_{47}\text{H}_{82}\text{N}_2\text{O}_5$: C, 74.75; H, 10.94; N, 3.71. Found: C, 74.59; H, 11.12; N, 3.31.

fraction 3: $R_f = 0.064$, 0.69 g, 47%, starting material **9**.

Preparation of diaminotriazine–uracil complexes, and study by microscopy.

1) 0.1850 g of triazine **6** and 0.1895 g of thiouracil **8** were dissolved in a hot ethanol/ dichloromethane mixture. Cooling resulted in crystallization of microneedles, containing both components in a 1:1 ratio as indicated by NMR. These needles turned to a highly viscous and sticky gum upon storage. Upon heating of the needles under polarizing microscope, the boundaries of the freshly obtained needles faded at 63–70°C; the edges of a spot of the very viscous gum also rounded also at 65°C, with a drop in viscosity. A moderately viscous and low birefringent liquid was present above 70°C. Isotropisation occurred at 105°C, with a sudden drop in viscosity.

2) 7.0 mg of triazine **6** and 7.0 mg of uracil **9** were codissolved in a warm ethanol/dichloromethane mixture. Cooling resulted in precipitation of a gel, but after prolonged standing (more than one year), dots of microneedles had crystallized, while the gel had disappeared mostly. The dots of tiny microneedles were harvested by spatula picking, and washed by suspending in ethanol and filtering. Filtration gave a sticky white powder, consisting of **6** and **9** in a 1:1 ratio as indicated by $^1\text{H-NMR}$. A sample under the polarizing microscope shows rounding of the boundaries at 95°C with a drop in viscosity. The slightly birefringent viscous gum turned isotropic at 115°C.

3) 7.4 mg of triazine **6** and 7.6 mg of uracil **11** were dissolved in ethanol. Cooling and evaporation in air resulted in the precipitation of a 1:1 complex, as indicated by $^1\text{H-NMR}$. As observed by polarizing microscopy, this gum melted to a liquid crystalline material of intermediate viscosity at 82°C. Isotropisation occurred at 105°C, with a sharp transition to a low viscous fluid.

References and Footnotes

- 1) F. Reinitzer, *Monatsch. Chem.*, **1888**, *9*, 421.

- 2) Approximately 5% of all organic compounds exhibit liquid crystalline behavior (*Liquid Crystals, the fourth state of Matter*, Ed. F.D. Saeva, Marcel Dekker Inc., New York, 1979).
- 3) For books on liquid crystallinity, see: (a) G. Vertogen, W.H. de Jeu, *Thermotropic Liquid Crystals, Fundamentals*, in: *Springer Series in Chemical Physics*, vol 45, Ed. V.I. Goldanskii, F.P. Schäfer, J.P. Thoenes, Springer Verlag, Berlin, 1988, (b) E.B. Priestley, D.J. Wojkiewicz, P. Sheng, *Introduction to liquid Crystals*, Plenum Press, New York, 1975, (c) G.W. Gray, *Molecular Geometry and the Properties of Nonamphiphilic Liquid Crystals*, in: *Advances in Liquid Crystals*, vol 2, Ed. G.H. Brown, Academic Press, New York, 1976.
- 4) (a) S. Chandrasekhar, B.K. Sadashiva, K. Suresh, *Pramana*, 1977, 9, 471, (b) C. Destrade, M.C. Mondon, J. Malthête, *J. Phys. Colloq. (Paris)*, 1979, 40B, C3.
- 5) For excellent reviews, see: (a) C.M. Paleos, D. Tsiourvas, *Angew. Chem. Int. Ed. Engl.*, 1995, 34, 1696, (b) T. Kato, *Supramolecular Science*, 1996, 3, 53.
- 6) For some examples, see: (a) H. Zheng, B. Xu, T.M. Swager, *Chem. Mater.*, 1996, 8, 907, (b) J. Barbera, C. Cativiela, J.L. Serrano, M.M. Zurbano, *Adv. Mat.*, 1991, 3, 602, (c) M.N. Abser, M. Bellwood, C.M. Buckley, M.C. Holmes, R.W. McCabe, *J. Mater. Chem.*, 1994, 4, 1173, (d) H. Zheng, P.J. Carroll, T.M. Swager, *Liquid Crystals*, 1993, 14, 1421, (e) N.J. Thompson, J.L. Serrano, M.J. Baena, P. Espinet, *Chem. Eur. J.*, 1996, 2, 214.
- 7) (a) M. v.d. Auweraer, C. Catry, L. Feng Chi, O. Karthaus, W. Knoll, H. Ringsdorf, M. Sawodny, C. Urban, *Thin Solid Films*, 1992, 210/211, 39, (b) A.R.A. Palmans, J.A.J.M. Vekemans, H. Fischer, R.A. Hikmet, E.W. Meijer, *Chem. Eur. J.*, 1997, 3, 300.
- 8) M.-J. Brienne, J. Gabard, J.-M. Lehn, I. Stilbor, *J. Chem. Soc., Chem. Comm.*, 1989, 1868.
- 9) (a) C. Fouquey, J.-M. Lehn, A.-M. Levelut, *Adv. Mat.*, 1990, 2, 254, (b) M. Kotera, J.-M. Lehn, J.-P. Vigneron, *J. Chem. Soc., Chem. Comm.*, 1994, 197.
- 10) (a) T. Kato, Y. Kubota, M. Nakano, T. Uryu, *Chem. Lett.*, 1995, 1127, (b) T. Kato, *Supramolecular Science*, 1996, 3, 53.
- 11) (a) T. Kato, J.M.J. Fréchet, *J. Am. Chem. Soc.*, 1989, 111, 919, (b) T. Kato, A. Fujishima, J.M.J. Fréchet, *Chem. Lett.*, 1990, 919, (c) T. Kato, H. Adachi, A. Fujishima, J.M.J. Fréchet, *Chem. Lett.*, 1992, 265, (d) M. Fukumasa, T. Kato, T. Uryu, J.M.J. Fréchet, *Chem. Lett.*, 1993, 65, (e) T. Kato, J.M.J. Fréchet, P.G. Wilson, T. Saito, T. Uryu, A. Fujishima, C. Jin, F. Kaneuchi, *Chem. Mater.*, 1993, 5, 1094.
- 12) L.J. Yu, J.M. Wu, S.L. Wu, *Mol. Cryst. Liq. Cryst.*, 1991, 198, 407.
- 13) (a) U. Kumar, T. Kato, J.M.J. Fréchet, *J. Am. Chem. Soc.*, 1992, 114, 6630, (b) T. Kato, H. Kihara, T. Uryu, A. Fujishima, J.M.J. Fréchet, *Macromolecules*, 1992, 25, 6836, (c) S. Malik, P.K. Dhal, R.A. Mashelkar, *Macromolecules* 1995, 28, 2159, (d) T. Kato, N. Hirota, A. Fujishima, J.M.J. Fréchet, *J. Polym. Sci., part A: Polym. Chem.*, 1996, 34, 57.
- 14) U. Beginn, G. Lattermann, *Mol. Cryst. Liq. Cryst.*, 1994, 241, 215.
- 15) (a) R. Kleppinger, C.P. Lillya, C. Yang, *Angew. Chem.*, 1995, 107, 1762, (b) R. Kleppinger, C.P. Lillya, C. Yang, *J. Am. Chem. Soc.*, 1997, 119, 4097.
- 16) J. Malthête, A. Collet, A.-M. Levelut, *Liq. Cryst.* 1989, 5, 123.
- 17) G. Lattermann, G. Staufer, *Liq. Cryst.* 1989, 4, 1303.
- 18) Few examples of hydrogen bonded systems have mesophase temperature ranges exceeding 50°C. We are aware of only one instance with mesophase ranges exceeding 100°C for hydrogen bonded mesogens, see ref 9a.
- 19) The compounds were crystallized from a solvent.
- 20) H. Ringsdorf, I. Voigt-Martin, J. Wendorff, R. Wuestefeld, R. Zentel in *Chemistry and Physics of Macromolecules*, Ed. E.W. Fischer, R.C. Schulz, H. Sillescu, VCH, Weinheim, 1991, 211.

Chapter 6

Reversible Linear Supramolecular Polymers, by Self-Complementary Quadruple Hydrogen Bonding of Bifunctional Compounds

Abstract:

Strong and unidirectional association via quadruple hydrogen bonding of self-complementary ureidopyrimidinone units is used to obtain linear polymers that are bonded non-covalently. This is achieved by linking two ureidopyrimidinone units by a spacer. The properties of such a bifunctional ureidopyrimidinone derivative, 3, are reminiscent of conventional polymers in many respects. A concentrated solution of this compound in chloroform shows a high viscosity. The viscosity is strongly concentration dependent, and the concentration dependence follows Cates's model for reversibly breakable polymers above the overlap concentration. The presence of linear supramolecular polymer structures of reversibly linked monomers in chloroform solution was further substantiated by the addition of a monofunctional compound. The latter acts as a chain stopper and limits the degree of polymerization, leading to a dramatic drop in viscosity even when added in very small amounts. From this chain-stopper experiment at 40 mM, an average degree of polymerization of at least 700 was deduced, with a corresponding dimerization constant exceeding $2 \times 10^6 \text{ M}^{-1}$.

In the solid state, the supramolecular polymers display properties normally observed for macromolecules, and not for organic molecules. The bulk material is viscous and rubbery at ambient temperatures, from which fibers can be drawn. In contrast to conventional polymers, however, the melt is a low viscous fluid at high temperatures. The molecules with alkyl chains as spacers tend to crystallize, rendering detailed study of the polymer properties in bulk impossible. Therefore, a synthetic route to siloxane-spaced bifunctional molecules was developed in collaboration with Ky Hirschberg and Huub van Aert. This route uses a double hydrosilylation coupling of a benzyl protected 3-butenyl pyrimidinone unit with α,ω -dihydro-siloxanes, and removal of the benzyl protecting group by hydrogenolysis after the hydrosilylation coupling. In contrast to the alkyl-spaced supramolecular polymers, these materials with flexible siloxane spacers do not crystallize from the melt. This opens the way to study visco-elastic properties in the bulk by rheology.

6.1 Introduction

Nowadays, polymers are virtually synonymous with macromolecules, which are very large molecules built by linking smaller units (monomers) by covalent bonds.¹ Macromolecules may be formed by numerous chemical reactions, such as free radical reactions, (trans)esterification, (trans)amidation or other condensation reactions, anionic or cationic addition reactions, and organometallic coordination reactions. The polymer chains may be linear (e.g. polyethylene, polytetrafluorethylene, polycaprolactam), carry short side chains (e.g. polystyrene, polybutadiene), or may even be branched, or the polymer may consist of an infinite network of cross-linked chains. Macromolecules occur widespread in natural systems, most often as construction materials, such as cellulose, which is a polysaccharide in plants, or collagen, a polypeptide in animals. Polymers have an enormous and intriguing range of unique properties, such as rubber elasticity and high solution viscosity. These are due to the length of the macromolecular chains, which become entangled above a certain critical chain length.

In the early days of polymer chemistry, it was not yet established that the unique properties of polymers are caused by the presence of long-chain macromolecules. The macromolecular concept was formulated by Hermann Staudinger in 1920, after being presented in a lecture in 1917. However, the new idea was under debate during the 1920s, and was opposed by many scientists. They argued that polymers are colloidal assemblies of organic molecules, kept together by VanderWaals interactions. Only at the end of the 1920 decade, the research results decisively pointed to the macromolecular nature of polymers.

Nowadays, supramolecular chemistry—using non-covalent interactions to assemble well-defined structures—has become increasingly important in polymer science.² Although hydrogen bonding and other weak, reversible interactions have been recognized to be very important in determining polymer properties, —e.g. in polyamides³— the design of new polymer architectures based on non-covalent interactions has started only recently. Substantial efforts are being undertaken to alter the properties of polymers by end-group functionalization,⁴ and hydrogen bonding has been used to obtain side-chain liquid crystalline polymers.⁵ These efforts rely mostly on cooperativity of many weak interactions, giving rise to phase-separation, such as formation of microcrystalline domains or induction of liquid crystallinity.

Although self-assembly by well-defined, cooperative non-covalent interactions is a well-recognized process in biological systems,⁶ the general concept of self-assembly of synthetic molecules by molecular recognition of complementary components received general attention only after it was integrated by Lehn in the field of supramolecular chemistry.⁷ As described by Lehn in 1988, one exciting challenge of supramolecular chemistry is to assemble linear, polymeric structures using non-covalent interactions. Monomeric molecules, with two

associating functional groups, are assembled reversibly into linear chains by non-covalent interactions of these functional groups (figure 6.1 gives an example of a copolymeric system with hydrogen bonding). A prerequisite for these linear supramolecular polymers—in which a reversible alternative for the covalent bond is used—is to incorporate strong, highly directional and reversible non-covalent interactions.

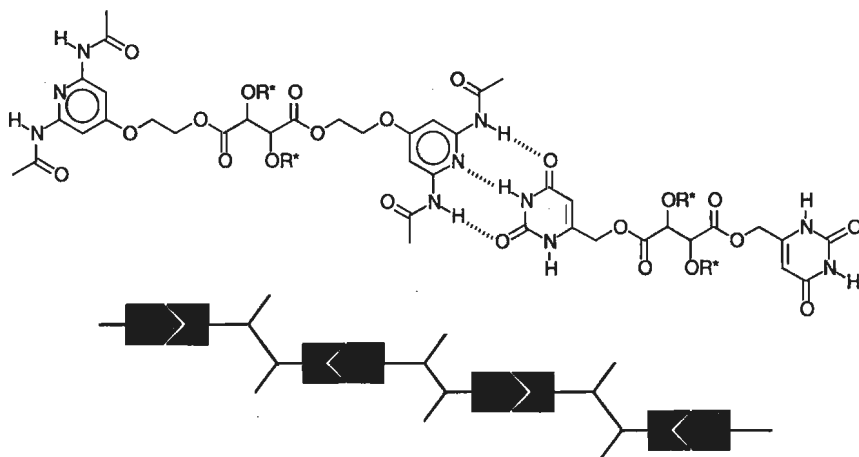


Figure 6.1: Supramolecular polymers reported by Lehn,⁷ obtained by mixing bifunctional compounds with the complementary couple di(acetylamino)pyridine–uracil in a 1:1 ratio.

The concept of supramolecular polymers has been known for years, but systems that are reversible, flexible, and have appreciable degrees of polymerization in the amorphous state or in dilute solution have scarcely been obtained.⁸ The reason is that the required sufficiently strong, yet highly directional and reversible secondary interactions were not available. Ionic interactions have sufficient strength, but lack directionality, giving rise to network formation and gelation,⁹ whereas coordination of metal ions shows limited reversibility and tunability.¹⁰

Multiple hydrogen bonds are renowned for their unique combination of strength and directionality. The hydrogen bonded copolymer systems Lehn reported (figure 6.1), obtained by mixing two bifunctional compounds with complementary hydrogen bonding units in a 1:1 ratio, indeed feature polymeric structures in bulk, in a liquid crystalline state with additional ordering. In solution, however, no polymeric structures were observed, probably because the chains were too short due to the low association constant of the di(acetylamino)pyridine–uracil couple. Other efforts to use highly directional multiple hydrogen bonds have been hampered mainly by the insufficient stability of single,¹¹ double,¹² or triple hydrogen bonds,¹³ or by the difficult preparation of the strongest couples.¹⁴

The finding that readily accessible derivatives of 2-ureido-4-pyrimidinone dimerize strongly and unidirectional by means of a *self-complementary* DDAA array of four hydrogen bonding sites (see chapter 4), prompted us to use this functionality as the associating end-group in reversible self-assembling polymer systems (see figure 6.2 for the concept).

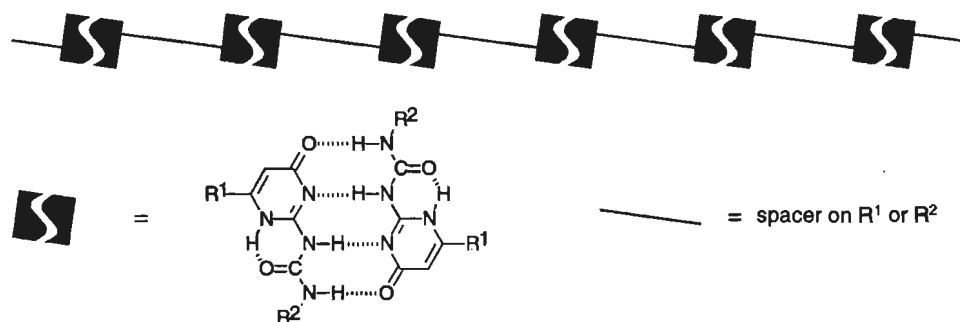


Figure 6.2: Schematic representation of reversible linear supramolecular polymers obtained from bifunctional compounds with the self-complementary 2-ureido-4-pyrimidinone unit.

The self-complementarity of the ureidopyrimidinone linking unit, resulting in a homopolymer, has two paramount advantages in comparison with the system of Lehn, who uses complementary groups that form a copolymer:

- (i) Less synthetic effort is required because only one unit has to be synthesized.
- (ii) It is not necessary to mix exact stoichiometric quantities.

As described in theoretical considerations of condensation polymerization,^{1a,1b} copolymerization of monomers A–A and B–B will only give long chains if the co-monomers are mixed in exactly 1:1 stoichiometries: a 1% excess of one of the components will limit the number-average degree of polymerization to at most 200. The formation of supramolecular polymers by linking via self-complementary units is comparable to condensation polymerization of a lactone or lactam, i.e. only one monomer. The molecular weight of this type of condensation polymerization is not limited by mixing of the monomers in stoichiometric quantities.

As also follows from the concept depicted in figure 6.2, a high degree of purity is required to obtain long polymer chains. Any impurity in the form of a monofunctional compound will act as a chain stopper, and considerably diminish the degree of polymerization. This occurs in the same way as the chain length of a condensation polymer of type A–B is limited by the presence of monofunctional impurities in the monomer.^{1a,1b}

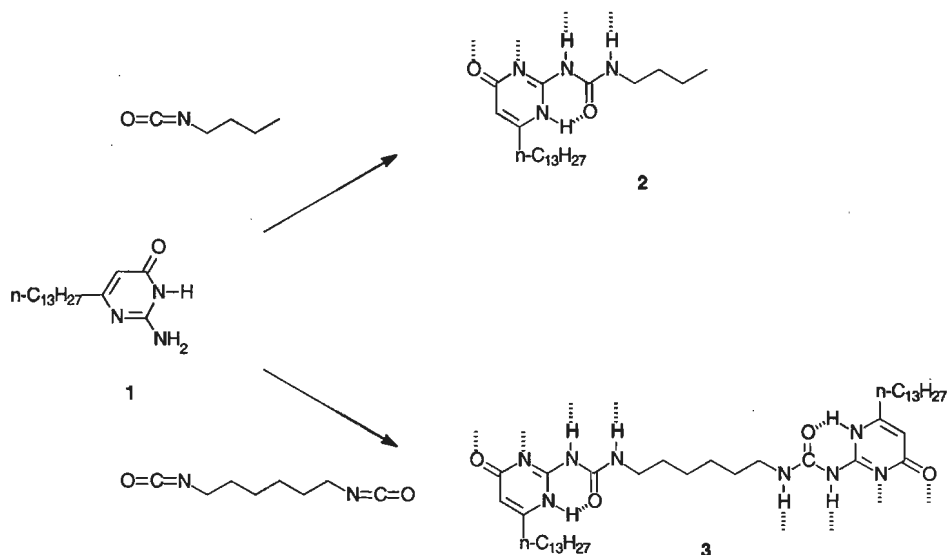
In this chapter, the development of synthetic routes to symmetrical compounds with two self-complementary arrays of four hydrogen bonding groups in one molecule is discussed. The synthesis includes extensive purification and impurities are carefully monitored by Electrospray Ionization Mass Spectrometry. To show the polymeric nature of

our supramolecular polymers, we focus on the behavior in solution using viscosimetry. The viscosity of a polymer solution is related to the length of the polymer chains.¹ The polymeric nature in the solid state is deduced from its physical appearance, qualitative mechanical experiments, and from preliminary microscopy results. The material properties are compared to those of conventional polymers, and the interesting features of this new system with respect to conventional macromolecular polymers are discussed.

6.2 Results & Discussion

6.2.1 Synthesis and characterization of supramolecular polymer

Synthesis. Based on our knowledge of the influence of substituents on tautomerism and bonding behavior of ureidopyrimidinones in solution (as in monofunctional derivative **2**, see chapter 4), aliphatic spacers were chosen in our first approach to link those units in the supramolecular polymers.¹⁵ 6-Tridecyl-isocytosine **1** (see chapter 4) was reacted with commercially available hexane diisocyanate, affording bifunctional compound **3** in one step (scheme 6.1). The reaction was performed by refluxing in dry pyridine for 48 hours. After the reaction time, the crude product **3** was isolated in 95% yield by precipitation in acetone.



Scheme 6.1: Synthesis of monofunctional compound **2**, and of bifunctional compound **3**.

Purification and ESI-MS characterization. The purity of **3** was only ~ 90% as deduced from $^1\text{H-NMR}$. The major impurity was identified as bifunctional molecule **4**, carrying an additional hexylurea spacer (figure 6.3). This impurity suggests partial hydrolysis and subsequent decarboxylation of an isocyanate group to afford the amine, which subsequently reacts with another isocyanate molecule.¹⁶

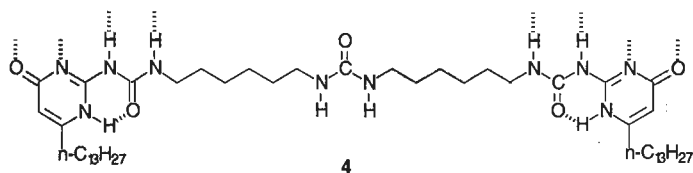


Figure 6.3: Likely impurity **4** in raw material of **3**.

Impurity **4** was removed by a column chromatographic separation on flash-silicagel using chloroform/ethanol 95:5 v/v as eluent, and **3** was obtained as a white powder by precipitation from chloroform into acetone. This material was sufficiently pure to obtain satisfactory elemental analysis. Since impurities, especially those capable of interfering with the formation of a hydrogen bonded polymer, had to be excluded rigorously to guarantee a high degree of polymerization, further purification was attempted. Repetitive precipitations from chloroform/ethyl acetate (by cooling of a hot solution) were found to result in a further improvement of the purity. The specific viscosity of a 40 mM solution in chloroform, a good qualitative measure for the length of a polymer chain, increased by these repetitive precipitations from 6.5 after the column chromatographic separation, to 11.7 after 5 precipitations, and then, the viscosity did not increase any more (see Experimental Section).

The impurities were monitored by Electrospray Ionization Mass Spectrometry (ESI-MS).¹⁷ ESI-MS spectra taken from the material after column chromatography, and after three precipitations from hot chloroform/ethyl acetate, are shown in figure 6.4.

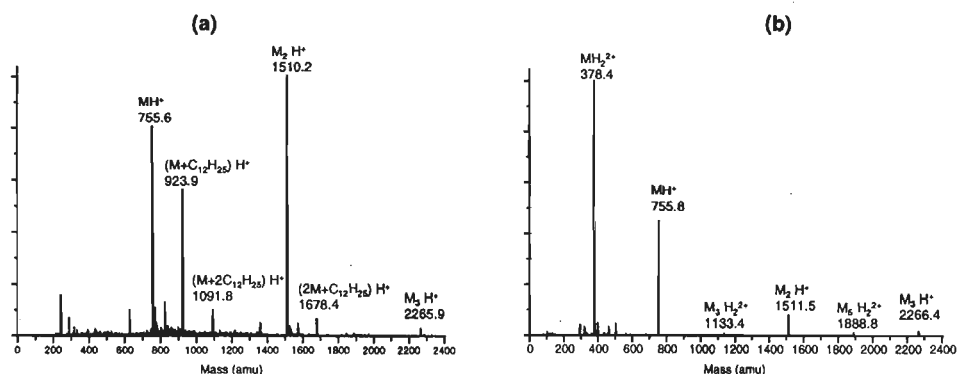
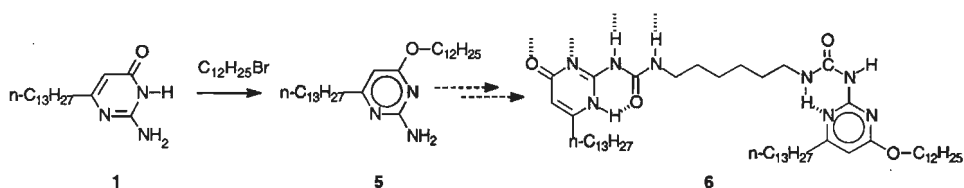


Figure 6.4: ESI-MS spectra of compound **3**: (a) after column chromatography and acetone precipitation, (b) after 3 precipitations from hot chloroform/ ethyl acetate.

An impurity with an additional dodecyl chain is present in the material after column chromatography and precipitation from acetone, which is removed by precipitations from hot chloroform/ethyl acetate. The structure of the impurity is assigned to **6**, based on a triplet signal at 3.7 ppm of this impurity in ^1H -NMR. Impurity **6** is likely to originate from *O*-alkylation of isocytosine **1** by dodecyl bromide (scheme 6.2).¹⁸ As further proof of the identity of this impurity, the *O*-alkylated isocytosine **5** was isolated from the mother liquor of the crude isocytosine reaction and unambiguously characterized as the *O*-alkylated derivative by ^1H -NMR and ^{13}C -NMR (see Experimental Section).



Scheme 6.2: Formation of impurity 6 in supramolecular polymer 3.

Based on integration of the signals in ^1H -NMR, impurity **6** is present in the product after column chromatography and precipitation in acetone in approximately 0.4%. This value corresponds well to the value deduced from chain stopper experiments performed with batches of different purity (vide infra). The large relative intensity of the signals attributed to the impurity **6** in the ESI-MS spectrum can be explained well by preferential protonation of the *O*-alkylated ureido-4-pyrimidinone end-group in **6**. This preferential protonation of an *O*-alkylated ureidopyrimidinone end-group probably occurs because it cannot dimerize via quadruple hydrogen bonding, and hence lacks the stabilization by dimerization. Furthermore, figure 6.4b shows that dimers, trimers, etc. are present even in dilute solutions, and in the presence of the strongly hydrogen bonding competitive solvent formic acid.

^1H -NMR dilution studies in chloroform. ^1H -NMR-studies were performed to gather insight into the hydrogen bonding behavior of **3** in solution. In ^1H -NMR spectra of concentrated CDCl₃ solutions of compound **3**, the region of N-H and alkylidene absorptions is similar to that of monofunctional compound **2** (figure 6.5) This indicates that the ureido-pyrimidinone groups of **3** are involved in dimerization. In dilute chloroform solutions, three new sets of peaks are present, of which the signals lie very close to the signals at high concentrations. Unfortunately, the ratios of the different forms could not be determined reliably — not even by deconvolution— due to strong peak overlap.

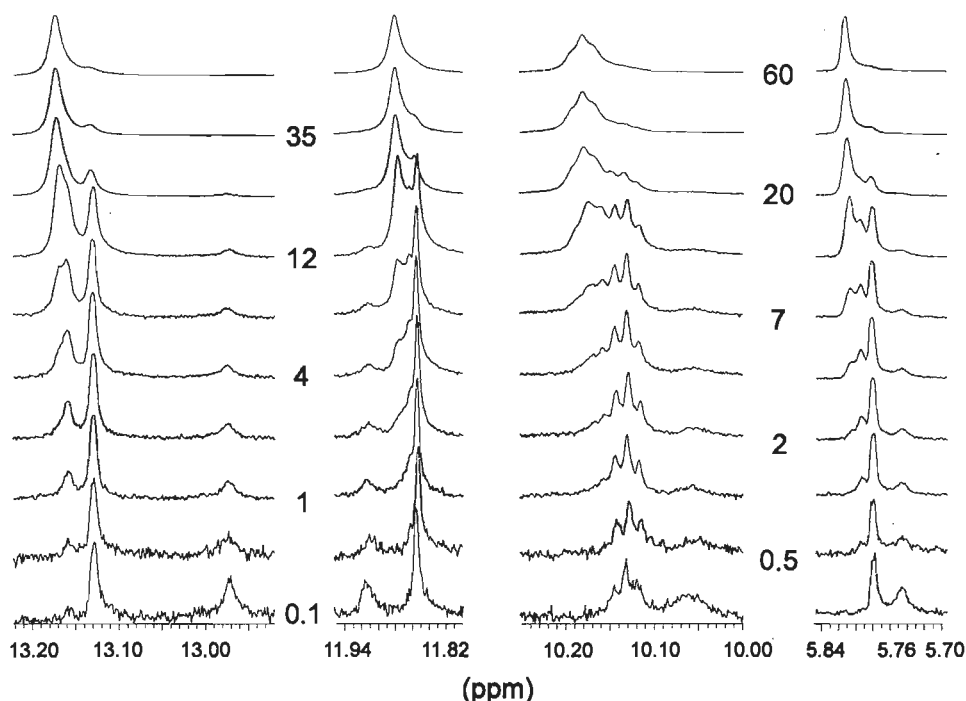


Figure 6.5: Concentration dependence (concentrations given in mM) of the three N–H signals and the alkylidene signal in the ^1H -NMR spectrum of supramolecular polymer **3** in CDCl_3 .

Their locations indicate, however, that the new signals originate also from dimerized ureidopyrimidinone units. Therefore, these signals are attributed to cyclic oligomeric structures of different size. The concentration dependence of the equilibria between cyclic oligomeric structures (at low concentrations) and linear polymeric structures (at high concentrations) is similar to the ring–chain equilibria in condensation polymerization described by Flory.^{1a}

6.2.2 Polymer properties in solution

Viscosity of chloroform solutions. Concentrated solutions of bifunctional compound **3** in chloroform are very viscous, and the viscosity is highly concentration and temperature dependent. A plot of the logarithm of the specific viscosity (for viscosity measurement procedures, see Experimental Section) versus the logarithm of the concentration is linear with a slope of 3.76, while a slope of 0.94 is found for monofunctional compound **2** (figure 6.6). The constant high slope of 3.76 for compound **3** suggests that, in the whole concentration range covered, molecules **3** behave like entangled polymers, following Cates's model for reversibly breakable polymers above the overlap concentration.¹⁹ Cates's model

predicts that the zero-shear viscosity of a solution of a reversible breakable polymer that undergoes scission–recombination, or end–interchange, quicker than reptation (cancelling of entanglements) is proportional to the volume fraction (or concentration) to the power of 3.7 and 3.5, respectively.

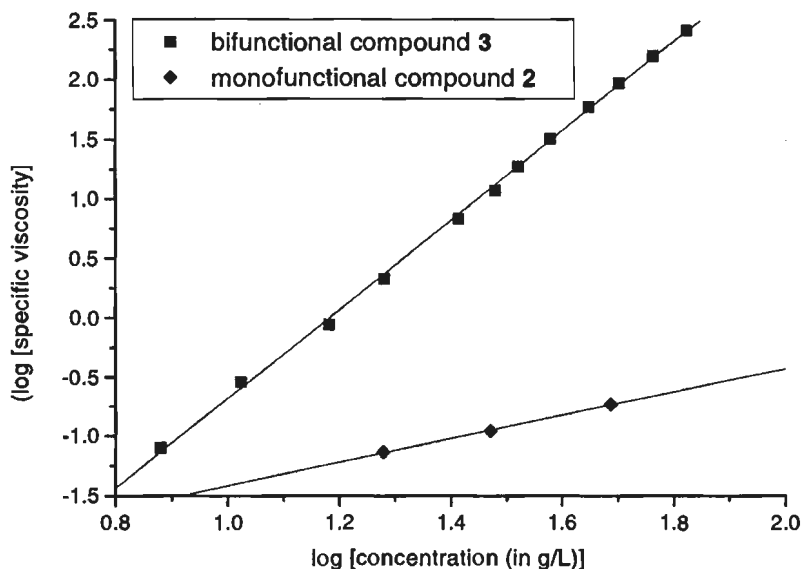


Figure 6.6: Specific viscosity of solutions in chloroform as a function of concentration (in g/L) of bifunctional derivative **3** and for monofunctional derivative **2**.

Chain stopper experiment. To confirm the unidirectionality of the quadruple hydrogen bonding interaction, the specific viscosity of a 40 mM solution of **3** in chloroform was monitored as increasing amounts of monofunctional compound **2**—which acts as a chain stopper for the supramolecular polymer— were added. A dramatic drop in viscosity was observed even upon addition of very small amounts of **2** (see figure 6.7). This observation proves the reversibility of the hydrogen bonding interaction, and implies that the high viscosity should be assigned to unidirectional interactions, and not to multidirectional gelation.

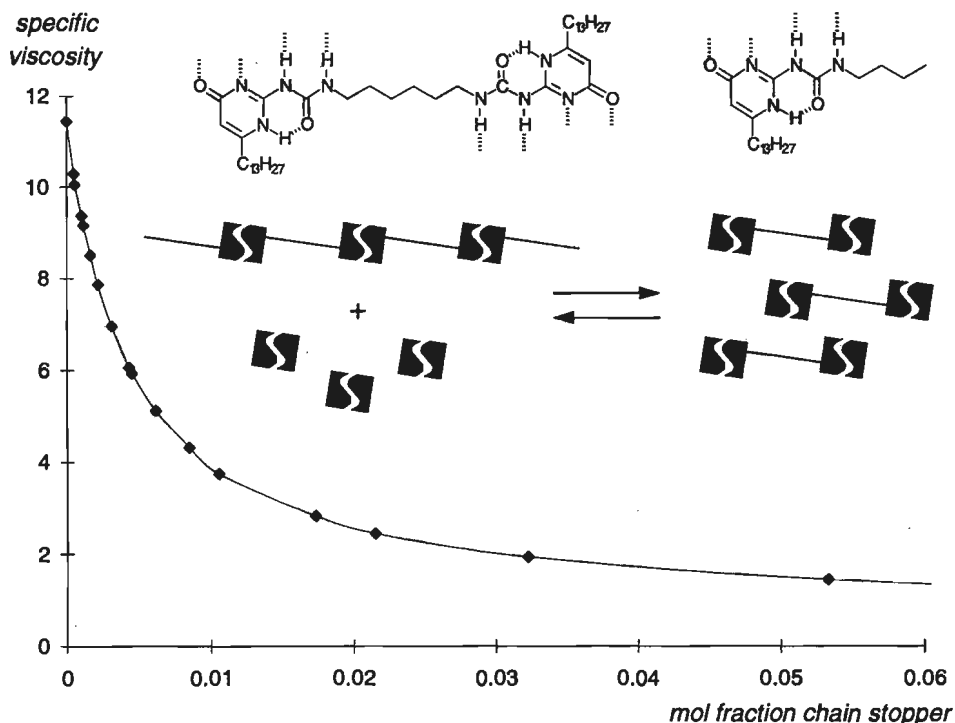


Figure 6.7: Specific viscosity of solutions of **3** in chloroform as a function of added monofunctional compound **2**.

This phenomenon is reminiscent to the limitation of the molecular weight of a condensation polymer by the addition of a monofunctional monomer.^{1a,1b} Monofunctional compound **2** (mol fraction chain stopper = x) limits the number-average degree of polymerization (DP) of bifunctional compound **3** to at most $DP_{\max} = 2/x$. DP is further determined by the degree of association, which is a function of concentration and association constant. The degree of polymerization (DP) of **3** is given by the following equation (see Experimental Section):

$$DP = \frac{2 \cdot ([\mathbf{3}] + [\mathbf{2}])}{[\mathbf{2}] - \frac{1}{4K} [1 - \sqrt{1 + 8K([\mathbf{2}] + 2 \cdot [\mathbf{3}])}]} \quad (1)$$

When an exponential relation between η_{sp} and DP is assumed in the form of $\eta_{sp} = p \times DP^a$,²⁰ the data fit well for $\eta_{sp} \sim (DP)^{0.78}$, and $K_{\text{dim}} = 2.2 \times 10^6 \text{ M}^{-1}$. Furthermore, it follows that the degree of polymerization of a 40 mM solution is ~ 700 , which corresponds to a molecular weight of approximately $5 \times 10^5 \text{ g} \cdot \text{mol}^{-1}$. A chain stopper experiment performed at 30 mM gives, as expected, a lower degree of association but also a lower association

constant, due to a higher degree of cyclization at lower concentrations. Because of this cyclization, and also because 100% purity is assumed in the fitting procedure, the obtained values are minimal values.

6.2.3 Polymeric properties in bulk

The bulk properties of reversible supramolecular polymers of type **3** are of great interest for possible applications as materials, and also very interesting from a fundamental point of view. As a consequence of the reversibility of the hydrogen bonding in the links between the monomers, entanglements of these supramolecular polymer chains will have only a certain and limited lifetime. Scission and recombination of the chains can occur, similar as dimers of type A–A and B–B exchange and form heterodimers A–B (see chapter 4, section 4.2.5 on heterodimers). The lifetime of the hydrogen bonded links is expected to be very dependent on temperature, as well as the association constant and hence the degree of polymerization. Therefore, the materials are expected to feature a large and interesting temperature dependency on their properties. The limited lifetime of the bonds permits the material to ‘immediately’ adjust its configuration to external stimuli, thus affording an interesting object for rheological studies of visco-elastic properties.

Bulk material of compound **3** appears as an amorphous white powder after precipitation from ethyl acetate, and melts at 160°C to a low viscosity fluid. Fibers can be drawn from the melt at that temperature, which on standing gradually turn brittle. However, the bulk visco-elastic properties of compound **3** could not be investigated, because this compound has a strong tendency to crystallize. Inspection by polarizing microscopy shows that the amorphous glass, obtained by quick supercooling of the fluid from 160°C to room temperature, crystallizes slowly upon standing. When the fluid is kept between 160°C and 180°C, needle-like crystals form slowly. Further heating results in melting of these crystals, and another type of crystals forms. The compound melts at 196°C to an isotropic liquid with low viscosity, but also decomposes slowly at that temperature.

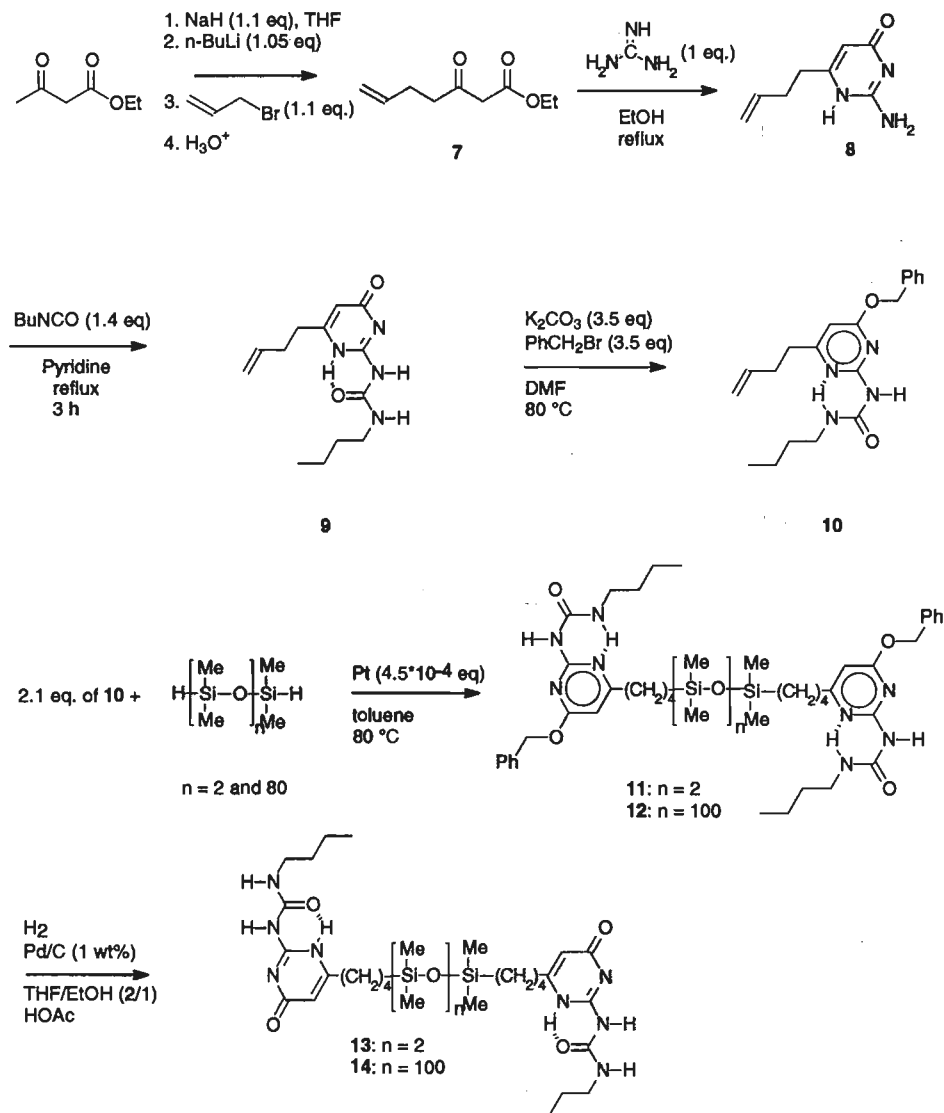
Synthesis of supramolecular polymers with siloxane spacers. Because a compound was desired that does not crystallize, a route to bifunctional compounds containing a flexible siloxane spacer was developed in close collaboration with Ky Hirschberg and Huub van Aert. To obtain bifunctional compounds with siloxane spacers, we have chosen to couple the unit as a whole entity onto both ends of a bifunctional hydrosiloxane core molecule via hydrosilylation, because:

- (i) Hydrosilylation is known to be compatible with many functional groups.²¹
- (ii) A precursor of the quadruple hydrogen bonding unit with an alkene functionality is readily accessible.²²

(iii) This approach has been proven to be feasible by Zimmerman et al, who also could couple (unprotected) hydrogen bonding functional groups —di(acylamino)pyridine units— functionalized with an alkene group onto siloxane polymers by hydrosilylation.²³

(iv) The approach of coupling the unit as a whole entity furthermore offers the possibility of polymer functionalization, and is not restricted by the availability of di-isocyanates.

The route we applied is depicted in scheme 6.3; the key step is double coupling of alkene functionalized ureidopyrimidinones with a bis-hydride terminated siloxane.



Scheme 6.3: Synthesis of bifunctional siloxane compounds.

Compound **13** was obtained as crystals by crystallization from ethyl acetate after several purifications. When these crystals are melted (mp 112°C), or when a chloroform solution is evaporated to dryness, an amorphous state is obtained that does not crystallize upon standing, even after weeks. This amorphous state appears at room temperature as a very viscous rubbery material, while the benzyl protected material **11** is a low viscous fluid. The polymer analogues **12** and **14** have also substantial differences in appearance; **12** is a low viscous oil, **14** is a rubbery material. Further details on the properties of **13** and **14**, including study of rheological behavior, are discussed elsewhere.²⁴

6.3 Conclusion

Linear supramolecular polymers, in which the monomers are linked non-covalently and reversibly, have been obtained by incorporating two 2-ureido-4-pyrimidinone units, which dimerize very strongly (yet still reversibly) via unidirectional quadruple hydrogen bonding, in one molecule. The bifunctional molecules that feature these properties can be synthesized by a very convenient and short synthesis. However — unavoidably in view of the concept — extensive purification of the crude products to a very high degree of purity (> 99.95% preferably) is necessary.

These linear supramolecular polymers show DPs by far exceeding those of existing self-assembled systems based on less than four hydrogen bonds. The very high association constant and the self-complementarity of the ureidopyrimidinone unit induce polymer-like behavior even in solution at low concentration. Furthermore, hydrosilylation allows for functionalization of short and long-chain dihydro-siloxanes with 2-ureido-4-pyrimidinone units at both ends. The flexible siloxane spacer in these molecules prevents crystallization of the material in bulk, in contrast to the molecules with *n*-alkyl spacers, offering a good object for study of bulk properties.

Concludingly, a new and unique class of materials with polymer-like behavior has become available. These supramolecular polymers enable fundamental studies on the effect of lifetime of the links between the monomeric units (and hence of entanglements) on polymer behavior, which has been the subject of recent speculations.²⁵ Because of the reversibility of the bonding, it should be easy to prepare random block-copolymers by mixing two comparable components. The chain length of the supramolecular polymers is adjustable by addition of chain stoppers, in a way similar to that of condensation polymers. Finally, cyclic structures of different size may be formed to a varying degree by simply varying the concentration.

6.4 Experimental Section

General methods. Chemicals were purchased from Acros Chimica, Fluka or Aldrich and used as received unless otherwise stated. All reactions were carried out under an atmosphere of dry nitrogen unless otherwise stated. Solvents were of technical grade unless otherwise stated. Analytical grade pyridine was dried over 4 Å molecular sieves. NMR-spectra were recorded on a Varian Gemini 300 or a Bruker AM400. Chemical shifts are given in ppm relative to TMS for ^1H and ^{13}C spectra. IR-spectra were recorded on a Perkin-Elmer 1600 FT-IR spectrometer. Melting points were determined on a Jenaval THMS 600 melting point microscope and are uncorrected. Electrospray Ionization Mass Spectrometry was performed on a Perkin Elmer Sciex API-300 LC-MS/MS (Norwalk, USA). Samples were prepared by dissolving approx. 1 mg sample in 10 mL chloroform p.a., and acidified with formic acid. Samples were measured in Flow Injection Analysis mode. Measurements were performed directly after preparation, since samples were found to deteriorate upon standing.

Viscosity measurements. Viscosities were measured in Schott Capillary Viscometer Ubbelohdes using a Schott Viscosity Measuring Unit AVS350 for exact time measurement, thermostated at 20.00°C using a Schott CT1650 waterbath. The solutions of the supramolecular polymers in chloroform (p.a. stabilized with amylene) were filtered through 5 µm before use. Dynamic viscosities $\eta = K \times (t - \theta)/\text{density}$ were determined from running times of the solution through the capillaries, using the capillary constant K of the ubbelohde, and a correction time θ that was given in tables enclosed with the ubbelohdes. The relative viscosity (η_{rel}) is defined as $\eta_{\text{solution}}/\eta_{\text{solvent}}$; the specific viscosity (η_{sp}) equals $\eta_{\text{rel}} - 1$. In the dilution experiment, ubbelohdes with different constants K were calibrated relative to each other to cover a large range.

Derivation of equation 1. The number average degree of polymerization (DP) is defined as the average of the number of molecules in a polymer chain. Since there are always two end-groups in a linear chain, DP equals the ratio of the total number of molecules in solution, divided by half the number of end-groups. Dimers of the stopper are thus treated as $\text{DP} = 2$; with small amounts of stopper, nearly all stopper molecules will end-cap polymer chains. The number of end-groups equals the sum of stopper molecules and non-complexed ureidopyrimidinone functional groups. We define several parameters:

DP	Number average degree of polymerization.
K_{dim}	K_{dim} , in chapter 4, since the complex dimerization constant determines the ratio between complexed ureidopyrimidinone units and non-bonded ureidopyrimidinone units.
[Dim]	Concentration of dimerized ureidopyrimidinone functional groups (not molecules).
[Mon]	Concentration monomeric (= non-complexed) ureidopyrimidinone functional groups.
[Bif]	Concentration bifunctional molecules (3).
[Stop]	Concentration monofunctional molecules (2).
[C _{tot}]	Total concentration of ureidopyrimidinone functional groups

Since the experiment is confined to a certain constant volume, the ratio of molecules is equal to the ratio of concentrations, so in formula we can write for DP:

$$\text{DP} = \frac{2 \times \{ [\text{Bif}] + [\text{Stop}] \}}{[\text{Stop}] + [\text{Mon}]}$$

The concentration of non-complexed ureidopyrimidinone *functional groups* is a function of K_{dim} and the concentration of the ureidopyrimidinone functional groups. It is assumed that the association constant is equal for the unit in compounds **3** and **2**, and is also independent of DP. This assumption is considered reasonable, since the differences in structure are remote from the ureidopyrimidinone unit. Furthermore, we neglect cyclization assuming all the chains are linear.

From the definition of K_{dim} and the total concentration of ureidopyrimidinone functional groups,

$$\text{Mon} + \text{Mon} \rightleftharpoons \text{Dim} \quad K_{\text{dim}} = \frac{[\text{Dim}]}{[\text{Mon}]^2} \quad C_{\text{tot}} = 2 \times [\text{Dim}] + [\text{Mon}]$$

it follows that the concentration of monomeric ureidopyrimidinone functional groups is derived from the following equation:

$$[\text{Mon}] = C_{\text{tot}} - 2 \times K_{\text{dim}} \times [\text{Mon}]^2$$

and solution of this quadratic equation gives:

$$[\text{Mon}] = \frac{-1 + \sqrt{1 + 8 \times K_{\text{dim}} \times C_{\text{tot}}}}{4 \times K_{\text{dim}}}$$

Since the total concentration of ureidopyrimidinone functional groups equals the sum of concentration of stopper (**2**) and twice the concentration of bifunctional molecules (**3**), DP is given by:

$$\text{DP} = \frac{2 \times \{ [\text{Bif}] + [\text{Stop}] \}}{[\text{Stop}] - \frac{1}{4 \times K_{\text{dim}}} \times \{ 1 - \sqrt{1 + 8 \times K_{\text{dim}} \times ([\text{Stop}] + 2 \times [\text{Bif}]) \}}}$$

N,N'-(1,6-Hexadiyl)-bis-(2-ureido-6-tridecyl-4-pyrimidinone) 3. A suspension of 6-tridecylisocytosine **1** (11.20 g, 40 mmol) in dry pyridine (80 mL) and toluene (10 mL) was heated to reflux. A clear solution was obtained, and 10 mL of solvent were distilled off. After cooling, 1,6-hexane diisocyanate (3.33 g, 19.8 mmol) was added via a syringe, and the solution was boiled under reflux for 72 h. After cooling, the solution was poured into acetone (1 L), and the suspension filtered. The crude product was purified by column chromatography (flash silica, 5% ethanol in chloroform, R_f = 0.10–0.30), and impure fractions were purified again analogously. The pure fractions were combined, and the solvent volume reduced to 100 mL. The solution was poured into acetone, and the white precipitate that formed filtered and dried, yield 66%. This material was of sufficient purity to obtain satisfactory elemental analysis. $^1\text{H-NMR}$ (CDCl_3) δ : 13.18 (s, 2H), 11.88 (s, 2H), 10.18 (s, 2H), 5.82 (s, 2H), 3.23 (s, 4H), 2.45 (t, 4H), 1.63 (d, 8H), 1.25 (m, 44H), 0.88 (t, 6H). $^{13}\text{C-NMR}$ (CDCl_3) δ : 173.2, 156.6, 154.7, 152.4, 105.8, 40.0, 32.7, 31.9, 29.4, 29.3, 29.1 (overlapping peaks), 26.8, 22.7, 14.1. IR (KBr) ν : 3220, 3139, 3030, 2924, 2852, 2605, 1699, 1660, 1586, 1525, 1460, 1252 cm^{-1} . Anal. calcd. for $\text{C}_{42}\text{H}_{74}\text{N}_8\text{O}_4$: C, 66.81; H, 9.88; N, 14.84. Found: C, 67.25; H, 9.77; N, 14.62.

The product was however purified more intensively by the following procedure that was applied repeatedly. The product was dissolved in hot chloroform, and two volumes ethyl acetate were added. Cooling caused the product to precipitate as a white powder, with a recovery of ~ 95% in every step. The specific viscosity of a 40 mM solution was monitored as a function of purification steps, and from the chain stopper experiments performed with those fractions, the purity with respect to monofunctional compounds (presumably **6**) was determined. After 5 precipitations, the specific viscosity of a 40 mM solution in chloroform had reached a maximum, and attempts to obtain a higher

specific viscosity by more precipitations were unsuccessful, and led to deterioration instead. The specific viscosities, and the estimated purity are given in the table below.

purification steps	crude product a	after column b	after 3 precipitations c	after 4 precipitations c	after 5 precipitations c
specific viscosity	low	6.50	10.05	11.14	11.67
estimated purity ^d	90%	99.6%	99.94%	99.96%	99.98%

^a product after precipitation of reaction mixture in acetone; ^b product after precipitation in acetone after column chromatography; ^c product after precipitations from hot chloroform/ethyl acetate; ^d estimated from chain stopper experiments and ¹H-NMR.

O-Alkylated isocytosine 5 (2-butylureido-4-dodecyloxy-6-tridecyl-pyrimidine). The reaction mixture of the synthesis of isocytosine 1 (see chapter 4) was cooled, and diluted with hexane and water. The white powder was filtered (isocytosine 1), and a fine white powder separated from the filtrate during filtration. This powder was filtered off, and consisted of a mixture of 1 and 5. Dissolution in chloroform, and filtration removed insoluble 1. The filtrate was evaporated to dryness, and the white powder crystallized from hexane, giving analytically pure 5 as white microneedles (2.37 g). ¹H-NMR (CDCl₃) δ: 5.77 (s, 1H), 5.36 (br, 2H), 3.90 (t, 2H), 2.31 (t, 2H), 1.69 (t, 2H), 1.58 (t, 2H), 1.25 (br, 38H), 0.88 (t, 6H). ¹³C-NMR (CDCl₃) δ: 166.6, 161.9, 153.7, 100.0, 76.0, 40.4, 36.2, 30.8, 28.6, 28.5–28.3 (multiple peaks), 27.0, 26.2, 25.9, 21.6, 13.1.

References and Footnotes

- (a) P.J. Flory, *Principles of Polymer Chemistry*, Cornell University Press, Ithaca, **1953**, (b) P.C. Painter, M.C. Coleman, *Fundamentals of Polymer Science*, Technomic Publishing Company, Lancaster, USA, **1994**, (c) U.W. Gedde, *Polymer Physics*, Chapman and Hall, London, **1995**.
- (a) C. Hilger, M. Dräger, R. Stadler, *Macromolecules*, **1992**, *25*, 2498, (b) A. Aggeli, M. Bell, N. Boden, J.N. Keen, P.F. Knowles, T.C.B. McLeish, M. Pitkeathly, S.E. Radford, *Nature*, **1997**, *386*, 259.
- F.W. Billmeyer Jr, *Textbook of Polymer Science*, 3rd Edn, Wiley Interscience, New York, **1984**.
- (a) M. Müller, A. Dardin, U. Seidel, V. Balsamo, B. Iván, H.W. Spiess, R. Stadler, *Macromolecules*, **1996**, *29*, 2577.
- Reviewed by C.T. Imrie in *Trends in Polymer Chemistry*, **1995**, *3*, 22, (b) U Kumar, T. Kato, J.M.J. Fréchet, *J. Am. Chem. Soc.*, **1992**, *114*, 6630, (c) T. Kato, H. Kihara, T. Uryu, A. Fujishima, J.M.J. Fréchet, *Macromolecules*, **1992**, *25*, 6836, (d) S. Malik, P.K. Dhal, R.A. Mashelkar, *Macromolecules* **1995**, *28*, 2159, (e) T. Kato, N. Hirota, A. Fujishima, J.M.J. Fréchet, *J. Polym Sci., part A: Polym. Chem.*, **1996**, *34*, 57.
- For a discussion of self-organization in biological systems, see: (a) M. Eigen, L. DeMayer, *Naturwissenschaften*, **1966**, *53*, 50, (b) M. Eigen, *Naturwissenschaften*, **1971**, *58*, 465. For a review on the assembly of the tobacco mosaic virus, see: A. Klug, *Angew. Chem. Int. Ed. Engl.*, **1983**, *22*, 565.

- 7) (a) J.-M. Lehn, *Angew. Chem. Int. Ed. Engl.*, **1988**, 27, 89, (b) J.-M. Lehn, *Angew. Chem. Int. Ed. Engl.*, **1990**, 29, 1304, (c) C. Fouquey, J.-M. Lehn, A.-M. Levelut, *Adv. Mater.*, **1990**, 2, 254, (d) J.-M. Lehn, *Makromol. Chem. Makromol. Symp.*, **1993**, 69, 1.
- 8) (a) A recent example of a unidirectional polymer chain undergoing scission/recombination, based on a complex of copper and an organic molecule with oxygen ligands: P. Terech, *Progr. Colloid. Polym. Sci.*, **1996**, 102, 64, (b) P. Terech, V. Schaffhauser, P. Maldivi, J.M. Guenet, *Langmuir*, **1993**, 8, 2104. This system, however, is rigid and forms a gel.
- 9) M. Möller, J. Omeis, E. Mühleisen, in: *Reversible Polymeric Gels and Related Systems*, Ed. P.S. Russo, *American Chemical Society Symposium series 350*, Chapter 7. (American Chemical Society, Washington DC, **1987**).
- 10) C.D. Eisenbach, A. Gödel, M. Terskan-Reinold, U.S. Schubert, *Makromol. Chem. Phys.* **1995**, 196, 1077.
- 11) (a) C. Alexander, C.P. Jariwala, C.-M. Lee, A.C. Griffin, *Macromol. Chem., Macromol. Symp.*, **1994**, 77, 283, (b) P. Bladon, A.C. Griffin, *Macromolecules*, **1993**, 26, 6604, (c) C.-M. Lee, C.P. Jariwala, A.C. Griffin, *Polymer*, **1994**, 35, 4550, (d) C.B.St. Pourcain, A.C. Griffin, *Macromolecules*, **1995**, 28, 4116.
- 12) (a) C.P. Lillya, R.J. Baker, S. Huette, H.H. Winter, Y.-G. Lin, J. Shi, L.C. Dickinson, J. C.W. Chien, *Macromolecules*, **1992**, 25, 2076, (b) Y. Ducharme, J.D. Wuest, *J. Org. Chem.* **1988**, 53, 5787.
- 13) (a) C. Fouquey, J.-M. Lehn, A.-M. Levelut *Adv. Mater.*, **1990**, 2, 254 (b) M. Kotera, J.-M. Lehn, J.-P. Vigneron, *J. Chem. Soc. Chem. Commun.*, **1994**, 197.
- 14) T. J. Murray, S.C. Zimmerman, *J. Am. Chem. Soc.*, **1992**, 114, 4010.
- 15) Alkyl substitution is favorable, because these substituents favor the 4[1H]-pyrimidinone tautomer, which dimerizes more strongly by a DDAA-motif than the DADA motif of the pyrimidin-4-ol tautomer (see chapter 4). Furthermore, compounds with alkyl substituents show better solubility.
- 16) We have tried to diminish the presence of small amounts of water by drying the isocytosine thoroughly, using dry solvent, working under an atmosphere of dry nitrogen, and drying the solution of isocytosine in pyridine by azeotropic distillation with toluene.
- 17) For the principles of Electrospray Ionization Mass Spectrometry, and its potential and application as analytical tool, the reader is referred to: R. Saf, C. Mirtl, K. Hummel, *Acta Polymer.*, **1997**, 48, 513.
- 18) Dodecyl bromide was still present in the crude keto-ester used.
- 19) (a) M.E. Cates, *J. Phys. Chem.*, **1990**, 94, 371, (b) M.E. Cates, S.J. Candau, *J. Phys.: Condens. Mater.*, **1990**, 2, 6869, (c) S. J. Candau, A. Khatory, F. Lequeux, F. Kern, *J. de Phys. IV, Colloque C1, Suppl. on J. de Phys. II*, **1993**, 3, 197, (d) C. Dammer, P. Maldivi, P. Terech, J.-M. Guenet, *Langmuir*, **1995**, 11, 1500.
- 20) For macromolecular polymers, the well-known empirical Kuhn-Mark-Houwink-Sakurada equation ($\eta_{\text{intrinsic}} = p \times DP^a$) holds. The intrinsic viscosity is the limit to zero concentration of η_{sp} divided by concentration. Hence, the equation holds for the non-entangled concentration domain. References for the Kuhn-Mark-Houwink-Sakurada equation: 1a, 1b, and: H.-G. Elias, *An Introduction to Polymer Science*, VCH, Weinheim (Germany), **1997**, p. 200–213. These supramolecular polymers, however, have an intrinsic viscosity of zero, and hence the Mark-Houwink relation does not hold. We therefore tried to fit our data assuming a similar relation between specific viscosity and the degree of polymerization, and the data fitted well.

The same scaling relation was also used by Cates for his model of reversible breakable polymers.

- 21) (a) W. Noll, *Chemistry and Technology of Silicones*, Academic Press, New York, **1968**, (b) C. Eaborn, *Organosilicon Compounds*, Butterworth Sci. Publ., London, **1960**, (c) C. Eaborn, R.W. Bott, in: *Organometallic Compounds of the group IV elements*, Vol.1, p 105, New York, **1960**, (d) F.O. Stark, J.R. Fallender, A.P. Wright, in: *Comprehensive organometallic Chemistry*, Ed. Sir G. Wilkinson, Vol. 2, p 305, New York, **1982**, (e) E. Lukevics, *Russ. Chem. Chem. Revs.*, **1977**, 46(3), 264, (f) I. Yilgör, J.E. Mc Grath, *Polysiloxane Containing Copolymers; A survey of Recent Development*, **1988**, (g) H.R. Kricheldorf, *Silicon in Polymer Synthesis*, Germany, **1996**.
- 22) The synthesis of a keto-ester with an alkene endgroup is reported: S.N. Huckin, L. Weiler, *J. Am. Chem. Soc.*, **1974**, 96, 1082.
- 23) S.C. Zimmerman, W.-S. Kwan, *Angew. Chem. Int. Ed. Engl.*, **1995**, 34, 2404.
- 24) (a) R.P. Sijbesma, F.H. Beijer, L. Brunsveld, B.J.B. Folmer, J.H.K.K. Hirschberg, R.F.M. Lange, J.K.L. Lowe, E.W. Meijer, *Science*, **1997**, 278, 1601, (b) J.H.K.K. Hirschberg, F.H. Beijer, R.P. Sijbesma, H.W.A. van Aert, E.W. Meijer, manuscript in preparation.
- 25) (a) T. McLeish, *Science*, **1997**, 278, 1577, (b) F. Lequeux, S. Candau in: *Theoretical Challenges in the Dynamics of Complex Fluids*, Ed. T. McLeish, Kluwer, Dordrecht (The Netherlands), **1997**.

Chapter 7

Crystal Engineering of Melamine–Uracil Complexes

Abstract:

Melamine forms crystalline complexes with uracil or thymine derivatives in either a 1:2 or a 1:3 stoichiometry.

*In the 1:2 crystalline complexes, as revealed by single crystal X-ray diffraction, two DAD sites of melamine are complexed by the ADA sites of two uracil molecules, thus forming a V-shaped wedge. Additional hydrogen bonding between the 1:2 complexes leads to the formation of herringbone-like infinite chains in the complexes with 1-N-methyl-6-tridecyluracil **4** and 1-N-methyl-6-hydroxymethyluracil **6**. In the 1:3 crystalline complexes, the three DAD sites of melamine are complexed by the ADA arrays of three uracil molecules, resulting in a rosette-like structure.*

6-Hydroxymethyl substituted uracils, which have functional groups capable of additional hydrogen bonding interactions, form cocrystals with melamine in a 1:2 as well as in a 1:3 ratio. In these cocrystals, infinite hydrogen bonding networks are present. Melamine and N-propylthymine form exclusively a 1:3 complex, which has a rosette-like structure with threefold symmetry. Because all potential hydrogen bond donors are involved in the rosette formation, there are no hydrogen bonding interactions between the 1:3 rosette-like structures. The exclusive formation of 1:3 complexes of melamine with N-propylthymine has been rationalized by the fact that the N-1-propyl and the 5-methyl substituents shield one acceptor site of two potential sites of the carbonyl groups in N-propylthymine.

7.1 Introduction

As early as 1962, it was proposed that 2,4,6-triamino-*s*-triazine (melamine) and 2,4,6-trihydroxy-*s*-triazine (cyanuric acid) form an infinite, two-dimensional lattice upon mixing, due to hydrogen bonding interactions in two directions (figure 7.1).¹

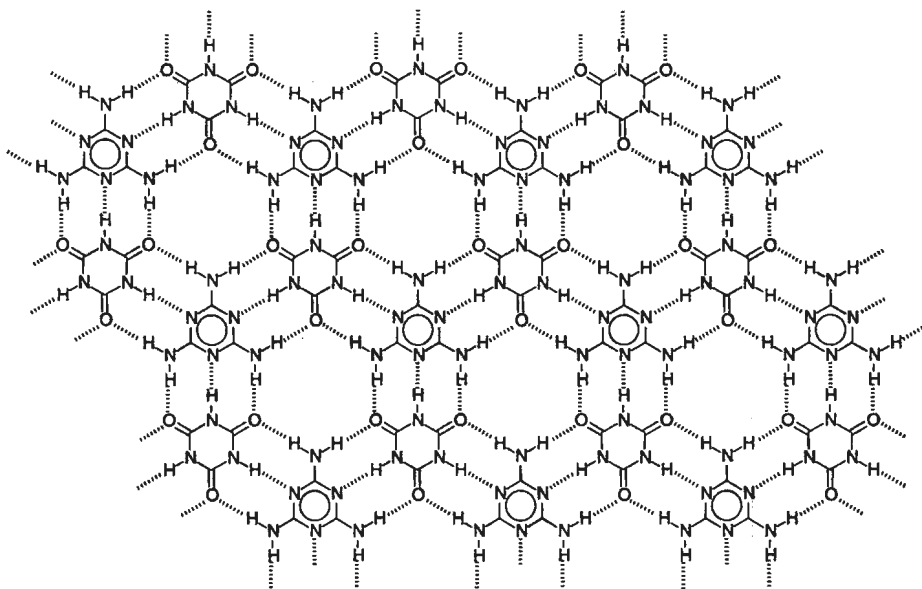


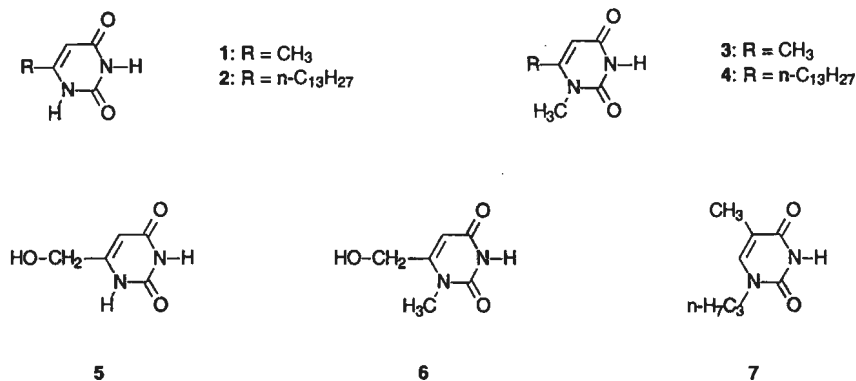
Figure 7.1: Proposed infinite, two-dimensional lattice formed by melamine and cyanuric acid.

Until now, the proposed structure could not be confirmed due to the impossibility to obtain crystals of sufficient quality for X-ray analysis.² A crystal structure of the hydrochloric acid salt of melamine and cyanuric acid has been reported.³ Model studies by several groups have been performed to mimic structures using this hydrogen bonding pattern. Whitesides⁴ has investigated several complexes using parts of this infinite, two-dimensional melamine–cyanuric acid lattice. If melamines and cyanuric acid (or barbiturates) were substituted, a variation of linear tapes, crinkled tapes, and rosettes (= cyclic hexamers) could be obtained. A variation of the linear tape, as well as a cyclic hexamer, were described by Lehn et al.⁵ Kunitake reported the formation of several helical and tube-like nanostructures from the complexation of di(alkyl) substituted melamines with a diimide.⁶ Rebek has reported strong complexation of melamine by a tris-imide acting as a molecular cleft.⁷

However, only few complexes containing parent melamine have been reported. Whitesides⁸ and Mingos⁹ have reported crystal structures of complexes of melamine and imides. In these complexes, the stoichiometry of melamine, having three DAD arrays, and the

imide, with its ADA array, is 1:2. As a consequence, one of the three DAD sites of melamine is not complexed with the ADA array of the imide, and a herringbone-structure is formed. Ronald Lange showed that 1:1 and 1:2 complexes were formed when melamine was cocrystallized with succinimide and glutarimide, respectively.¹⁰ Recently, Takuda also reported the formation of a 1:1 complex between melamine and succinimide.¹¹ Despite the resemblance in the crystal structures of both 1:1 complexes between melamine and succinimide, polymorphism is present.

Ronald Lange showed that it was possible to molecularly dissolve melamine in the alternating copolymer of styrene and maleimide, up to a 1:3 ratio of melamine and imide groups.¹² A 1:3 rosette-like architecture of three imides around the melamine molecule was proposed. However, up to our model studies,^{10b} no examples of crystalline 1:3 complexes with melamine were disclosed, while the C_3 symmetry of melamine suggests that it should be possible to obtain a 1:3 complex with a rosette-like structure. With a variety of ADA-units in the form of uracil derivatives at hand (compounds 1–7, see chapter 2 for their preparation), cocrystallization with melamine from water or other polar solvents was attempted in order to obtain a crystalline 1:3 complex. The complexes were studied by single crystal X-ray diffraction.



7.2 Results

7.2.1 Cocrystallization of melamine with uracils

Cocrystallization experiments were generally performed in water, because this is a solvent in which melamine is moderately soluble. Furthermore, water is known to be an excellent solvent for such cocrystallizations, due to hydrophobic effects. When uracils were too insoluble in water, mixtures of water and ethanol were used.

Attempts to obtain X-ray quality crystalline complexes of melamine with uracils 1–3 were unsuccessful. Cooling of a dilute solution of melamine and uracil 1 in a 1:3 ratio in hot

water quickly resulted in the precipitation of a fine precipitate. The melamine–uracil ratio of this precipitate did not have a constant and discrete ratio, indicating precipitation of a mixture of crystals. The solubility of melamine and 6-alkyluracil **2** in aqueous ethanol differed so much that only the uracil precipitated. With *N*-1-methylated uracils **3** and **4**, only crystalline complexes with a 1:2 stoichiometry were formed. The crystals of the melamine complex with uracil **3** had the appropriate size for X-ray analysis, yet their quality was judged insufficient because they were bent and twinned. The crystals of the 1:2 complex of melamine and uracil **4** were small and of poor quality, yet good enough to obtain a reasonably well-refined single X-ray crystal structure.

With the expectation that higher solubility would improve the chance of obtaining good crystals, melamine was cocrystallized with the water soluble uracils **5** and **6**, and large plate- and needle shaped crystals, respectively, indeed separated slowly. ¹H-NMR in DMSO-*d*₆ indicated that both these complexes had a 1:3 stoichiometry. However, upon standing of the 1:3 crystals in the mother liquor, these crystals gradually redissolved, and, simultaneously, 1:2 complexes crystallized. Although we did not study elaborately the factors that determine the choice for the formation of 1:2 and 1:3 crystals, the experiments performed showed a general trend that the 1:3 complexes formed initially when crystallization experiments were performed at high concentrations, or with melamine–uracil ratios exceeding 1:3, while 1:2 complexes resulted at low concentrations or with melamine–uracil ratios below 1:3.

In search of a compound that would form 1:3 complexes exclusively, our attention was turned to the moderately water soluble *N*-propylthymine **7**. Cocrystallization in water of melamine with **7** in various ratios between 1:1 and 1:5 resulted in the formation of crystalline complexes with a 1:3 stoichiometry, sometimes accompanied by crystals of melamine. Since the crystals of the 1:3 complex obtained from water were severely twinned and irregular (bent) and therefore judged to be unsuitable for X-ray analysis, cocrystallization experiments in ethanol (96%) were attempted. These experiments were initially frustrated by the insolubility of the crystals of melamine, and the melamine and *N*-propylthymine **7** were first thoroughly grinded together in a mortar in a 1:3 ratio. Now, we were able to obtain a homogeneous solution in ethanol. Slow cooling of this solution gave crystals of sufficient quality for X-ray crystal structure determination.

7.2.2 Crystal structures

The crystal structure of the 1:2 complex of melamine and 1-*N*-methyl-6-tridecyluracil **4** features V-shaped wedges, consisting of one melamine and two uracil molecules. These wedges form herring-bone like infinite chains by two single hydrogen bonds of the two remaining melamine N–H donor sites to two remaining uracil carbonyl acceptor sites at C4 (figure 7.2). Because all the available hydrogen bond donor functional groups are involved in

the formation of the herring-bone structure, one of the melamine ring nitrogen acceptor sites remains unused. The herring-bone like chains form layers, with two adjacent chains in an antiparallel fashion. These layers form a plate-like crystal; the chains lie slightly translated above each other, and are also antiparallel.

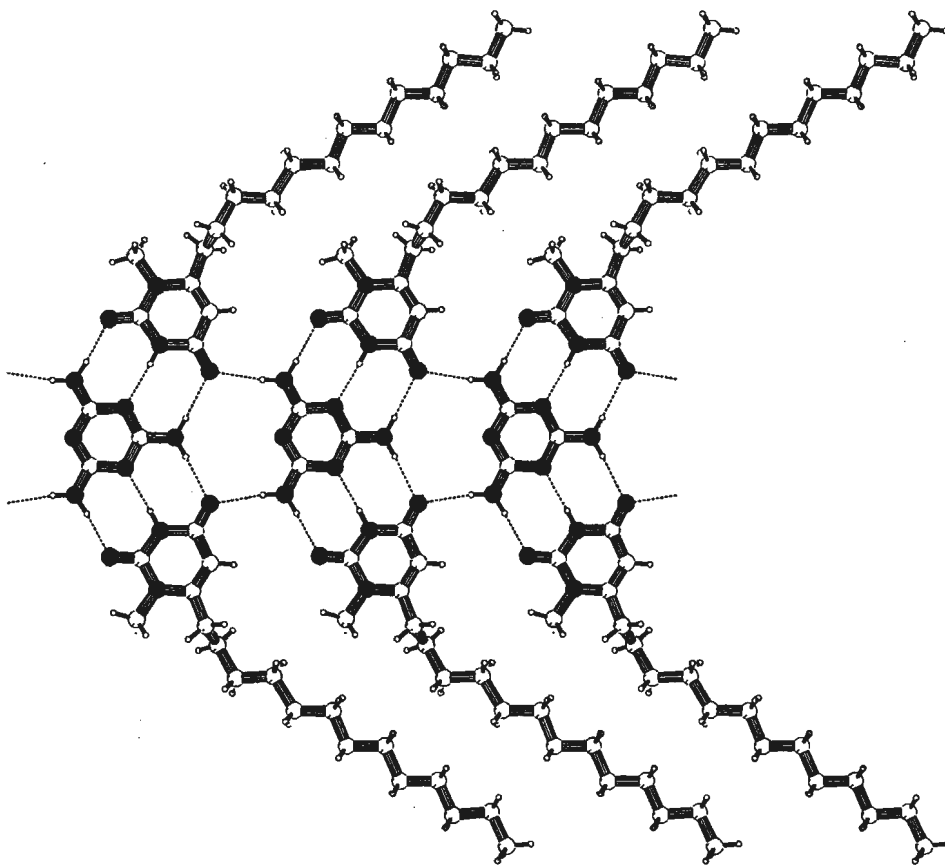


Figure 7.2: PLUTON representation of the crystal structure of the 1:2 cocrystal **melamine•4**, featuring the herringbone structure formed by an infinite chain of V-shaped wedges of one melamine and two uracil molecules.

The crystal structure of the initially formed 1:3 complex of melamine and 6-hydroxymethyluracil **5** could not be determined by single crystal X-ray diffraction, because the plate-like crystals were too thin. The 1:2 complex of melamine and **5**, which formed upon prolonged standing in the mother liquor, appeared to contain also three molecules of crystal water per unit. In the crystal, melamine and two uracil molecules form a V-shaped wedge, with two DAD–ADA hydrogen bonding contacts (figure 7.3a). These wedges form infinite chains by dimerization of uracil via two hydrogen bonds. The infinite chains are connected

via hydrogen bonds of the uracil hydroxymethyl to a uracil carbonyl group in another chain, thus forming a (pleated) plane (figure 7.3b). These pleated planes fit on top of each other, and the planes are connected via an extensive hydrogen bonding network formed by the hydroxymethyl groups of the uracil molecules, and three molecules of crystal water (figure 7.3c). These water molecules form hydrogen bonds with the remaining two melamine N-H donors and the remaining melamine ring nitrogen atom, and with a uracil carbonyl at C4 of one of two uracil molecules.

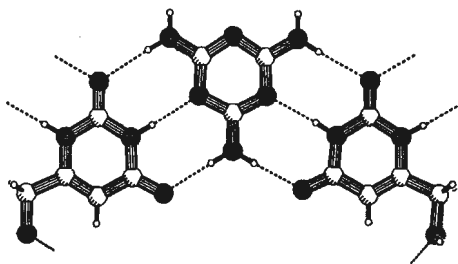


Figure 7.3a: PLUTON representation of the crystal structure of the 1:2 cocrystal **melamine•5**, featuring a V-shaped wedge formed by one melamine molecule and two molecules of uracil **5**.

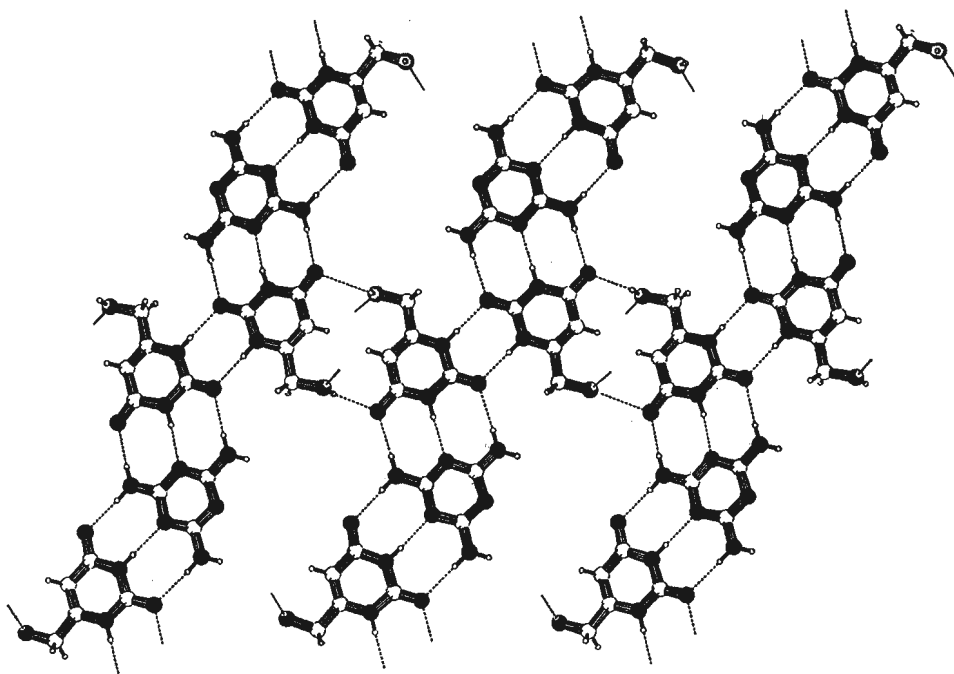


Figure 7.3b: PLUTON representation of the crystal structure of the 1:2 cocrystal **melamine•5**, featuring formation of a pleated plane by uracil dimerization and interaction between the chains. The three molecules of crystal water have been omitted for clarity.

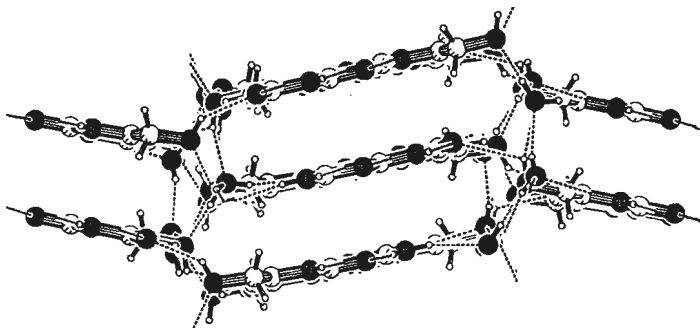


Figure 7.3c: PLUTON representation of the crystal structure of the 1:2 cocrystal **melamine•5**. View in the direction of the infinite chains, showing stacking of the complexes. An extensive network of hydrogen bonds of hydroxymethyl groups with three molecules of crystal water is present in the lattice.

The 1:2 complex of melamine and 1-*N*-methyl-6-hydroxymethyluracil features a herringbone structure of V-shaped wedges of melamine and two uracil molecules (figure 7.4a), similar as observed in the previously discussed crystal structure of melamine and 1-*N*-methyl-6-tridecyluracil. In this crystal structure, the hydroxymethyl groups of other, parallel, herring-bone like structures form hydrogen bonds to the remaining melamine ring nitrogen atom acceptor site. This results in a pleated sheet structure (figure 7.4b).

The hydrogen bonds of the hydroxyl group to the melamine ring nitrogen are significantly longer ($D-H\cdots A$ distance is $3.164(2) \text{ \AA}$) than the other hydrogen bonds ($D-H\cdots A$ distance in the range $2.82\text{--}2.97 \text{ \AA}$), suggesting the former hydrogen bonds are weaker.

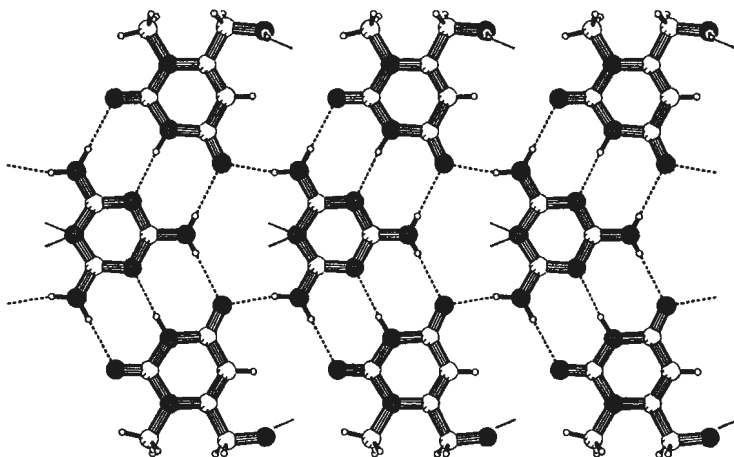


Figure 7.4a: PLUTON representation of the crystal structure of the 1:2 cocrystal **melamine•6**, featuring a herringbone structure formed by an infinite chain of V-shaped wedges of melamine and two uracil molecules.

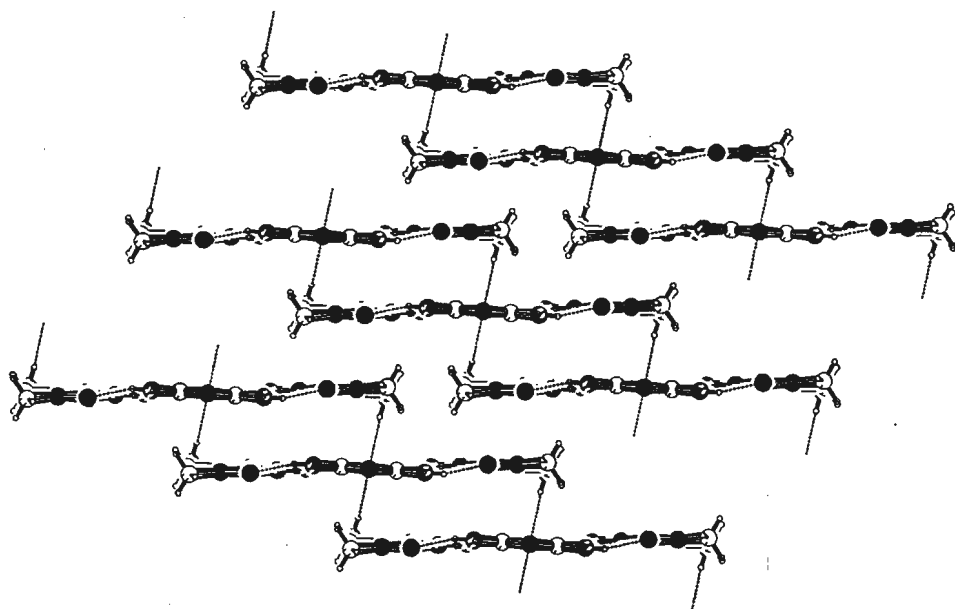


Figure 7.4b: PLUTON representation of the crystal structure of the 1:2 cocrystal **melamine•6**, with a view in the direction of the herringbones, showing the connection of the herring bones.

The crystal structure of the 1:3 complex between 1-*N*-methyl-6-hydroxymethyluracil **6** and melamine features a 1:3 rosette-like architecture (figure 7.5a). The V-wedge fragment found in the 1:2 cocrystal forms a part of the 1:3 rosette, and hence there is no symmetry in a 1:3 rosette-like structure. These 1:3 rosette-like structures form a pleated plane by connection via a hydrogen bond from a hydroxymethyl group to a uracil carbonyl acceptor site in one direction, and via a hydrogen bond between two hydroxymethyl groups of two different 1:3 rosette-like structures in the other direction (figure 7.5b). Alternatingly on top and below of these 1:3 rosette-like structures in one pleated plane, another 1:3 rosette-like structure is present with different orientation, connected by two single hydrogen bonds of hydroxymethyl groups (figure 7.5c). More hydrogen bonds between hydroxymethyl substituents result in a three-dimensional network.

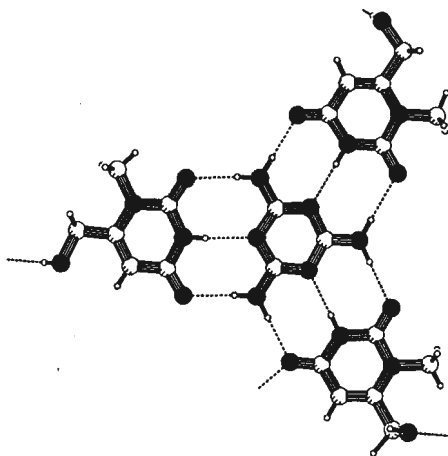


Figure 7.5a: PLUTON representation of the crystal structure of the 1:3 cocrystal **melamine•6**, featuring a rosette-like structure of one melamine and three uracil molecules.

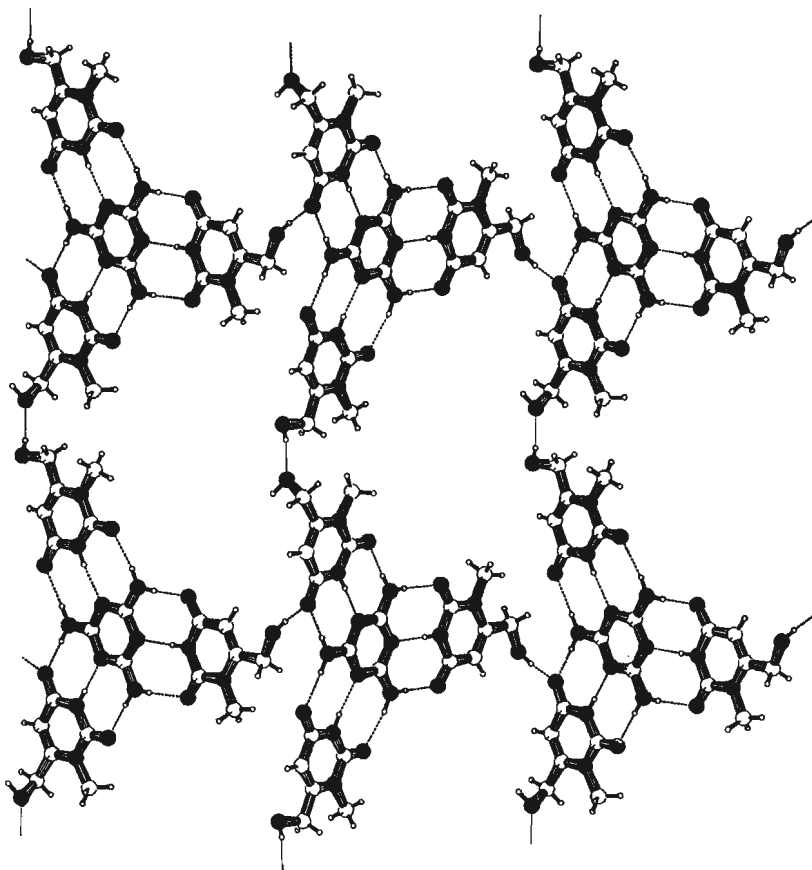


Figure 7.5b: PLUTON representation of the crystal structure of the 1:3 cocrystal **melamine•6**, featuring a pleated plane structure of rosette-like structures.

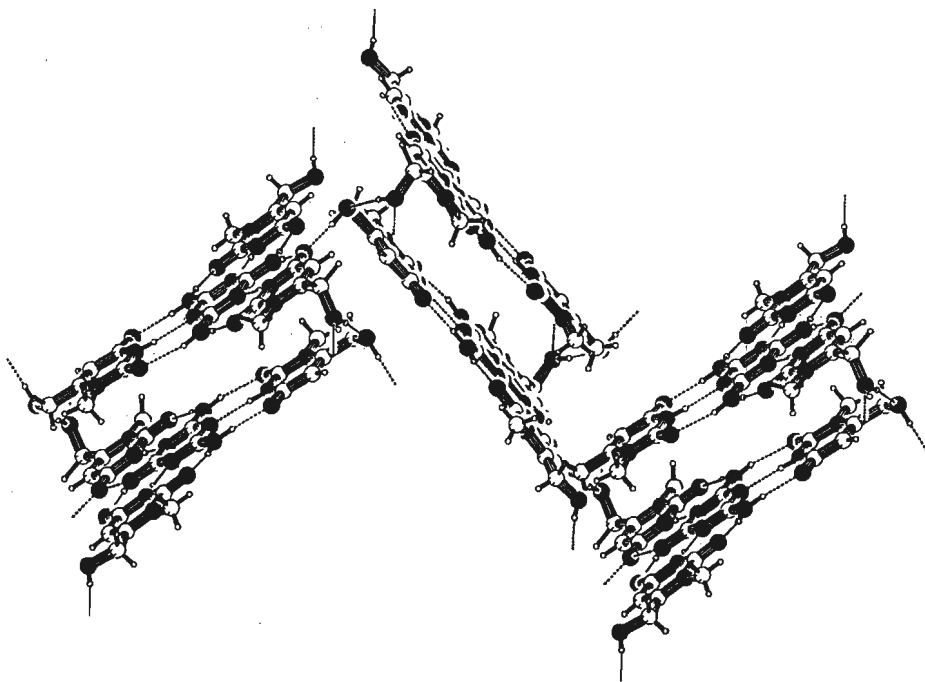


Figure 7.5c: PLUTON representation of the crystal structure of the 1:3 cocrystal **melamine•6**, featuring alternating packing on top and below of 1:3 rosette-like structures.

C_3 -symmetrical and planar rosette-like structures of one melamine and three *N*-propylthymine molecules are present in the crystal structure of the 1:3 complex of melamine and *N*-propylthymine (figure 7.6a). Since all hydrogen bond donors are involved in the formation of the 1:3 rosette-like structures, there are no hydrogen bonding interactions between the 1:3 rosette-like structures. Layers are formed by hexagonal packing in the *a,b* plane, around sixfold axes in the *c*-direction and perpendicular to the layers (figure 7.6b). The next layer is centered around the 6_3 -axis, but it is rotated by 60 degrees (figure 7.6c). In this way, infinite channels are formed, which are filled with disordered solvent, and the propyl chains, which are disordered over four positions.

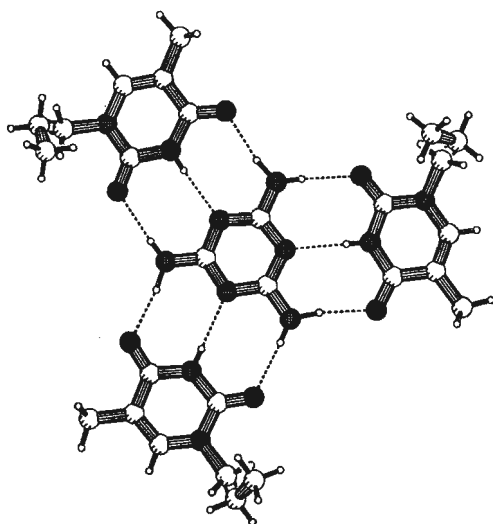


Figure 7.6a: PLUTON representation of the rosette-like structures with threefold symmetry in the crystal structure of the 1:3 cocrystal **melamine•7**.

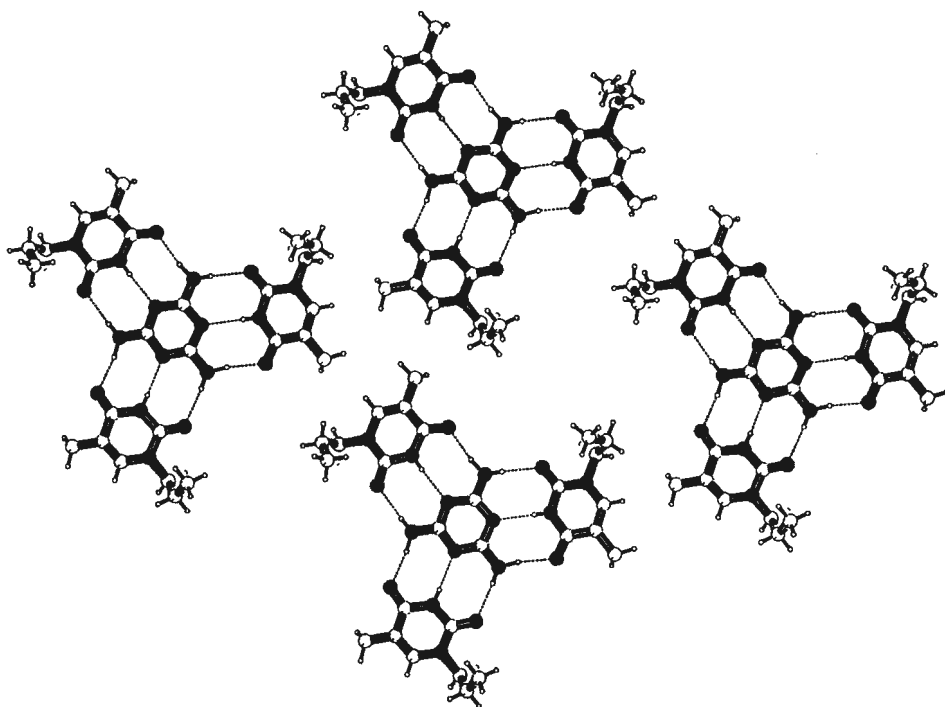


Figure 7.6b: PLUTON representation of the crystal structure of the 1:3 cocrystal **melamine•7**, featuring the hexagonal packing of the rosette-like structures in the in the a,b-plane.

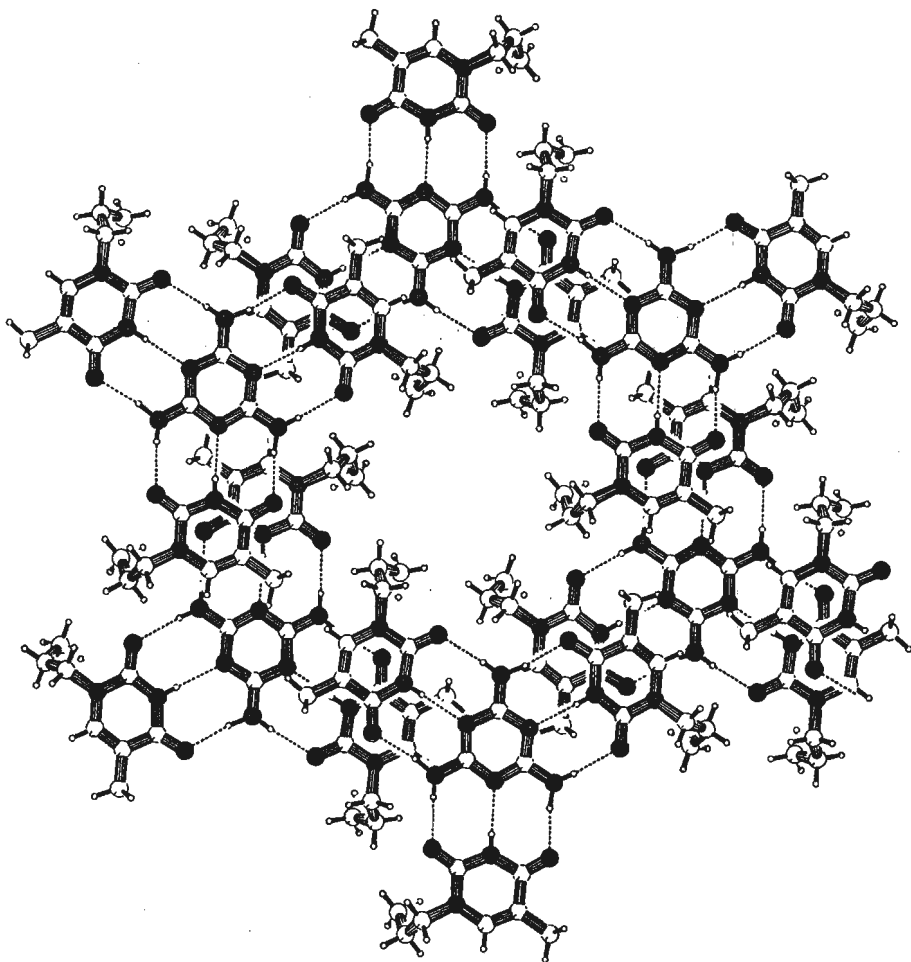


Figure 7.6c: PLUTON representation of the crystal structure of the 1:3 cocrystal **melamine•7**, with a view perpendicular on the infinite channels.

7.3 Discussion of Complex Stoichiometries

Melamine forms crystalline complexes with various imides in a 1:1, 1:2, as well as a 1:3 stoichiometry. The complex stoichiometry is very dependent on the nature of the imide: (two different polymorphs of) 1:1 complexes are formed with succinimide,^{10,11} a 1:2 complex is formed with glutarimide,¹⁰ with dibromobarbituric acid,⁸ and with a ADA array of a metal chelate.⁹ Complexes in a 1:2 as well as a 1:3 stoichiometry result with uracil and thymine derivatives, indicating the influence of structural variations even within one class of compounds. No well-defined crystalline complexes with a discrete melamine/uracil ratio are

formed with uracils **1** and **2**, *N*-1-unsubstituted and without a 6-hydroxymethyl substituent, while *N*-1-methylated uracils **3** and **4** give complexes with a 1:2 stoichiometry only. With 6-hydroxymethyl substituted uracils **5** and **6**, both 1:2 as well as 1:3 complexes result. Most strikingly, melamine forms exclusively 1:3 complexes with *N*-propylthymine **7**. We recently reported an explanation for this trend in complex stoichiometries.^{10b}

In the complexes, all potential hydrogen bonding donors are involved in the hydrogen bonding scheme. However, potential acceptor sites are sometimes not involved in the hydrogen bonding scheme. The discrepancy between potential donor and acceptor sites seems to drive the complex stoichiometry: the stoichiometry with a minimal discrepancy between the number of donor and acceptor sites is favored. The availability of the acceptor sites for hydrogen bonding is strongly influenced by the geometry of the imide, and by substituents.

In the 1:2 complex of melamine with 6-hydroxymethyluracil **5**, all uracil carbonyls are involved in hydrogen bonding twice; also the three melamine ring nitrogen acceptor sites are bonded.¹³ In the 1:2 complex of melamine with 1-*N*-methyl-6-tridecyluracil **4** with the herring-bone structure, one melamine ring nitrogen acceptor site is not involved in hydrogen bonding, because all potential donors are used in the formation of the herring-bone. Of the four potential acceptor sites of the uracil carbonyl groups, three sites are involved in hydrogen bonding: the acceptor site not hydrogen bonded is the one adjacent to the *N*-1-methyl substituent. Also in the other 1:2 complexes with a herring-bone like structure, of melamine and 1-*N*-methyl-6-hydroxymethyluracil **6**, and of melamine and glutarimide,^{10b} one of the four potential acceptor sites (of two carbonyl groups) in the imide is not involved in hydrogen bonding. In the 1:2 complex with uracil **6**, this is also the carbonyl group adjacent to the *N*-1-methyl substituent. While one melamine acceptor site is not involved in the hydrogen bonding scheme in the 1:2 complexes of melamine with *N*-1-methyl-6-tridecyluracil **4** (and with glutarimide^{10b}), the similar melamine ring nitrogen in the herring-bone like 1:2 complex of melamine and 1-*N*-methyl-6-hydroxymethyluracil **6** accepts a hydrogen bond from the hydroxymethyl substituent of **6**, while the hydroxy acceptor site remains unused. The formation of a hydrogen bond to the melamine acceptor site is in line with the empirical rule described by Etter,¹⁴ stating that hydrogen bonds are generally formed from the strongest donor to the strongest acceptor: the melamine ring nitrogen is a much stronger acceptor than the oxygen of the hydroxymethyl.¹⁵

In the 1:3 complex of melamine with *N*-propylthymine **7** with the rosette-like structure, every uracil carbonyl group is involved in hydrogen bonding only once. In the 1:3 structure with 6-hydroxymethyluracil **6**, the carbonyl groups of two uracil molecules also accept only once, while every third uracil molecule in a 1:3 rosette-like structure has three acceptor sites of two carbonyls used, owing to an additional hydrogen bond from a hydroxymethyl. From these results, combined with the structures reported by Lange,^{10a-b} the following guidelines are deduced:

- (i) Complexes with a 1:2 stoichiometry result when one of the potential four carbonyl acceptor sites of the two carbonyls of the imide is shielded by a substituent, as in *N*-1 methylated uracils **3** and **4**.
- (ii) Complexes with a 1:3 stoichiometry are formed when two of four potential carbonyl acceptor sites of the two carbonyls of the uracil are shielded by adjacent substituents at *N*-1 and at the 5-position, as in *N*-propylthymine **7**.
- (iii) Additional hydrogen bonding interactions in hydroxymethyl substituted uracils **5** and **6** cause that both the 1:3 stoichiometry and the 1:2 stoichiometry are observed.

7.4 Conclusion

The stoichiometry of supramolecular complexes of melamine and uracils can be tuned by the accessibility of the carbonyl acceptor sites of the uracil molecules, through introducing substituents at *N*-1 and at the 5-position. This result shows that uncovering assembly rules governing the crystallization of a distinctive group of related complexes is a useful approach to the design of crystalline solids, and hence represents a distinctive step forward towards crystal engineering.¹⁶

7.5 Experimental Section

General methods. The synthesis of uracil molecules has been described in chapter 2. Melamine was recrystallized from water with filtering hot before use in the cocrystallizations.

Cocrystallizations. Unless otherwise stated, cocrystals were obtained by recrystallization from excess hot water by slow cooling, followed by slow evaporation in air. The crystals of the 1:3 melamine-*N*-propylthymine complex from ethanol and from water have identical IR spectra.

X-ray single crystal structure analyses. Crystals suitable for X-ray structure determination were mounted on a Lindemann-glass capillary and transferred to an Enraf-Nonius CAD4-T diffractometer on rotating anode (MoK α radiation, graphite monochromator, $\lambda = 0.71073$ Å, $T = 150$ K). Data were corrected for Lorentz-polarization effects and for linear instability in the periodically measured reference reflections, but not for absorption. The unit-cell parameters were checked for the presence of higher lattice symmetry.¹⁷ Unless otherwise stated, the structures were solved by automated direct methods (SHELXS-86¹⁸), and refined on F^2 by full-matrix least-squares techniques (SHELXL-93¹⁹). No observance criterion was applied during refinement. All hydrogen atoms were located on different Fourier maps; their coordinates were included as parameters in the refinement. All non-hydrogen atoms were refined with anisotropic thermal parameters. Hydrogen atoms were refined with a fixed isotropic thermal parameter related to the value of the equivalent isotropic displacement parameter of their carrier atoms.

Crystal data for 1:2 complex melamine•4: C₃H₆N₃•2 C₁₈H₃₂N₂O₂; $M_r = 743.05$, colourless, plate-shaped crystal (0.01 x 0.1 x 0.3 mm), monoclinic, space group C2/c (no. 15) with $a = 23.843$ (7), $b = 8.4059$ (16), $c = 20.874$ (3) Å, $\alpha = 90$, $\beta = 94.038$ (18), $\gamma = 90^\circ$, $V = 4173.3$ (16) Å³, $Z = 4$, $D_c = 1.183$

$\text{g}\cdot\text{cm}^{-3}$, $F(000) = 1624$, $\mu(\text{Mo K}\alpha) = 0.8 \text{ cm}^{-1}$. 4494 Reflections measured, 2722 independent reflections, $R_{\text{int}} = 0.149$, ($1.0^\circ < \theta < 25.0^\circ$), and 239 parameters. Data collected on an Enraf-Nonius FAST area detector on rotating anode, $T = 100\text{K}$. The structure was solved with SHELXS-86, and refined using SHELXL-97. Hydrogen atoms were included in the refinement on calculated positions riding on their carrier atoms. Part of the 6-alkyl chain of 1-N-methyl-6-tridecyluracil is disordered over two positions. Final $wR2 = 0.1716$, $w = 1/[\sigma^2(F^2) + (0.0010P)^2 + 20P + 5000]$, $R1 = 0.0983$ (for $1060 I > 2\sigma(I)$), $S = 1.197$, $-0.42 < \Delta\rho < 0.44 \text{ e } \text{\AA}^{-3}$.

Crystal data for 1:2 complex melamine•5: $\text{C}_3\text{H}_6\text{N}_6 \cdot 2 \text{ C}_5\text{H}_8\text{N}_2\text{O}_3 \cdot 3 \text{ H}_2\text{O}$; $M_r = 464.40$, colourless, needle-shaped crystal ($0.01 \times 0.1 \times 0.7 \text{ mm}$), monoclinic, space group $P2_1/c$ (no. 14) with $a = 7.2903(16)$, $b = 21.948(13)$, $c = 12.148(7) \text{ \AA}$, $\alpha = 90^\circ$, $\beta = 98.46(3)$, $\gamma = 90^\circ$, $V = 1922.6(17) \text{ \AA}^3$, $Z = 4$, $D_c = 1.6044(14) \text{ g}\cdot\text{cm}^{-3}$, $F(000) = 976$, $\mu(\text{Mo K}\alpha) = 1.4 \text{ cm}^{-1}$. 16893 Reflections measured, 3393 independent reflections, $R_{\text{int}} = 0.0684$, ($0.93^\circ < \theta < 25.0^\circ$), and 303 parameters. The structure was solved by SHELXS-86, and refined using SHELXL-96. Hydrogen atoms were included on calculated positions. Final $wR2 = 0.2187$, $w = 1/[\sigma^2(F^2) + (0.06P)^2]$, $R1 = 0.0815$ (for $1221 I > 2\sigma(I)$), $S = 0.942$, $-0.34 < \Delta\rho < 0.36 \text{ e } \text{\AA}^{-3}$.

Crystal data for 1:2 complex melamine•6: $\text{C}_3\text{H}_6\text{N}_6 \cdot 2 \text{ C}_6\text{H}_8\text{N}_2\text{O}_3$, $M_r = 438.40$, colourless, plate-shaped crystal ($0.1 \times 0.2 \times 0.5 \text{ mm}$), monoclinic, space group $C2$ (no. 5) with $a = 15.8345(10)$, $b = 8.0746(7)$, $c = 7.2945(14) \text{ \AA}$, $\alpha = 90^\circ$, $\beta = 101.644(11)$, $\gamma = 90^\circ$, $V = 913.5(2) \text{ \AA}^3$, $Z = 2$, $D_c = 1.5938(3) \text{ g}\cdot\text{cm}^{-3}$, $F(000) = 460$, $\mu(\text{Mo K}\alpha) = 1.3 \text{ cm}^{-1}$. 2434 Reflections measured, 1131 independent reflections, $R_{\text{int}} = 0.0684$, ($2.63^\circ < \theta < 27.5^\circ$), and 175 parameters. Positional parameters of the hydrogen atoms were refined. Final $wR2 = 0.0847$, $w = 1/[\sigma^2(F^2) + (0.0568P)^2 + 0.09P]$, $R1 = 0.0345$ (for $1112 I > 2\sigma(I)$), $S = 1.033$, $-0.31 < \Delta\rho < 0.32 \text{ e } \text{\AA}^{-3}$.

Crystal data for 1:3 complex melamine•6: $\text{C}_3\text{H}_6\text{N}_6 \cdot 3 \text{ C}_6\text{H}_8\text{N}_2\text{O}_3$, $M_r = 594.55$, colourless, plate-shaped crystal ($0.15 \times 0.50 \times 0.55 \text{ mm}$), monoclinic, space group $P2_1/c$ (no. 14) with $a = 9.5342(6)$, $b = 22.6908(12)$, $c = 12.3059(9) \text{ \AA}$, $\alpha = 90^\circ$, $\beta = 106.666(7)$, $\gamma = 90^\circ$, $V = 2550.4(3) \text{ \AA}^3$, $Z = 4$, $D_c = 1.5484(2) \text{ g}\cdot\text{cm}^{-3}$, $F(000) = 1248$, $\mu(\text{Mo K}\alpha) = 1.2 \text{ cm}^{-1}$. 7821 Reflections measured, 5827 independent reflections, $R_{\text{int}} = 0.0451$, ($0.9^\circ < \theta < 27.5^\circ$), and 462 parameters. Positional parameters of the hydrogen atoms were refined, except for the hydrogen atoms of methyl group C(12), which were included in a disorder model. Final $wR2 = 0.1543$, $w = 1/[\sigma^2(F^2) + (0.0539P)^2 + 1.46P]$, $R1 = 0.0606$ (for $3370 I > 2\sigma(I)$), $S = 1.033$, $-0.28 < \Delta\rho < 0.48 \text{ e } \text{\AA}^{-3}$.

Crystal data for 1:3 complex melamine•7: $\text{C}_3\text{H}_6\text{N}_6 \cdot 3 \text{ C}_8\text{H}_{12}\text{N}_2\text{O}_2$, $M_r = 1261.41$, colourless, block-shaped crystal ($0.1 \times 0.2 \times 0.5 \text{ mm}$), hexagonal, space group $P6_3/m$ (no. 176) with $a = 17.212(2)$, $b = 17.212(2)$, $c = 6.3697(5) \text{ \AA}$, $\alpha = 90^\circ$, $\beta = 90^\circ$, $\gamma = 60^\circ$, $V = 1634.2(3) \text{ \AA}^3$, $Z = 2$, $D_c = 1.282(2) \text{ g}\cdot\text{cm}^{-3}$, $F(000) = 672$, $\mu(\text{Mo K}\alpha) = 1.0 \text{ cm}^{-1}$. All data are given without disordered solvent contribution (vide infra). 4825 Reflections measured, 1366 independent reflections, $R_{\text{int}} = 0.14$, ($1.37^\circ < \theta < 27.5^\circ$), $T = 100 \text{ K}$, and 113 parameters. The *N*-propyl moiety is disordered over four positions, two of which are generated by the space group symmetry. The occupancy ratio of the two unique conformations was included as a parameter in the refinement. The unit cell contains a channel parallel to the *c*-axis and passing through the origin, filled with disordered solvent (probably water). This density was modeled by introducing two partially occupied oxygen sites in the channel. Hydrogen atoms were included on a difference Fourier map, and subsequently included in the refinement. All non-hydrogen atoms were refined with anisotropic thermal parameters, except for the carbon atoms in the disordered propyl chain. Hydrogen atoms were refined with a fixed isotropic thermal parameter related to the value of the equivalent isotropic displacement parameter of their carrier atoms by a factor of 1.5 for the methyl, disordered methylene, and amine hydrogen atoms, and by a factor 1.2 for

the other hydrogen atoms. Final $wR2 = 0.179$, $w = 1/[\sigma^2(F^2) + (0.0483P)^2 + 1.81P]$, $R1 = 0.065$ (for 690 $I > 2\sigma(I)$), $S = 1.07$, $-0.26 < \Delta\rho < 0.28 \text{ e } \text{\AA}^{-3}$.

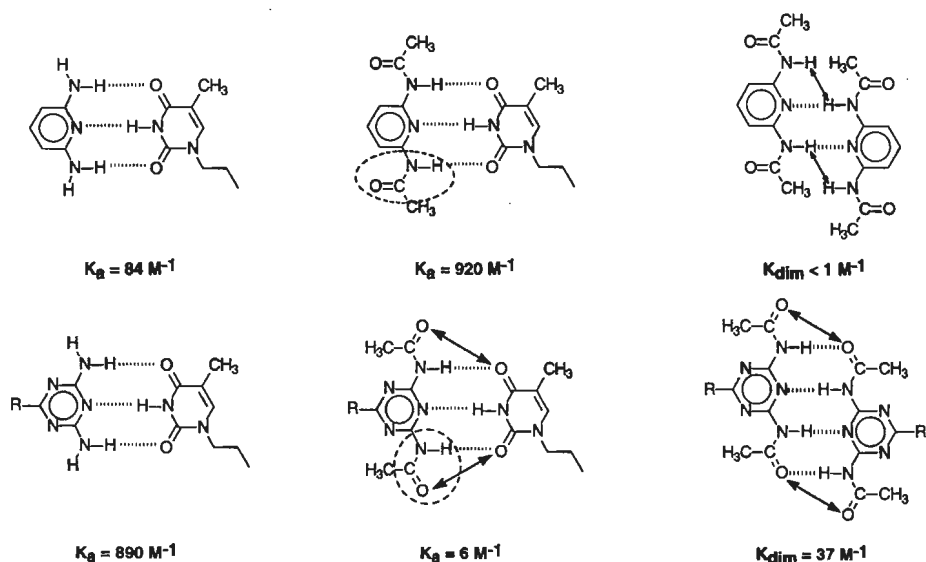
References and Footnotes

- 1) G. Ostragorich, R. Bacaloglu, *Tmisoara. Studii Cercetari Stiint. Chim.*, **1962**, *9*, 273, (b) A.I. Finkel'shtein, O.S. Rukevich, *Zh. Prikl. Spektrosk.*, **1983**, *38*, 327.
- 2) J.A. Zerkowski, J.C. MacDonald, C.T. Seto, D.A. Wierda, G.M. Whitesides, *J. Am. Chem. Soc.*, **1994**, *116*, 2382.
- 3) Y. Wang, B. Wei, Q. Wang, *J. Crystallogr. Spectrosc. Res.*, **1990**, *20*, 79.
- 4) For a review see: G.M. Whitesides, E.E. Simanek, J.P. Mathias, C.T. Seto, D.N. Chin, M. Mammen, D.M. Gordon, *Acc. Chem. Res.*, **1995**, *28*, 37.
- 5) (a) J.-M. Lehn, M. Mascal, A. DeCian, J. Fischer, *J. Chem. Soc., Chem. Comm.* **1990**, 479. (b) J.-M. Lehn, M. Mascal, A. DeCian, J. Fischer, *J. Chem. Soc., Chem. Comm.* **1992**, 461.
- 6) (a) N. Kimizuka, T. Kawasaki, K. Hirata, T. Kunitake, *J. Am. Chem. Soc.*, **1995**, *117*, 6360, (b) N. Kimizuka, S. Fujikawa, H. Kuwahara, T. Kunitake, A. Marsh, J.-M. Lehn., *J. Chem. Soc., Chem. Comm.*, **1995**, 2103.
- 7) J. Rebek Jr., *Pure & Appl. Chem.*, **1989**, *61*, 2103.
- 8) Crystal structure of melamine with two molecules of dibromobarbituric acid: J.A. Zerkowski, J.C. MacDonald, G.M. Whitesides, *Chem. Mat.*, **1994**, *6*, 1250.
- 9) A.D. Burrows, C.-W. Chan, M.M. Chowdhry, J.E. McGrady, D.M.P. Mingos, *Chem. Soc. Rev.*, **1995**, 329.
- 10) (a) R.F.M. Lange, PhD. Thesis, Eindhoven University of Technology, **1997**, (b) R.F.M. Lange, F.H. Beijer, R.P. Sijbesma, R.W.W. Hooft, H. Kooijman, A.L. Spek, J. Kroon, E.W. Meijer, *Angew. Chem. Int. Ed. Engl.*, **1997**, *36*, 969.
- 11) H. Tukada, Y. Mazaki, *Chem. Lett.*, **1997**, 441.
- 12) (a) R.F.M. Lange, E.W. Meijer, *Macromolecules*, **1995**, *28*, 782, (b) R.F.M. Lange, E.W. Meijer, *Macromol. Symp.*, **1996**, *102*, 301, (c) reference 10a.
- 13) The carbonyl between the two N-H groups (on C2) is involved in the DAD-ADA bonding and in uracil dimerization, while the carbonyl at C4 is involved in a hydrogen bond with a hydroxymethyl group, or a water molecule. Also the third melamine ring nitrogen atom is hydrogen bonded to a water molecule.
- 14) M.C. Etter, *Acc. Chem. Res.*, **1990**, *23*, 120.
- 15) (a) G.A. Jeffrey, W. Saenger, *Hydrogen Bonding in Biological Structures*, Springer Verlag, Berlin, **1994**, (b) G.A. Jeffrey, *An Introduction to Hydrogen Bonding*, Oxford University Press, Oxford, **1997**.
- 16) (a) C.B. Aakeröy, K.R. Seddon, *Chem. Soc. Rev.*, **1993**, 397, (b) G.R. Desiraju, *Angew. Chem. Int. Ed. Engl.*, **1995**, *34*, 2328.
- 17) Spek, A.L. *J. Appl. Crystallogr.*, **1988**, *21*, 578.
- 18) G.M. Sheldrick, SHELXS-86, *Program for crystal structure determination*, University of Göttingen, Germany, **1986**.
- 19) G.M. Sheldrick, SHELXL-93, *Program for crystal structure refinement*, University of Göttingen, Germany, **1993**.

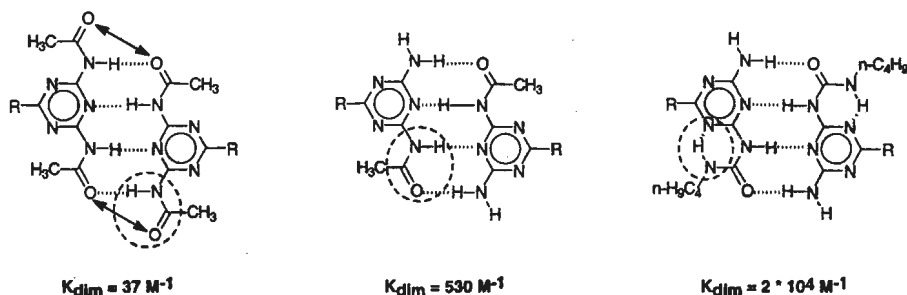
Samenvatting

Dit proefschrift beschrijft gedetailleerde studies om nieuwe meervoudige waterstofbrugeenheden te verkrijgen welke sterkte en unidirectionaliteit van binding combineren met gemak in synthese, evenals enkele supramoleculaire toepassingen hiervan. Het relatief nieuwe gebied van de supramoleculaire chemie, met zijn principes, doelen en uitdagingen, wordt omschreven in het inleidende hoofdstuk 1. Door hun unieke combinatie van sterkte, specificiteit en gerichtheid zijn meervoudige waterstofbruggen een van de favoriete niet-covalente interacties om zelf-geassembleerde functionele materialen te verkrijgen. Daarom wordt uitgebreid ingegaan op de principes van waterstofbrugvorming, en op de factoren die de bindingssterkte van rijen van meervoudige waterstofbruggen bepalen. Waterstofbrugeenheden die sterkte en gerichtheid combineren met een gemakkelijke synthese—welke ten grondslag kunnen liggen aan diverse nieuwe supramoleculaire polymeerarchitecturen—zijn echter sporadisch aanwezig in de supramoleculaire literatuur.

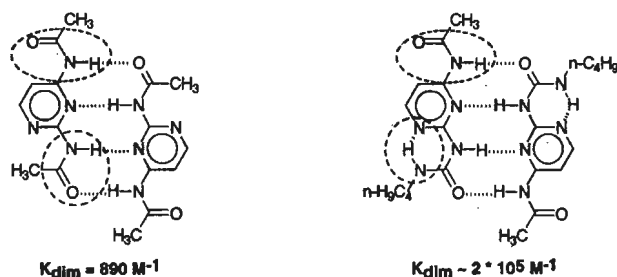
Een poging om sterke complexatie via drievoudige waterstofbruggen te verkrijgen tussen de (gemakkelijk toegankelijke) combinatie di(acyl)aminotriazine–uracil wordt beschreven in hoofdstuk 2. Gedetailleerde ^1H -NMR en IR studies in chloroform oplossing zijn gebruikt ter bestudering van het effect van acylering van de aminogroepen in enerzijds 2,4-diaminotriazines en anderzijds 2,6-diaminopyridine op de waterstofbrugvorming. Een tegengesteld effect op de bindingssterkte van complexen met uracillen treedt op, terwijl dimerisatieconstanten van di(acylamino)triazines veel hoger zijn dan die van di(acylamino)pyridines. Deze twee fenomenen zijn mede het gevolg van verschillende conformationele voorkeuren van de amides in di(acylamino)triazines en di(acylamino)pyridines, zoals associatieconstanten van complexen in CDCl_3 in onderstaande figuur aangeven.



In hoofdstuk 3 wordt de eerder vermelde capaciteit van 2,4-di(acylamino)triazines om te dimeriseren via viervoudige waterstofbruggen verder uitgewerkt, met het doel de dimerisatie te versterken. Zoals in onderstaande figuur is weergegeven, is het mogelijk sterkere dimerisatie via een lineaire DADA rij van waterstofbrugfunctionaliteiten te verkrijgen door twee afstotende interacties ten gevolge van overbodige carbonylen weg te nemen, simpel door het gebruiken van mono-geacyleerde diaminotriazine derivaten. Sterkere dimerisatie wordt bovendien verkregen door pre-organisatie toe te passen middels een intramoleculaire waterstofbrug, door een amide te vervangen door een (butyl)ureido substituent.

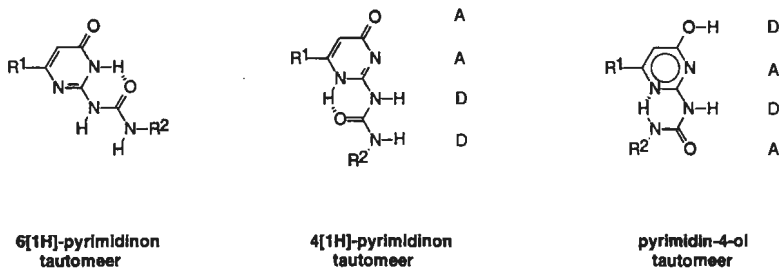


Het tweede deel van hoofdstuk 3 laat zien dat dimerisatie via zelf-complementaire DADA rijen van waterstofbrugfunctionaliteiten ook aanwezig is in geacyleerde derivaten van 2,4-diaminopyrimidine, en dat voor-organisatie door een intramoleculaire waterstofbrug ook in pyrimidine derivaten een substantiële toename van de stabiliteit van de dimeren teweeg brengt. Daar de dimerisatieconstanten in pure CDCl_3 zo groot zijn dat bepaling hiervan onmogelijk is door de te lage gevoeligheid van $^1\text{H-NMR}$ en FT-IR, zijn studies in gemengde oplosmiddelcombinaties van chloroform en methanol gebruikt om, door middel van extrapolatie, een schatting te verkrijgen voor de waarde in pure CDCl_3 . Deze worden weergegeven in onderstaande figuur.



Hoofdstuk 4 beschrijft studies naar viervoudige waterstofbrugvorming in 2-ureido-4-pyrimidinon derivaten, en toont aan dat deze verbindingen exceptioneel sterk kunnen dimeriseren via voor-georganiseerde DDAA rijen van waterstofbruggen, dit in verbindingen

die heel gemakkelijk zijn te synthetiseren. Het complexatiegedrag van deze ureido-pyrimidinonen is echter gecompliceerd door het optreden van evenwichten tussen drie mogelijke tautomere vormen. Het 6[1H]-pyrimidinon tautomeer wordt waargenomen als de (meest stabiele) monomere vorm, terwijl dimeren gevormd kunnen worden zowel via DDAA rijen van het 4[1H]-pyrimidinon tautomeer alswel in een DADA rij van het pyrimidin-4-ol tautomeer.



Deze tautomere evenwichten worden beïnvloed door begrepen, en dus stuurbare, substituenteffecten, en zijn afhankelijk van het oplosmiddel en de concentratie. Extrapolatie van complexe dimerisatieconstanten, waarin een tautomerisatie is inbegrepen, in $\text{CDCl}_3/\text{DMSO}-d_6$ oplosmiddelmengsels geeft aan dat de dimerisatieconstante in pure CDCl_3 groter is dan $4.5 \times 10^5 \text{ M}^{-1}$ voor 6-trifluoromethyl-2-butylureido-pyrimidin-4-ol, welke stof voorkomt als een DADA dimeer van het pyrimidin-4-ol tautomeer, en zelfs substantieel groter dan 10^6 M^{-1} is voor 6-methyl-2-butylureido-4-pyrimidinon, welke verbinding voorkomt als een DDAA dimeer van het 4[1H]-pyrimidinon tautomeer.

Hoofdstuk 5 beschrijft de vorming van vloeibaar kristallijne fasen van schijfvormige mesogenen, welke gevormd worden door viervoudig waterstofgebrugde dimeren gefunctionaliseerd met alkoxy staarten. Polarisatie microscopie, differentiële scanning calorimetrie, infrarood, en röntgen verstrooiing studies laten zien dat in het algemeen discotische hexagonale fasen verkregen worden in opmerkelijk brede temperatuurstrajecten.

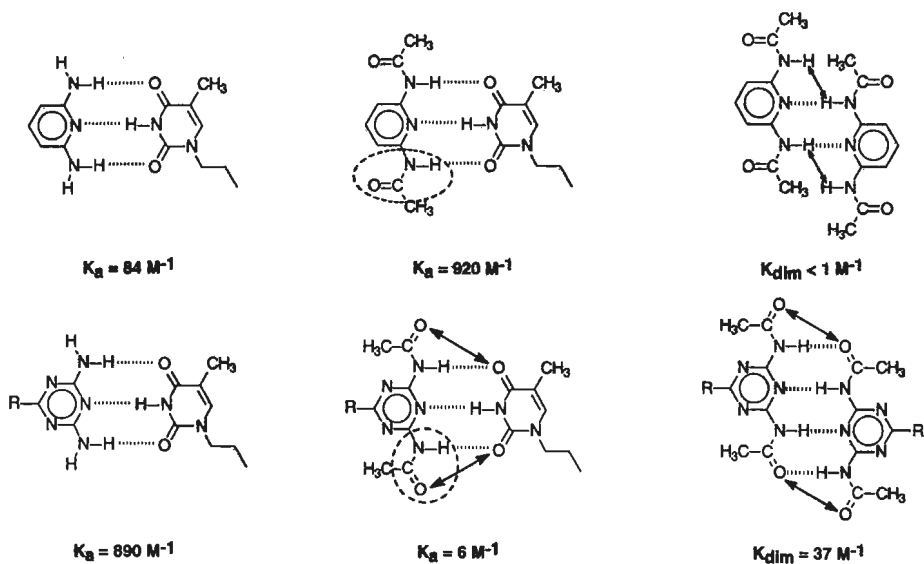
Hoofdstuk 6 laat zien dat lineaire supramoleculaire polymeren, in welke de bindingen tussen de monomeren van niet-covalente aard zijn, verkregen worden door twee zelf-complementaire ureidopyrimidinon eenheden, welke sterk en unidirectioneel dimeriseren via viervoudige waterstofbruggen, in één molecuul in te bouwen. Als een gevolg van de sterke, maar reversibele binding tussen de monomeren laten deze supramoleculaire polymeren een unieke en niet eerder vertoonde combinatie van eigenschappen zien, die, afhankelijk van de condities, karakteristieken van zowel organische moleculen als van macromoleculen hebben.

Hoofdstuk 7 beschrijft kristalstructuurontwerp in melamine-uracil complexen. Door de toegankelijkheid van de carbonyl acceptoren in de uracil moleculen te beïnvloeden, dit door introductie van substituenten op de N-1- en/of op de C-5-positie, kan de vorming van 1:2 visgraatstructuren of 1:3 rozet-achtige architecturen gestuurd worden.

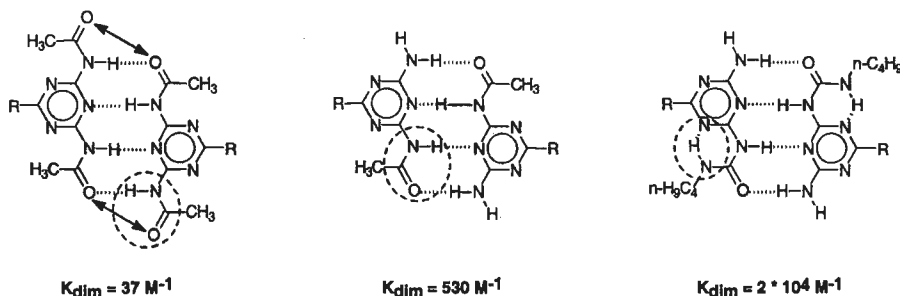
Summary

This thesis describes detailed studies to obtain novel multiple hydrogen bonding units that combine strong and unidirectional binding with ease of synthesis, as well as some supramolecular applications thereof. The relatively young field of supramolecular chemistry, including its principles, aims and challenges, is described in the introductory chapter 1. Because of their unique combination of strength, specificity and directionality, multiple hydrogen bonding is one of the most applied non-covalent interactions to obtain self-assembling functional materials. Hence, the principles of hydrogen bonding, and factors that determine the strength of multiple hydrogen bonding arrays, are elaborated in detail. However, multiple hydrogen bonding units that combine strong and unidirectional binding with ease of synthesis, which could be useful for several new supramolecular polymer architectures, are only scarcely reported in supramolecular literature.

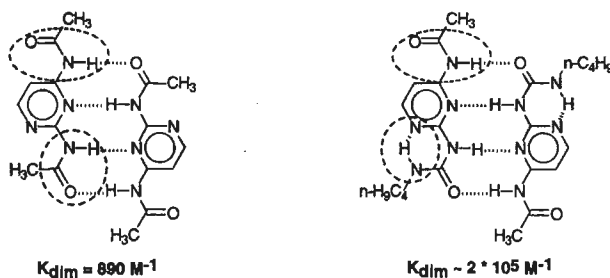
Chapter 2 describes an attempt to induce strong complexation via triple hydrogen bonding between the (synthetically easily accessible) combination di(acyl)aminotriazine–uracil. Detailed ^1H -NMR and IR investigations in chloroform solution allowed the study of the effect of acylation of the amino groups of 2,4-diaminotriazines and 2,6-diaminopyridine on hydrogen bonding. A remarkable, opposite effect of acylation with respect to complexation with uracils occurs, while the dimerization constants of di(acylamino)triazines are significantly higher than those of the corresponding di(acylamino)pyridines. These two phenomena presumably arise from different conformational preferences of the amides in di(acylamino)triazines and di(acylamino)pyridines, as the association constants of complexes given in CDCl_3 in the figure below indicate.



In chapter 3, the previously observed capacity of 2,4-di(acylamino)triazines to dimerize via quadruple hydrogen bonding is elaborated, with the intention to strengthen the tendency for dimerization. As shown in the figure below, stronger dimerization via linear DADA arrays is achieved by removal of two spectator repulsions, by using mono-acylated diaminotriazine derivatives. Stronger dimerization is also achieved by pre-organization of the DADA-array by an intramolecular hydrogen bond, through replacement of the amide group by a (butyl)ureido group.

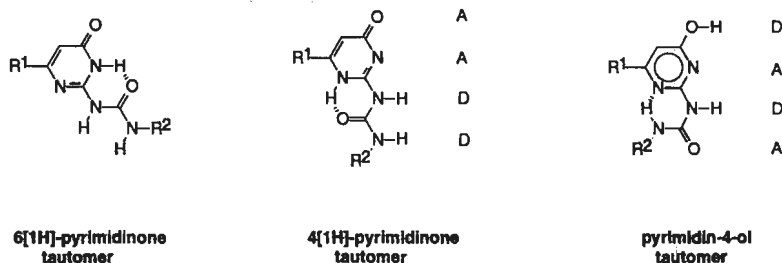


The second part of chapter 3 shows that dimerization via self-complementary DADA arrays is also present in acylated derivatives of 2,4-diaminopyrimidine, and that pre-organization by an intramolecular hydrogen bond effects a substantial increase in the stability of dimers also in pyrimidine derivatives. Since the dimerization constants in pure chloroform are so large that their determination is hampered by the sensitivity of ^1H -NMR and FT-IR being too low, studies in chloroform/methanol solvent mixtures were performed to get, by extrapolation, an estimate for the value in pure CDCl_3 as given in the figure below.



Chapter 4 describes studies of quadruple hydrogen bonding in 2-ureido-4-pyrimidinone derivatives, and shows that it is possible to obtain exceptionally strong dimerization via (pre-organized) DDAA arrays of hydrogen bonding groups in compounds that are readily accessible. The complexation behavior of these ureidopyrimidinones is, however, complicated by the occurrence of equilibria between three tautomeric forms. The 6[1H]-pyrimidinone tautomer is observed as the (most stable) monomeric form, while dimers

may be formed via DDAA arrays of the 4[1H]-pyrimidinone tautomer, as well as by DADA arrays of the pyrimidin-4-ol tautomer.



These tautomeric equilibria are influenced by understood, and hence steerable, electronic substituent effects, and are dependent on solvent and concentration. Extrapolation of complex dimerization constants, which include a tautomerization, in $\text{CDCl}_3/\text{DMSO-}d_6$ mixtures indicate that dimerization constants in pure CDCl_3 exceed $4.5 \times 10^5 \text{ M}^{-1}$ for 6-trifluoromethyl-2-butylureido-pyrimidin-4-ol, which dimerises via a DADA array of the pyrimidin-4-ol tautomer, and even substantially exceed 10^6 M^{-1} for 6-methyl-2-butylureido-4-pyrimidinone, which dimerises via a DDAA array of the 4[1H]-pyrimidinone tautomer.

Chapter 5 describes the formation of liquid crystalline phases of disk-like mesogens formed by quadruply hydrogen bonded dimers functionalized with alkyl chains. Polarization microscopy, differential scanning calorimetry, and X-ray diffraction studies indicated that, in general, discotic hexagonal phases are obtained in remarkably broad temperature ranges.

Chapter 6 shows that linear supramolecular polymers, which are bonded non-covalently, originate from the strong and unidirectional association via quadruple hydrogen bonding of self-complementary ureidopyrimidinone units in bifunctional compounds. As a result of the strong, yet reversible, binding between the monomers, these supramolecular polymers feature, depending on conditions, a unique and unprecedented combination of properties, reminiscent both of organic molecules and of macromolecules.

Chapter 7 describes crystal engineering in melamine-uracil complexes. By tuning the carbonyl acceptor accessibility in uracil molecules, through introducing substituents at the *N*-1- and/or at the C-5-position, the formation of 1:2 herringbone-like structures or 1:3 rosette-like architectures is regulated.

Curriculum Vitae

Felix Beijer werd op 14 mei 1970 geboren te Tiel. Na het brugjaar aan de voormalige Rijks Scholen Gemeenschap te Tiel (heden: Lingecollege) werd aldaar 4 jaar gymnasium opleiding genoten. De resterende twee jaar van het VWO werden gevolgd op het Newman College te Breda. Het examen, met als vakken Nederlands, Engels, Latijn, Wiskunde A, Wiskunde B, Natuurkunde, Scheikunde en Biologie, werd behaald in mei 1988.

Aansluitend op het behalen van het VWO diploma werd op 1 september 1988 de studie Scheikunde aan de Universiteit Utrecht aangevangen. Het propaedeutisch examen werd in augustus 1989 (cum laude) behaald. De studie werd in juni 1993 succesvol afgerond (met genoegen), met als specialisaties Fysisch Organische Chemie (Prof.dr. L.W. (Leo) Jenneskens, Dr. J.W. (Jan) Zwikker), Chemiedidactiek (Dr. O. (Onno) de Jong) en NMR-spectroscopie (Dr. H.W.A. (Huub) Biessels), en als afstudeerrichting Preparatieve Organische Chemie (Prof.dr. L. (Lambert) Brandsma). Tevens was de auteur in die periode tweemaal in dienst van de Universiteit Utrecht als student-assistent voor het scheikunde-praktikum van de studenten Natuurwetenschappen.

Na zijn afstuderen heeft de auteur zijn voorliefde voor organische chemie vorm gegeven tijdens zijn promotie-onderzoek, daartoe in de gelegenheid gesteld door Prof.dr. E.W. (Bert) Meijer van de vakgroep Organische Chemie aan de Technische Universiteit Eindhoven. In de periode september 1993 tot en met augustus 1997 heeft de auteur daar, in dienst als AIO-4, zijn promotieonderzoek uitgevoerd, onder begeleiding van Dr. R.P. (Rint) Sijbesma. De belangrijkste resultaten van dat onderzoek staan beschreven in dit proefschrift.

List of Publications

Hydrogen-bonded Complexes of Diaminopyridines and Diaminotriazines: Opposite Effect of Acylation on Complex Stabilities: Felix H. Beijer, Rint P. Sijbesma, Jef A.J.M. Vekemans, E.W. Meijer, Huub Kooijman, and Anthony L. Spek, *J. Org. Chem.*, **1996**, *61*, 6371–6380.

Crystal Engineering of Melamine–Imide Complexes; Tuning the Stoichiometry by Steric Hindrance of the Imide Carbonyl Groups: Ronald F.M. Lange, F.H. Beijer, R.P. Sijbesma, R.W.W. Hooft, H. Kooijman, A.L. Spek, J. Kroon, E.W. Meijer, *Angew. Chem. Int. Ed. Engl.*, **1997**, *36*, 969–971.

Self-complementarity Using Quadruple Hydrogen Bonding: Felix H. Beijer, Rint P. Sijbesma, Huub Kooijman, Anthony L. Spek, and E.W. Meijer, *Angew. Chem.*, **1998**, *110*, 79; *Angew. Chem. Int. Ed. Engl.*, **1998**, *37*, 75

Strong Dimerization of 4[1H]-ureidopyrimidinones via Quadruple Hydrogen Bonding in a Donor–Donor–Acceptor–Acceptor Array: Felix H. Beijer, Rint P. Sijbesma, Huub Kooijman, Anthony L. Spek, E.W. Meijer, *J. Am. Chem. Soc.*, submitted.

Reversible Polymers from Self-Complementary Monomers, Using Quadruple Hydrogen Bonding, R.P. Sijbesma, F.H. Beijer, L. Brunsveld, B.J.B. Folmer, K. Hirschberg, R.F.M. Lange, J.K.L. Lowe, E.W. Meijer, *Science*, **1997**, *278*, 1601–1602.

Discotic Liquid Crystals from Quadruply Hydrogen Bonded Dimers, Felix H. Beijer, H. Fischer, R.P. Sijbesma, E.W. Meijer, manuscript in preparation.

Supramoleculair Polymeer: Rint P. Sijbesma, Felix H. Beijer, Luc Brunsveld, E.W. Meijer; (concept) octrooiaanvraag nr. 1004192 voor het principe van viervoudige waterstofbruggen voor polymeer-eigenschappen (DSM-Research), October 4 **1996**.

Design, Synthesis and Characterisation of New Hydrogen Bonding Units for Supramolecular Polymer Chemistry, lecture at SON meeting, section Organic Chemistry, October 4, **1996**.

Self-Complementary Quadruple Hydrogen Bonding Units for Supramolecular Polymer Chemistry, F.H. Beijer, J.K.L. Lowe, J.H.K.K. Hirschberg, R.P. Sijbesma, E.W. Meijer, poster presentation at Bayreuth Polymer Symposium, Germany, April 7–9 **1997**, 2nd prize in the poster presentation.

Stellingen

behorende bij het proefschrift

Cooperative Multiple Hydrogen Bonding in Supramolecular Chemistry

1. De introductie van een grafische methode om uit een verdunningsreeks de dimerisatieconstante te bepalen, is weinig zinvol vanwege de beschikbaarheid van het computerfitten van de resultaten middels de niet-lineair kleinste kwadraten methode.

J.-S. Chen, C.-Y. Fang, J.K. Baird, *Z. Physikal. Chem.*, **1997**, *199*, 49.

2. Het niet kunnen reproduceren van de ooit gemeten hoge ET(30) polariteit waarde van chloroform is waarschijnlijk het gevolg van het gebruik in het verleden van chloroform gestabiliseerd met 1% ethanol.

J.G. Dawber, J. Ward, R.A. Williams, *J. Chem. Soc., Faraday Trans. I*, **1988**, *84*, 713.

3. De hydrosilyleringskoppeling van quinidine met siloxanen resulteert niet in de door de auteurs voorgestelde structuur.

A. Bachrach, A. Zilkha, *Eur. Polym. J.*, **1984**, *20*, 493.

4. De grens tussen dendrimeren en sterk vertakte polymeren wordt steeds vager door het gebruik van de term dendritische structuur.

G.R. Newkome, C.D. Weis, C.N. Moorefield, G.R. Baker, B.J. Childs, J. Epperson, *Angew. Chem. Int. Ed. Engl.*, **1998**, *37*, 307.

5. De bepaling van het gehalte actieve zuurstof in verbinding X zegt niets over dat gehalte in onafhankelijke verbinding Y.

Y. Ishii, K. Yamawaki, T. Ura, H. Yamada, T. Yoshida, M. Ogawa, *J. Org. Chem.*, **1988**, *53*, 3587.

6. De term 'rapid' in de titel van het tijdschrift doet bij sommige publicaties vermoeden, dat inderdaad geen tijd is genomen een goede referee te raadplegen.

M. Yoshikawa, J. Izumi, T. Kitao, S. Sakamoto, *Macromol. Rapid. Comm.*, **1997**, *18*, 761.

7. Subtiele tekstveranderingen door tijdschriftredacteurs om de tekst mooier en duidelijker te maken, leveren niet altijd het gewenste resultaat.

F.H. Beijer, H. Kooijman, R.P. Sijbesma, A.L. Spek, E.W. Meijer, *Angew. Chem. Int. Ed. Engl.*, **1998**, *37*, 75.

8. De voorspelde waarden van de bindingsterkte van viervoudige waterstofbrugkoppels, gebaseerd op de extrapolatie van 'regels' afgeleid uit koppels met minder dan vier waterstofbruggen, had men beter experimenteel bevestigd.
 1. J. Sartorius, H.-J. Schneider, *Chemistry, Eur. J.*, **1996**, *2*, 1446,
 2. F.H. Beijer, *dit proefschrift*.
9. Het meerdere malen publiceren van dezelfde resultaten is een jammerlijk gevolg van het door de huidige wetenschappelijke gemeenschap gehanteerde idee dat de lengte van de publicatielijst het voornaamste criterium is van iemands wetenschappelijke kwaliteiten.
 - 1: R. Kleppinger, C.P. Lillya, C. Yang, *Angew. Chem.*, **1995**, *107*, 1762,
 - 2: R. Kleppinger, C.P. Lillya, C. Yang, *J. Am. Chem. Soc.*, **1997**, *119*, 4097.
10. Het gebruik van de term 'self-assembly' in publicaties wekt ten onrechte de indruk dat de auteurs zelf op moleculaire schaal kunnen organiseren.
11. Eén kristalstructuur zegt vaak meer dan duizend woorden.
12. Door de bereidheid tot donatie van organen te koppelen aan de wens te ontvangen, zal het tekort aan donororganen sterk verminderen.
13. De NS zou de toename van het reizigersvervoer per trein in de presentatie van hun jaarcijfers gemakkelijk nog spectaculairder kunnen laten lijken door niet het aantal reizigerskilometers, maar het aantal reizigersuren te gebruiken.
14. Gezien alle aandacht in het nieuws en het politieke belang van het milieu kan het niet lang meer duren, voordat iemand meent een verband tussen 'El Nino' en het door de mens veroorzaakte 'broeikas-effect' aangetoond te hebben.
15. Het geeft zwaar te denken dat juist onder hoger opgeleide en wetenschappelijk onderbouwde mensen veel aanhang is te vinden voor de Montignac-eetstijl.
16. Het argument van rokers, dat roken moet mogen omdat je iemands behoeften moet respecteren, gaat voorbij aan de behoefte van vele mensen aan schone lucht.
17. Klonen leidt tot tweedeling.
18. Zonder weerstand kom je niet vooruit.

